



JRC SCIENCE FOR POLICY REPORT

Atlas of the Human Planet 2020

*Open geoinformation for
research, policy, and action*

2020



This publication is a Science for Policy report by the Joint Research Centre (JRC), the European Commission's science and knowledge service. It aims to provide evidence-based scientific support to the European policymaking process. The scientific output expressed does not imply a policy position of the European Commission. Neither the European Commission nor any person acting on behalf of the Commission is responsible for the use that might be made of this publication. For information on the methodology and quality underlying the data used in this publication for which the source is neither Eurostat nor other Commission services, users should contact the referenced source. The designations employed and the presentation of material on the maps do not imply the expression of any opinion whatsoever on the part of the European Union concerning the legal status of any country, territory, city or area or of its authorities, or concerning the delimitation of its frontiers or boundaries.

Contact information

Name: Thomas Kemper
Address: Via Fermi, 2749 21027 ISPRA (VA) - Italy - TP 267
European Commission - DG Joint Research Centre
Space, Security and Migration Directorate
Disaster Risk Management Unit E.1
Email: thomas.kemper@ec.europa.eu
Tel.: +39 0332 78 55 76

EU Science Hub

<https://ec.europa.eu/jrc>

JRC122364

EUR 30516

PDF	ISBN 978-92-76-27388-2	ISSN 1831-9424	doi:10.2760/16432
Print	ISBN 978-92-76-27389-9	ISSN 1018-5593	doi:10.2760/562514

Luxembourg: Publications Office of the European Union, 2020

© European Union, 2020



The reuse policy of the European Commission is implemented by the Commission Decision 2011/833/EU of 12 December 2011 on the reuse of Commission documents (OJ L 330, 14.12.2011, p. 39). Except otherwise noted, the reuse of this document is authorised under the Creative Commons Attribution 4.0 International (CC BY 4.0) licence (<https://creativecommons.org/licenses/by/4.0/>). This means that reuse is allowed provided appropriate credit is given and any changes are indicated. For any use or reproduction of photos or other material that is not owned by the EU, permission must be sought directly from the copyright holders.

All content © European Union, 2020, except:

Figure 1 © Adobe Stock, 2020, p. 7
Figure 3 © Adobe Stock, 2020, p. 11
Figure 4 © Adobe Stock, 2020, p. 12
Figure 14 © Adobe Stock, 2020, p. 23
Figure 17 Adobe Stock, 2020, p. 25
Figure 41 © Adobe Stock, 2020, p. 51
Figure 60 © DG ECHO, 2020, p. 71
Figure 79 © Adobe Stock, 2020, p. 91
Figure 94 © Adobe Stock, 2020, p. 107
Figure 95 © Adobe Stock, 2020, p. 108
Figure 97 © Adobe Stock, 2020, p. 110
Figure 101 © Adobe Stock, 2020, p. 114
Figure 103 © Adobe Stock, 2020, p. 116
Figure 105 © Adobe Stock, 2020, p. 120

Cover Image: © Adobe Stock

How to cite this report: European Commission, Joint Research Centre, Atlas of the Human Planet 2020 – Open geoinformation for research, policy, and action, EUR 30516, European Commission, Luxembourg, 2020, ISBN 978-92-76-27388-2, doi:10.2760/16432, JRC122364.

Atlas of the Human Planet 2020

*Open geoinformation for
research, policy, and action*

2020

Contents

Abstract.....	1
Foreword of the Director General of the Joint Research Centre	2
Foreword of the Director of the Group on Earth Observations Secretariat.....	3
Acknowledgements	4
Executive Summary.....	5
1 Introduction.....	8
1.1 Big Earth Data Intelligence: from Earth Observation data to AI-driven decision making	8
1.2 The GEO Human Planet Initiative.....	9
1.3 GHSL evolution from data to tools.....	9
1.4 Open geoinformation for research, policy and action.....	10
2 Fundamentals.....	13
2.1.1 From Earth's surface to built-up area.....	15
2.1.2 From Built-up area to population grid	16
2.1.3 From built-up area and population to settlement grids	17
2.1.4 From Urban Centres spatial delineation to a 4-D city database.....	18
2.1.5 From Urban Centres to Functional Urban Areas.....	19
2.1.6 From population layers to urban and rural classification of territorial units	20
2.1.7 GHSL workflow real case synthetic example	21
3 Applications of GHSL data in research, policy and action.....	24
3.1 Disaster Risk Management	26
3.1.1 The Disaster Risk Management Knowledge Centre - Risk Data Hub, web platform to facilitate management of disaster risks	27
3.1.2 Epidemic Risk Exposure and Urbanisation	29
3.1.3 Mapping the COVID-19 Pandemic and Potential Risk Factors.....	31
3.1.4 Advancing exposure and risk assessment in the EU by modelling population distribution in daily and seasonal cycles	33
3.1.5 Mapping drought hazard, exposure and vulnerability for drought risk reduction.....	35
3.1.6 Developing the European Wildfire Risk Assessment (WRA)	37
3.1.7 GloFAS Rapid Risk Assessment.....	39
3.1.8 New Estimates of Global Population and Land in the Low Elevation Coastal Zone Using GHSL-based Datasets.....	41
3.1.9 Flood Risk and Impact in Urban Areas Using Social Media.....	43
3.1.10 Saving time in satellite mapping in case of large disasters: the automatic identification of Areas of Interest based on the Global Human Settlement (GHS) - Settlement Model grid (SMOD).....	45
3.1.11 GHSL datasets in the Mapping component of the Copernicus Emergency Management Service	47
3.1.12 After conflicts in Iraq.....	49

3.2	Urbanisation.....	52
3.2.1	Cities in the World	53
3.2.2	The Future of Cities.....	55
3.2.3	Metropolitan Spaces in Africa	57
3.2.4	The Degree of Urbanisation.....	59
3.2.5	Delineating boundaries of metropolitan areas in the world using GHSL data.....	61
3.2.6	ESPON FUORE - Functional Urban Areas and other regions in Europe	63
3.2.7	The structure of urban settlements in European functional urban areas	65
3.2.8	Population agglomeration and dispersion in Emerging Europe.....	67
3.2.9	Analysing global megacities with GHSL data	69
3.3	Development.....	72
3.3.1	Rural electrification planning tool for Burkina Faso	73
3.3.2	Estimating Small-Area Population Density in Sri Lanka using Surveys and Geospatial Data.....	75
3.3.3	Estimating travel time to urban areas of different population sizes*	77
3.3.4	GHSL: A crucial input for LUISA4Africa	79
3.3.5	Estimating climate change induced migration	81
3.3.6	Estimates of Rural and Urban Displacement Trends.....	83
3.3.7	Detecting spatial patterns of inequality from Earth Observation.....	85
3.3.8	Tracking Infrastructural Transitions using Multi-Temporal GHSL, Black Marble, and GPW Population Data.....	87
3.3.9	SDG Voluntary Local Reviews: using GHSL layers to measure SDGs in European cities	89
3.4	Supporting the European Green Deal with new knowledge	92
3.4.1	Monitoring Arctic populations dynamics and urbanisation.....	93
3.4.2	Population changes and urbanisation in mountain ranges of the world.....	95
3.4.3	Global air pollutant emissions in urban centres.....	97
3.4.4	The possibility for renewable electricity autarky in Europe.....	99
3.4.5	Using the European Settlement Map to assess the rooftop solar photovoltaic potential in the European Union.....	101
3.4.6	The European Settlement Map (ESM 2015) green component.....	103
3.4.7	The structure of urban green in European functional urban areas	105
4	Challenges and trends in human settlements research.....	108
4.1	Fine scale global mapping of human settlements.....	109
4.2	Multi-sensor monitoring of human settlements	110
4.3	Human settlements spatial patterns and typologies.....	111
4.4	Describing the vertical component of built-up areas over large scales	112
4.5	Mitigating sensor-dependent built-up area estimation.....	113
4.6	Improving the mapping of global population distribution.....	115
4.6.1	Mapping and assessing present population and their dynamics	115
4.6.2	Spatially-explicit, high resolution population projections.....	116

4.7 Capacity building.....	117
4.8 Way Forward.....	119
5 Conclusions.....	121
References.....	122
List of Figures.....	126
List of Boxes.....	131

Abstract

The 2020 edition of the Atlas of the Human Planet presents policy-relevant examples provided by users of Global Human Settlement Layer (GHSL) products. Following a call for contribution, 37 showcases cover the domains of disaster risk reduction and crisis management, environment, urbanisation, and sustainable development. They were provided by members of the GEO Human Planet Initiative, the European Commission, international organisations including the Organisation for Economic Cooperation and Development, the International Organisation for Migration, the World Bank, and the European Bank for Reconstruction and Development, academia as well as the private sector. Each of the showcases demonstrates the added value of open and free geoinformation and provides policy recommendations for its domain.

The Atlas discusses also challenges and limitations of current global data sets and provides an outlook on the upcoming GHSL data release 2020 as well as the plan for a future production of the GHSL data under the umbrella of the Copernicus services.

Foreword of the Director General of the Joint Research Centre



The mandate and ambition of the Joint Research Centre is to provide science-based evidence for EU policy making. Yet the hurdles to use new evidence in policymaking are many: the evidence must be robust, methods must be transparent, results must be truly understood, and outcomes must be accepted by all sides of the policy debate before it is trusted and used.

I believe that the Global Human Settlement Layer is a showcase in this regard. Over the past ten years, it has succeeded in transforming earth observation data into accepted statistics on global human built-up and population. This revolutionary project has turned an exploratory research approach into a solid methodology, culminating in March 2020 when the UN Statistical Commission, on the basis of the GHSL data, adopted a worldwide definition of cities and urban areas for the first time ever.

Detailed knowledge about population and infrastructure is crucial also for sustainable development. This was recognized when 193 world leaders agreed upon the 17 Sustainable Development Goals (SDGs) in 2015, and promised to “leave no one behind.” Nevertheless, without reliable and timely population data linked to location, we cannot ensure that everyone is accounted for and that no one will be left behind. Even without the COVID-19 pandemic, many countries were struggling to update their census frequently. The GHSL data can help fill these data gaps and obtain informed and fine grained updates on population and infrastructure.

We now have clear and ample evidence that the GHSL data has inspired much progress. With this Atlas of the Human Planet 2020, we provide more than thirty examples of applications of the GHSL data covering very relevant policy domains, from disaster risk management to urbanisation, sustainable development and the green deal. I hope that this new Atlas can inspire even more people to further explore and use this source of knowledge, helping to overcome the limitations of traditional tools and methodologies.

The present GHSL achievements were possible thanks to the free and open data access to the data as well as networking in the GEO Human Planet Initiative. The training actions organised by the JRC have contributed to disseminate the knowledge all over the world, and as requested by the UN Statistical Commission we shall continue to train policy makers and scientists in the months to come.

Now that GHSL has reached the necessary maturity, it makes sense to move the provision of the baseline data into operational production in the Copernicus Emergency Service, which will ensure regular updates of the data. This will be the next challenge for us, in order to be able to offer a real operational service to the benefit of the whole world.

Stephen Quest
Director General
European Commission Directorate General Joint Research Centre

A handwritten signature in blue ink, appearing to read 'Stephen Quest', written over a light blue background.

Foreword of the Director of the Group on Earth Observations Secretariat



It is a great honour for me to introduce the Atlas of Human Planet 2020 that provides over 30 policy-relevant, action-oriented applications of the Global Human Settlement Layer (GHSL) data. As an intergovernmental partnership brokering the largest amount of publicly funded environmental data in the world, GEO has always advocated for broad and open data sharing policies and practices. We believe that harnessing Earth observations for the benefit of society can only be fully achieved through open access and sharing of data, information, knowledge, products, and services.

The Atlas 2020 is a deliverable of the GEO Human Planet Initiative, that is supporting global policy processes with agreed, actionable, and goal-driven metrics by developing a new generation of measurements and information products. By promoting cross-disciplinary cooperation, the initiative encourages innovation in the production and harmonization of high quality data products and services. The breadth of applications showcased in the Atlas 2020 amplifies and broadens the evidence base for open data sharing policies and practices, showcasing the opportunities and benefits of open data.

The high level applications span four thematic areas relevant to international development strategies: disaster risk reduction, crisis management, environment, urbanization, and sustainable development, and are a reflection of the wide and multi-disciplinary community of GHSL data users. From policymakers to researchers to practitioners, the future of decision making will rely on the ability of these expert multi-disciplinary communities to leverage partnerships and open EO data, to provide innovative knowledge for transformative policies.

We look forward to 2021 when the GHSL will increase its thematic accuracy with the integration of Copernicus Sentinel-2 data from 2018 onwards and continue seeing GHSL users providing scalable and policy-relevant examples for the benefit of our planet.

Prof. Dr. Gilberto Camarra
Director
Group on Earth Observations Secretariat

A handwritten signature in blue ink, appearing to read 'G. Camarra', written in a cursive style.

Acknowledgements

The editors Thomas Kemper, Michele Melchiorri, Daniele Ehrlich and Sergio Freire wish to express their gratitude to Christina Corbane, Martino Pesaresi and Marcello Schiavina who contributed to shaping the GHSL Outlook.

The **GHSL team**, led by Thomas Kemper (JRC) comprises in 2020 Donato Airaghi (Engineering), Damiano Binda (JRC), Christina Corbane (JRC), Daniele Ehrlich (JRC), Sergio Freire (JRC), Luca Maffeni (UniSystems), Michele Melchiorri (Engineering), Martino Pesaresi (JRC), Panagiotis Politis (ARHS Developments), Filip Sabo (ARHS Developments), Marcello Schiavina (JRC), Pierpaolo Tommasi (Fincons). Fabio Bortolamei (Fincons) designed the Atlas Cover.

The Atlas of the Human Planet 2020 core chapter 3 collects more than 30 contributions sourced among the wide community of GHSL data users. The following 100+ experts co-authored the showcases (in alphabetical order):

Alasdair Rae *University of Sheffield*, Alessandro Annunziato *European Commission Joint Research Centre*, Alex de Sherbinin *Center for International Earth Science Information Network*, Alexandra Hays *Center for International Earth Science Information Network*, Alfredo Alessandrini *European Commission Joint Research Centre*, Alfredo Branco *Arcadia SIT*, Alice Siragusa *European Commission Joint Research Centre*, Ana Barbosa *TAF EU Technical Assistance Facility*, Ana I. Moreno-Monroy *Organisation for Economic Co-operation and Development*, Ana Luisa Barbosa *RANDBEE*, Ana Maria Valdes *Délégation de l'Union Européenne au Burkina Faso*, Andrea Cattaneo *Food and Agriculture Organization of the United Nations*, Andrea Leone *Directorate-General for International Cooperation and Development*, Andrea Mandrici *Arcadia SIT*, Andy Nelson *University of Twente*, Annett Wania *European Commission Joint Research Centre*, Antigoni Maistralli *European Commission Joint Research Centre*, Arnulf Jäger-Waldau *European Commission Joint Research Centre*, Beatriz Martín *UNIGE*, Brigitte Koffi *European Commission Joint Research Centre*, Calum Baugh *European Centre for Medium-Range Weather Forecasts*, Carlo Lavallo *European Commission Joint Research Centre*, Carlos Castillo *Universitat Pompeu Fabra*, Carolina Perpiña Castillo *European Commission Joint Research Centre*, Charlotte Hoole *University of Birmingham*, Chiara Proietti *European Commission Joint Research Centre*, Chris Jacobs-Crisioni *European Commission Joint Research Centre*, Christina Corbane *European Commission Joint Research Centre*, Claudia Baranzelli *European Commission Joint Research Centre*, Daniel J. Weiss *University of Oxford*, Daniela Ghio *European Commission Joint Research Centre*, Daniele de Rigo *Arcadia SIT*, Daniele Ehrlich *European Commission Joint Research Centre*, David Newhouse *The World Bank*, Davide Ferrari *Engineering Ingegneria Informatica S.p.A.* *Commission Joint Research Centre*, Deborah Balk *City University of New York*, Diego Guizzardi *European Commission Joint Research Centre*, Domenico Nappo *Unisystems SA*, Duarte Oom *European Commission Joint Research Centre*, Eduardo Zambrano *International Organization for Migration*, Efrain Larrea *MCRIT*, Eleanor Stokes *Earth from Space Institute USRA*, Ellen Hamilton *The World Bank*, Fabrizio Natale *European Commission Joint Research Centre*, Federica Marando *European Commission Joint Research Centre*, Felipe Batista e Silva *European Commission Joint Research Centre*, Filip Sabo *ARHS Developments*, Francesco Dottori *European Commission Joint Research Centre*, Francisco Domingues *UAB*, Giacomo Delli *Arcadia SIT*, Giorgio Libertà *European Commission Joint Research Centre*, Gloria Passarello *UNIGE*, Gordon McGranahan *Center for International Earth Science Information Network*, Grazia Zulian *European Commission Joint Research Centre*, Grégoire Dubois *European Commission Joint Research Centre*, Gretchen Bueermann *International Organization for Migration*, Gustavo Naumann *European Commission Joint Research Centre*, Hans Pfeiffer *Arcadia SIT*, Hasim Engin *Center for International Earth Science Information Network*, Hogeun Park *The World Bank*, Hristo Tanev *European Commission Joint Research Centre*, Ine Vandecasteele *European Commission Joint Research Centre*, Kytt MacManus *Center for International Earth Science Information Network*, Inès Joubert-Boitat *Unisystems SA*, Ioannis Kougias *European Commission Joint Research Centre*, Jacob van Etten *Bioversity International*, Jacques Michelet *UNIGE*, Jawoo Koo *International Food Policy Research Institute*, Jean-Philippe Aurambout *European Commission Joint Research Centre*, Jesus San-Miguel-Ayanz *European Commission Joint Research Centre*, Joachim Maes *European Commission Joint Research Centre*, Joao Porto de Albuquerque *University of Warwick*, Johan Lilliestam *Institute for Advanced Sustainability Studies*, Jorge López *UAB*, Juan Arevalo *TAF EU Technical Assistance Facility*, Julian Wilson *European Commission Joint Research Centre*, Juliane Klatt *International Organization for Migration*, Jürgen V. Vogt *European Commission Joint Research Centre*, Karen Seto *Yale University*, Karmen Poljanšek *European Commission Joint Research Centre*, Katalin Bódis *University of Pannonia*, Katerina Jupova *GISAT*, Konstantin Rosina *European Commission Joint Research Centre*, Lewis Dijkstra *European Commission Directorate-General for Regional and Urban Policy*, Lia Brum *World Association of the Major Metropolises*, Luca Vernaccini *Fincons S.p.A.*, Magda Moner-Girona *European Commission Joint Research Centre*, Marcello Schiavina *European Commission Joint Research Centre*, Marco Martino *TAF EU Technical Assistance Facility*, Maria José Ramos *UAB*, Marzia Santini *European Commission Joint Research Centre*, Michael Sutcliffe *City Insight (Pty) Ltd*, Michele Melchiorri *Engineering Ingegneria Informatica S.p.A.*, Milan Kalas *Freelance consultant*, Monica Crippa *European Commission Joint Research Centre*, Montserrat Marin Ferrer *European Commission Joint Research Centre*, Narcisse Sawadogo *TAF EU Technical Assistance Facility Burkina Faso*, Nathaniel Young *European Bank for Reconstruction and Development*, Nigel Taylor *European Commission Joint Research Centre*, Oriol Biosca *MCRIT*, Pamela Probst *European Commission Joint Research Centre*, Paolo Veneri *Organisation for Economic Co-operation and Development*, Paulo Barbosa *European Commission Joint Research Centre*, Peter Salamon *European Commission Joint Research Centre*, Peter Spruyt *European Commission Joint Research Centre*, Peter Vogt *European Commission Joint Research Centre*, PIERALBERTO MAIANTI *Arcadia SIT*, Robert Chen *Center for International Earth Science Information Network*, Roberto Boca *Arcadia SIT*, Roger Milego *UAB*, Rosana Grecchi *Arcadia SIT*, Rya Inman *Center for International Earth Science Information Network*, Ryan Engstrom *George Washington University*, Silvia Migali *European Commission Joint Research Centre*, Sándor Szabó *European Institute of Innovation & Technology*, Sergio Freire *European Commission Joint Research Centre*, Stefan Pfenninger *ETH Zurich*, Stefano Luoni *Unisystems SA*, Stefano Paris *European Commission Joint Research Centre*, Sue Bannister *City Insight (Pty) Ltd*, Theresa S. McMenomy *Food and Agriculture Organization of the United Nations*, Thomas Petroliaqkis *European Commission Joint Research Centre*, Tiberiu Eugen Antofie *European Commission Joint Research Centre*, Tim Tröndle *Institute for Advanced Sustainability Studies*, Tomás Artes Vivancos *European Commission Joint Research Centre*, Tracy Durrant *Engineering Ingegneria Informatica S.p.A.*, Valerio Lorini *European Commission Joint Research Centre*, Vanni Zavarella *European Commission Joint Research Centre*, Vidhya Soundararajan *Institute of Management*, Zintis Hermansons *ESPON EGTG*.

Executive Summary

The Atlas of the Human Planet 2020 collects contributions from more than 100 users of Global Human Settlement Layer data sets among decision makers, researchers and practitioners. The showcases are grouped in four thematic areas with a close link to four policy domains disaster risk management (the Sendai Framework for Disaster Risk Reduction), urbanisation (SDG 11 and New Urban Agenda), Development (the 2030 Agenda for Sustainable Development), environment and sustainability (European Green Deal and UNFCCC Paris Agreement). All applications show action oriented, transformative and scalable solutions to make progress in the aforementioned policy frameworks. This year's Atlas also highlights challenges and strategic directions related to human settlements mapping as well as an outlook of the upcoming release of the GHSL (Global Human Settlement Layer) increasingly relying on Copernicus Sentinel data.

Policy Context

Spatial data from the Global Human Settlement Layer has been the knowledge base to develop the Degree of Urbanisation (DegUrba) a method that delineates cities, urban and rural areas for international comparisons. This methodology was endorsed by the UN Statistical Commission in March 2020. DegUrba is essential for monitoring progress in achieving the goals of the 2030 Agenda for Sustainable Development¹ by providing a tool for harmonised data collection disaggregated in urban and rural areas.

This Atlas also shows the progress made in exploiting Copernicus Sentinel satellite data to map human settlements, in particular by developing original methods for information extraction.

The Atlas of the Human Planet 2020 is a deliverable to the GEO (Group on Earth Observations) Human Planet Initiative². The initiative maximises the use of (big) open data and artificial intelligence (AI) and combines Earth Observation (EO) data with socio-economic and other data. By developing a new generation of measurements and information products, the initiative provides new scientific evidence and a comprehensive understanding of the human presence on the planet that can support policy processes with agreed, actionable and goal-driven metrics.

Key Conclusions

This Atlas collects more than 30 different applications of GHSL data and tools for addressing societal challenges and priorities. GHSL datasets and models are used by a wide variety of stakeholders, across a number of policy areas. Applications in disaster risk management benefit from reliability and wide spatiotemporal coverage of GHSL data. Showcases on urbanisation leveraged on local yet globally consistent data with high level of spatial detail and long temporal coverage. Applications in the framework of development exploited GHSL data to generate scientific models to plan and scale policies at regional and global scales. Furthermore, several showcases highlighted actionable and scalable solutions for a transition towards greener and more inclusive economies. Next to applications derived from currently available GHSL data, the Atlas suggests possible directions for future research and innovation, ensuring the next generation of GHSL data continues to assist science for policy applications in the 2030 policy horizon and beyond.

Main Findings

In disaster risk management, the showcases highlight that GHSL data support all the different phases of the disaster risk management cycle. In the field of urbanisation, GHSL data unravel the relationship between urbanisation and development looking at the whole spectrum of settlement typologies by taking into account also functional linkages between settlements. In the thematic area of development, it has been recorded how GHSL data clearly fulfil the mission of filling data gaps and provide scalable solutions for Sustainable Development Goals targets estimation and monitoring. On aspects related to environment, sustainability and the opportunities posed by the European Green Deal it emerges how much knowledge GHSL data can help co-create when the essential societal variables of population and built-up areas are combined with other socio-economic, ecological or environmental data to address sustainable development.

Related and Future JRC work

At the core of the GHSL project is the understanding of the societal and environmental processes of planet Earth. The project supports several Knowledge Centres in the Commission (Disaster Risk, Territorial Policies, Migration and Demography). The GHSL project is one of the key test cases of the Joint Research Centre Earth

¹ <https://sustainabledevelopment.un.org/post2015/transformingourworld>

² <https://www.earthobservations.org/activity.php?id=119>

Observation Data and Processing Platform (JEODPP). The processing power and storage of JEODPP are essential for the success of GHSL, which relies on artificial intelligence approaches applied to large fine scale data sets.

In the process of uptake of the Degree of Urbanisation as methodology for delineation of cities and urban and rural areas for international and regional statistical comparison purposes the JRC will increasingly work as technical partner of DG REGIO, EUROSTAT and other five International Organisations (OECD, World Bank, FAO, ILO, and UN-HABITAT) to improve capacities of National Statistical Offices and other institutional stakeholders.

Following the successful 'fitness for purpose' test of the GHSL products, the JRC is working with the Directorate-General for Regional and Urban Policy (DG REGIO) and Directorate-General for Defence Industry and Space (DG DEFIS), on an integration of the Global Human Settlement Layer products in the Emergency Management Service of the Copernicus programme.

Quick guide

The Atlas of the Human Planet 2020 is the fifth edition of the GHSL Atlas series and it relies on the extended network of GHSL data users to showcase high-impact applications in four thematic areas at the core of global development agendas. This edition of the Atlas hosts more than 30 contributions sourced from a network of more than 100 experts across various disciplines and regions of the world. The knowledge contained in this report supports policy areas in regional policy, external actions, development and cooperation and are a key contribution to the baseline information for the 2030 Development Agenda.



1.0

1 Introduction

The world's population reached 7.7 billion at the end of 2019 (World Population Prospects 2019³), and will likely increase to 8.5 billion by 2030, when the 2030 Agenda for Sustainable Development comes to an end. The countries of sub-Saharan Africa are likely to account for more than half of this growth. Unfortunately, we have little understanding of the exact location and the conditions under which many people live, in particular the most vulnerable. Such information is vital to design policies to promote the transition to greener economies for the years to come, but also to improve disaster risk management and crisis response now. New open, inclusive and consistent data – including those used in this report – can be utilised to assess humanity's impact on the planet, access to resources, and exposure to risk. These new data allow generating actionable information to support decision making by governments, organizations and individuals. The development of new methods and the production of accurate geospatial data on population and settlements is the first step for an effective monitoring of the 2030 Development Agenda and its thematic agreements (the Sendai Framework for Disaster Risk Reduction, the Sustainable Development Goals, the Paris Climate Agreement and the New Urban Agenda).

The Global Human Settlement Layer project of the European Commission's Joint Research Centre addresses these needs with spatially detailed information on population and settlements. The GHSL framework relies on three pillars that reflect recent developments in the scientific-technological landscape:

1. A remarkable increase of free and open data including Earth Observation (e.g. Landsat, Copernicus Sentinel satellites) and volunteered geographic information (e.g. Open Street Map) at global scale;
2. A boost in data technology including storage (e.g. online cloud storage), processing (e.g. high-performance computing) and methodological development (e.g. artificial intelligence and machine learning);
3. The promotion of open collaboration, coordinated and sustained data sharing and infrastructure for better research, policy making, decisions and action by initiatives such as the Group on Earth Observations (GEO).

1.1 Big Earth Data Intelligence: from Earth Observation data to AI-driven decision making

Big data has been seen as a 'strategic highland' in the new data-intensive era (Guo 2017). In particular, the development of Earth observation technology is generating an enormous amount of Big Earth Data (BED) describing our planet. The world of Earth observation is dramatically changing driven by rapid advances in sensor and digital technologies. There is an increasing need to mine the large amount of Earth observation data delivered by the new generation of satellites including the Copernicus Earth Observation Programme that is providing open and free satellite imagery to monitor the state of our planet and its changes. Artificial Intelligence (AI) is enabling scalable exploration of big data and bringing new insights and predictive capabilities.

BED and AI are merging into a synergistic relationship, where BED and AI feed each other. Learning from available BED, AI can generate that intelligence promised by the recent digital transformation of the Earth Observation sector. By processing data faster and on a larger scale, AI pushes the boundaries of big data analytics. AI can accelerate the production of global information layers, drive the development of autonomous decision-making and improve policy-making by providing critical insights as long as it meets some key recommendations (Craglia et al. 2018):

- The outputs of AI should correspond to actionable evidence that can be easily understood by decision-makers, investors, consumers and citizens alike to maximize participation and accountability;
- It is needed to develop human-interpretable solutions by creating a bridge between EO (Earth Observation) and AI communities;
- AI applications supporting policy making have to be transparent, comprehensible, monitorable and accountable;
- AI should be backed up by frameworks for auditing and evaluating with agreed international standards;
- We should challenge the shortcomings of AI and work towards strong evaluation strategies, as well as transparent and reliable systems.

³ UN DESA World Population Prospects 2019: https://population.un.org/wpp/Publications/Files/WPP2019_Highlights.pdf

The GHSL framework deploys advanced AI machine learning to satellite imagery for accurate and rapid mapping of built-up areas at global scale. In doing so GHSL adheres to the principles outlined in Craglia et al. (2018) and to the European Commission approach to human-centric AI.

1.2 The GEO Human Planet Initiative

The third pillar of the GHSL framework, next to the growing availability of open and free EO data and the Big Earth Data and Artificial Intelligence advances, is the interaction and collaboration with other scientists and decision makers through the network of the Group on Earth Observations and the Human Planet Initiative. The initiative brings together various needs of decision makers with scientists fostering collective knowledge building and co-design of actionable solutions.

The Group on Earth Observations (GEO) is a voluntary partnership of governments and organisations that envisions ‘a future wherein decisions and actions for the benefit of humankind are informed by coordinated, comprehensive and sustained Earth observations and information’. The Human Planet Initiative (HPI) is committed to developing a new generation of global measurements of human presence on planet Earth. The HPI contributes to the Group on Earth Observation’s (GEO)⁴ work plan and shares GEOs core aim of improving the availability, access and use of Earth observations for a more sustainable planet.

The Human Planet uses the advances of Earth Observation technologies and geospatial data analytics for improving our understanding of settlement spatial patterns and processes and their effect on urbanisation. The HPI develops consistent geospatial data – including built-up and population density – that are used to understand human presence on planet Earth (Atlas of the Human Planet 2016 Pesaresi, Melchiorri, et al. 2016) as well as urbanisation (Atlas of the Human Planet 2018 and 2019 (European Commission , Joint Research Centre 2018; 2019), disaster risk (Atlas of the Human Planet 2017 (Pesaresi et al. 2017)) and the societal impact, and use of resources (this Atlas).

The HPI work is coordinated by two leading institutions: the Center for International Earth Science Information Network (CIESIN) and the Joint Research Centre. The Human Planet Initiative groups more than 200 scientists and policy makers from 85 different organisations including academies, international institutions, governmental bodies and the private sector. The HPI work is conducted based on specific areas including the development of global built-up layers, population density grids, harmonising global population datasets.

HPI information products are used to report across the post-2015 international frameworks: the 2030 Agenda for Sustainable Development (SDGs), the UN Framework Convention on Climate Change (UNFCCC), the Sendai Framework for Disaster Risk Reduction 2015-2030, and the New Urban Agenda. For example, HPI supplies the three variables used to compute indicator SDG 11.3.1 – the land use efficiency indicator. The HPI has also supported a number of policy institutions and researchers in their quest for data. For example, the Degree of Urbanisation Method – requested and co-developed with a number of policy institutions – was endorsed at the 51st session of the UN Statistical Commission as methodology to delineate cities, urban and rural areas for international comparison.

1.3 GHSL evolution from data to tools

The GHSL global data set – first published at the Habitat III Conference in 2016 – was the most complete, consistent, detailed, free and open dataset on human settlements that provided harmonised information on population and settlement development from 1975-2015.

The GHSL framework followed an evolutionary design across various domains: EO data segment, thematic products output, tools suite, and capacity building. The first release in 2016 was trained with a mix of low spatial resolution data sets including the MODIS Urban Extent, MERIS GlobCover and LandScan (Pesaresi, Ehrlich, et al. 2016) (Figure 2). With the advent of the Copernicus Sentinel satellites (starting with the Sentinel-1 radar system), new consistent free and open imagery with better spatial resolution became available. Consequently, the global built-up map based on Sentinel-1 was trained with the Landsat-based built-up map (Corbane et al. 2017). The Sentinel-1 data revealed much better smaller settlements especially in rural contexts. Therefore, the Landsat data were reprocessed leading to the second GHSL release based on Landsat data in 2019 (Corbane, Pesaresi, et al. 2019). The latest step in this evolution is the current integration of Sentinel-2 data (Corbane, Syrris, et al. 2020). Over the past four years, the process of information extraction from EO innovated in both the sources of EO data, and in the methods employed.

⁴ Group on Earth Observations: http://earthobservations.org/documents/gwp20_22/gwp2020_summary_document.pdf

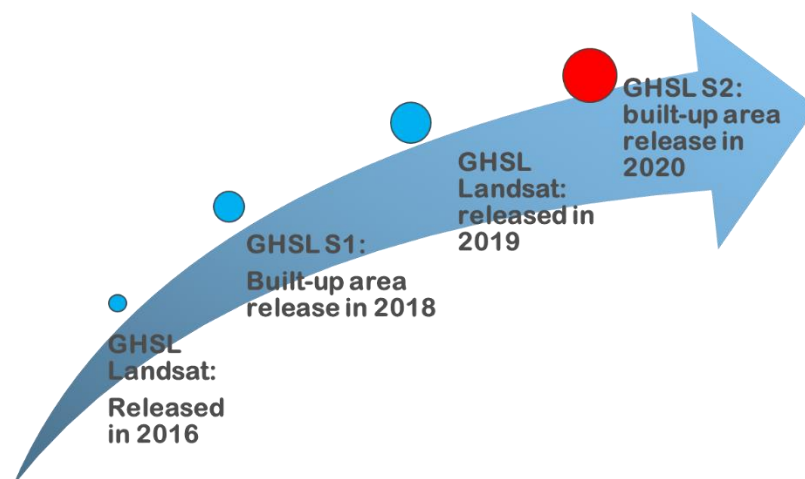


Figure 2. The evolutionary concept of GHSL EO data segment

The GHSL framework integrates Earth Observation derived data (level 0) i.e. imagery with other data sources (i.e. training data) to develop higher-level information. The first step in this thematic evolution is the generation of built-up area grids, from which population grids are derived by distributing residential population into the built-up areas mapped from the EO data (level 1). The population grids are subsequently used to delineate and classify the cities, urban and rural areas in the settlement model (level 2). The settlement model in turn allows delineating all cities in the world for the Urban Centre Database and the calculation of Functional Urban Areas (level 3). More information on the thematic layers will be provided in Chapter 2 (p. 13). Therefore, over time the thematic products produced in the framework of GHSL also expanded from three baseline products in 2016 to more than nine products in 2020. The three core products based on Landsat imagery (GHS-BUILT, GHS-POP, and GHS-SMOD) still represent primary information, yet, more sophisticated products derived from modelling and data integration (i.e. GHS-UCDB, GHS-FUA) have been developed. Products based on Copernicus data are also growing expanding, with the 2012 and 2015 versions of the European Settlement Map, the GHS-Sentinel 1 built-up layer, and the recent GHS-Composite S2, the latter at the base of experiments to map human settlements at global scale with Sentinel 2 optical data.

The GHSL framework includes also a growing number of tools that allow production of population grids, settlements classification etc. in compliance to GHSL models and workflows. The publication of methods in the scientific literature is necessary for openness and transparency, but often not sufficient for multilateral democratization of the information production and collective knowledge building. The suite of GHSL Tools allows users to extract features from EO data, apply the Degree of Urbanisation method and conduct GIS analytics also in the framework of the SDGs. More details on the tools will be provided in the following chapter.

1.4 Open geoinformation for research, policy, and action

The Atlas of the Human Planet 2020 has two objectives. After five years since the first public release of global data, it provides a multidisciplinary review of GHSL data applications to policy areas related to disaster and crisis management, urbanisation, development, environment and sustainability. At the same time, it provides an outlook to the next phase of data provision that will include an extension of the time series, better spatial resolution and an operational production in the context of the Copernicus Programme. This year's Atlas leverages on the wide community of GHSL data users across policymaking, research, and non-governmental organisations and on the 2019 GHSL Data Package release.

After this introduction that highlighted the importance of the three features (i) free and open EO data, (ii) big earth data and artificial intelligence and (iii) a collaborative network for the GHSL framework, the second chapter explains the fundamentals of GHSL providing simple and essential information about its products. In this edition the GHSL Urban Centre Database, the GHSL Functional Urban Areas and the GHSL Tools are newly featured.

The core chapter of the 2020 edition of the Atlas is Chapter 3 (p. 24) that contains 37 showcases of GHSL data applications in support to policymaking and scientific research. The chapter is organised into four thematic domains with strong linkages to global and EU policy agendas.

Chapter 4 (p. 108) introduces a number of emerging challenges brought by the evolution of GHSL products, and by the new data acquisition, processing and analysis frameworks. The section also highlights thematic areas of particular concern to grant accurate and up-to date data production.

The last section of the Atlas 4.8 (p. 119) introduces the way forward for GHSL, identifying directions to strengthen partnerships, ties with the industry and a mature relationship with policy support.



Figure 3 © Adobe Stock

The background is a dark, teal-toned abstract composition. It features a dense field of binary digits (0s and 1s) that appear to be floating or falling from the top right towards the bottom left. Interspersed among the digits are numerous bright, glowing white and light blue particles, some of which are larger and more intense than others, creating a sense of depth and movement. The overall effect is reminiscent of a digital rain or a data stream visualization.

2.0

2 Fundamentals

The GHSL is framed around three general principles (Pesaresi 2018):

- i) operating in an open and free data and methods access policy (open input, open method, open output);
- ii) enabling reproducible, scientifically defensible, fine-scale, synoptic, complete, planetary-size, and cost-effective information production;;
- iii) facilitating information sharing and multilateral democratization of the information production, and collective knowledge building.

The first and second principle call for public, scientific control of the data and the information production methods generating the GHSL information and derived findings. The second and third principle call for automatic information production methods being able to process systematically the large mass of baseline data lowering down the cost of the information production. This moves the human efforts from the information extraction to the discussion of the observed facts and ultimately to derive decisions. In the frame of the above, there are three main principles applied in the design of the GHSL automatic information production system. They are shortly recalled here: i) test and apply real-word (big) data scenarios, ii) produce evidence-based output analytics, and iii) facilitate repeatability of the results. The principles are comprehensively presented as example to policy support in the SDG context in (Melchiorri et al. 2019).

The Global Human Settlement Layer (GHSL) project combines state-of-the-art AI machine learning with satellite data from Copernicus Sentinel and Landsat and census data to generate science-based information. The GHSL deploys a human centric approach to artificial intelligence implementing the EU efforts to promote technological solutions that are transparent and accountable to people.

GHSL products are highly integrated and dependent. The baseline information layer is the GHS-BUILT; it is obtained by processing large amount of satellite imagery and other reference datasets to detect built-up areas. The information on the spatial distribution of global built-up areas is then combined with population information (suitable spatial information on population counts) to generate a population map (GHS-POP). Information on the distribution of built-up areas and resident population is then combined according to the settlement model to classify seven different settlement typologies (GHS-SMOD) based on population density and size and grid cells contiguity. The transitions from satellite imagery to settlements classification is simplified in Figure 6.

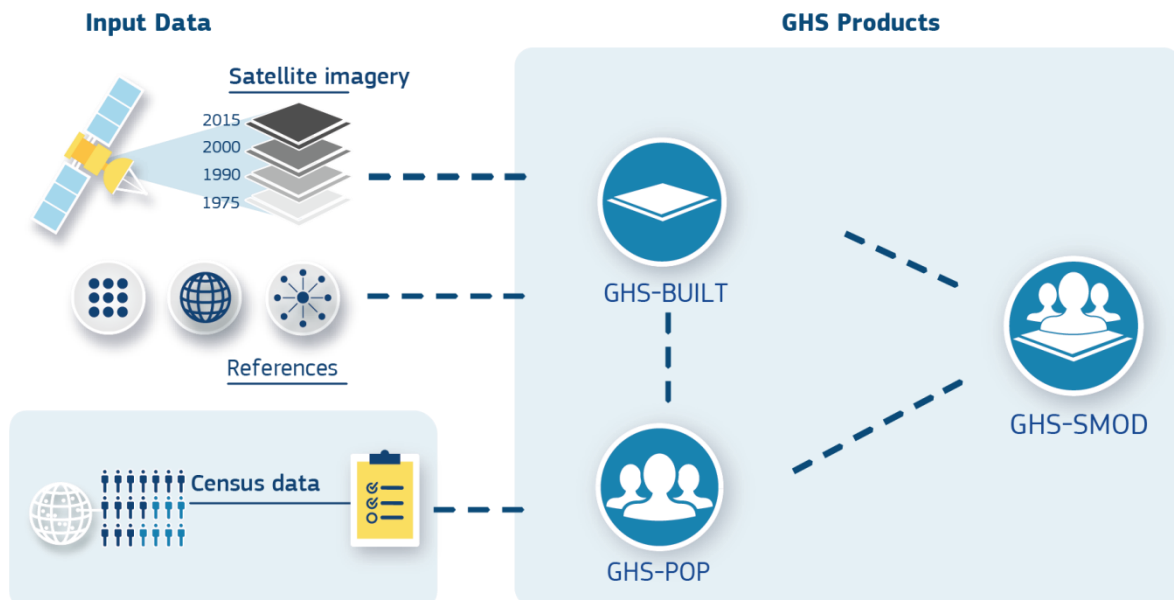


Figure 5 Schema of dependencies between input data and GHS products

The following sections help the reader to understand fundamental concepts of GHSL and its data. The first subparagraph deals with extraction of information from satellite imagery (2.1.1) and built-up definition.

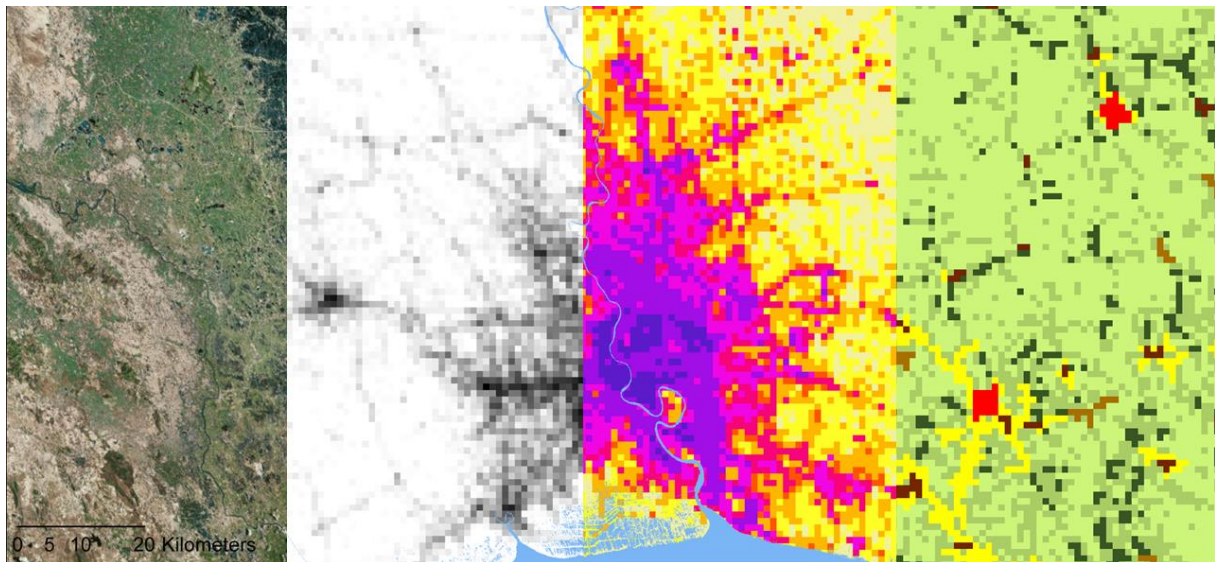


Figure 6 Transition from Landsat imagery to built-up areas extraction (GHS-BUILT), population modelling (GHS-POP), and settlements classification (GHS-SMOD), examples in the area of Bangkok (Thailand) information layers of the epoch 2015.

The second paragraph describes the process to combine built-up grids with census data to produce the population grids (2.1.2). The third paragraph (2.1.3) illustrates the key elements and rules of the GHS-SMOD Grid, derived from the New Degree of Urbanization (Lewis Dijkstra and Hugo Poelman 2014): specifically, the rules for defining *Urban Centres*, *Urban Clusters* and rural settlements are illustrated.

Paragraph 2.1.4 and 2.1.5 explain two analytical datasets derived from core GHSL layers. The former shows the basics of the GHS-UCDB a global multi-dimensional and multi-temporal database covering 10,000 urban centres. The latter shows the basics of the GHS-FUA, a global database on functional urban areas derived from the GHSL epoch 2015.

The sixth paragraph (2.1.6) explains the synergistic use of the suite of GHSL tools to apply the Degree of Urbanisation method. The graphic (Figure 12) explains the steps and the corresponding GHS Tools for: the construction of a regular-spaced population grid from given geospatial population data in the form of points or polygons (first step); the application of the degree of urbanisation methodology to a given population grid and additional optional layers (second step); the classification of small spatial units into cities, towns and semi dense areas, or rural areas (third step).

The last sub-section (2.1.7) explains with simple images, and examples of three GHSL datasets (GHS-BUILT, GHS-POP and GHS-SMOD) for the area of Madrid, Spain. The following sections are non-technical explanation of the scientific workflows deployed for the production of GHSL data, documented in the GHSL Data Package 2019 (Florczyk et al. 2019) and in the GHS Tools user guides.

2.1.1 From Earth's surface to built-up area

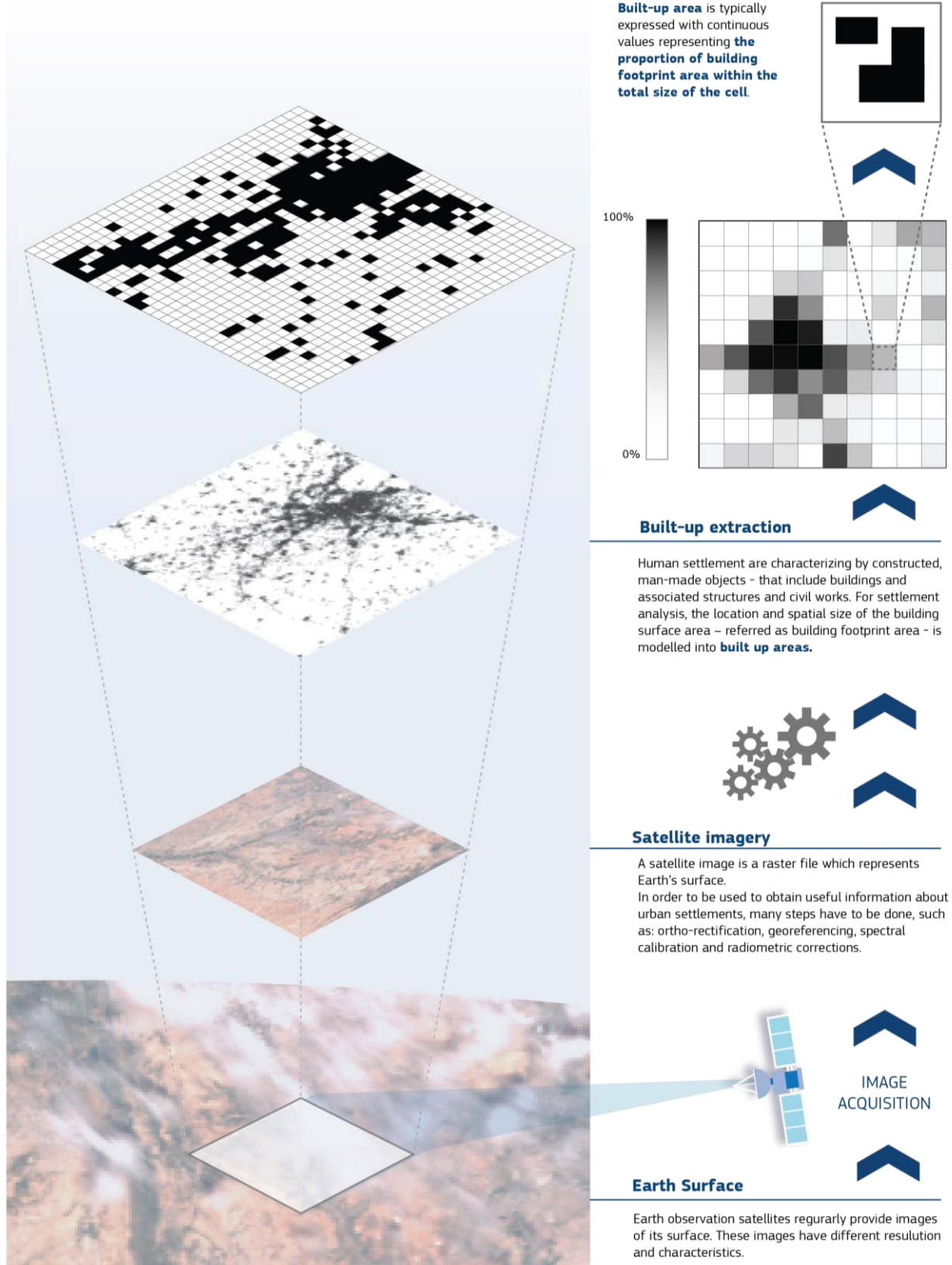


Figure 7 Information extraction process from the satellite images of the earth surface (bottom) to the built-up area extraction (middle) to the aggregated built-up area density (top).

2.1.2 From Built-up area to population grid

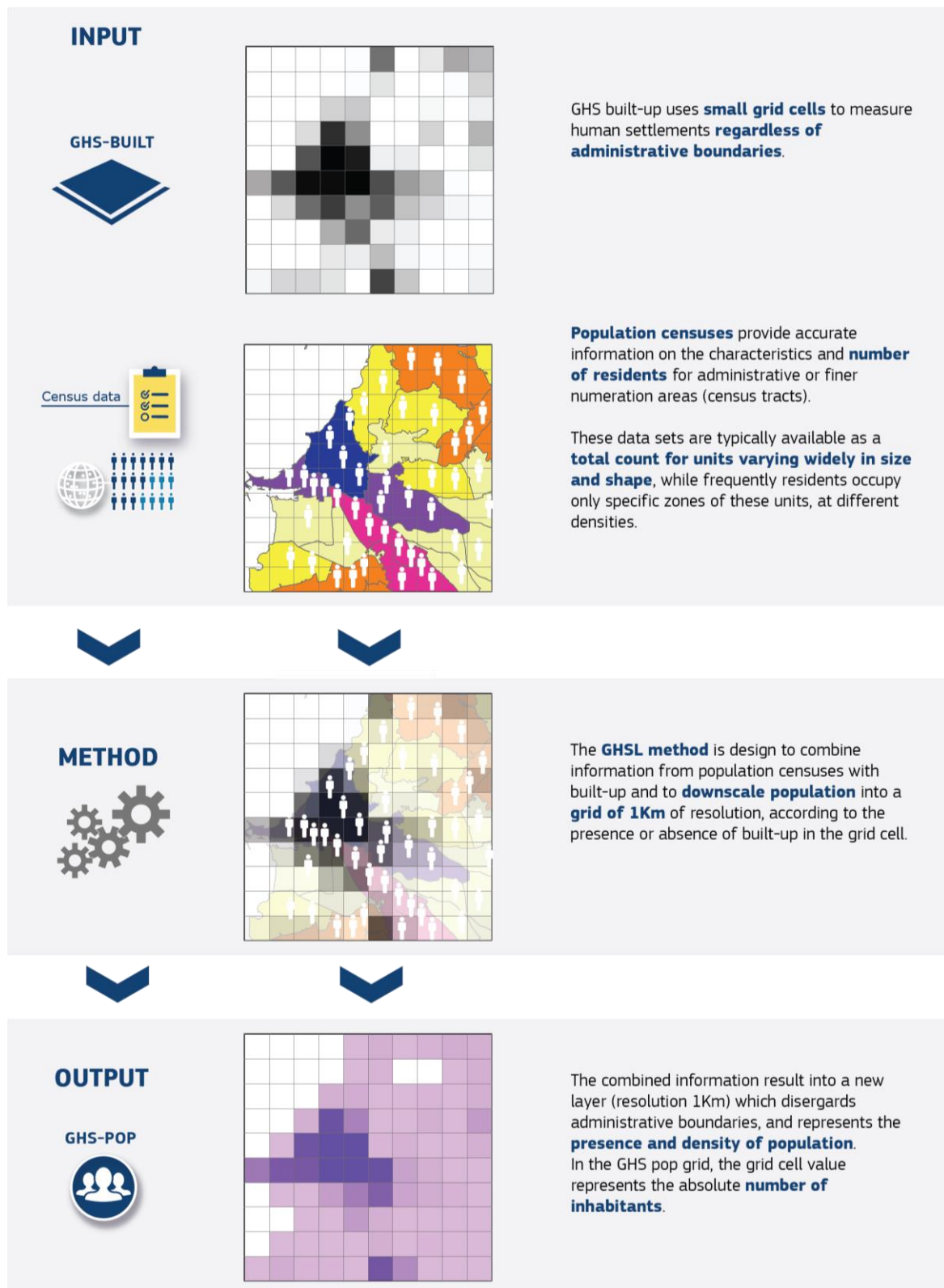


Figure 8 Combination of GHS-BUILT with the census data to produce a regular fine scale grid of population density.

2.1.3 From built-up area and population to settlement grids

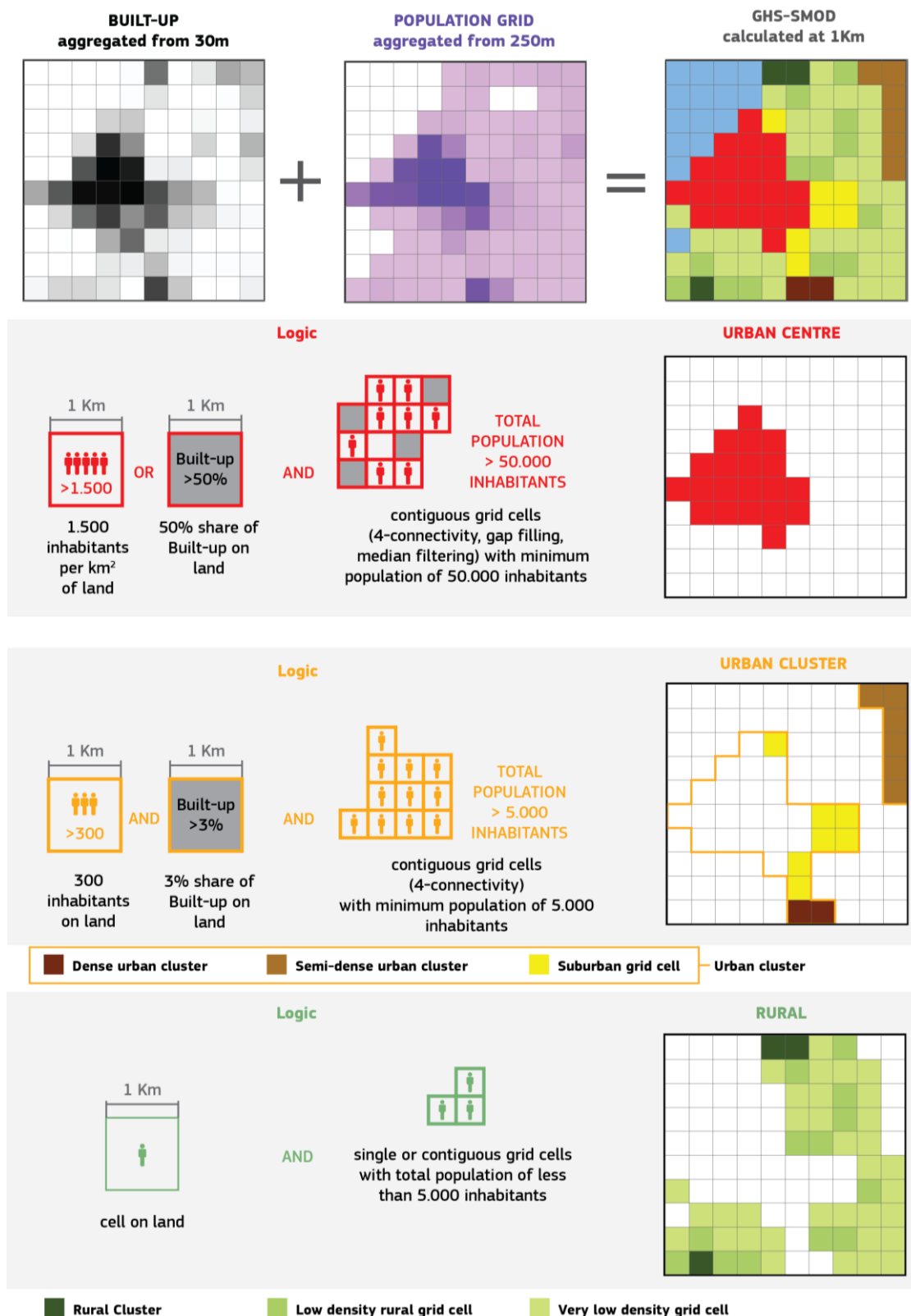


Figure 9 Synthetic explanation of GHS-SMOD logics and definitions. An example from the area of Trapani (Italy)

2.1.4 From Urban Centres spatial delineation to a 4-D city database

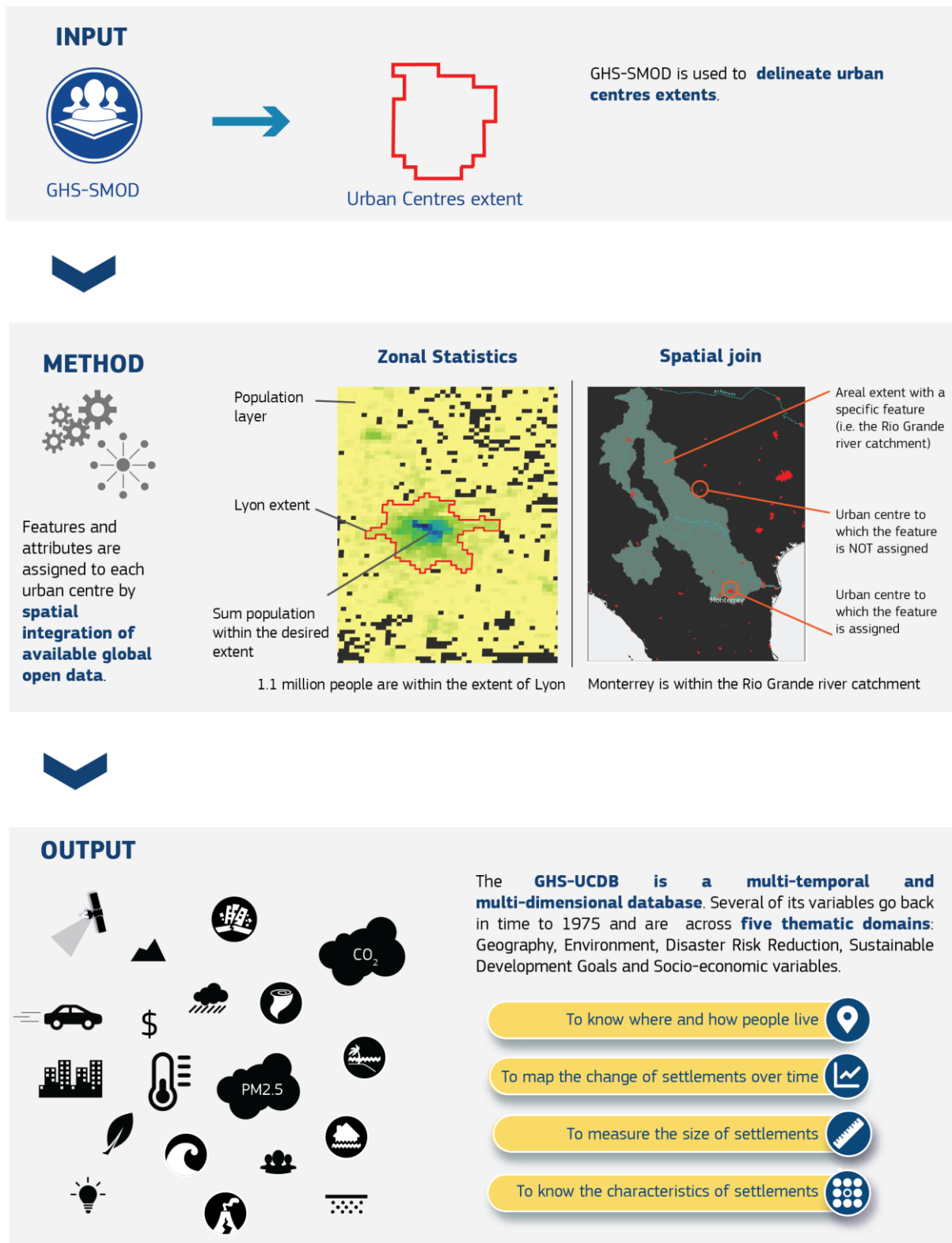


Figure 10 Combination of GHS-SMOD urban centres and other variables to obtain the GHS-UCDB with geospatial data integration processing

2.1.5 From Urban Centres to Functional Urban Areas

INPUT



GHS-UCDB



GHS-POP

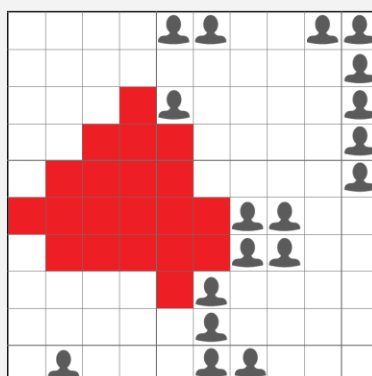
GHS-UCDB is used to **delineate urban centres**. GHS-POP outlines the possible origins for **commuting** to the cores.



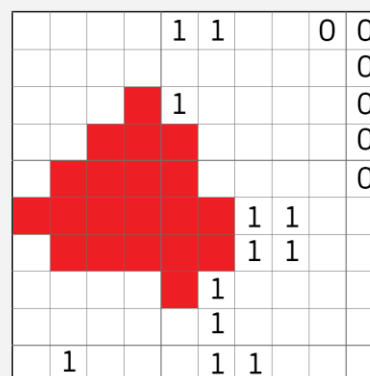
METHOD



By statistical modeling origins and destinations are tested to assign a cell to the commuting zone. the approach combines travel time, GDP per capita and area and population of the urban centre



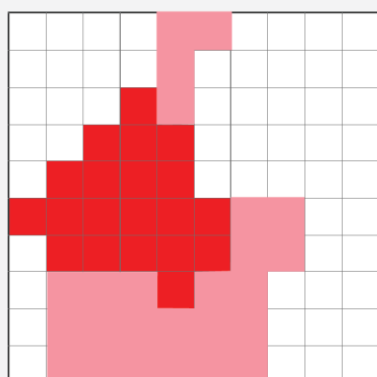
Identify populated places as possible travel origins



Statistical model to test viability of travel



OUTPUT



Delineate Functional Urban Area boundaries

The **GHS-FUA is a geospatial database** delineating commuting areas of urban centres for the entire globe in 2015.

To know how many people commute



To measure the size of economic influence



To analyse metropolitan population dynamics



GHS-FUA ports to the globe the EC-OECD definition of Functional Urban Area.

Figure 11 Delineation of GHS-FUA as commuting area for all urban centres on the planet for the epoch 2015

2.1.6 From population layers to urban and rural classification of territorial units

The Degree of Urbanisation classifies the entire territory of a country along the urban-rural continuum. It combines population size and population density thresholds to capture the full settlement hierarchy. It is applied in a two-step process: First, 1 km² grid cells are classified based on population density, contiguity and population size. Subsequently, local units are classified based on the type of grid cells their population resides in. The operationalisation of this process is enabled by tools developed in the framework of the Global Human Settlement Layer.

When the population grid is not available, it is possible to produce it with GHSL solutions. For the construction of a regular-spaced population grid from given geospatial population data (as points or polygons) the GHS-POP2G Tool can be used (Figure 12).

Then, the first step to apply the Degree of Urbanisation can be implemented applying the methodology to a given population grid (i.e. the one just produced with the POP2G) and additional optional layers (with the GHS-DUG Tool). Finally, in the second step, the derived grid cell classification is used to classify small spatial units into cities, towns and semi dense areas, or rural areas (with the GHS-DU-TUC Tool). Figure 12 explains the key steps and the corresponding input data and output information. As displayed, the suite of GHSL tools works in cascade allowing the classification of administrative units providing geospatial information about population and optionally other information layers. GHSL Tools come with comprehensive user guides (Maffenini, Schiavina, Freire, et al. 2020; Maffenini, Schiavina, Melchiorri, et al. 2020a; 2020b). Additional Tools like the GHS-Pop Warp Tool can be used to pre-process population data available to the user to ease the deployment of the GHS-DUG Tool.

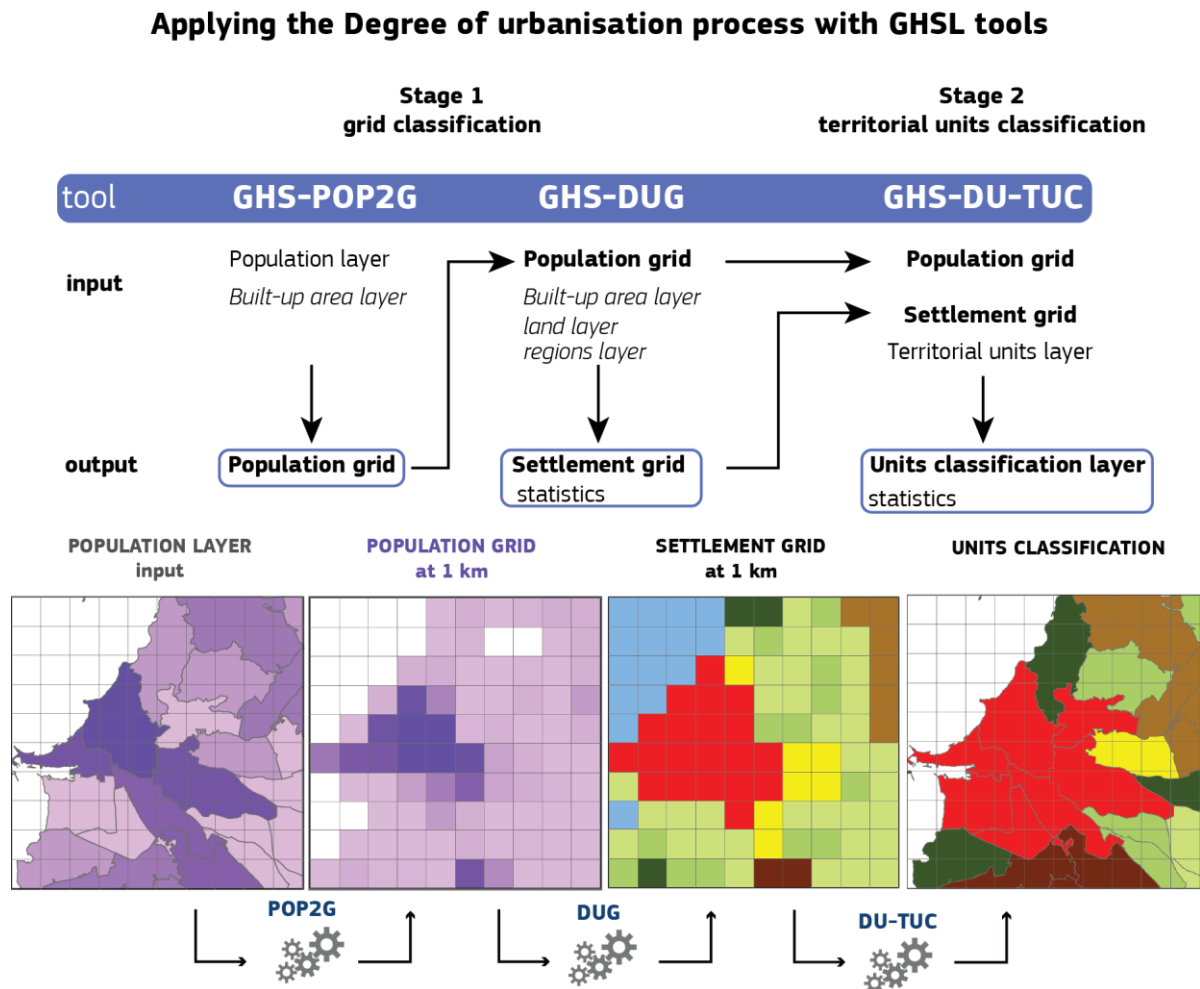
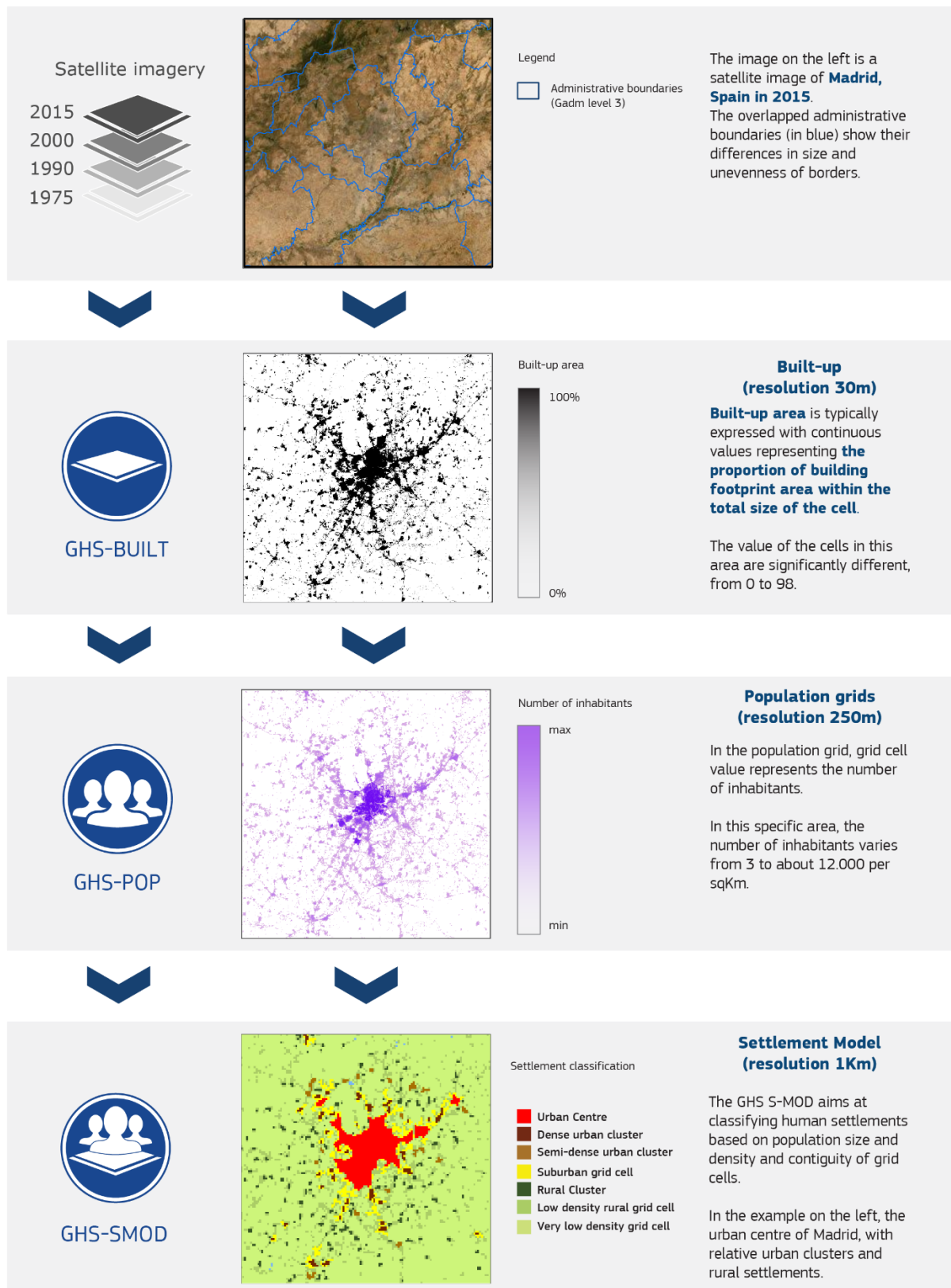


Figure 12 Applying the Degree of Urbanisation process with GHSL Tools

2.1.7 GHSL workflow real case synthetic example



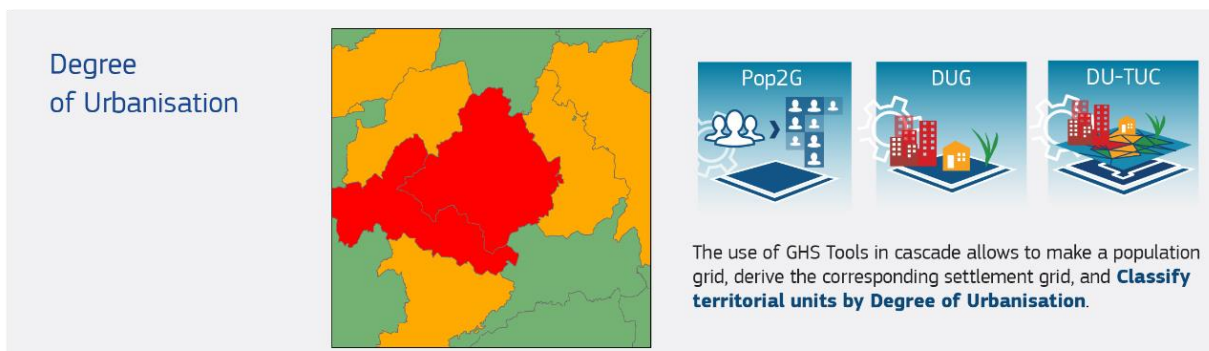
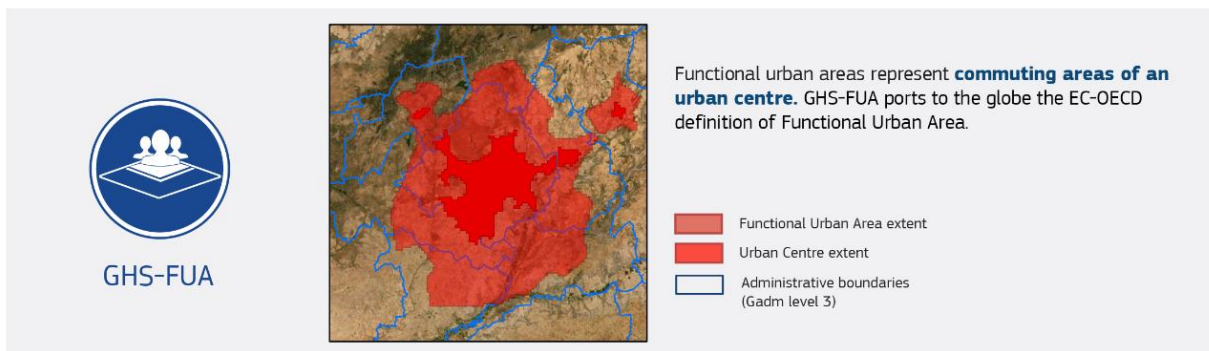


Figure 13 GHSL process from imagery to settlement map in the area of Madrid (geospatial layers of the epoch 2015)



3.0

3 Applications of GHSL data in research, policy and action

The GEO Human Planet and the GHSL project aim to support a novel, evidence-based assessment of the human presence on the planet Earth based on free and open data. The availability of open and free GHSL data has supported the generation of a wide body of scientific and institutional knowledge. This chapter presents a selection of policy relevant research and data analysis carried out with GHSL data.

These applications make use of the full range of data sets of the 2019 data release including the refined GHS-BUILT (based on an improved workflow for built-up area extraction from satellite image), GHS-POP (improved with updated population estimates and refined built-up area input layers), and GHS-SMOD (introducing a more detailed classification of settlements in two levels). In addition, the GHS-UCDB, a global database of urban centres, and GHS-FUA, a global database of functional urban areas and the European Settlement Map (ESM) were used.

Showcases are concise two-page briefs presenting an application of GHSL data to address societal and policy related challenges especially in the framework of international agendas like the Sustainable Development Goals, the Sendai Framework for Disaster Risk Reduction, the Paris Agreement (UNFCCC), and the New Urban Agenda. All are underlying the six priorities of the European Commission Priorities.

This chapter includes 37 applications and organises them in four thematic areas (Figure 16): Disaster Risk & Crisis Management (12 showcases), Urbanisation (9 showcases), Development (9 showcases), and Environment and Sustainability (7 showcases). The following sub-sections introduce the showcases by thematic domain.

Showcases thematic areas

Policy Agendas

Disaster Risk and Crisis Management



Urbanisation



Development



Environment and Sustainability



Figure 16 Showcases by thematic area and main policy linkage



3.1

Disaster Risk Management

3.1 Disaster Risk Management

Disasters unfold from the impact of natural hazards, and from intentional (i.e. conflict) or unintentional (i.e. toxic spills) human activities. Disasters affect millions of people and cause billions of Euros in damage each year. The EU provides needs-based humanitarian assistance to people hit by such disasters with particular attention to the most vulnerable victims. In fact, the EU (Member States and EU institutions collectively) is among the leading donors of humanitarian aid in the world. The EU has developed the Civil Protection Mechanism to deliver aid in preparation for or immediate aftermath of a disaster in Europe and worldwide.

Although many of these disaster events are impossible to predict precisely, it is possible to prepare to reduce their effects. Disaster preparedness efforts include plans made in advance of an emergency that help individuals and communities get ready. Disaster response during or immediately following an emergency focusses on efforts to save lives and to prevent further damage. Disaster recovery aims for a return of the affected community to its pre-disaster state, and possibly to make it less vulnerable to future risk. At a strategic level, disaster mitigation measures try to prevent future emergencies or minimize their negative effects.

The different phases of the disaster cycle all require detailed knowledge about the presence of population, settlements and infrastructure assets. The GHSL data were originally developed to meet these needs. This section will showcase different application examples covering the full disaster cycle, starting with risk analysis and assessment activities. The showcases include the **Risk Data Hub**, a web-based knowledge platform developed to facilitate management of disaster risks between different actors (3.1.1). Addressing epidemic risk has been a priority in disaster risk management since before the COVID-19 global pandemic. The **INFORM epidemic** showcase combines the INFORM Risk index methodology with GHSL data to estimate epidemic exposure by settlements classes (3.1.2). In the current COVID-19 pandemic, GHSL data were incorporated in the SEDAC Global COVID-19 Viewer, as presented in the **Mapping the COVID-19 Pandemic and Potential Risk Factors** showcase (3.1.3).

Hazardous events (natural or man-made) can have different disaster outcomes depending on the time of the day that impact occurs. The **ENACT project** addresses this need in the EU with seamless night-time and daytime population density grids for each month of the year (3.1.4).

While the impact of Earthquakes or volcano eruptions are challenging or impossible to predict that of other hazards can be anticipated. The Copernicus Emergency Management Service addresses this in its early warning and monitoring component. The Drought Observatory assesses the **drought risk for Europe and the globe** (3.1.5). The European Forest Fire Information System (EFFIS) monitors forest fire activity in near-real time and uses the European **Wildfire Risk Assessment** (WRA) to provide harmonized assessments for EU Member States and across the Middle East and North Africa (3.1.6). For **rapid flood risk assessment**, the Global Flood Awareness Systems (GloFAS) produces daily streamflow forecasts for major river networks and uses total population and land cover within the flood extent to assess potential flood impact (3.1.7). Sea level rise is also a threat for coastal settlements. Figures on global exposure are presented in the showcase **New Estimates of Global Population and Land in the Low Elevation Coastal Zone** (3.1.8)

In order to improve this assessment for urban areas, the **FIUME project** integrates information derived from social media, authoritative data (numerical models, sensors and remote sensing) and socio-economic data (3.1.9).

When a disaster occurs, emergency managers need to receive detailed information about the impact and extent of the event. The rapid mapping service of Copernicus provides this information and makes use of the Global Disaster Alert and Coordination System (GDACS) and the GHSL data to **automatically identify the most affected areas of a disaster** in order to target the prompt acquisition of satellite images (3.1.10). As soon as the imagery is available, the damages are delineated and the **affected population** can be assessed (3.1.11).

In the post-crisis recovery phase, population continues to require support from donors, in particular vulnerable groups such as **Internally Displaced Persons (IDPs) and returnees**. The showcase from Iraq illustrates the importance of gathering information disaggregated by urban and rural areas, because the needs are very different (3.1.12).

3.1.1 The Disaster Risk Management Knowledge Centre - Risk Data Hub, web platform to facilitate management of disaster risks

Exposure Analysis Module of the DRMKC Risk Data Hub

Antofie, T., E., Luoni, S., Montserrat, M.F.

The Disaster Risk Management Knowledge Centre (DRMKC) has been working since its launch in September 2015 in the challenging task of developing collective disaster risk related knowledge based on solid partnerships involving scientists, policymakers and operational authorities (i.e. civil protections, and emergency responders). The DRMKC Risk Data Hub has been developed to provide a concrete platform where these different communities could share knowledge and information and profit from the possibility of working together. The need for a multi-hazard platform to link science and policy, past and future, local and global dimensions was identified after reviewing the National Risk Assessments prepared by the Union of Civil Protection Mechanism's (UCPM) participant countries and then submitted to the European Commission. There was an evident gap between the knowledge developed by the scientific community and the one reaching the National Risk Assessments due under the UCPM. The DRMKC Risk Data Hub is a concrete answer to this need. It facilitates the actions that Member States need to take in order to meet risk management related obligations such as Disaster Loss Databases, National Risk Assessment and finally Risk Management Plans. The present version of the DRMKC Risk Data Hub covers two phases of the disaster risk management (DRM) cycle: the pre-event phase of prevention, and the post-event phase of recovery. In the prevention phase, the DRMKC Risk Data Hub focuses on anticipation of impact areas in order to reduce, or avoid, the potential losses. Identification of the impact areas is assessed by means of exposure analysis. Spatial extent of hazards' extreme events' metrics, such as severities, frequencies or intensities are superimposed with exposure layers. In this way, we establish the spatial extent of the hazardous event which becomes accountable for potential impact and the spatial location of exposed assets. Understanding the exposure will contribute to effective preparation, monitoring and response to various hazards and will increase communities' resilience to disasters.

We measure exposure to hazards of infrastructure, built-up space (commercial and residential), land cover, protected areas or human lives. Residential built-up space and residential population are two main groups of assets that are represented currently across various types of analysis within the DRMKC Risk Data Hub. The sources of the two types of exposure layers are ESM (European Settlement Map, 2016)⁵ for the built-up space and Global Human Settlement Layer (GHSL, 2016) for the population. To discriminate the residential topology for the artificial areas both for population and for built-up area, the Corine Land Cover (CLC, EEA 2016) is used. Spatial data analysis is performed across geographical scales (countries or local administrative units) and across multiple hazards. Moreover, in order to assign the exposure analysis to different settlement types, the exposure layers (e.g. ESM, GHSL) are masked by the "degree of urbanisation" layer, selecting in this way three types of human settlements: Rural, Urban Clusters and Urban Centres (Figure 18). The GHSL settlement grid model (that classifies human settlements on the base of the built-up and population size and density) was used to assess the "degree of urbanisation". Mapping the exposure from multiple hazards has been prepared considering either the extent of the hazard or the intensity levels. As examples, the exposure analysis for river flood and coastal floods considers the water levels: < 1m, <2m, <4m, <6m. The analysis is done using flood layers at 100m resolution for the entire European domain. Using GHSL products was an obvious choice as it provides high gridded data resolution.

The result of our analysis is the anticipation of the areas expected to suffer significant impact from hazards. By integrating hazard data along with the exposure layers (Figure 19), we provide a starting point for prioritized local case studies on impacts from multiple hazards, as well as setting the basis for the development of mitigation strategies. However In order to account for the exposure not only as a coincidence of the geographical location of hazard and assets, a greater level of information that includes attributes of the assets is needed. This information is often available only at local scale, part of cadastral plans, critical infrastructure engineering, census, etc., and administrated by different institutions at national level making difficult to be accessed. Also, incorporating the temporal projection of human densities can be a key factor in assessing the impact from future change in climate. These aspects are considered in the analysis implemented on the Risk Data Hub and is anticipating the future, already considered developments of the GHSL products.

⁵ New versions of the ESM (ESM_BUILT_VHR2015_EUROPE_R2019) are available and considered for disaster risk analysis future use on the DRMKC Risk Data Hub

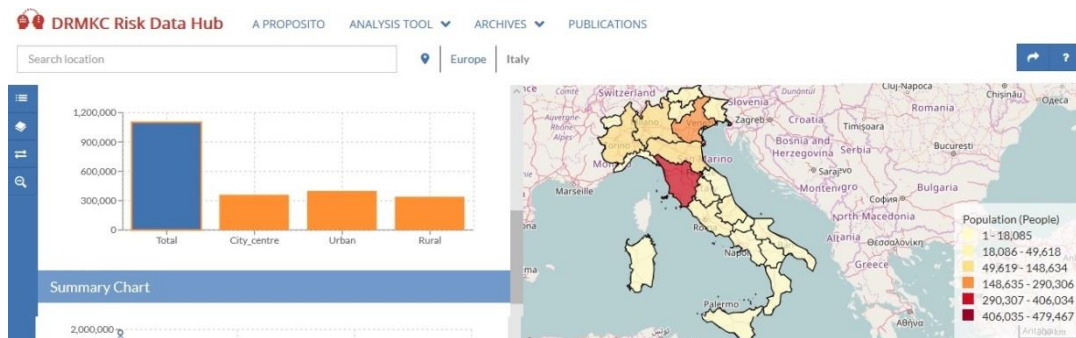


Figure 18 Population exposure analysis considering the degree of urbanisation, GHS-SMOD layer

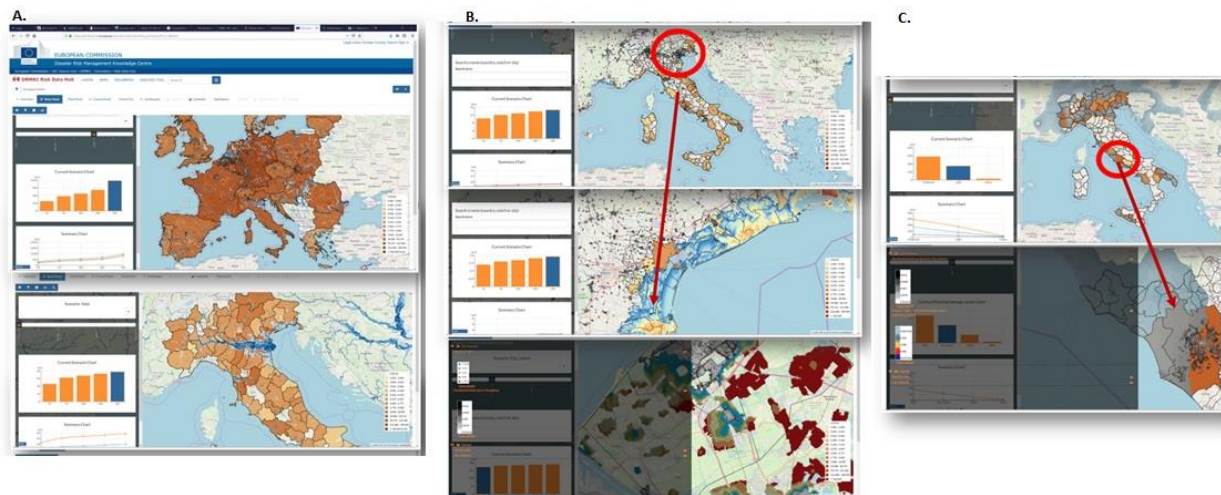


Figure 19 Across-scale population exposure analysis using GHSL layers for A. River flood, B. Coastal Flood, C. Earthquake, hosted on the Risk Data Hub.

References:

GHS-POP: Schiavina, Marcello; Freire, Sergio; MacManus, Kytt (2019): GHS population grid multitemporal (1975, 1990, 2000, 2015) R2019A. European Commission, Joint Research Centre (JRC) DOI: 10.2905/42E8BE89-54FF-464E-BE7B-BF9E64DA5218 PID: <http://data.europa.eu/89h/0c6b9751-a71f-4062-830b-43c9f432370f>

GHS-BUILT: Corbane, Christina; Florczyk, Aneta; Pesaresi, Martino; Politis, Panagiotis; Syrris, Vasileios (2018): GHS built-up grid, derived from Landsat, multitemporal (1975-1990-2000-2014), R2018A. European Commission, Joint Research Centre (JRC) doi: 10.2905/jrc-ghsl-10007 PID: <http://data.europa.eu/89h/jrc-ghsl-10007>

GHS-SMOD: Pesaresi, Martino; Florczyk, Aneta; Schiavina, Marcello; Melchiorri, Michele; Maffeni, Luca (2019): GHS settlement grid, updated and refined REGIO model 2014 in application to GHS-BUILT R2018A and GHS-POP R2019A, multitemporal (1975-1990-2000-2015), R2019A. European Commission, Joint Research Centre (JRC) DOI: 10.2905/42E8BE89-54FF-464E-BE7B-BF9E64DA5218 PID: <http://data.europa.eu/89h/42e8be89-54ff-464e-be7b-bf9e64da5218>

Flood hazard map: Alfieri, L., Salamon, P., Bianchi, A., Neal, J., Bates, P.D., Feyen, L., 2014. Advances in pan-European flood hazard mapping, Hydrol. Process., 28 (18), 4928-4937, doi:10.1002/hyp.9947.

3.1.2 Epidemic Risk Exposure and Urbanisation

Estimating population exposure to epidemics across the rural-urban continuum

Vernaccini, L., Poljanšek, K., Melchiorri, M.

The COVID-19 global pandemic pushes the epidemic risk to be a priority in disaster risk management at the global and national level. Combining the INFORM Risk index methodology (De Groeve, 2014) with GHSL data on population density (GHS-POP) to estimate exposure and Degree of Urbanisation Settlement Grid (GHS-SMOD) to characterise settlements, epidemic exposure can be analysed by epidemic type and settlements classes.

The INFORM Risk Index is a composite indicator developed by the Joint Research Centre of the European Commission (JRC) that identifies countries at risk of humanitarian crisis and disaster. The INFORM Risk Index methodology is very flexible and it can be adapted to specific risks. In the 2018 JRC developed the INFORM Epidemic Risk Index (Poljanšek, 2018) in close collaboration with the World Health Organization (WHO). As from its sixth release in 2019 the INFORM Risk Index includes also an epidemic hazard component. For the first time, the INFORM Risk Index allows to assess epidemics in a multi-hazard risk assessment at the global level within a single framework (Figure 20).

The first step in an epidemic risk assessment is to identify the areas with the possible presence of the pathogens and the population exposed. We benefited from existing models of environmental suitability for the transmission of a virus from environmental sources into human populations to establish regions at risk of spill over infections. We used the GHS Global Population Grids to estimate the numbers of individuals exposed within each country. The GHS population grid fits all the INFORM's requirements: global coverage, open source, transparent methodology and high resolution.

A pilot study on Nigeria combined the gridded information on epidemic exposure extracted by the INFORM Risk Index with the settlement classification from GHSL to characterize people exposure to epidemic in rural areas, towns and peri-urban areas, and urban centres. The characterisation of epidemic exposure in the three settlement classes is subject to the geographic spread of the pathogen. Dengue and Malaria territorial range potentially affect the whole country, while Marburg virus disease (MVD) and Ebola (EVD) affected approximately 2.5% of Nigeria's total population. Overall the share of population exposed to epidemics is lower in rural areas compared to urban areas. On average 20% of rural areas inhabitants and 80% of urban ones are exposed to each of the diseases included in the Index. For example, 70% of urban centre population is exposed to Zika, compared to 50% of urban cluster population and 40% of the rural one (Figure 21). Moreover, while about 2% of Nigeria population is exposed to MVD, half of the exposed population is in urban centres, 40% in urban clusters and 10% in rural areas. Information about hotspots of human exposure to epidemics is significant for addressing development policy and healthcare infrastructure siting and operations. The Nigeria pilot demonstrated the flexibility of the GHS-SMOD to apply geographic location disaggregation to other existing data. This and many other data integration challenges greatly support analysis of progress made in meeting SDG 3 on health and wellbeing capturing the urban/rural diversification with a globally consistent approach. The showcase shed lights on the potential disaggregation of several indicators in the INFORM Risk Index by geographical location and on the value of fine-scale up-to-date population data.

In response to the COVID-19 pandemic, in April 2020 JRC has also released an INFORM COVID-19 Risk Index (Poljanšek, 2020) to support the specific decision-making needs such as identify high priority risk areas and prioritize resources for prevention, preparedness, capacity development and medium-long term risk monitoring and evaluation. As COVID-19 impacted urban and rural areas differently, disaggregated exposure data would better support preparedness in urban settlements, which is critical for effective national, regional and global responses to COVID-19 (WHO, 2020).

Exposure to epidemics - INFORM RISK INDEX 2020

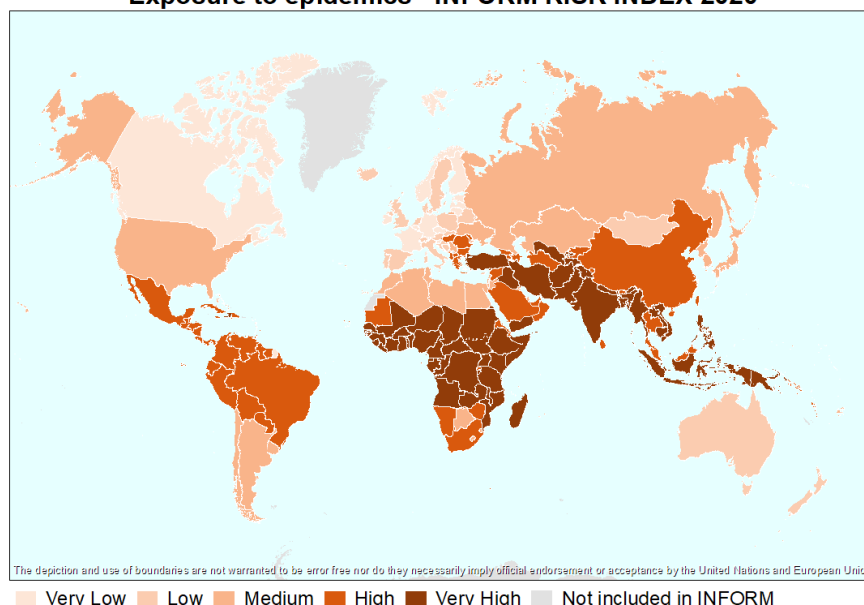


Figure 20 Global exposure to epidemics (INFORM Risk Index 2020)

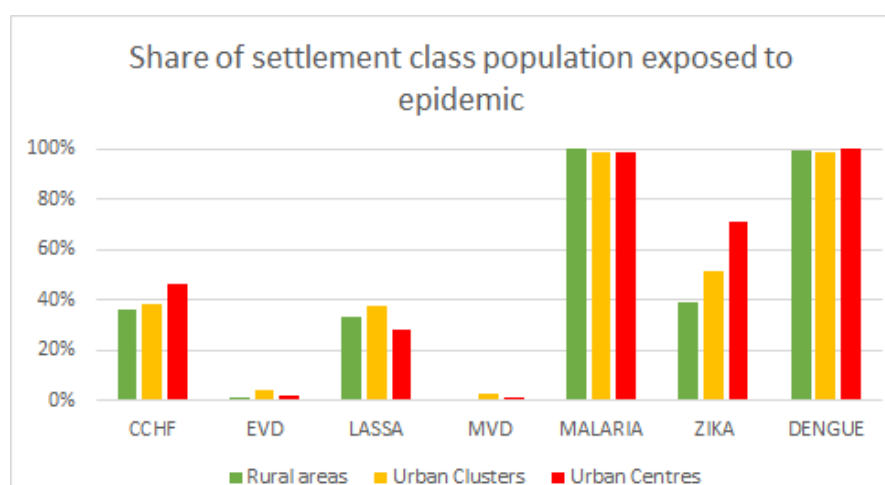


Figure 21 Population exposed in Nigeria to selected epidemics by Degree of Urbanization grid settlement class at Level 1

References:

European Commission, Joint Research Centre (JRC); Columbia University, Center for International Earth Science Information Network - CIESIN (2015): GHS population grid, derived from GPW4, multitemporal (1975, 1990, 2000, 2015). European Commission, Joint Research Centre (JRC).

Pesaresi, Martino; Florczyk, Aneta; Schiavina, Marcello; Melchiorri, Michele; Maffenini, Luca (2019): GHS-SMOD R2019A - GHS settlement layers, updated and refined REGIO model 2014 in application to GHS-BUILT R2018A and GHS-POP R2019A, multitemporal (1975-1990-2000-2015). European Commission, Joint Research Centre (JRC)

De Groeve, T., Poljanšek, K., and Vernaccini, L., *Index for Risk Management INFORM Concept and Methodology Report*, EUR 26528 EN, Publications Office of the European Union, Luxembourg, 2014, ISBN 978-92-79-33669-0, doi:10.2788/78658, JRC87617.

Poljanšek, K., Marin-Ferrer, M., Vernaccini, L., Messina, L., *Incorporating epidemics risk in the INFORM Global Risk Index*, EUR 29603 EN, Publications Office of the European Union, Luxembourg, 2018, ISBN 978-92-79-98669-7, doi:10.2760/990429, JRC114652.

Poljanšek, K., Vernaccini, L. and Marin Ferrer, M., *INFORM Covid-19 Risk Index*, EUR 30240 EN, Publications Office of the European Union, Luxembourg, 2020, ISBN 978-92-76-19203-9, doi:10.2760/596184, JRC120799.

Strengthening preparedness for COVID-19 in cities and other urban settings: interim guidance for local authorities. Geneva: World Health Organization; 2020 (WHO/2019-nCoV/ Urban_preparedness/2020.1).

3.1.3 Mapping the COVID-19 Pandemic and Potential Risk Factors

Development of an Interactive Viewer to Support Visualization and Analysis of COVID-19 Prevalence and Mortality Around the World

Chen, R.S., MacManus, K., de Sherbinin, A.

The rapid increase in Coronavirus Disease 2019 (COVID-19) cases around the world throughout 2020 has highlighted the many uncertainties in how the disease spreads through communities, across national borders, and between continents. In early 2020, there was widespread speculation about risk factors that might contribute or inhibit exposure to the virus and vulnerability to its impacts. Reporting of COVID-19 cases and mortality was incomplete and inconsistent, and the ability to detect COVID-19 infections in both symptomatic and asymptomatic individuals was still developing. The Johns Hopkins University & Medicine (JHU) Coronavirus Resource Center, in collaboration with Esri, developed the widely viewed COVID-19 Dashboard⁶ that gathered and visualized case, mortality, and testing data from around the world, providing an ongoing overview of the pandemic. However, this Dashboard mainly focused on total cases and deaths by country and available subnational units, and did not provide data on the overall population that could be exposed to the virus. With this in mind, the NASA Socioeconomic Data and Applications Center (SEDAC), operated by the Center for International Earth Science Information Network (CIESIN) at Columbia University, decided to create the SEDAC Global COVID-19 Viewer⁷ to support visualization and analysis of COVID-19 cases and deaths in relationship to the population in areas of interest to users around the world. Given initial observations that COVID-19 was spreading more quickly in densely settled urban areas, it was clear that population density was a key variable of concern, and one that was incorporated into many epidemiological models for predicting the virus' spread (e.g., Chinazzi *et al.*, 2020). Furthermore, it became evident that the elderly had higher mortality risk, and that males were more at risk than females, indicating the relevance of a population's age and sex structure in interpreting mortality data and assessing future COVID-19 vulnerability (Heuveline and Tzen, 2020). Other potential risk factors included exposure to poor air quality, degree of urbanization, elevation, and air temperature (Petroni *et al.*, 2020; Segovia-Juarez *et al.*, 2020).

To create the Global COVID-19 Viewer, SEDAC drew on readily available data sources, including data on *Basic Demographic Characteristics* from its Gridded Population of the World version 4.11 (GPWv4.11) collection, *Degree of Urbanization* from the Global Human Settlement Layer Settlement Model (GHS-SMOD), *Elevation* from the Altimeter Corrected Elevations, v2 (ACEv2) dataset, and *Aerosol Optical Depth* (AOD) from the Moderate Resolution Imaging Spectroradiometer (MODIS) instrument on NASA's Terra and Aqua satellites (a measure of air pollution). SEDAC quickly repurposed code and interface designs from other interactive mapping tools and integrated open data services from both internal and external providers, including an Application Programming Interface provided by JHU and three Hosted Feature Layers from JHU supported by Esri's Living Atlas. The initial version of the Viewer was released in April 2020. It provided the ability to create age-sex "pyramids" for custom areas of interest defined by the user for comparison with available JHU case and mortality data. A second release in July 2020 added data on rates of COVID-19 cases and mortality per 100,000 people and visualization of trends. As the pandemic evolved, it became increasingly important to track existing and developing COVID-19 "hotspots," as well as areas that had managed to keep the pandemic under control. The latest version of the Viewer, released in September 2020, expanded visualization of trends on different time scales, providing choropleth maps updated daily with 7-day moving averages of mortality and prevalence rates per 100,000 population (Figure 22). The Viewer also displays trends in daily cases and deaths, and 7-day moving averages, for time scales of one, three, and six months, and since the pandemic began (Figure 23). Charts based on *Degree of Urbanization* from GHS-SMOD show population and land area by settlement classes for both existing and user-defined geographic areas (Figure 23). SEDAC received extensive feedback from users, including its User Working Group, and continues efforts to improve the Viewer to meet the needs of diverse users. With COVID-19 still spreading rapidly in many parts of the world in late 2020, and with vaccines expected to be distributed widely in 2021, the need to monitor and predict the course of the virus remains critical. Information services such as the JHU COVID-19 Dashboard and SEDAC's Global COVID-19 Viewer are essential to gathering, integrating, and communicating complex data about this deadly disease that has dramatically affected our Human Planet during 2020.

⁶ <https://coronavirus.jhu.edu/map.html>

⁷ <https://sedac.ciesin.columbia.edu/mapping/popest/covid-19/>

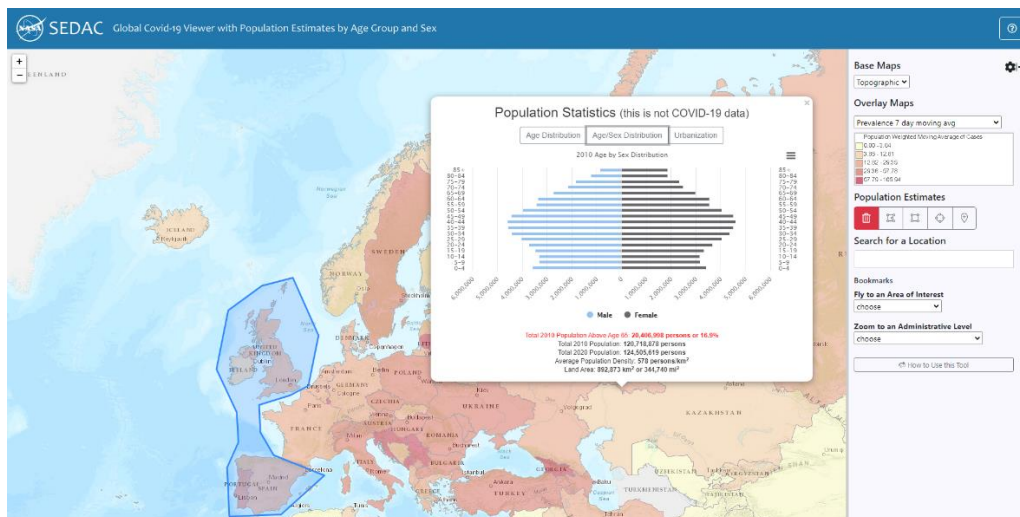


Figure 22 SEDAC Global COVID-19 Viewer showing a population-weighted 7-day moving average of cases in Europe as of 1 December 2020 and an age pyramid for the combined populations of the UK, Spain, and Portugal.

COVID-19 Statistics for India

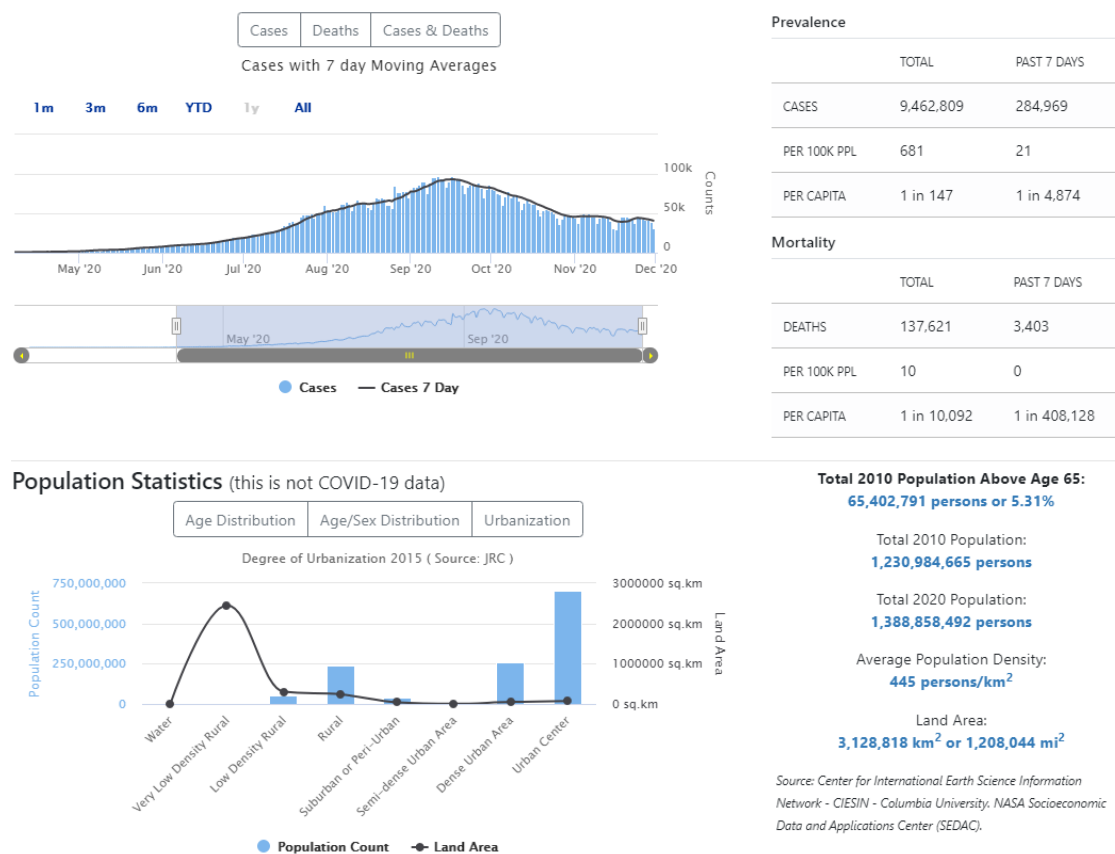


Figure 23 SEDAC Global COVID-19 Viewer showing charts of daily and 7-day moving average of COVID cases, and degree of urbanization population and land area estimates for India

References

- [Chinazzi et al. 2020](#). Preliminary assessment of the International Spreading Risk Associated with the 2019 novel Coronavirus (2019-nCoV) outbreak in Wuhan City.
- [Heuveline and Tzen. 2020](#). Beyond Deaths per Capita: Comparative CoVID-19 Mortality Indicators.
- [Petroni et al. 2020](#). Hazardous air pollutant exposure as a contributing factor to COVID-19 mortality in the United States.
- [Segovia-Juarez et al. 2020](#). High altitude reduces infection rate of COVID-19 but not case-fatality rate.

3.1.4 Advancing exposure and risk assessment in the EU by modelling population distribution in daily and seasonal cycles

An application of the ENACT project for Disaster Risk Management

Freire S., Schiavina M., Corbane C., Rosina K., Batista e Silva F.

Exposure, i.e. the presence of people or assets in dangerous areas, is a core component of disaster risk, without which there would be no direct impacts from hazards. Particularly for some types of natural hazards, risk can only be significantly reduced by decreasing exposure and vulnerability, as the hazard component of the equation is quite inflexible. For example, earthquakes and volcanic eruptions are still difficult to predict and we cannot control or reduce the magnitude of events.

Earthquakes are the second deadliest natural hazards after heat waves, causing more than 30,000 deaths in Europe in the last three decades. Southern Europe frequently experiences seismic activity that often causes destruction of entire settlements and leaves thousands of people homeless. Earthquakes are sudden and unpredictable events, whose risk of injury varies significantly between night and day, leading to the recommendation that vulnerability and exposure be assessed in this temporal cycle.

Since people are the most vital element to protect from hazards, adequate planning, mitigation, and reaction to disasters requires knowing the location of people and their characteristics. Human activities (work, study, leisure) result in large fluctuations in population distribution at a range of spatio-temporal scales. These population dynamics can greatly modify the patterns and assessment of population exposure, particularly for rapid onset hazard events such as earthquakes, tsunamis, and floods. However, due mostly to lack of data on population spatio-temporal dynamics, these implications have been largely overlooked in risk analyses or considered only for small areas and in case studies. Therefore, assessments of population exposure have typically relied on population distribution maps representing resident population as derived from census information.

In the frame of the project ENACT (ENhancing ACTivity and population mapping), we produced for Europe (EU-28) a set of seamless nighttime and daytime population density grids for each month of the year 2011 (census year), taking into account human activities and induced major daily and monthly variations (Figure 24). We created these new spatio-temporal grids by mining and combining official statistical data at regional level with geospatial data from conventional and non-conventional data sources. Updated, detailed, and consistent geospatial data on distribution and density of human settlements is fundamental to know where and how we live. Built-up areas mapped in the European Settlement Map (ESM 2012, release 2017), produced in frame of the Global Human Settlement Layer (GHSL) project, were used both to improve the disaggregation of population distribution and to further detail the new pan-European land use map created to inform the location of daytime activities (Rosina et al. 2020). The final population grids, at 1km resolution, are validated and are freely available to the public here: https://jeodpp.jrc.ec.europa.eu/ftp/jrc-opendata/ENACT/ENACT_POP_2011_EU28_R2020A/

Availability of such data sets enables unprecedented comparable and detailed analysis of the daily and seasonal variations of population exposure and risk across 28 countries inhabited by more than 500 million people. By combining these population grids with the most recent data on seismic hazard (ESHM-Corbane et al. 2017), we are able to map and quantify variations of population exposure, to study their spatio-temporal patterns, and to eventually identify potential daily and seasonal exposure hot spots. Regarding population exposure to highest seismic levels (MMI>VI), Figure 26 shows different patterns in Spain and Greece: while in Spain potential exposure is higher in nighttime period and reaches maximum in January, in Greece it is higher in daytime, reaching maxima in summer months.

Although most useful for baseline risk assessment, especially when also combined with information on vulnerabilities, such population grids can potentially benefit all stages of the Disaster Management cycle, from risk analysis and assessment to mitigation, preparedness and response. These data can substantially contribute to advancements in natural hazard risk assessment models, in this way responding to requests of the Sendai Framework for Disaster Risk Reduction and the 2030 Agenda for Sustainable Development.

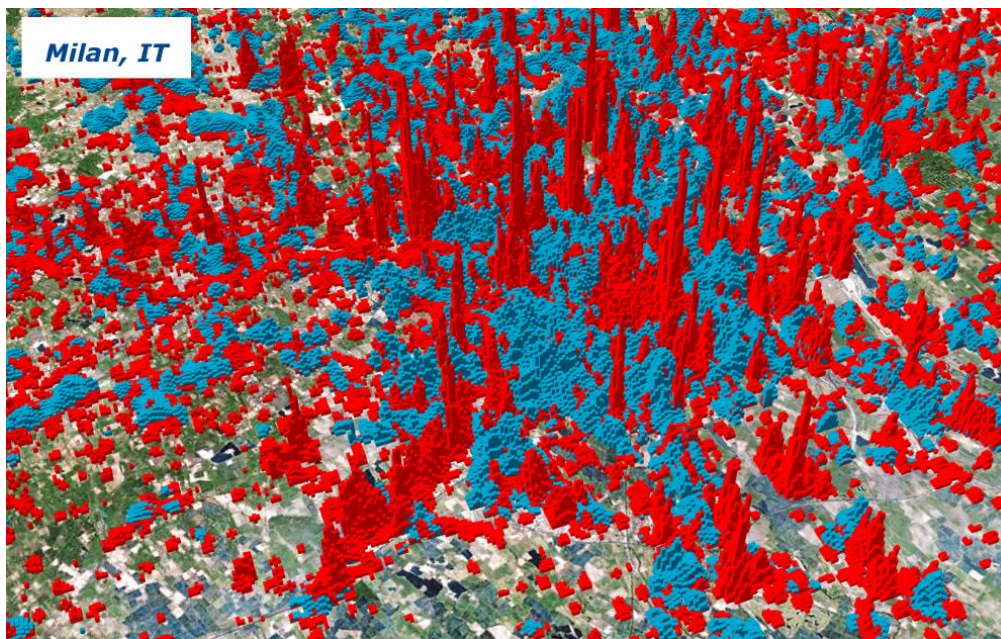


Figure 24 Estimated difference in daytime (red) vs nighttime (blue) population in Milan, Italy, in 2011. Height of the bars is directly proportional to its population density.

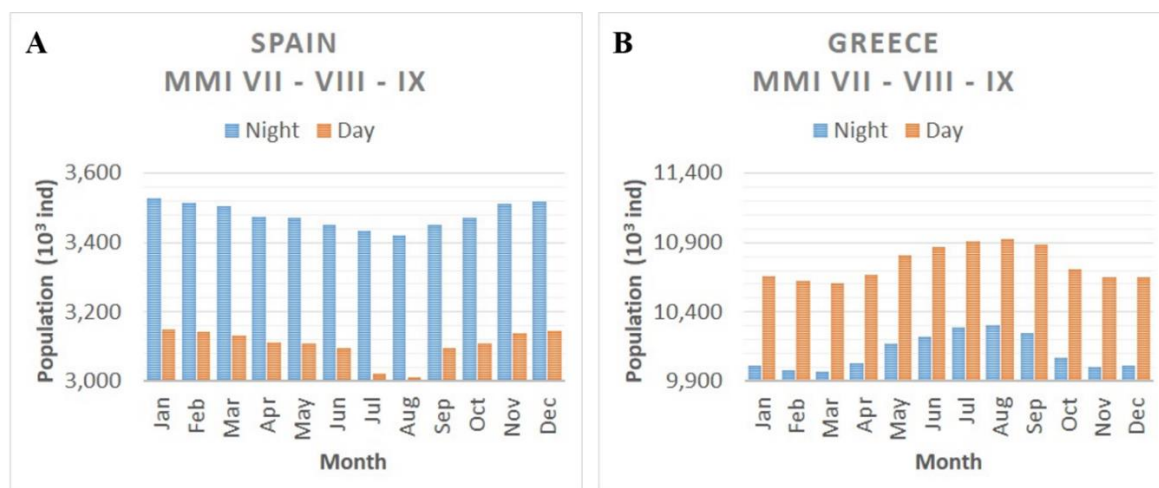


Figure 25 Variation of potential population exposure to seismic hazard per month in 2011, for (A) Spain; (B) Greece, for Modified Mercalli Intensity (MMI) levels > VI (Strong). Blue bars represent nighttime exposure; orange bars represent daytime exposure.

References:

ENACT-POP: Schiavina, Marcello; Freire, Sergio; Rosina, Konstantin; Ziemba, Lukasz; Marin Herrera, Mario; Craglia, Massimo; Lavalle, Carlo; Kemper, Thomas; Batista e Silva, Filipe (2020): ENACT-POP R2020A - ENACT 2011 Population Grid. European Commission, Joint Research Centre (JRC) [Dataset] doi:10.2905/BE02937C-5A08-4732-A24A-03E0A48BDCDA PID: <http://data.europa.eu/89h/be02937c-5a08-4732-a24a-03e0a48bdcd>

ESM 2012 R2017: Stefano FERRI, Alice SIRAGUSA, Filip SABO, Maria PAFI, Matina HALKIA; The European Settlement Map 2017 Release. Methodology and output of the European Settlement Map; EUR 28644 EN; doi:10.2760/780799

Rosina, K., F. Batista e Silva, P. Vizcaino, M. Herrera, S. Freire & M. Schiavina (2020) Increasing the detail of European land use/cover data by combining heterogeneous data sets, International Journal of Digital Earth, 13:5, 602-626, DOI: 10.1080/17538947.2018.1550119

ESHM: Corbane, C., Hancilar, U., Ehrlich, D., De Groeve, T., (2017). Pan-European seismic risk assessment: a proof of concept using the Earthquake Loss Estimation Routine (ELER). Bull Earthquake Eng 15:1057-1083

3.1.5 Mapping drought hazard, exposure and vulnerability for drought risk reduction

From spatially explicit assessment to management

Naumann G., Barbosa P., Vogt. J.

The preparation of Drought Management Plans (DMPs) must be linked to an agreed conceptual framework for drought management and based on a clear drought definition as well as spatially explicit information on the exposure and vulnerability of different affected sectors (Vogt et al. 2018). National Drought Policies are required to support the development of such DMPs, adapted to the particular local conditions of each country. Drought policies should not simply be a post facto response to disasters, but should be a permanent concern of governments and society. In that sense, as proposed by the High-level Meeting on National Drought Policy (HMNDP 2013) and Vogt et al. (2018), any drought policy should be based on three pillars: 1- drought monitoring, forecasting, and early warning; 2- vulnerability, and impact assessments, and 3- drought preparedness, mitigation and response. The UNCCD 2018-2030 Strategic Framework includes a new strategic objective (SO3) on the consideration of drought in national action programmes. With particular reference to vulnerability and impact assessment, the Decision 29 of UNCCD COP 13⁸ focused on the opportunities for the Parties to consider completing drought risk assessments for sectors, population groups and regions vulnerable to drought.

In that context, COP 13 requested the development of the UNCCD drought toolbox as part of the UNCCD Drought Initiative in order to provide drought stakeholders with easy access to tools, case studies and other resources to support the design of National Drought Plans. The aim is to boost the resilience of people and ecosystems to drought. A National Drought Plan should include a risk assessment to ensure that preparedness, response and drought mitigation activities are effective, efficient and targeted at those who need them most. In the UNCCD toolbox launched during COP 14, the drought risk assessment relies on the methodology and assessment developed by the European Commission's Joint Research Centre (Vogt et al., 2018). It is calculated as the probability of harmful consequences or the likelihood of losses resulting from interactions between drought hazard (the probability of drought events), drought exposure (such as the GHS-POP population layer, sources of livelihood and assets in an area in which drought events may occur) and drought vulnerability (the propensity of exposed elements to suffer adverse effects when impacted by a drought event) (Carrão et al., 2016; Vogt et al., 2018). To assess drought risk at global scale, each component of drought risk was calculated independently, based on global-scale indicators of different spatial resolutions: 1) Hazard has been computed from historical sequences of monthly precipitation deficits for the period between 1901 and 2010; 2) Exposure has been computed at the sub-national level using GHS-POP indicators of population and livestock density, as well as information on crop cover and baseline water stress; 3) Vulnerability has been derived from a combination of factors of social, economic and infrastructural indicators.

Figure 26 shows the three determining factors of drought risk (hazard, exposure and vulnerability) that result in the drought risk map focused on agricultural production. In this case, the scores for each component are not an absolute measure, but a relative statistic that provides a regional ranking of hotspots where to target and prioritise actions to reinforce adaptation plans and mitigation activities. Drought risk has been found to be driven by an exponential growth of regional exposure while hazard and vulnerability exhibited a weaker relationship with geographic distribution of risk values. This kind of analysis can be refined at higher spatial resolution to obtain meaningful results at different scales of analysis. These can range from the local to continental level, allowing an assessment of the spatial distribution of the drought risk within a given area of interest (e.g. farm, province, river basin, country, region, or continent). Figure 27 shows the implementation of the risk assessment in the UNCCD Drought Toolbox⁹. This framework is data driven and the main limitation for obtaining reliable estimates is the availability and accuracy of relevant information at different administrative levels. In that sense, the GHS-POP proves to be a suitable and unique exposure dataset to depict human exposure able to inform the risk assessment at different scales.

⁸ ICCD/COP(14)/CST/7. Outcomes of the work of the Committee on Science and Technology on a monitoring framework for the strategic objective on drought. CST 14, New Delhi, India, 2019. <https://www.unccd.int/official-documents/cst-14-new-delhi-india-2019/iccdcop14cst7>

⁹ <https://knowledge.unccd.int/drought-toolbox/page/vulnerability-and-risk-assessment>

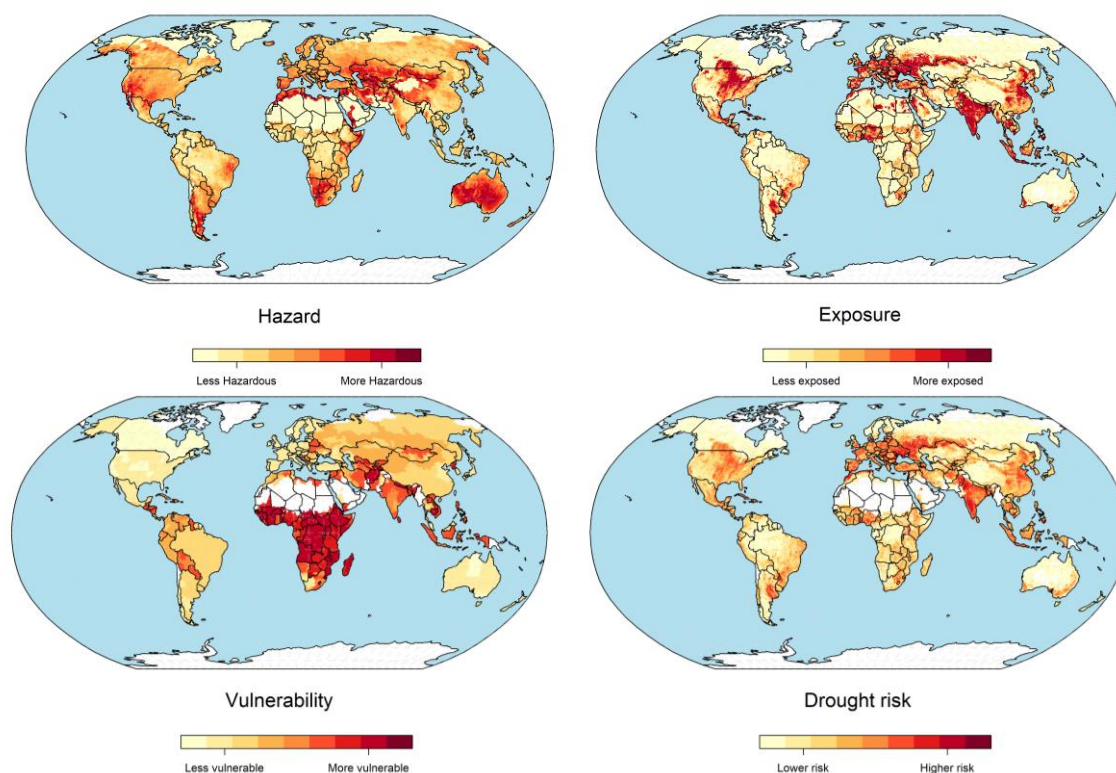


Figure 26 Global drought hazard, exposure (including GHS-POP layer), and vulnerability as well as the risk resulting from the combination of all factors. Adapted from Vogt et al., 2018

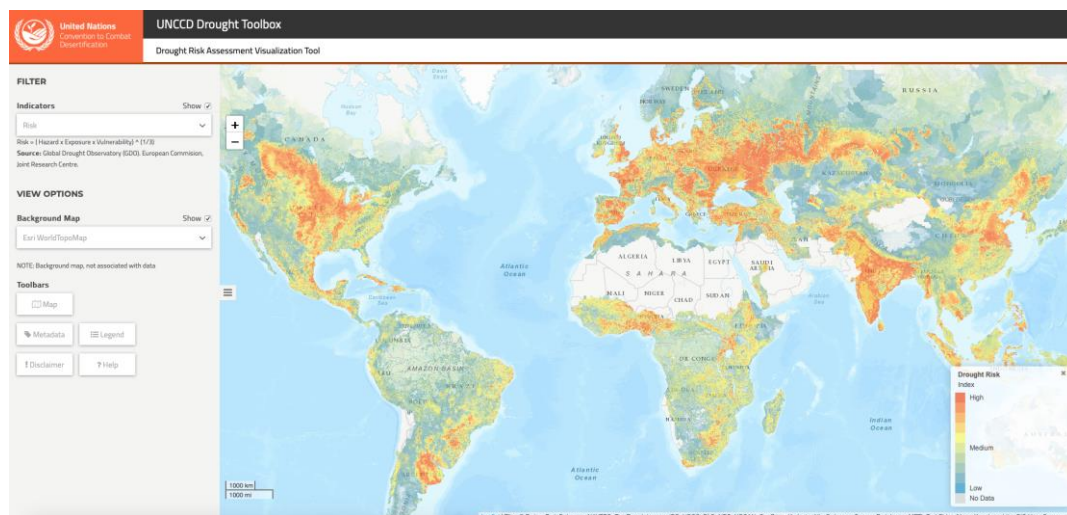


Figure 27 Drought risk assessment in the UNCCD Drought toolbox. Source: <https://maps.unccd.int/drought/>

References:

Carrão H., G. Naumann, P. Barbosa, 2016. Mapping global patterns of drought risk: an empirical framework based on sub-national estimates of hazard, exposure and vulnerability. *Glob Environ Change*, 39, 108-124.

HMNDP – High Level Meeting on National Drought Policies (2013). Towards More Drought Resilient Societies. Geneva, 11 – 15 March 2013.

Schiavina, M; Freire, S; MacManus, K (2019): GHS population grid multitemporal (1975, 1990, 2000, 2015) R2019A. European Commission, Joint Research Centre (JRC).

Vogt, J., Naumann, G., Masante, D., Spinoni, J., Cammalleri, C., Erian, W., Pischke, F., Pulwarty, R., Barbosa, P. (2018). Drought Risk Assessment. A conceptual Framework. EUR 29464 EN, Publications Office of the European Union, Luxembourg, 2018. ISBN 978-92-79- 97469-4

3.1.6 Developing the European Wildfire Risk Assessment (WRA)

The contribution of the GHSL

Oom D., de Rigo D., Pfeiffer H., San-Miguel-Ayanz J., Grecchi R., Durrant T., Libertà G., Artes Vivancos T., Boca R., Maianti P., Branco A., Ferrari D.

The assessment of wildfire risk is critical to develop prevention and mitigate the damages caused by wildfires at European and global scales. The development of a pan-European approach follows from a series of EU regulations that require the European Commission to have a wide overview of the wildfire risk in the European region, to support the actions of its Member States and to ensure compliance in the implementation of EU regulations related to wildfires. The conceptualization of the European Wildfire Risk Assessment (WRA) as the product of hazard, exposure, and vulnerability follows the definition by San-Miguel- *et al.*, 2017 and will support the inter-comparison of WRA among countries, complementing existing national WRA with a simpler, but harmonised, methodology. Additionally, it can serve as a first approach to assess wildfire risk in those countries that have not yet performed a national WRA. The Global Human Settlement data were used in two dimensions: directly, on the identification of areas where the fires could occur (potential burnable mask); and indirectly, on the identification of key vulnerable areas in the proximity of human dwellings (wildland urban interface - WUI). These areas have a significant share of burnable wildland, and are close to where people live, so that wildfire events are typically more frequent and directly expose the local population.

The burnable mask (Figure 28) refers to any type of vegetation fuel, so it includes wildland, but also cropland, or any other typology of land with vegetation components that could actually burn. This mask acts as a filter to avoid false alarms, i.e. to prevent that fire observations not corresponding to vegetation fires bias the final output. It was developed under the Global Wildfire Information System (<https://gwis.jrc.ec.europa.eu/>) framework, estimating on a high-spatial resolution the potential burnable area where vegetation fuels are found, irrespective of the particular fuel type. The GHSL built-up product was used directly together with the JRC's Global Water Layer (Pekel *et al.*, 2016; <https://global-surface-water.appspot.com/>) and the Annual Maximum Normalized difference vegetation index (NDVI) value derived from Copernicus Sentinel imagery. The data processing was initially implemented at pixel level with spatial resolution of 30 meters, and then aggregated at the spatial resolution of the WCRP¹⁰. A pixel was masked (considered as a non-burnable pixel) if occupied by GHSL built-up, or by water or if the maximum annual value of NDVI in the pixel was lower than 0.2 (assuming that such values correspond to bare soil). In populated areas close to natural or semi-natural areas, the expansion of natural vegetation or settlements into the other class generates an interface designated as WUI (Figure 29). In assessing the European wildfire risk, we used the WUI modelled to assess the vulnerable population by proximity to wildland fuels in a changing climate, under the PESETA project (Costa *et al.*, 2020). The European Settlement Map was used to identify settlements in vulnerable areas and GHSL population data (GHS-POP) were used to identify the population exposed in the WUI (Freire *et al.*, 2016). Two complementary components characterize the WUI modelled in PESETA, the first accounting for the effect of local fires very close to the WUI, and the second for the effect of large wildfires able to affect areas in their proximity, even if not directly contiguous to the fire (Costa *et al.*, 2020). The local component is due to the more frequent ignition of areas where people can have an easier, direct access to wildland. As a consequence of accidental or deliberate fire started by people (the two most common causes of fire in Europe), these areas are more vulnerable to suffer wildfire damage and are identified where settlements are intermixed with wildland vegetation. Once a given fire is ignited close to the WUI, the locations nearby are also threatened due to the fire propagation, and additional people may be directly at risk or large areas of vegetation fuels may burn. When large areas of vegetation burn, a large amount of biomass fuel is affected and a correspondingly high amount of energy may be released (potentially leading to burning particles, such as firebrands and embers, to move far from the original fire). These large wildfires may affect population in near areas even if not directly contiguous to the fire. The second (non-local) component of the WUI accounts for these areas (Costa *et al.*, 2020). In the present climatic conditions, two areas with a comparable level of fire danger – but one within and the other outside the WUI – have a different fire risk, higher in the WUI. Under a changing climate, the co-occurrence of an increasing fire danger, and the presence of people potentially exposed in the vulnerable WUI interface, indicates an increasing fire risk (Costa *et al.*, 2020).

¹⁰ European grid of the Coordinated Regional Climate Downscaling Experiment (CORDEX) by World Climate Research Programme (WCRP). Archived at <https://tinyurl.com/y85nxfdw>. The standard grid EUR-11 is used (grid cell resolution of approximately 0.11 degrees, or about 12.5 km).

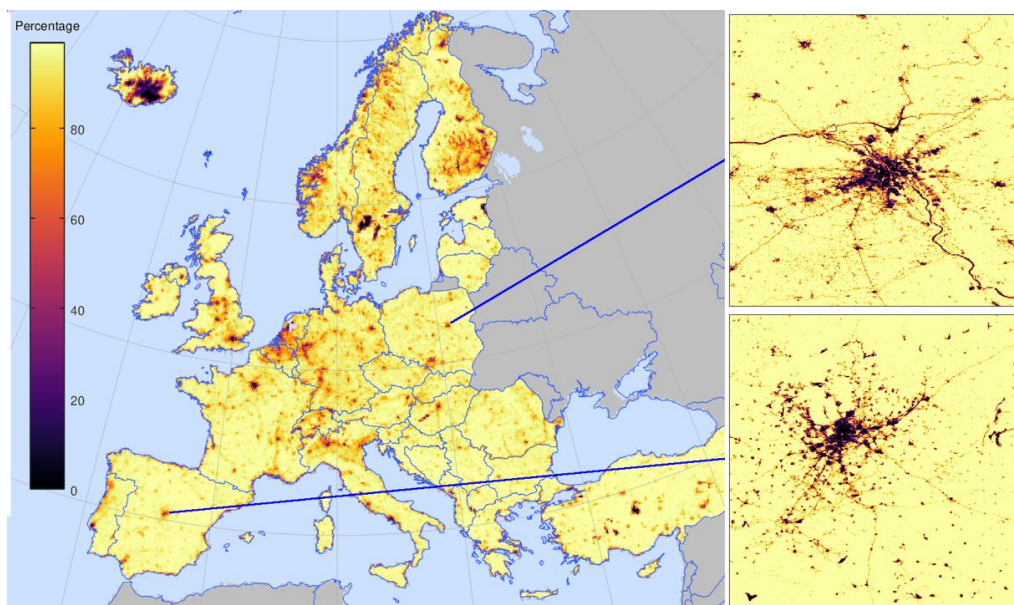


Figure 28 Potential Burnable Area Proportion (0-100 %)

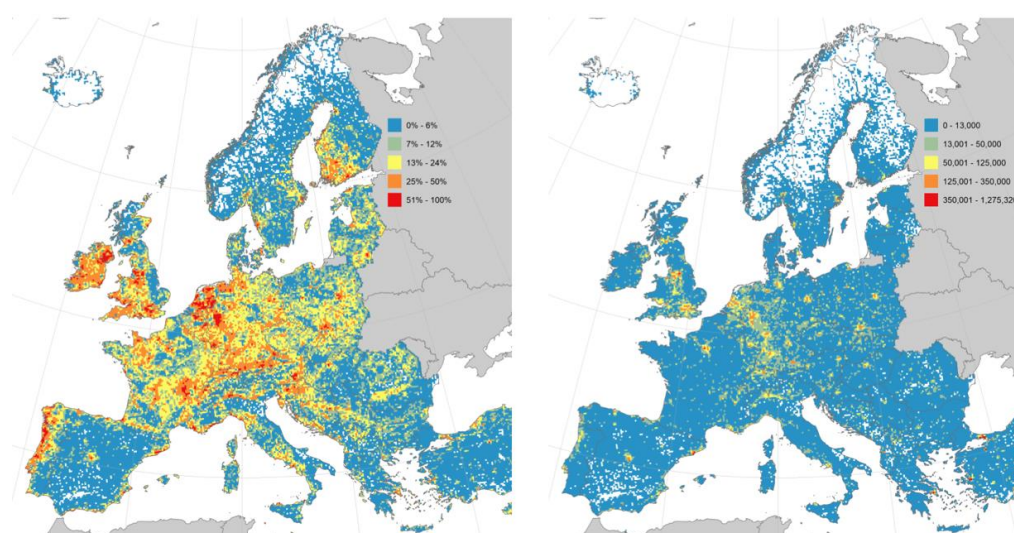


Figure 29 WUI in Europe, 2012: percentage of WUI land area (left), and population living in the interface (right). Population data from 2015, WCRP EUR-11 grid cell size: approximately 12.5 km (see footnote). From Costa et al., 2020.

References:

- Costa, H., de Rigo, D., Libertà, G., Houston Durrant, T., San-Miguel-Ayanz, J., 2020. European wildfire danger and vulnerability in a changing climate: towards integrating risk dimensions. *Publications Office of the European Union*, Luxembourg, 59 pp. ISBN:978-92-76-16898-0, <https://doi.org/10.2760/46951>
- Freire, S., MacManus, K., Pesaresi, M., Doxsey-Whitfield, E., Mills, J., 2016. Development of new open and free multi-temporal global population grids at 250 m resolution. In: *Proceedings of the 19th AGILE International Conference on Geographic Information Science*.
- Pekel, J.-F., Cottam, A., Gorelick, N., Belward, A.S., 2016. High-resolution mapping of global surface water and its long-term changes. *Nature* 540, 418–422. <https://doi.org/10.1038/nature20584>
- San-Miguel-Ayanz, J., Chuvieco, E., Handmer, J., Moffat, A., Montiel-Molina, C., Sandahl, L., Viegas, D., 2017. Climatological risk: wildfires. In: Poljanšek, K., Marín Ferrer, M., De Groeve, T., Clark, I. (Eds.), *Science for disaster risk management 2017: knowing better and losing less*. *Publications Office of the European Union*, Luxembourg, pp. 294–305.

3.1.7 GloFAS Rapid Risk Assessment

Operational procedure for rapid flood risk assessment

Kalas M., Dottori F., Salamon P., Baugh C.

The development of methods for rapid flood mapping and risk assessment is a key step to increase the usefulness of flood early warning systems and it is crucial for effective emergency response and flood impact mitigation. Currently, flood early warning systems rarely include real-time components to assess potential impacts generated by forecasted flood events. In this context, the European Commission has developed a dedicated procedure within the Global Flood Awareness System (GloFAS), which provides operational flood predictions in major rivers at the global scale as part of the Copernicus Emergency Management Services. The service is operational and publicly available since end of 2019 to local hydrometeorological services with responsibility for flood warning, emergency responders, NGOs.

GloFAS produces daily streamflow forecasts for major river networks with a lead time of 30 days. Where the flood peak magnitude is forecasted to exceed local flood protections, flood-prone areas are delineated using a pre-simulated catalogue of local flood maps derived at ~1km spatial resolution. Then, total population and land cover areas within the flood extent are extracted and aggregated into administrative regions. The resulting values are used to define the Rapid Impact Assessment as a risk matrix (Figure 30) based on the maximum population affected and the timing of the flood peak. The number of people affected is calculated using the Global Human Settlement Layer (GHS-POP). The land cover data are taken from the European Space Agency - Climate Change Initiative (ESA-CCI). One of the main goals of GloFAS is to provide globally harmonized information about upcoming flood events at the global scale. In order to forecast the possible impacts on population it is paramount to use exposure information which is available and consistent at the global scale, regularly maintained, well documented and based on a robust methodology. The GHSL datasets fit perfectly to such description and were therefore chosen to represent population density and distribution.

The Rapid Risk Assessment (RRA) procedure has been tested in recent large-scale flood events such as the floods caused by typhoon Kenneth in Mozambique and the Brahmaputra floods in 2019 in India (Figure 31). We used observations of inundated areas and population affected to validate the RRA estimates. These tests showed the potential of RRA to provide near-real time delineation of flood-prone areas, and to identify populated places at risk. The proposed methodology of the impact assessment has supported the European Response Coordination Centre (ERCC) during the real flood events (e.g. Mozambique 2019, Iran 2019).

Providing reliable and timely information about the location of people exposed to upcoming floods is a crucial piece of information for emergency responders and local governments. As such, GloFAS can provide an important support in areas where flood early warning systems are not available, or where flood impact forecasts are not routinely produced.

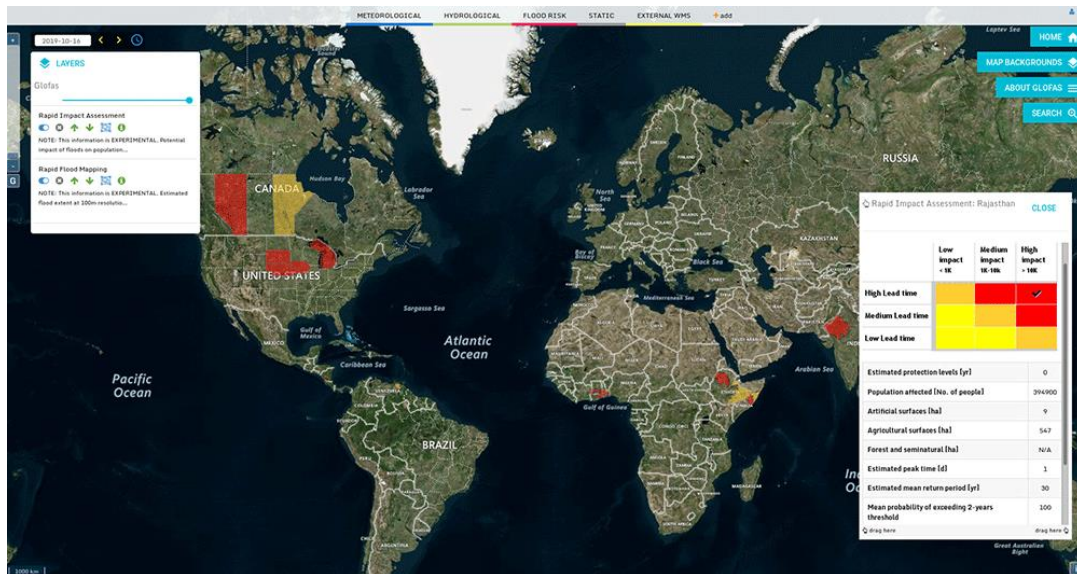


Figure 30 View of the Rapid Risk Assessment available on the GloFAS website The Global administration regions are shaded according to an impact matrix (shown below) which combines the total population exposure to the flood hazard with the lead time of the flood event. Categories along the top of the matrix refer to the total number of people who live within the flood inundation footprint.

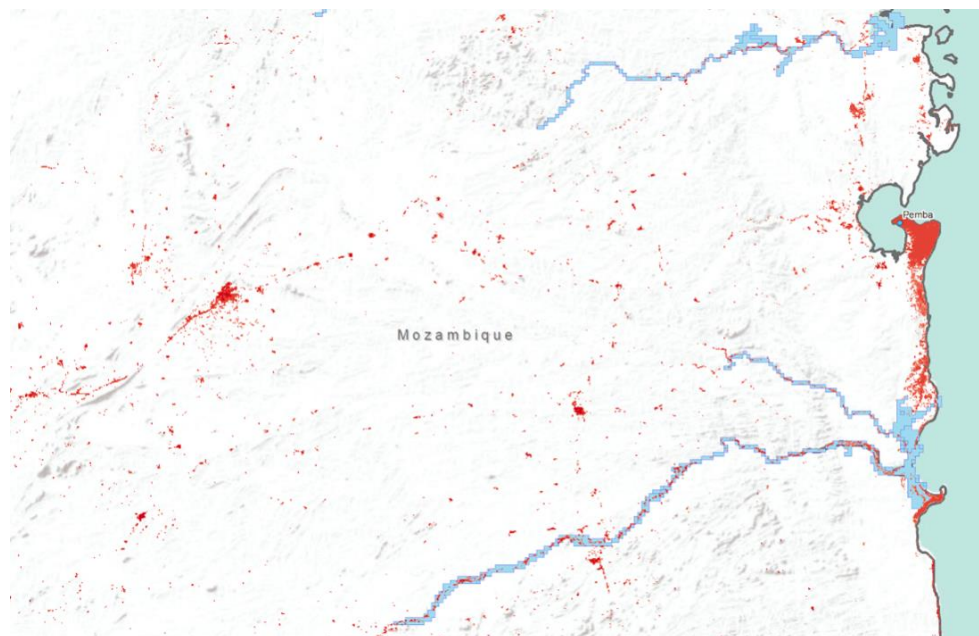


Figure 31 Application of the GloFAS RRA for the case study in Mozambique. The map shows overlay of the population density (in red) with the areas predicted to be flooded (in blue).

References:

ESA CCI <https://www.esa-landcover-cci.org/>

Schiavina, M; Freire, S; MacManus, K (2019): GHS population grid multitemporal (1975, 1990, 2000, 2015) R2019A. European Commission, Joint Research Centre (JRC).

3.1.8 New Estimates of Global Population and Land in the Low Elevation Coastal Zone Using GHSL-based Datasets¹¹

MacManus K., Balk D., Engin H., McGranahan G., Inman R., Hays A.

Projections for global sea level rise, along with data regarding a region's geographic and demographic characteristics, can be used to assess exposures and to manage risk and vulnerability. In a seminal 2007 study¹², McGranahan, Balk and Anderson estimated the urban and rural population and land exposure in a low elevation coastal zone (LECZ) globally. Subsequent work demonstrated the large influence of data resolution and population modelling assumptions on determining the number of people potentially exposed. New revisions, presented here, use Global Human Settlement Layer (GHSL) datasets to classify settlements along a rural-urban continuum, to quantify population and built-up densities at risk in 1990, 2000 and 2015. New elevation models/datasets are also used to improve the estimation of the exposure zone itself, and to allow for refined exposure estimates below 5 meters and 5-10 meters (contiguous to coastline), and above 10 meters.

Variations in settlement categorizations, and corresponding population models, result in vastly different estimates of the number of exposed people, potentially excluding vulnerable groups from risk and damage assessments associated with climate change scenarios. Thus it is of utmost importance to be transparent about which underlying data sets were used and why. The new estimates for the population living within LECZs correct for many of the issues that arose with prior datasets, which in some instances failed to account for populations living in relatively smaller geographic areas. The 2007 study was based on data from GRUMP (the Global Rural Urban Mapping Project), where total population was allocated at 30 arc seconds (~1km) horizontal resolution, based on circa 1995 DMSP-OLS night-time lights derived urban and rural areas within the census-based spatial units. The work presented here uses GHS-POP (Figure 32), which increases horizontal resolution to 9 arc seconds (~300m) and positional accuracy by utilizing the GHS-BUILT time series.

GHS Settlement Model Grid (GHS-SMOD) constructs a typology of settlement types defined by GHS-BUILT, and population density (derived from GHS-POP) that classifies pixels into 7 categories along a "rural-to-urban continuum". For comparability with other data sets, we simplify GHS-SMOD into three classes: rural, quasi-urban (such as towns, suburbs and semi-dense areas) and urban (Figure 32C). The estimates (presented here) use the Multi-Error-Removed Improved-Terrain Digital Elevation Model (MERIT-DEM) (Figure 32A), which addressed many of the widely studied shortcomings of the Shuttle Radar Topography Mission (SRTM) DEM that was previously used. A sensitivity analysis compares these estimates with those based on other population, urban area proxies, and elevation datasets. The population and settlement layers were then conditioned so that they could be summarized by two LECZ areas (and outside the LECZ), and by country.

Consistent with the 2007 study, the new results place 671M persons or 10.7% of the global population in 2000 living below 10m contiguous to seacoast. This share continued to increase to 11.1 % (815M persons) in 2015 (Figure 32E). Additionally, the new estimates by settlement type place 14.1% of the population of urban centers and 10.7% of those living in quasi-urban areas in the LECZ in 2015 (Figure 32E), with the pie chart showing much higher fractions of urban and quasi-urban residents in the LECZ than beyond it. Similarly, urban land -- while a small fraction of total land -- is disproportionately greater in the LECZ than beyond it. Among urban dwellers living in the LECZ, 31% of those living in urban centers and 43% of those living in quasi-urban centers, live in the higher risk 0-5m zone. Deltaic countries with large cities contribute disproportionately to these estimates. In particular, several countries in Asia have especially large shares of their urban and total population in the LECZ, as shown here for Viet Nam (Figure 32A).

The findings demonstrate the uneven distribution of population living in LECZs, due to the historic and continued development of cities and towns along the coast. With the overwhelming share of population growth to occur in the city and towns of the world, particularly those in Asia, Africa and Latin America, it is crucial that policymakers have spatially accurate population and elevation data such as those presented here in order to project and plan for potential damages from gradual sea level rise and the threat of storm surge flooding, and encourage mitigation.

¹¹ Preliminary Release Data available at <http://www.ciesin.columbia.edu/data/lecز-urban-rural-population-land-area-estimates-v3/>

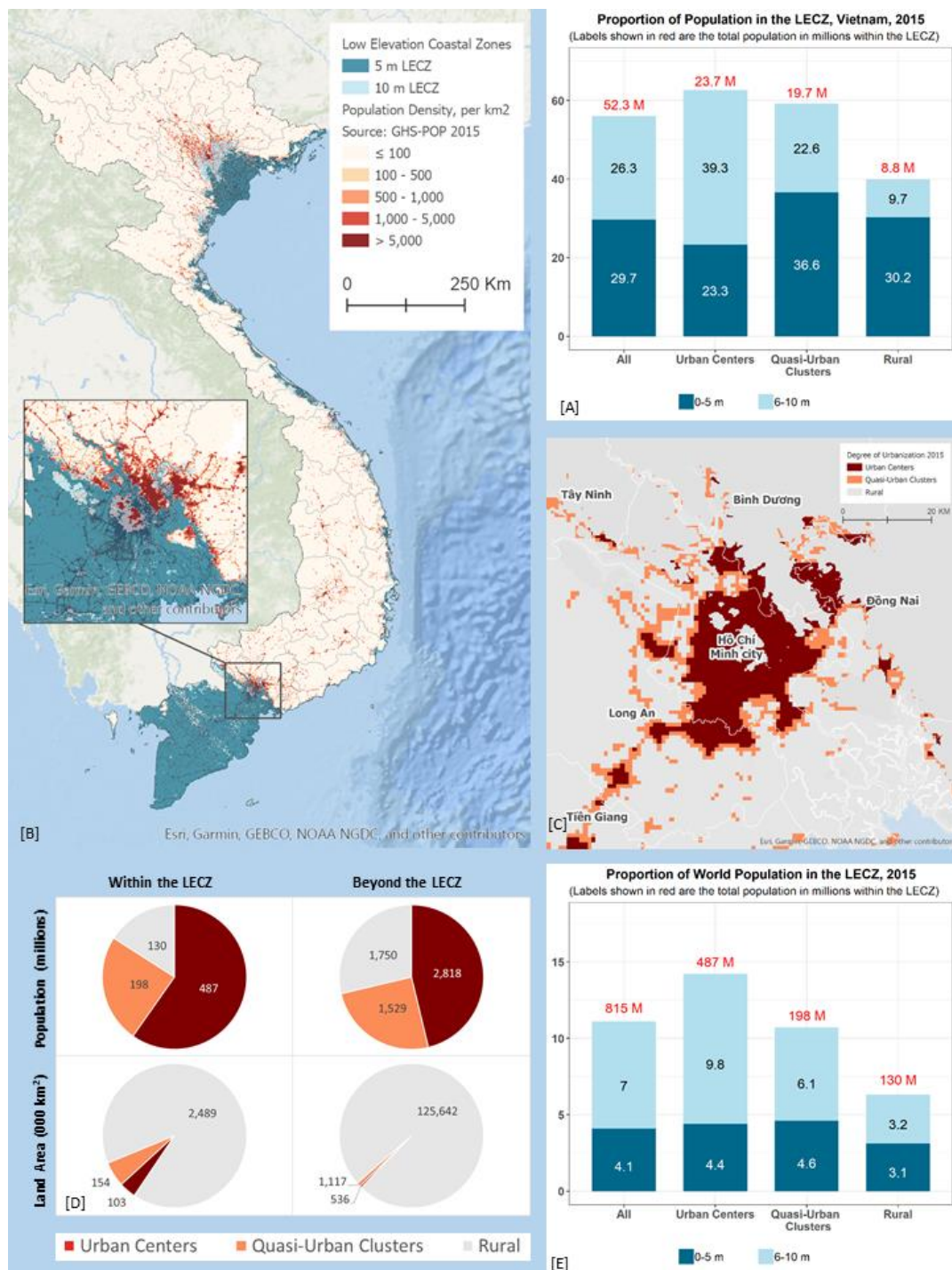


Figure 32 Population in low elevation coastal zones in Vietnam analysed using GHS-POP and settlements classification

References

- Coalition for Urban Transitions (2019): Climate Emergency, Urban Opportunity: How National Governments can Secure Economic Prosperity and Avert Climate Catastrophe by Transforming Cities. World Resources Institute <https://urbantransitions.global/wp-content/uploads/2019/09/Climate-Emergency-Urban-Opportunity-report.pdf>
- European Commission, Joint Research Centre (JRC); Columbia University, Center for International Earth Science Information Network - CIESIN (2015): GHS population grid, derived from GPW4, multitemporal (1975, 1990, 2000, 2015). European Commission, Joint Research Centre (JRC).
- McGranahan, Gordon, Deborah Balk, and Bridget Anderson. 2007. "The Rising Tide: Assessing the Risks of Climate Change and Human Settlements in Low Elevation Coastal Zones." *Environment and Urbanization* 19 (1): 17–37. <https://doi.org/10.1177/0956247807076960>.
- Pesaresi, Martino; Florczyk, Aneta; Schiavina, Marcello; Melchiorri, Michele; Maffneni, Luca (2019): GHS-SMOD R2019A - GHS settlement layers, updated and refined REGIO model 2014 in application to GHS-BUILT R2018A and GHS-POP R2019A, multitemporal (1975-1990-2000-2015). European Commission, Joint Research Centre (JRC)

3.1.9 Flood Risk and Impact in Urban Areas Using Social Media

The FIUME exploratory research project

Lorini V., Nappo D., Salamon P., Zavarella V., Tanev H., Castillo C., Porto de Albuquerque J.

Urban areas can flood due to intense precipitation events, rapid snowmelt, and rises in sea, lake, river, and groundwater levels. Major reasons for urban flooding are poor drainage systems, lack of maintenance, and poorly controlled growth of urban areas, especially in developing countries. Due to the complexities of urban environments, urban flood modelling and prediction of flood prone areas face many challenges, therefore it is of the utmost importance to provide timely risk assessment at the highest possible resolution.

The aim of this project is integrating information derived from social media, authoritative data (numerical models, sensors and remote sensing) and socioeconomic data to improve disaster risk management capacity in urban areas and to study the correlation between social media activity and flood impacts with ad-hoc Machine Learning (ML) models. Social media can be seen as a form of distributed cognition. The interactions among users are a form of collective intelligence, as they allow to collectively make sense of a developing situation. Social media during a crisis generates a wealth of data that can be used to better situational awareness. During a crisis, social media users can contribute to create a “sensor” for “citizen generated data” assimilated to direct or remote earth observation systems. In the Framework of (i) the Decision No 1313/2013/EU of the European Parliament and of the Council on a Union Civil Protection Mechanism¹³ and (ii) the Sendai Framework for Disaster Risk Reduction¹⁴, the implementation of a System for channelling aggregated Social Media information will have a very positive impact on both DG JRC internal stakeholders as a tool for research and external stakeholders (other DGs and Copernicus EMS users) as an additional layer of data for situational awareness. Copernicus EMS will have access to an additional toolbox for analysis and projections.

Two pilot cities (two languages, Barcelona ES and Sao Paulo BR) are selected as ‘test cases’ where to define if social media could be useful to detect high resolution extent and impacts of urban floods in densely populated cities where social media and socioeconomic data are expected to be abundant as more citizens are actively connected. The project relies on existing systems at the JRC, such as the Global Flood Awareness System (GloFAS¹⁵), the Global Human Settlement Layer (GHSL¹⁶), the Social Media for Flood Risk (SMFR¹⁷) and the activity of text and data mining at the European Media Monitoring group (EMM¹⁸). Once heavy precipitation is forecasted over one of the pilot cities, ML models are trained to detect impacts on population, infrastructures and services from text (Figure 33 upper). Nevertheless, the aggregation of such information must be mapped against a geographical unit. The signals collected from social media posts are aggregated per unit as defined by GHSL (Figure 33 lower). To hyper geolocate the tweets, we built two specific gazetteers with data extracted from open data such as OpenStreetMap (preliminary data in Figure 3). Social media aggregated information will be coupled with GHSL statistical data such as population distribution for a dynamic risk assessment. GHSL combined with its global Urban Centre Database data will be used also as a statistical baseline for population density for comparing/validating the magnitude of signal detected from social media and studying a correlation between the population in an area and the impact on population and services (preliminary result shown in Figure 34).

We are confident the project will better the situational awareness during the response stage, after a natural hazard event heighten the risk of impacts to people, services or infrastructures in an Urban Area, where current physical modelling is extremely difficult. Validation of the research’s outcomes will be performed for a number of urban flood events, according to data availability from the Copernicus Emergency Management Services (CEMS). The developed tools for social media monitoring will be activated according to CEMS early warning systems such as GloFAS. The combination of news provided by EMM and damage assessment as well as GHSL population indicators will be used to evaluate the quality of the methodologies developed throughout the activity.

¹³ <https://eur-lex.europa.eu/legal-content/EN/TXT/?qid=1401179579415&uri=CELEX:32013D1313>

¹⁴ <https://www.undrr.org/publication/sendai-framework-disaster-risk-reduction-2015-2030>

¹⁵ <https://www.globalfloods.eu>

¹⁶ <https://ghsl.jrc.ec.europa.eu>

¹⁷ <https://arxiv.org/abs/1904.10876>

¹⁸ <https://emm.newsbrief.eu/overview.html>

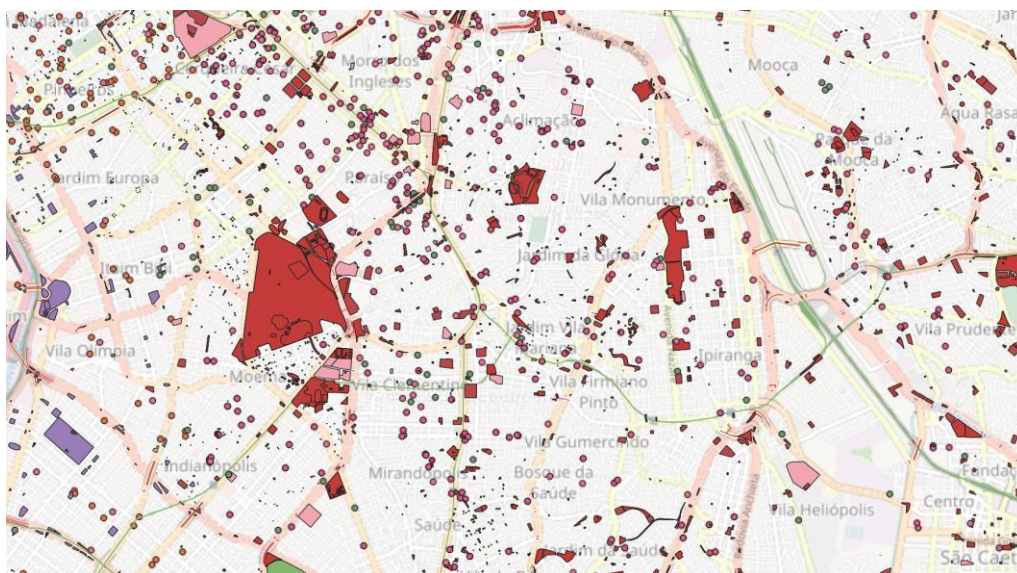
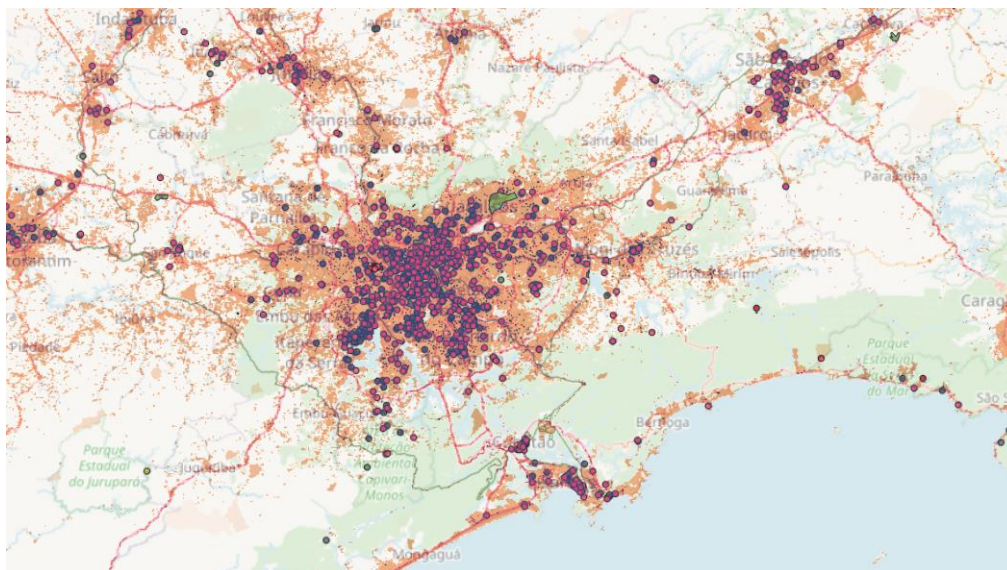


Figure 33 (upper) infrastructures extracted from free open data for Sao Paulo (Brazil) Urban Area overlaid with the corresponding GHSL layer; (lower) map of infrastructures that are used as gazetteers to place tweets in a GHSL cell on the map



Figure 34 Aggregation of classified tweets according to different classes of impact

3.1.10 Saving time in satellite mapping in case of large disasters: the automatic identification of Areas of Interest based on the Global Human Settlement (GHS) - Settlement Model grid (SMOD)

Results of the automatic methodology used to generate areas for the tasking of satellite acquisitions in the preparedness and early response phase of a disaster

Annunziato A., Joubert-Boitat I., Paris S., Probst P., Proietti C., Santini M., Wania A.

Satellite mapping is a tool that is widely used by disaster managers to rapidly and remotely assess the impact of disasters. A lot of effort has been focused over the years to improve the timeliness and reliability of the satellite-based impact assessments. Statistics from the satellite-based emergency mapping performed during the past eight years under the Copernicus Emergency Management Service (CEMS - Rapid Mapping) clearly show that one of the main bottlenecks in the process remains the fast access to new images required for providing timely post-event assessments. Knowing as soon as possible over which areas the satellite acquisitions should focus is essential to shortening this phase in order to save time. Identifying areas at risk at an early stage also increases the chance of acquiring pertinent images because the focus is put on areas where losses in terms of human life and property are likely to be higher.

Early warning and alert systems have great potential to support this process and recently a fruitful collaboration was established among the Global Disaster Alert and Coordination System (GDACS) and CEMS. The overall objective was to setup and test an automatic procedure to identify the most affected areas of a disaster in order to target the prompt acquisition of satellite images (Area of Interest - AoI). CEMS-Rapid Mapping is an on-demand service for authorised users (one per European Member State and other countries participating in the European Civil Protection Mechanism plus DG ECHO's Emergency Response Coordination Centre in Brussels; other users such as UN emergency services can trigger the service through authorised users). Most of the satellite missions used by the service need to be tasked over a specific area for a given date. Besides identifying AoIs for disasters which have just occurred (e.g. earthquakes), the challenge is also to define AoIs for disasters, where a GDACS alert is issued in view of an upcoming disaster such as tropical cyclones (i.e. in the preparedness phase). With the proposed methodology this process can be optimised in order to have imagery available once the user decides to activate.

The adopted methodology relies on the hazard-specific data and the characteristics of the satellite acquisition process. In particular, the procedure starts with issuing a Red alert from GDACS, meaning that the impact of a specific disaster is estimated to have the potential to evolve in a request for international humanitarian support from the affected countries. The available hazard intensity data (e.g. shake maps for earthquakes, wind, precipitation and storm surge forecasts for tropical cyclones) are automatically combined with the GHSL Settlement Model grid (GHS-SMOD) to identify the most critical areas in terms of exposure. In particular, for this analysis, the Degree of Urbanisation Level 1 classes are considered. From the combination of the two information layers, a priority for acquisitions over the impacted area can be determined based on the hazard intensity and number of exposed population, facilitating the decision process of where to focus first. Criteria for the ranking are the impact category and the number of inhabitants that are both provided for each AoI. The number of inhabitants is derived from the population dataset of the Global Human Settlement Layer (GHSL-POP).

This methodology has been developed and operationally tested during the last two years with promising results. The figures below show two activation examples. Figure 35 shows the comparison between the location of some of the AoIs generated by GDACS and areas analysed for impacts by the respective CEMS-Rapid Mapping activation (EMSR423) for an Earthquake, which occurred in January 2020 in Turkey (EQ1203232). The satellite-based impact assessment in the AoIs identified by this methodology allowed to detect the most significant damages caused by the earthquake. Figure 36 shows how the automatically generated AoIs can be used to point satellite data providers to task acquisitions for an upcoming disaster such as Typhoon Kammuri in the Philippines in December 2019 (TC1000636). The efficiency of the second application is under review for possible integration in CEMS operations. This collaborative effort in improving the disaster impact estimation and the automatic identification of the AoIs for the acquisition of satellite images is showing promising results in the view of pre-tasking of satellite acquisitions, allowing to fastening the process both for the identification of the AoI and for the timely acquisition of the satellite images.

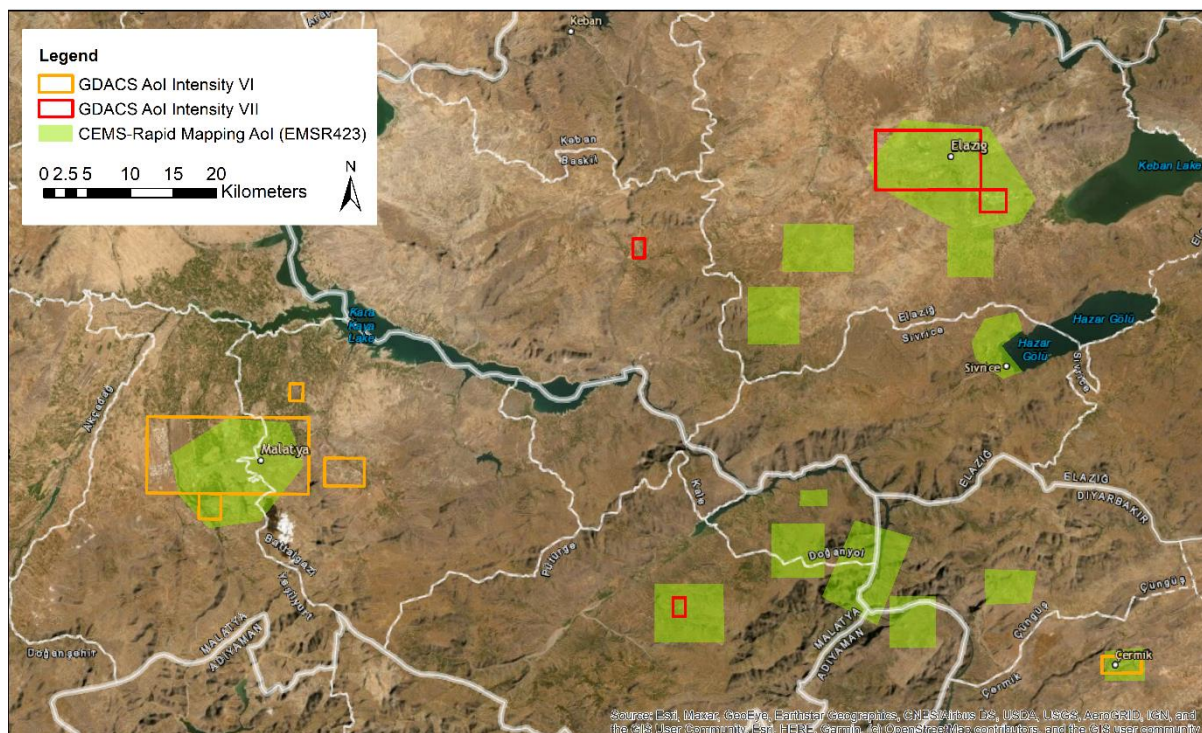


Figure 35 Earthquake in Turkey 24 January 2020: comparison of Aols generated by GDACS and the areas which were analysed under CEMS-Rapid Mapping for actual impact using satellite images. The satellite-based impact assessment confirmed damages in the GDACS Aols of the highest intensity class.

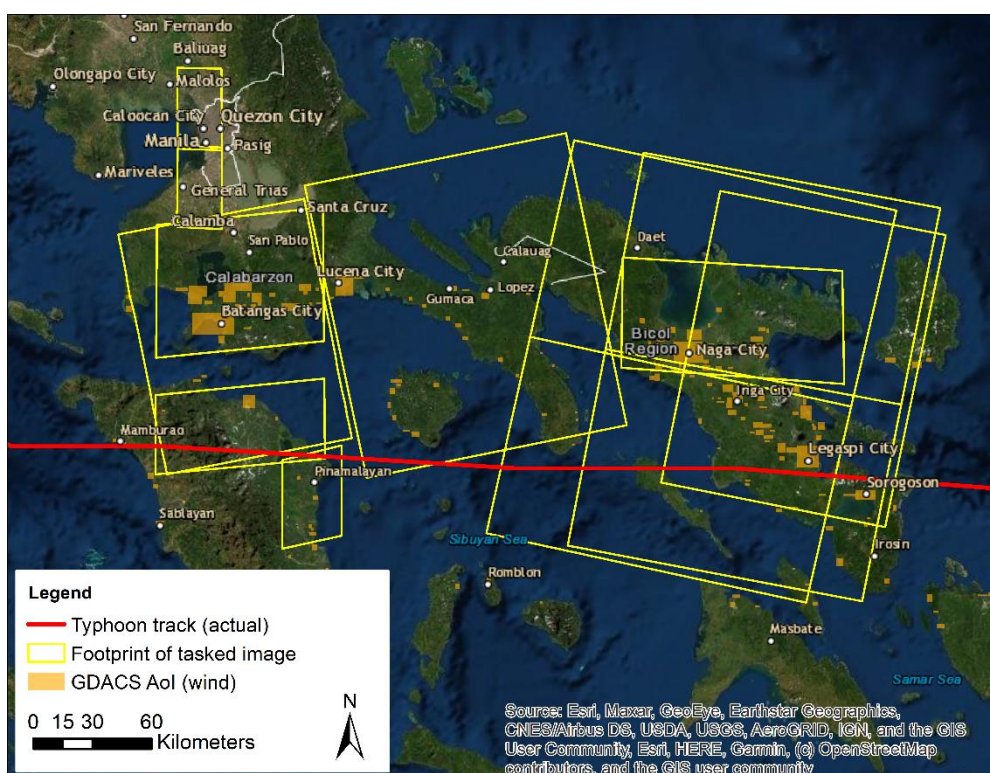


Figure 36 Typhoon Kammuri December 2019: comparison of Aols generated by GDACS (wind impact), actual storm track and the footprint of pro-actively tasked satellite images.

3.1.11 GHSL datasets in the Mapping component of the Copernicus Emergency Management Service

Relevant datasets to provide estimates on the population exposed to natural disasters

Wania A., Spruyt P., Joubert-Boitat I.

The Copernicus Emergency Management Service (CEMS) uses the analysis of satellite images to support the management of emergencies and to support the assessment of disaster risk. . Since 2012 it supports actors involved in disaster management with timely information for all phases of the disaster management cycle (before, during and after an event). Its mapping component offers for a specific disaster event anywhere in the world on-demand information, which is mostly derived from satellite imagery and combined with other ancillary information. The Rapid Mapping Service provides geo-spatial information in support of emergency management activities immediately following an emergency event. The Risk & Recovery Mapping is targeting the support of emergency management activities not related to the immediate response and in particular to activities dealing with prevention, preparedness, disaster risk reduction and recovery phases.

Both Rapid- and Risk & Recovery Mapping are typically providing information on the exposed population and assets. For this, the information extracted from the satellite imagery is combined with other ancillary datasets enabling users to e.g. locate assets, identify access routes, define measures to save lives or measures which reduce the impact from or even prevent a potential future disaster. Knowing how many people are possibly affected by a disaster and where they are located with respect to the impacted area is an important piece of information and the GHSL collection provides very relevant datasets for Rapid- and Risk & Recovery Mapping activations. The strengths of the collection are its open access, usability, reliability and global coverage. In Rapid Mapping the population dataset is used as default to provide an estimate of the people living in or close to the affected area. Open datasets are the preferred solution in Rapid Mapping, because they can be integrated in the highly standardised production workflow before the service is triggered by a user and therefore allow a smooth and fast generation and delivery of the products to emergency response actors. The products contain a so-called consequences table, which provides in tabular form a summary of the disasters' estimated consequences (exposure) on assets and population. Figure 37 below shows one of the output formats – a ready to print map – which provides a visual of the consequences table.

In the Risk & Recovery module, GHSL datasets are occasionally used. In a recent activation (EMSN054) they were used to assess the risk of flooding and its economic impact within a transboundary area. The area corresponds to the Drin river catchment area and more specifically to the part which extends into four (out of the five) countries, namely Albania, Kosovo, North Macedonia and Montenegro. The products were supporting the Drin River Cooperation agreement in the sustainable management of water resources in the Drin catchment area with the provision of relevant information for risk preparedness and sustainable development. More specifically, the European Settlement Map and GHS population grid were used to facilitate the downscaling of economic information from the Global Assessment Report (GAR) to a higher resolution providing an adequate representation of the built-up areas in general and specifically in areas with small/sparse urban densifications. Consequently, the population layer from GHSL was used to distribute population with a good level of accuracy, covering both urban and rural areas. Figure 38 below shows the transnational Drin River Basin Area of Interest.

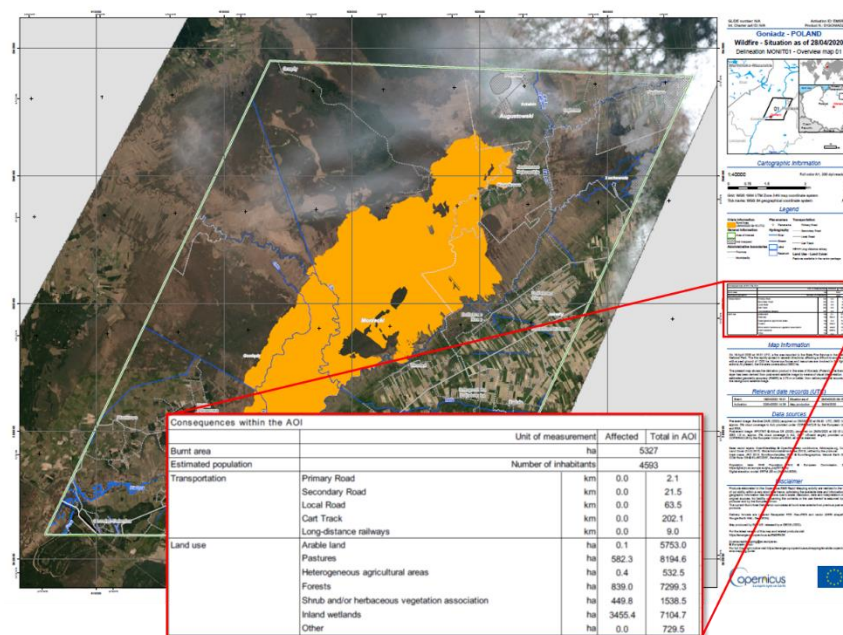


Figure 37 Example of one of the output formats of CEMS-Rapid Mapping products - a ready to print map - which provides a visual of the consequences table displaying among others the estimated population in the area of interest (Copernicus EMS © 2020, [EMSR436: Fire in Podlaskie Voivodeship, Poland: Delineation product, Monitoring 01])

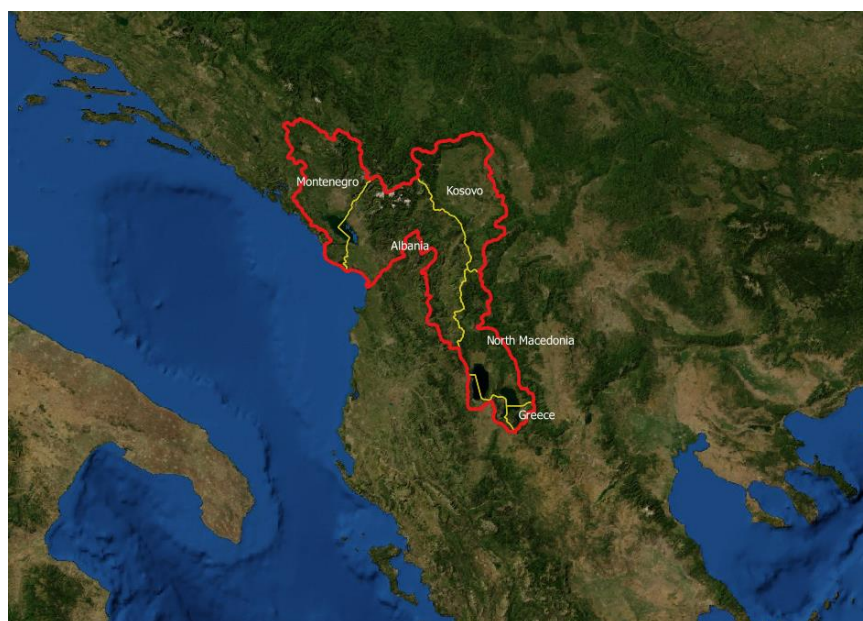


Figure 38 Area of interest of the Risk & Recovery Mapping activation (EMSN054) extending over the transnational Drin River Basin. The European Settlement Layer and GHS population grid were used to facilitate the downscaling of economic information from the Global Assessment Report.

References:

CEMS - Rapid Mapping activation EMSR436: Fire in Podlaskie Voivodeship, Poland. April 2020, access <https://emergency.copernicus.eu/EMSR436>

CEMS - Risk & Recovery Mapping activation EMSN054: Assessment of flood risk and economic impact, Drin river basin, Balkans. August 2019. <https://emergency.copernicus.eu/EMSN054>

3.1.12 After conflicts in Iraq

How to support displaced and vulnerable returnees

Park H., Hamilton E.

Since 2014, about 6.1 million Iraqis have been forcibly displaced due to armed conflicts and unstable conditions. Of these, about 1.4 million remain displaced while 4.7 million have returned. For this analysis, we focus on the 1.4 million Internally Displaced Persons (IDPs) as well as the 0.23 million vulnerable returnees who returned to their home areas but did not return to their previous residences. Despite overall declines in violence, displaced households and returnees are at higher risk of poverty and more likely to live in inadequate housing with limited access to basic services. 40% of IDPs reside in camps, informal settlements, and abandoned buildings, and more than 10% of returnees could not stay in their habitual residences in Diyala and Salah al-Din governorates. To better assist these vulnerable groups, it is essential to understand their locations since potential solutions differ in cities, peri-urban, and rural areas.

This showcase analyses IDPs and vulnerable returnees by location using the newly UN-endorsed global definition of cities, urban, and rural areas. By combining survey data from the International Organization for Migration's (IOM) geo-referenced Displacement Tracking Matrix (DTM) with the GHSL Settlement Model grid (GHS-SMOD), we enhanced our understanding of the spatial distributions of returnees and IDPs across Iraq. Since the DTM collected the geo-coordinates (i.e., neighbourhoods) of returnees and IDPs, we were able to map the locations of them accurately and then quantitatively assess the number and characteristics of vulnerable returnees and IDPs in urban, suburb, and rural settings.

The IDPs and vulnerable returnees are mostly found in cities (43%) or peri-urban areas (23%). In Nineveh and Erbil governorates, those vulnerable people residing in the city are 160 thousand and 145 thousand, respectively. The proportion of vulnerable urban households vary across governorates (from 21% to 86%). This analysis helps us to think about how to identify, design, improve and run policy interventions, as well as where support is needed. Displacement from conflict tends to be protracted. The population profiled here has been displaced for years and have not returned to their original dwellings even as others have. The common problem is that these IDPs have no unit to return to; it may have been destroyed or occupied by someone else. Some of those still displaced may prefer not to return to their original areas for other reasons connected with security or changes in ethnic composition. Regardless of the reason for continued displacement, this group of displaced and vulnerable returnees is in urgent need of integrated support, enabling them to overcome the challenging living conditions they find themselves in.

By analysing the locations of IDPs and vulnerable returnees, as shown in Figure 39, we can see the divergent spatial patterns of the two groups. In much of the country, the groups are spatially separated, but in some areas, such as Mosul and Tikrit, the groups live side by side. In Mosul, as can be seen in Figure 40, the IDPs and returnees coexist within the same neighbourhood. This spatial proximity has important policy implications given the importance of a place-based approach in a conflict-affected area facing complex and multisectoral challenges. First, the sectoral and/or target group programs aimed only at one group (say vulnerable returnees) may create grievances by excluding those living close by under similar conditions who are considered to be displaced, not returnees. Second, spatial proximity creates an opportunity to support returnees, displaced, and other urban poor living in the same vulnerable conditions through place-based interventions such as urban upgrading and recovery planning. One advantage of place-based approaches is that it does not require identifying specific people for support and instead benefits all in a community. Ultimately, it aims to provide a platform to bring diverse stakeholders together in order to improve social cohesion, which has deteriorated during the conflicts.

This short synthesis is aimed to illustrate how combining the settlement typologies— i.e., GHS-SMOD—and DTM data provides improved information useful for better decision making. Although done for Iraq, this kind of approach would be useful in other conflict contexts as well.

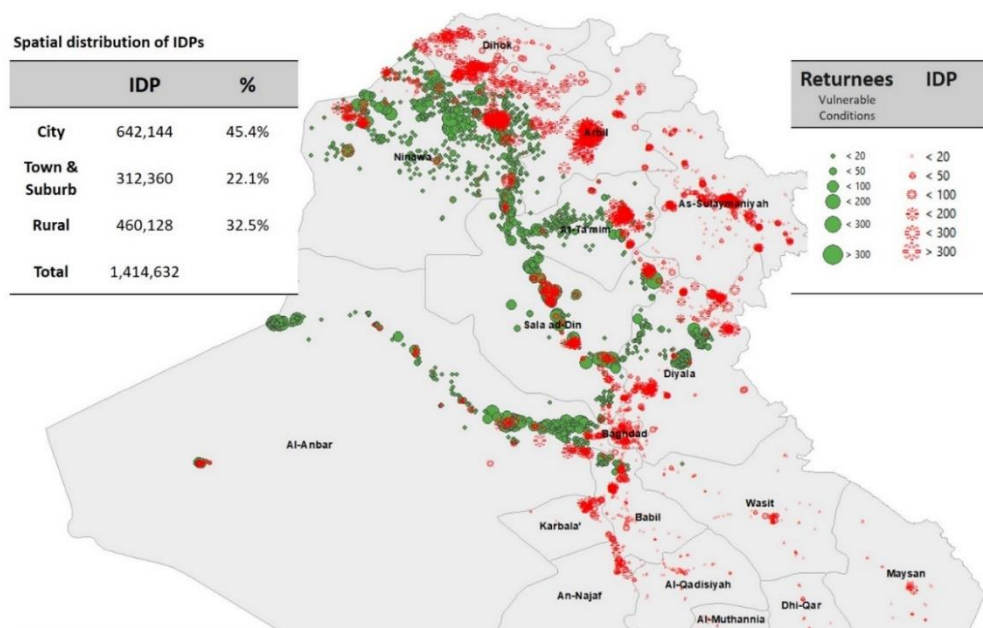


Figure 39 Spatial distribution of IDPs and Returnees with the vulnerable condition across entire Iraq

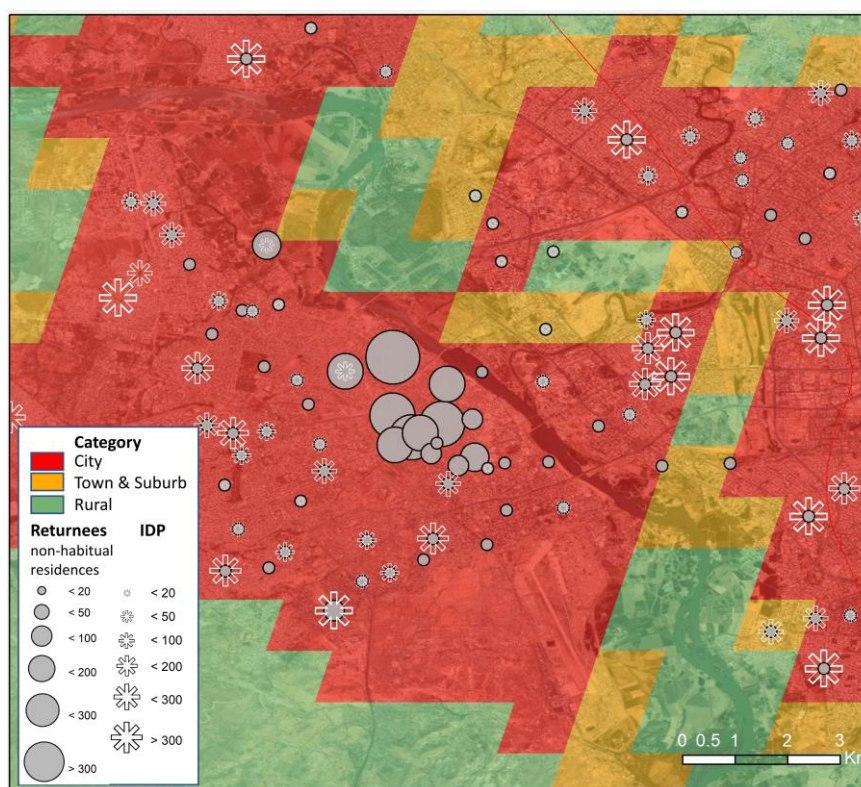


Figure 40 Snapshot of Mosul, Iraq, by combining the GHS-SMOD layer and DTM data

References:

Pesaresi, Martino; Florczyk, Aneta; Schiavina, Marcello; Melchiorri, Michele; Maffenini, Luca (2019): GHS settlement grid, updated and refined REGIO model 2014 in application to GHS-BUILT R2018A and GHS-POP R2019A, multitemporal (1975-1990-2000-2015), R2019A. European Commission, Joint Research Centre (JRC)

IOM (2019): Iraq Displacement Tracking Matrix (DTM) Round 113, retrieved from <http://iraqdtm.iom.int/archive/Home.aspx>

ESRI(2019) World Imagery, Sources: Esri, DigitalGlobe, GeoEye, i-cubed, USDA FSA, USGS, AEX, Getmapping, Aerogrid, IGN, IGP, swisstopo, and the GIS User Community

3.2

Urbanisation



3.2 Urbanisation

Urban areas host the majority of global population, and this proportion continues to grow everywhere. Urbanisation is among the most emblematic aspects of collective human activities, and this continuous process is one of the current societal megatrends. Over the last decades, the increase of the urban population share and the physical expansion of urban areas has given a clear urban character to contemporary societies. New technologies and datasets help improving the collective understanding of the process of urbanisation. This process is characterised by rapid change both in social and economic aspects, but also have a clearly spatial manifestation. As complex systems, urban areas require more integrated tools for their analysis and multi-sectoral policies to funnel significant change. As the global governance elaborated a common strategy for sustainable urbanisation, local yet globally consistent multi-temporal data on human settlements are increasingly perceived as a need for policymaking.

This section presents nine showcases where GHSL data enables production of new information, knowledge and information systems on different aspects of urbanisation, at European, regional and global levels.

The **Cities in the World** report (3.2.1) takes a new look at global urbanisation by analysing GHSL data in combination with other socio-economic datasets. The **Future of Cities** (3.2.2) relies on GHSL analytics to frame what is a city, urbanisation trends, the status of urban development challenges, and to report about the relationship between space and the city. The third showcase highlights key trends of **Metropolitan spaces in Africa** (3.2.3) and their implications on urban governance. The **Degree of Urbanisation** showcase (3.2.4) shows the main features of the method to delineate cities, urban and rural areas for international statistical comparisons and its further integration with GHSL data to monitor indicators.

The second stream of contributions focuses on functional urban areas. The showcase on **Delineating metropolitan areas boundaries in the world using GHSL data** (3.2.5) explains the application of GHSL data to implement a new model for estimating the boundaries of metropolitan areas at global level. The **ESPON FUORE - Functional Urban Areas and other regions in Europe** (3.2.6) shows the use of built-up area data as ancillary data (GHS-BUILT and ESM) to downscale indicators in FUA in Europe and other regions to fill data gaps. GHS-BUILT and European Functional Urban Areas as defined by EUROSTAT are analysed in the showcase **the structure of urban settlements of European functional urban areas** (3.2.7) explaining the morphological modifications that the process of spatial expansion of human settlements is causing in Europe.

The third dimension of showcases on urbanisation focuses on demography. **Population agglomeration and dispersion in Emerging Europe** (3.2.8) examines 25 years of population shifts in human settlements in the European region, mapping diverging trends and patterns concerning population density, supporting economists in the study of agglomeration economies. The last showcase **Analysing global megacities with GHSL data** (3.2.9) dissects the demographics on a sample of 30 such cities and highlights how all of them doubled in population between 1975 and 2015.

3.2.1 Cities in the World

A new perspective on urbanisation enabled by information from the Global Human Settlement Layer
OECD and EC editors

Over the past 40 years, global population has almost doubled. As a result, the size of rural areas, towns and especially cities has also grown rapidly. Today, cities are home to almost half of the global population and this share is projected to reach 55% by 2050. Global megatrends such as the climate emergency, demographic change and digitalisation will affect cities, towns and rural areas in different ways. This underlines the importance of designing efficient and coherent policy responses that are place-specific and cut across different policy domains. Despite the fact that cities are home to around half of the global population, definitions of what a city or a rural area is vary widely by country. Such differences hinder robust international comparisons and prevent accurate monitoring of the United Nation's Sustainable Development Goals (SDGs), as both are highly sensitive to the definitions of those areas.

The *Cities in the World report* (the Report hereafter), a joint initiative by the Organisation for Economic Cooperation and Development and the European Commission (Directorate General for Regional and Urban Policy, and Directorate General Joint Research Centre) analysed GHSL data and integrated it with other data sources, such as the Gallup World Poll geocoded data, to shed lights on the drivers and consequences of urbanisation. The study is based on the application to the entire world of two globally consistent definitions, the degree of urbanisation and the functional urban area, both implemented with GHSL data due to the long temporal coverage and the global scope.

In 1975, 37% of the world's population lived in cities (Figure 42). This share grew to 48% in 2015. It is projected to further increase to 55% by 2050. This shows that urbanisation is slowing down. Up to 2015, the city population share increased by almost 3 percentage points in a decade, while up to 2050 it would be less than 2 percentage points. The rural population share has been shrinking, from 30% in 1975 to 24% in 2015. The projection indicates this reduction would also slow down. Up to 2015, rural population shares dropped by almost 2 percentage points per decade, while afterwards, this is likely to be less than 1. Furthermore, when focusing on the analysis of city growth, the Report shows that the growth of city population has occurred in three ways. One-quarter of the growth was due to the doubling of the number of cities with more than 50 000 inhabitants from approximately 5 000 to 10 000. Half of the growth occurred through densification within original city boundaries. The remaining quarter was due to the spatial expansion of existing cities, which almost doubled in area. In metropolitan areas population has grown most strongly in larger ones. Large metropolitan areas with over 1 million inhabitants grew half a percentage point faster per year than smaller metropolitan areas and have increased by over 400 million new inhabitants since 2000. The fastest growth occurred in metropolitan areas with populations above 5 million. Due to the growth of smaller metropolitan areas, the number of metropolitan areas with more than 5 million inhabitants doubled in just 25 years.

When combining the Degree of Urbanisation with socio-economic data, i.e. on life satisfaction from the Gallup World Poll, it was found that satisfaction with one's standard of living and with life in general differ significantly between cities, towns and semi-dense areas, and rural areas in 111 countries across the world. On average, 18.6% of residents in cities are satisfied with their lives, compared to 16.5% of residents in rural areas (Figure 43). Other evidences suggest that cities and towns and semi-dense areas offer large income premiums, in terms of significantly higher wages and much higher income levels compared to rural areas. The economic benefits of living in densely populated places are even more striking for total household income, which combines income from self-employment, labour, capital and land. In cities, households have income levels more than two and a half times higher than households in rural areas do, although price differences across space are not taken into account. The Report further examines how educational attainment, health outcomes, crime and safety differ across cities, towns and rural areas establishing a precious knowledge base to analyse urbanisation and development policy.

By categorising, measuring and comparing complex patterns of human settlements consistently across the world, the Report helps identify current and future needs to promote prosperous and inclusive cities, towns and rural areas. It also provides a new tool for policymakers to monitor and pursue the United Nations Sustainable Development Goals, and thus makes an active contribution to achieving economic, social, and environmental sustainable development in all areas.

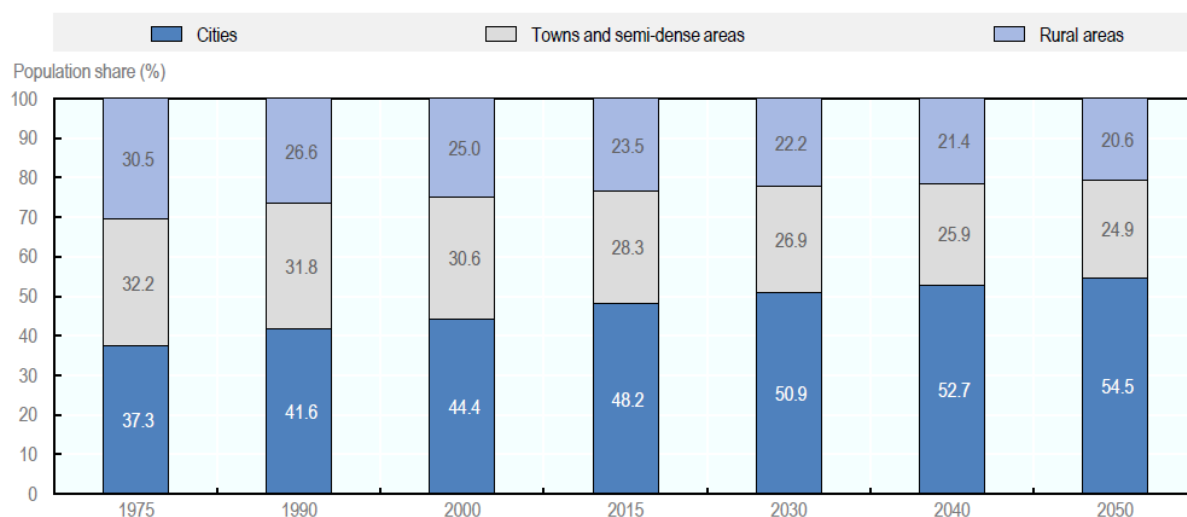


Figure 42 World population shares by degree of urbanisation, 1975-2050. In *Cities of the World* (OECD and EC, 2020) p. 17

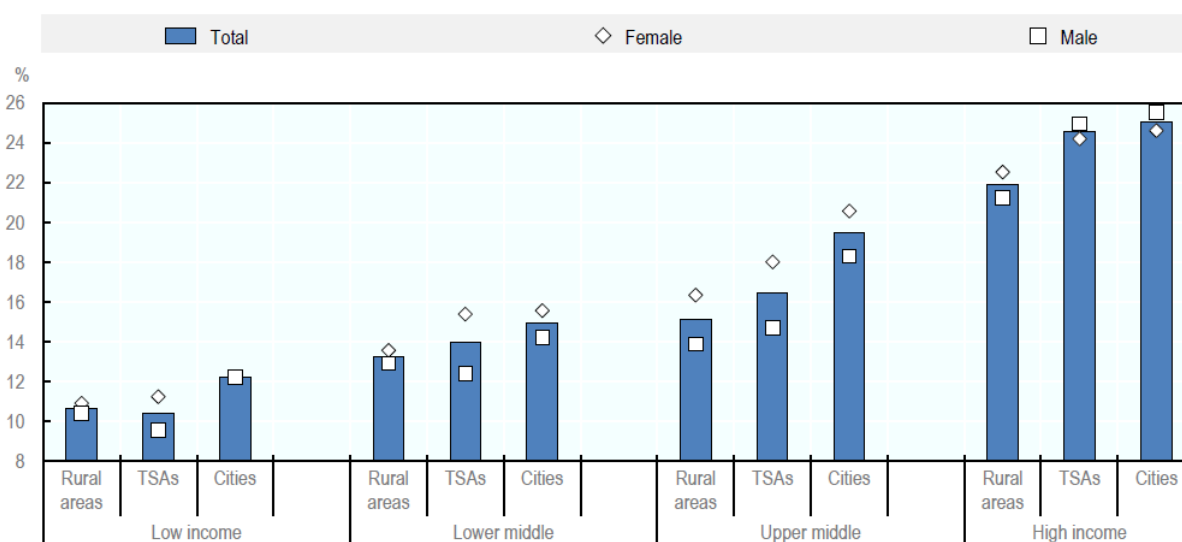


Figure 43 Life satisfaction by degree of urbanisation, income group and gender. Based on Gallup World Poll, 2016-17, <https://www.gallup.com/analytics/232838/world-poll.aspx>; elaborated by EC and OECD, 2019. In *Cities of the World* (OECD and EC, 2020) p. 41

References:

OECD/European Commission (2020), *Cities in the World: A New Perspective on Urbanisation*, OECD Urban Studies, OECD Publishing, Paris, <https://doi.org/10.1787/d0efcbda-en>.

Florczyk, Aneta; Corbane, Christina; Ehrlich, Daniele; Freire, Sergio; Kemper, Thomas; Maffenini, Luca; Melchiorri, Michele; Pesaresi, Martino; Politis, Panagiotis; Schiavina, Marcello; Sabo, Filip; Zanchetta, Luigi (2019) GHSL Data Package 2019. JRC117104. Publications Office of the European Union, Luxembourg. DOI: 10.2760/062975 <http://publications.jrc.ec.europa.eu/repository/handle/JRC117104>

3.2.2 The Future of Cities

Analyzing urbanization trends with the Global Human Settlement Layer (GHSL)
Vandecasteele I., Baranzelli C., Siragusa A., Aurambout J.

The Future of Cities report, published in June 2019, and accompanied by an online platform, was part of a series of Flagship JRC reports produced to inform the incoming European Commission at the end of 2019. The report focussed on the challenges faced in urban areas now and towards the future, and the ways in which cities manage them. Wherever possible, data and statistical analyses were used as evidence to identify and quantify trends in urban areas. The data and analysis provided by the GHSL and the Urban Centre Database were instrumental in this.

Firstly, the GHSL data helped to address the question "What is a City?" – the Degree of Urbanisation was detailed, and used as main city definition wherever possible in the further chapters of the report. In fact, a main message of the report was that, according to this definition, the world is already much more urbanised than previously thought, estimating that 75% of the world population currently live in urban areas, 72% in Europe (EU-28) in 2015.

Secondly, the main urbanisation trends were assessed at a global level using GHSL data. The Urban Centre Database identified and compared global megacities (those with more than 10 million inhabitants): highlighting that the number of large cities has increased significantly over the last 30 years - in 1990, there were 16 megacities worldwide; in 2015, there were 32 (Figure 44). Nearly 40% of overall built-up expansion and nearly 80% of population growth has taken place in the last 25 years in urban areas (Florczyk et al., 2019).

One of the main chapters addressing potential strategies to mitigate challenges faced by cities looked at the use of public and green space in urban areas. Also here, GHSL data provided a main source of evidence for trends. Analysis using GHSL data emphasized that urban sprawl and the inefficient use of land remains a problem, with cities globally having grown in size by an area equal to that of Greece since 1975, and 59% of cities having also seen an increase in land consumed per new resident (Melchiorri, 2018). The importance of green infrastructure in urban areas was also emphasized, and GHSL analysis revealed that while globally the greenness of cities has grown by 12%, in Europe it has increased by 38% over the last 25 years (Pesaresi et al., 2016).

The report was a first collaborative project produced by the newly-formed Community of Practice on Cities and was well-received. It is currently being used as source material for the re-drafting of the Leipzig Charter on Sustainable European Cities (Figure 45).

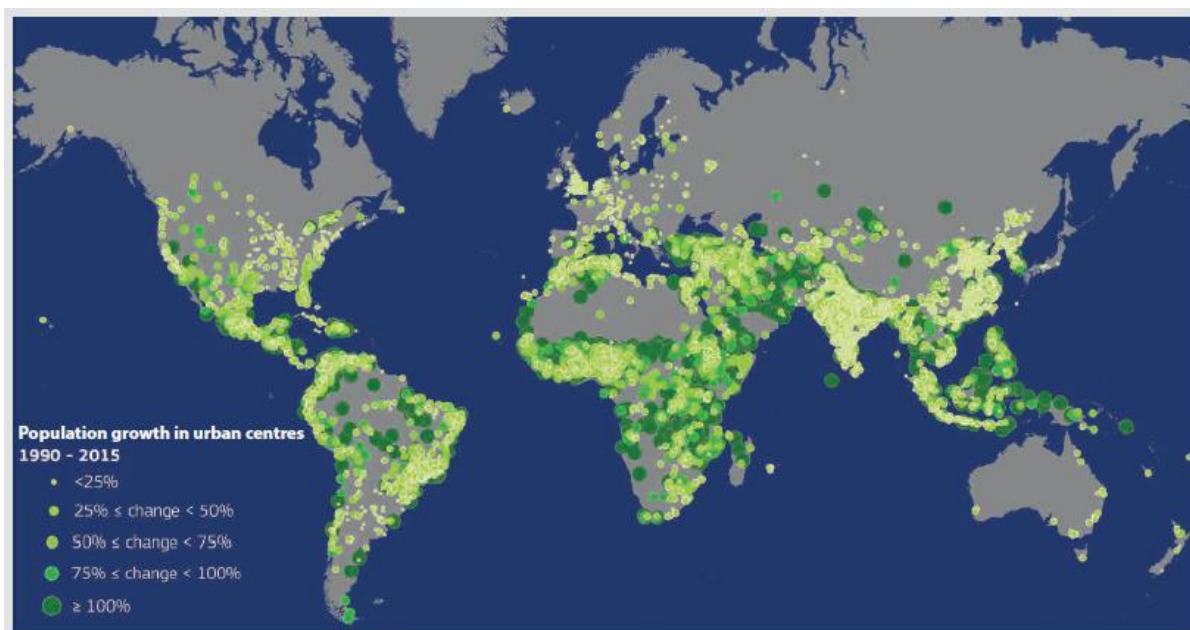


Figure 44 .Population Growth in urban centres 1990-2015, from the Urban Centres Database, as published in the Future of Cities Report. Web visualisation of the GHSL urban centre database in the Urban Data Platform Plus



Figure 45 Infographic showing one of the main key messages on demographics in European cities taken from the Future of Cities Report

References:

Vandecasteele, I., Baranzelli, C., Siragusa, A. and Aurambout, J. editors, Alberti, V., Alonso Raposo, M., Attardo, C., Auteri, D., Ribeiro Barranco, R., Batista E Silva, F., Benczur, P., Bertoldi, P., Bono, F., Bussolari, I., Louro Caldeira, S., Carlsson, J., Christidis, P., Christodoulou, A., Ciuffo, B., Corrado, S., Fioretti, C., Galassi, M., Galbusera, L., Gawlik, B., Giusti, F., Gomez Prieto, J., Grosso, M., Martinho Guimaraes Pires Pereira, A., Jacobs, C., Kavalov, B., Kompil, M., Kucas, A., Kona, A., Lavallo, C., Leip, A., Lyons, L., Manca, A., Melchiorri, M., Monforti-Ferrario, F., Montalto, V., Mortara, B., Natale, F., Panella, F., Pasi, G., Perpiña Castillo, C., Pertoldi, M., Pisoni, E., Roque Mendes Polvora, A., Rainoldi, A., Rembges, D., Rissola, G., Sala, S., Schade, S., Serra, N., Spirito, L., Tsakalidis, A., Schiavina, M., Tintori, G., Vaccari, L., Vandyck, T., Vanham, D., Van Heerden, S., Van Noordt, C., Vespe, M., Vetter, N., Vilahur Chiaraviglio, N., Vizcaino, M., Von Estorff, U. and Zulian, G., The Future of Cities, , EUR 29752 EN, Publications Office of the European Union, Luxembourg, 2019, ISBN 978-92-76-03847-4 (online),978-92-76-03848-1 (print), doi:10.2760/375209 (online),10.2760/364135 (print), JRC116711.

3.2.3 Metropolitan Spaces in Africa

Metropolis and the GHSL Urban Centre Database
Brum L., Bannister S., Sutcliffe M.

Metropolis is the metropolitan section of the World Organisation of United Cities and Local Governments (UCLG). To understand the scale of changes caused by factors such as urbanisation, climate change and changing demographics amongst its members, the governments of major cities across the globe, Metropolis has collected data for a range of indicators on governance, economic development, social cohesion, gender equality, environmental sustainability and quality of life.

In order to analyse and contextualise this data, Metropolis commissioned the first study in a series to analyse the data for specific regions, in the African Metropolitan Report. Metropolis defines metropolisation as the process of urban areas growing together into a larger functional urban space without regard for the specific jurisdictional definition of the units concerned, and data for the indicators is collected for the functional metropolitan spaces which are often made up of one or more administrative units. This methodology aligns with the Global Human Settlement Layer (GHSL) approach which allows for analysis beyond administrative borders. Importantly, though, the approach taken in this work combined the GHSL data with data on a wide range of indicators collected for 17 African metropolitan spaces.

Figure 46 indicates the urban spaces in Africa, classified by city population size, while Figure 47 uses this data to show changes over time. In 2015, there were 65 African settlements that each accommodated over one million residents, containing 192 million people and characterised by high growth rates, high densities, low levels of access to services, and high levels of poverty.

The 17 African metropolitan areas analysed show that whilst rates of growth are slowly declining, they are still significantly higher than those in urban areas in the rest of the world, providing significant governance and service delivery challenges. Population density is relatively high compared to world averages, but varies significantly across cities and is not always aligned to economic density.

The governance of African metropolises has a slightly higher degree of metropolitan coordination compared to other world regions, and a lower level of fragmentation. Policy leadership is also higher than the average for the rest of the world, yet budgets are proportionally lower, effectively allowing metropolises to have a greater say over what gets done, but often without the necessary fiscal power to implement it.

Social indicators show that African metropolises have lower levels of female leadership, higher murder levels and lower levels of literacy. Africa is highly vulnerable to climate change due to its dependency on climate related activities and low adaptive capacity. African metropolises have significantly lower levels of GDP per capita compared to all other world regions, and poverty rates are more than double the world average, with the youth shouldering a large portion of the total unemployment. Economic growth is also compromised by the relatively high dependency on work in the primary sector, where employment is characterized by relatively low wages and high levels of inequality.

The African Metropolitan Report was launched at a forum of African mayors and governors during the 6th Congress of United Cities and Local Governments (UCLG) in November 2019.

The project provides further evidence that metropolisation does lead to improvements in governance, economy, social development, gender disparities and the ability to address climate change and improve environmental sustainability. Given that African metropolisation rates are higher than global rates, as these spaces develop it is expected that in time the disparities between African metropolitan spaces and the rest of the world will reduce. However, this is only likely to happen if the trends towards the decentralisation of developmental powers and functions to sub-national and particularly metropolitan levels of governance continue. In particular, the provision or facilitation of basic services, including water, electricity, sanitation and waste removal, reduction of disparities and the like should all contribute to this process of improved governance.

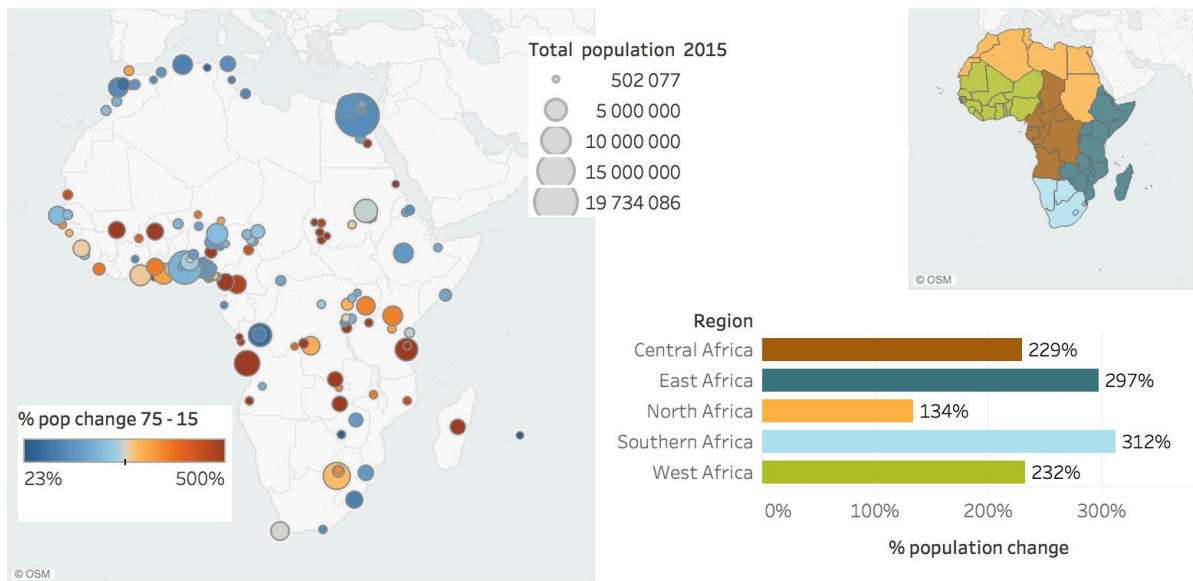


Figure 46 Population growth in large cities in Africa 1975 - 2015

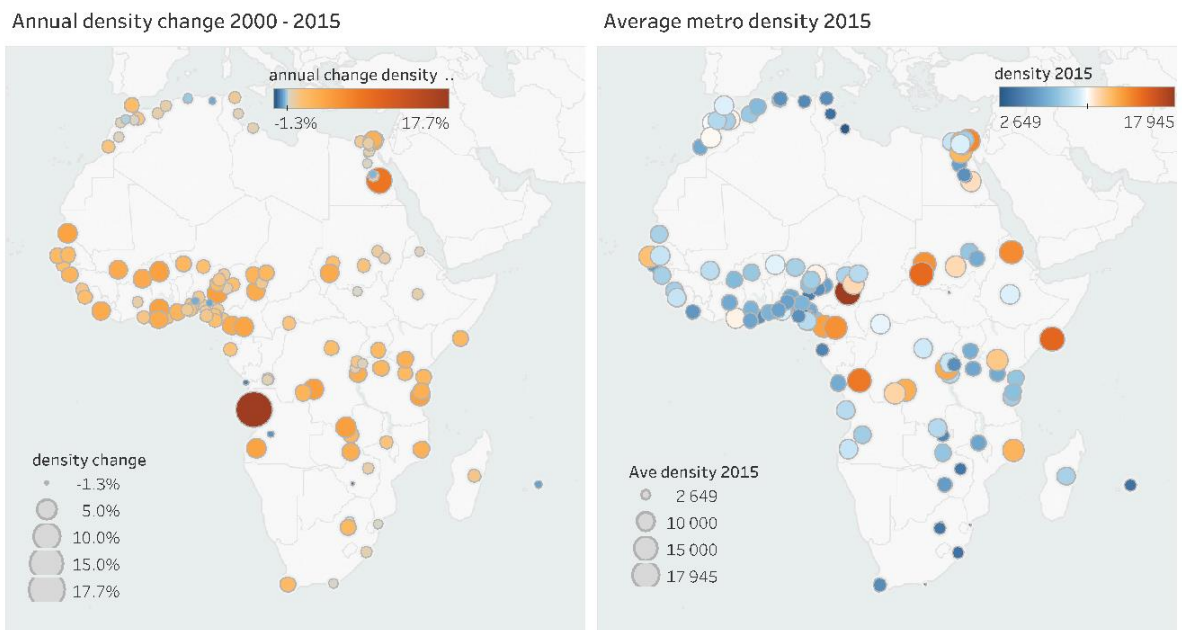


Figure 47 Map of annual density change for metropolises between 2000 and 2015 and average density in 2015

References:

Florczyk, A.J., Melchiorri, M., Corbane, C., Schiavina, M., Maffneni, M., Pesaresi, M., Politis, P., Sabo, S., Freire, S., Ehrlich, D., Kemper, T., Tommasi, P., Airaghi, D. and L. Zanchetta, Description of the GHS Urban Centre Database 2015, Public Release 2019, Version 1.0, Publications Office of the European Union, Luxembourg, 2019, ISBN 978-92-79-99753-2, doi:10.2760/037310, JRC115586.

Metropolis, <https://www.metropolis.org/projects/metropolitan-indicators>

2018 revision of the World Urbanization Prospects by UN DESA's Population Division

3.2.4 The Degree of Urbanisation

A new global definition of cities, urban and rural areas enabled by GHSL

Melchiorri M., and Dijkstra L.

National definitions of urban and rural areas differ significantly from one country to another, and this makes it difficult to compare areas across national borders. If the performance of urban and rural areas cannot be compared across countries, then policy transfer and statistical comparison become less reliable. In addition, several new global agendas call for the collection of harmonised indicators disaggregated by cities, and by urban and rural areas. That is why six international organisations, the European Union, The Food and Agriculture Organization of the United Nations (FAO), the International Labour Office (ILO), the Organization for Economic Co-operation and Development (OECD), United Nations Human Settlements Programme (UN-Habitat) and the World Bank, have been working closely together to develop a harmonised method to facilitate international statistical comparisons. The work towards a harmonised people-based definition of cities and settlements was launched at the Habitat III conference in 2016 with the explicit aim to organise global consultations and present the new method to the UN Statistical Commission for endorsement. The 51st Session of the UN Statistical Commission has endorsed the Degree of Urbanisation as recommended method to delineate cities, urban and rural areas for international statistical comparisons.

The Degree of Urbanisation classifies the entire territory of a country along the urban-rural continuum. It combines population size and population density thresholds to capture the full settlement hierarchy. It is applied in a two-step process: First, 1 km² grid cells are classified based on population density, contiguity and population size (Figure 48, left). The Degree of Urbanisation is applied to a 1 km² population grid to identify: Urban Centre grid cells, Urban Cluster grid cells, and Rural grid cells. Subsequently, local units are classified based on the type of grid cells where the majority of their population resides in. This method works best with small administrative or statistical units, such as municipalities or census enumeration areas (Figure 48, right), units are classified as: Cities if a local unit has at least 50% of its population in urban centres; Towns and semi-dense areas if a local unit has less than 50% of its population in urban centres and less than 50% of its population in rural grid cells; and Rural areas if a local unit has at least 50% of their population in rural grid cells.

The Degree of Urbanisation has several advantages: it is simple and transparent, relying on the simple combination of population size and density applied to the population grid; it helps monitoring progress on the SDGs because many indicators require urban/rural disaggregation or are sensitive to the ways boundaries are drawn; it captures agglomeration economies because the definition is based on the spatial concentration of the population.

The Degree of Urbanisation was applied by EUROSTAT and DG-REGIO in Europe since 2011. Thanks to the GHSL (GHS-POP and GHS-BUILT) it was first applied to the globe in 2016, and subsequently refined with a second hierarchical level (Level 2). The Degree of Urbanisation level 2 is a sub-classification level 1. It was created to identify medium and small settlements, i.e. towns and villages, identifying 7 settlement types. The Degree of Urbanisation at Level 2 was publicly released by JRC in 2019 as GHS-SMOD. The GHSL was the core information for a global consultation with 86 countries organised jointly by UN-Habitat and the European Commission in 2018 – 2019. The consultations were held across the globe involving representatives of National Statistical Offices, Land, Housing and Planning Ministries. To serve these needs and additional capacity building requirements, the GHSL was used to produce *Country Fact Sheets* for 224 countries and territories to support discussions and refinements of the Degree of Urbanisation.

The Degree of Urbanisation portrays a different situation of global urbanisation when compared to the World Urbanization Prospects. It estimates about half of global population lived in urban centres in 2015, 28% lived in towns and semi-dense areas and 24% in rural areas. Combining the Degree of Urbanisation with GHSL data on built-up and population, JRC researchers identified that in the majority of countries in the Global North, the built-up area per capita in 2015 is at least 25% higher than global average, and in several countries it is even double or more the global average (Figure 49). The built-up area per capita is an effective metric to support the SDG indicator on land consumption (11.3.1). With the continued update of GHSL this change can be monitored.

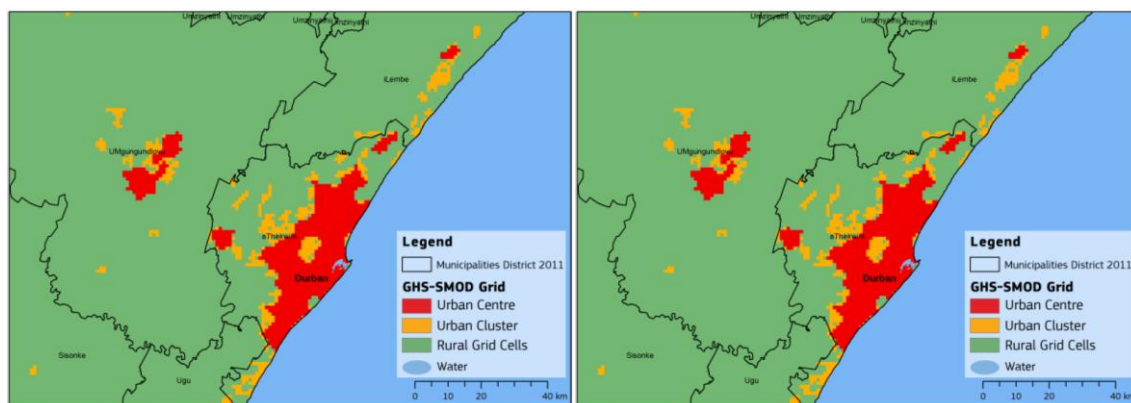


Figure 48 Degree of Urbanisation at level 1 in the area of Durban displayed at grid level GHS-SMOD on the left, and applied to local units on the right

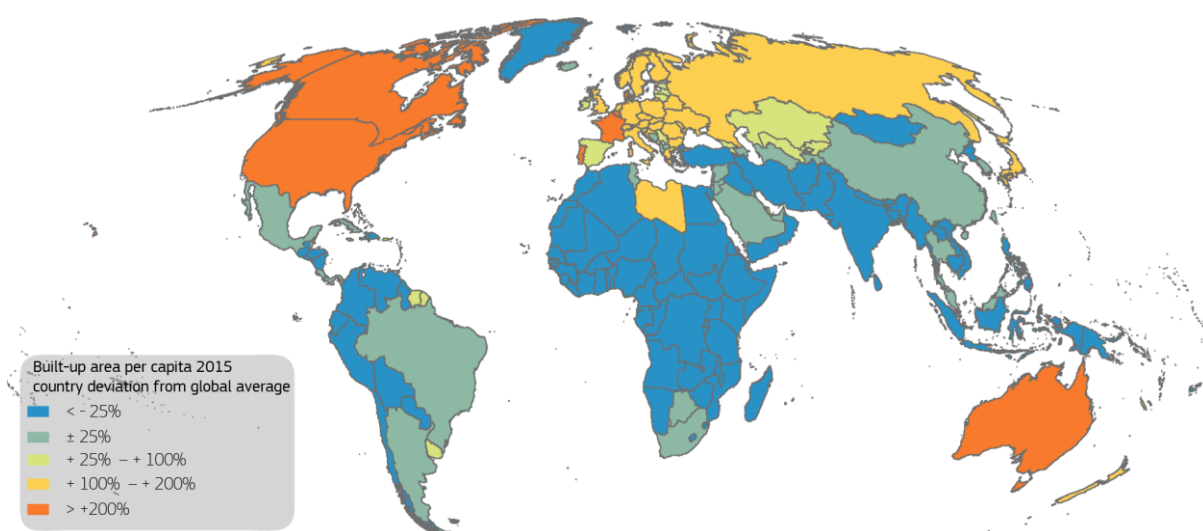


Figure 49 Country deviation from global average built-up area per capita 2015

References:

Florczyk, Aneta; Corbane, Christina; Ehrlich, Daniele; Freire, Sergio; Kemper, Thomas; Maffenini, Luca; Melchiorri, Michele; Pesaresi, Martino; Politis, Panagiotis; Schiavina, Marcello; Sabo, Filip; Zanchetta, Luigi (2019) GHSL Data Package 2019. JRC117104. Publications Office of the European Union, Luxembourg. DOI: 10.2760/062975 <http://publications.jrc.ec.europa.eu/repository/handle/JRC117104>

European Commission (2019), Atlas of the Human Planet 2019 — A compendium of urbanisation dynamics in 239 countries, JRC 118979, EUR 30010 EN, Publications Office of the European Union, Luxembourg.

3.2.5 Delineating boundaries of metropolitan areas in the world using GHSL data

A new method to estimate functional urban areas at the global level

Moreno-Monroy A., Schiavina M., Veneri P.

The OECD, in collaboration with the European Commission, has developed a method to estimate the boundaries of metropolitan areas. According to the OECD-EU method, metropolitan areas are defined as “Functional Urban Areas” (FUAs), which are composed of cities plus their surrounding commuting zones (OECD, 2012; Dijkstra, Poelman and Veneri, 2019). The purpose of the concept of FUA is to support robust international comparative analysis on socio-economic, environmental and well-being issues related to metropolitan areas and, more in general, to the agglomeration of people in space. In addition, a consistent definition of metropolitan areas’ boundaries is crucial to ensure comparability of statistical indicators at this scale and to support decision making in many policy domains, including transport, land-use, housing and spatial planning more in general.

The backbone of the method to delineate functional urban areas relies on gridded population data in order to perform the first step of the method, which consist in defining urban centres (clusters of grid cells with at least 50,000 inhabitants and a density of at least 1,500 inhabitants per square kilometre). The urban centre is subsequently adapted to local unit (i.e. municipalities) boundaries to define a ‘city’. Finally, other municipalities that surround the city and send to the latter at least 15% of their workforce on a daily basis are included in the FUA as part of the ‘commuting zone’. This EU-OECD method was applied to all European and OECD countries.¹⁹

More recently the OECD and EC Joint Research Centre developed a method to estimate the boundaries of FUAs at the global level (Moreno-Monroy, Schiavina, Veneri, 2020). The challenge was to delineate FUAs in the absence of any information on local unit boundaries and commuting data, which are not available on a global scale. For that purpose, the method uses only gridded data available at a global scale. GHSL data was a crucial data source, which allowed to define urban centres at a global scale.

Once the urban centre was defined, the global method estimates the extent of commuting zones through a probabilistic approach performed through a logistic regression model. The latter is trained using information on actual FUA boundaries in OECD countries where the EU-OECD definition was already available.

The method delineates about 9,000 estimated functional urban areas of at least 50,000 inhabitants, worldwide. Figure 50 (left) shows the boundaries of the FUA of Medellin (Colombia), distinguishing urban centre and its estimated commuting zone. Overall, More than half of the world population live in functional urban areas, with the largest share in North America (72%) and the lowest in Africa (44%). High-income countries tend to have large proportions of population living in FUAs, as well as an average larger size of FUAs.

An important advantage of FUA is that they allow assessing the population living outside cities, but in their close proximity, meaning in the commuting zones. Population in the commuting zones represent 17% of total FUA population and about 9% of the world population. What is clear from the results is that large commuting zones are a feature of rich countries (Figure 50 right). North America and Europe have the largest shares (close to 30%) FUA population in commuting zones. The full set of estimated FUAs can be explored, along with a set of indicators on population, built-up areas and air quality, in a dedicated web-tool available at the url: www.worldciestool.org, whose layout is depicted in Figure 51.

The tool allows to visualise all World FUAs in a simple interactive map. FUAs can be selected individually and by country. The user can select a specific FUA or urban centre, the indicator to be shown and the year of reference for the indicators, which ranges between 1975 and 2015. The tool includes a function to easily download all the statistical indicators visualised in the map, as well as the shape file for the FUAs’ digital boundaries.

¹⁹ See <http://www.oecd.org/regional/regional-statistics/functional-urban-areas.htm>

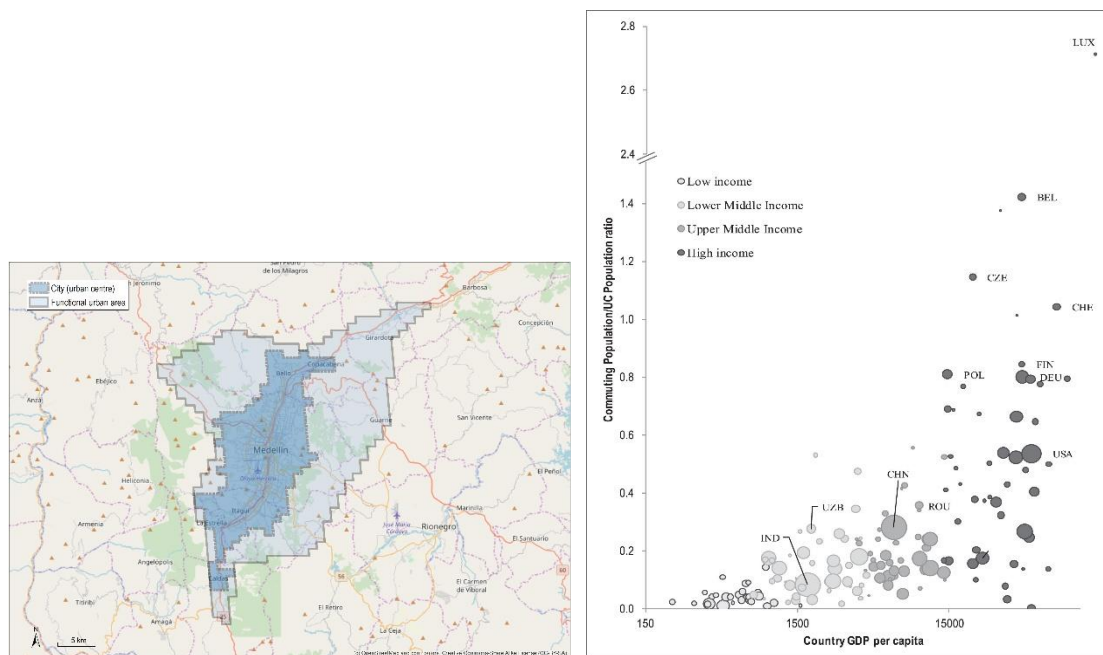


Figure 50 (left) The metropolitan area of Medellin, Colombia. (right) Development level and importance of commuting zones



Figure 51 A web-tool to explore Functional Urban Areas across the world. Source: www.worldcitiestool.org

References:

- Dijkstra, L., H. Poelman and P. Veneri (2019), "The EU-OECD definition of a functional urban area", *OECD Regional Development Working Papers*, No. 2019/11, OECD Publishing, Paris, <https://doi.org/10.1787/d58cb34d-en>.
- Moreno-Monroy, A., Schiavina, M., Veneri, P. (2020) Metropolitan areas in the world. Delineation and population trends, *Journal of Urban Economics*, DOI: <https://doi.org/10.1016/j.jue.2020.103242>
- OECD (2012), Redefining "urban". A New way to understand metropolitan areas. OECD Publishing, Paris.

3.2.6 ESPON FUORE - Functional Urban Areas and other regions in Europe

Using ESM and GHSL for downscaling demographic indicators across Europe

Milego R., Ramos M. J., Domingues F., López J., Michelet J., Martín B., Arévalo J., Passarello G., Barbosa A., Jupova K., Larrea E., Biosca O., Hermansons Z.

In order to improve the relevance, efficiency and effectiveness of the policymaking and implementation process regarding functional urban areas and other functional regions, it is essential to have data, indicators and analysis tools that can help to better understand the drivers for growth and inclusive social development in these areas. However, data required for decision-making, such as statistical figures and indicators, are generally available only for administrative territorial units. The *ESPON FUORE - Functional Urban Areas and Other Regions in Europe* project has developed a methodology (figure 1) to estimate different demographic, socio-economic and environmental indicators (by nine different functional regions (namely Functional Urban Areas, Coastal areas, Maritime Service Areas, Mountain massifs, Sparsely populated areas, Border areas (narrow and wide), and Green Infrastructure areas). The base indicators are spatially reported following two different Nomenclature of Territorial Units for Statistics (NUTS): NUTS2 (basic regions for the application of regional policies) and NUTS3 (small regions for specific diagnoses). From these base indicators the FUORE method can generate more detailed maps (i.e., downscaling), in terms of spatial resolution, using “ancillary” datasets which covariate with the source indicator. The downscaled data are eventually aggregated to the different functional regions.

In the context of the methodology developed, specifically in the case of the demographic indicators, the main ancillary dataset guiding the downscaling process is the European Settlement Map (ESM), whereas for socioeconomic and environmental indicators the Statistical classification of economic activities in the European Community (NACE at LAU level) has been used. However, ESPON spatial extent covers Europe, including Turkey and the Balkans, as well as French outermost regions in America and Africa. Therefore, the disaggregation of ESPON indicators requires a specific ancillary dataset covering those areas. In this way, the Global Human Settlement Layer built-up grid (GHS-BUILT) guided the disaggregation of demographic indicators for regions not covered by the European Settlement Map (ESM). A final refinement of the estimates is latterly conducted for all indicators, using Corine Land Cover-Refine (CLC-R) as additional ancillary dataset.

The estimation of indicators is based on a complex methodology of disaggregation by means of the different ancillary datasets, inspired by Batista e Silva and Poelman (2016). Particular weights from the ancillary variables (ESM, GHSL, NACE, CLC-R) were derived and used to populate each 1x1 km grid cell with an estimate of the ancillary variable. The downscaled indicators are eventually aggregated back from the 1x1 km cells to the different functional regions. Whenever official statistics do not exist or there are breaks in time series, FUORE methodology can provide consistent long time-series indicators.

All the new indicators generated by means of the FUORE methodology are presented in the *FUORE Analytical Tool*²⁰. This user-friendly Web Tool allows the users to inspect the complete time series of about 300 estimated indicators through interactive maps and charts (figure 2). In this way, the *FUORE Analytical Tool* provides a unique opportunity to analyse the current situation and trends, and benchmark the different functional regions, covering demography, employment, economy and society, , by means of several analytical functionalities. In addition, and embedded in the same Analytical Tool, a *Custom Disaggregation Tool* allows registered users to easily run the disaggregation-aggregation algorithm themselves, as well as to visually check and validate the outputs resulting from the process. The users of the Disaggregation Tool may provide any NUTS-based indicator and estimate it by functional area, making use of the built-in disaggregation matrices. User-generated data can be eventually added as new data to the *FUORE Analytical Tool*.

²⁰ <https://fuore.espon.eu/>

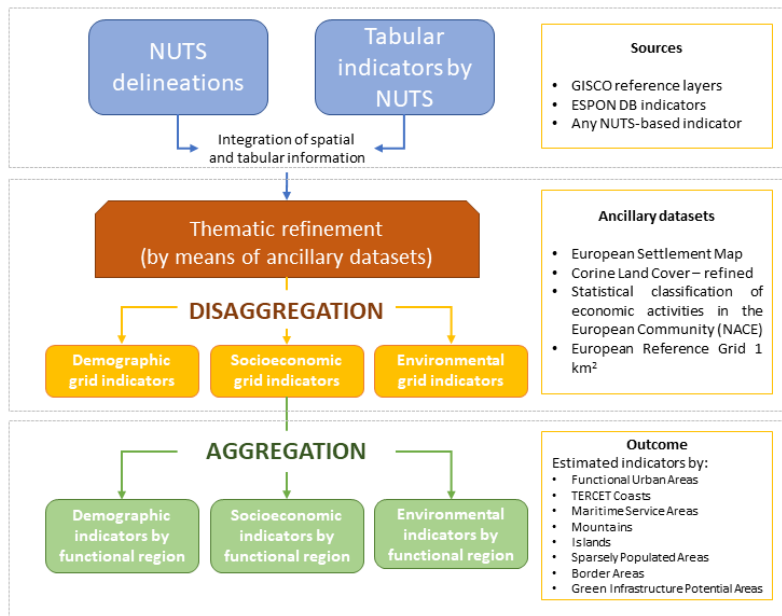


Figure 52 General schema of the disaggregation/aggregation method. (source: ESPON FUORE)

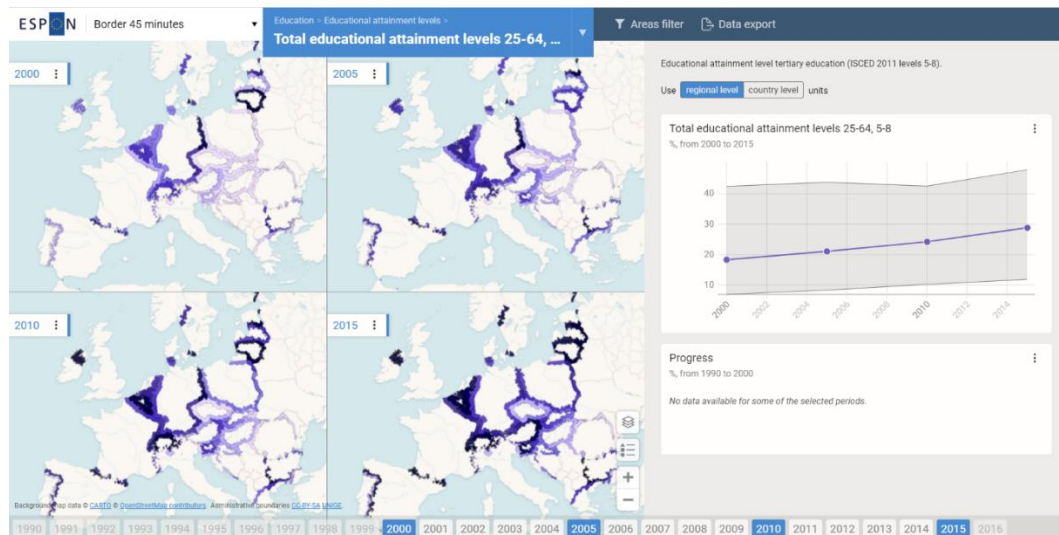


Figure 53 High education attainment levels evolution in border areas (2000-2005-2010-2015), estimated by means of the FUORE methodology using ESM and GHSM as ancillary dataset. Source: Screenshot from the FUORE Analytical Tool

References:

- Batista e Silva, F. & Poelman, H. (2016) Mapping population density in Functional Urban Areas - A method to downscale population statistics to Urban Atlas polygons. JRC Technical Report no. EUR 28194 EN. doi:10.2791/06831.
- Corine Land Cover-Refine (CLC-R): Rosina, K., Batista e Silva, F., Vizcaino-Martinez, Pl, Marín Herrera M.A., Freire, S. & Schiavina, M. 2018. An improved European land use/cover map derived by data integration AGILE 2018 – Lund, June 12-15, 2018
- European Settlement Map (ESM): Ferri, S., Siragusa, A., Sabo, F., Pafi, M., Halkia, M. 2017. The European Settlement Map 2017 Release. Methodology and output of the European Settlement Map; EUR 28644 EN; doi:10.2760/780799
- Global Human Settlement Map (GHSM): Pesaresi, Martino; Ehrlich, Daniele; Florczyk, Aneta J.; Freire, Sergio; Julea, Andreea; Kemper, Thomas; Soille, Pierre; Syrris, Vasileios (2015): GHS built-up grid, derived from Landsat, multitemporal (1975, 1990, 2000, 2014). European Commission, Joint Research Centre (JRC) [Dataset] PID: http://data.europa.eu/89h/jrc-ghsl-ghs_built_ldsmt_globe_r2015b
- Statistical classification of economic activities in the European Community (NACE): <https://ec.europa.eu/eurostat/documents/3859598/5902521/KS-RA-07-015-EN.PDF>

3.2.7 The structure of urban settlements in European Functional Urban Areas

A trend analysis from 1975 to 2014

Zulian G., Maes J.

Understanding and measuring urban growth and settlement patterns is key to effective and sustainable land management. Changes in settlement patterns are related to morphological modifications of urbanized areas and to the diffusion of artificial elements in the urban fringe. The phenomenon involves the transformation of large patches of natural habitats into smaller ones, which tend to be isolated from the original natural habitat (Saganeiti et al. 2018), in many cases having an impact on the structure and connectivity of them. For this reason, peri-urban rural landscape and peri-urban forests suffer the most from this dynamic. Moreover, the urban form has an impact on city performance in terms of mobility, ecosystem services and biodiversity (Cortinovis et al. 2019).

The current analysis of settlement patterns in European functional urban areas is based on the GHS built-up area grid (GHS-BUILT) (Corbane et al. 2019). The dataset represents a comparable, high resolution data set available at a global scale, which allowed a consistent assessment of long and short term trends.

The current methodology is a spatially explicit estimate of the degree of dispersion of built-up areas through a purely geometric point of view (Saganeiti et al. 2018). Assuming the circular form as the most “compact” possible, the index is based on the calculation of distances between different built-up areas on a 2 km buffer around each 1 km grid cell. The higher the value, the higher the degree of land fragmentation. Values greater than 100 represent no-built up areas. In terms of changes, negative values represent a progressive densification of built-up areas. To make the interpretation easier, the indicator has been classified in six key categories, which represent the types of settlement pattern having an impact on city performance (Figure 54).

European cities present a relatively high share of dense settlements, with commuting zones (or the cluster of municipalities around the core city) often assuming the characteristics of conurbations. Between 1975 and 2014 a progressive densification process is reported at EU level (Figure 55. A). An intense transition versus a very dense structure (red and orange dots) characterizes FUAs in England, Belgium and The Netherlands. In the short term, between 2010 and 2014 the process demonstrates a relatively rapid urbanization in eastern, Nordic and Mediterranean cities, probably connected with different stages of socio-economic development of European cities (Figure 55. B).

The current analysis was implemented for the assessment of the state and trends of European ecosystems. In this context key questions were how ecosystems have changed over the last decades and how have these changes impacted people through the altered delivery of ecosystem services (Maes et al, 2020). How cities develop and grow, is strongly related to physical and socio-economic characteristics of the area. Urban form and its dynamic has an impact on land use, in terms of residential, commercial, industrial, public open space, transport and mobility, on the condition of urban ecosystems and on their capacity to provide ecosystem services such as flood control, microclimate regulation or nature based recreation activities.

Since urban ecosystems are expanding very fast in Europe and globally, spatially explicit indicators providing a consistent and synthetic overview of a complex process are very important to support policy making.

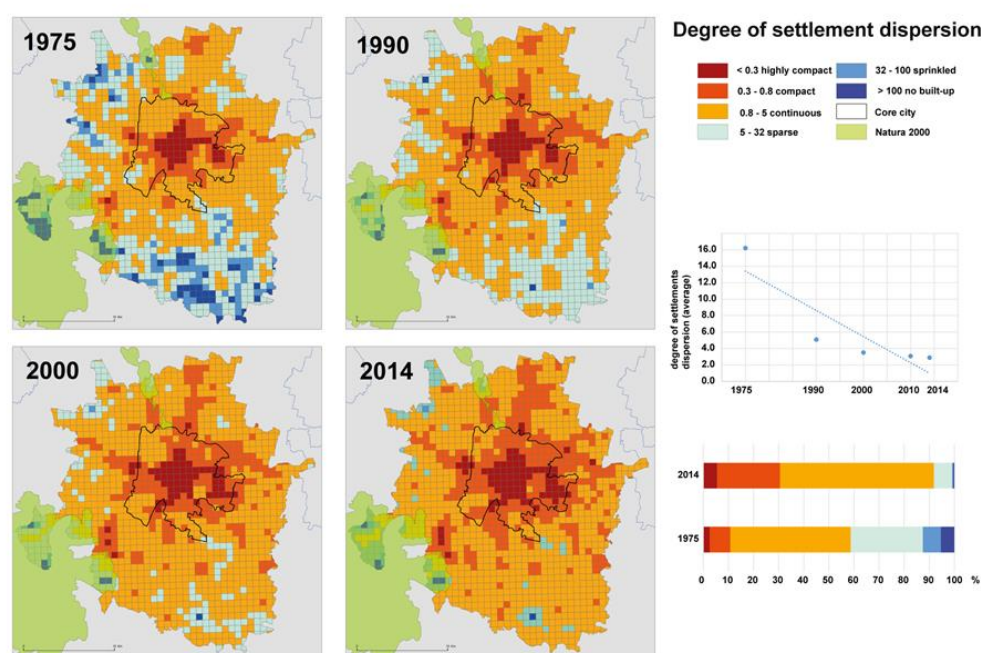


Figure 54 Settlement patterns in Padova (Italy) in 1975 – 1990 -2000 - 2014. (Maes et al., 2020)

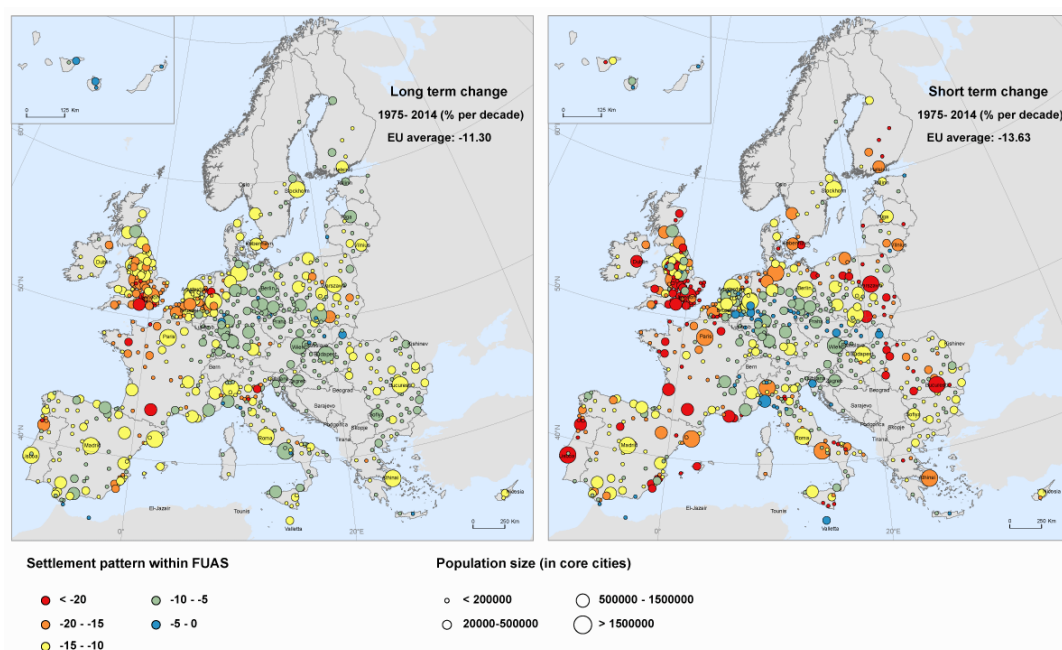


Figure 55 Settlement pattern in European functional urban areas, short and long-term trends. (Maes et al., 2020).

References:

Corbane, C., Pesaresi, M., Kemper, T., Politis, P., Florczyk, A.J., Syrris, V., Melchiorri, M., Sabo, F., Soille, P., Automated global delineation of human settlements from 40 years of Landsat satellite data archives. *Big Earth Data* 3(2), 2019, 140–169. doi: 10.1080/20964471.2019.1625528

Saganeiti, L., Favale, A., Pilogallo, A., Scorza, F., Murgante, B., Assessing urban fragmentation at regional scale using sprinkling indexes. *Sustain* 10(9), 2018, 1–23. doi: 10.3390/su10093274

Maes, J., et al., Mapping and Assessment of Ecosystems and their Services: An EU ecosystem assessment, EUR (where available), Publications Office of the European Union, Ispra, 2020, JRC120383.

3.2.8 Population agglomeration and dispersion in Emerging Europe

Opportunities and challenges across a changing urban-rural landscape
Young N.

The European Bank for Reconstruction and Development (EBRD) is a multilateral development bank that uses investment as a tool to build market economies in the post-Cold War era. Initially focused on the countries of the former Eastern Bloc, EBRD today supports development in nearly 40 countries from central Europe to central Asia and the southern and eastern Mediterranean, plus the West Bank and Gaza. The EBRD's Office of the Chief Economist produces an annual flagship publication, the Transition Report, which examines key issues affecting the economies in which the EBRD invests. The chapter titled, "Geographic Transition," in the 2018-19 report considers the evolution of population clusters in the EBRD regions since the beginning of transition in the early 1990s.

The gridded population data from the GHSL span the EBRD regions, providing consistent measures at a fine geographic resolution across time. Figure 56 maps an aggregated sketch of the geographical shift in population between 1990 and 2015 based on these data. Metropolitan areas showed substantial increases in population. To construct a measure of the population density experienced by an individual at a given one-kilometer square cell, the analysis sums the number of people residing in all nearby geographic cells (applying a 5 km radius), discounting people more with distance. This measure, termed "localized population density," became the basis for analysis at the cell, city, and country level.

Comparing localized population density across time revealed that populations are becoming increasingly concentrated in larger cities throughout the EBRD regions. Using an algorithm to cluster contiguously populated cells, "cities" of various sizes were identified in the GHSL waves for 1990, 2000 and 2014. About half of the inhabitants of cities with populations greater than 500,000 experienced large increases in localized population density between 2000 and 2014. Another 23 per cent experienced moderate increases. This growth appears to be fueled by emigration from secondary cities and rural areas. During the same period, over half of the inhabitants remaining in smaller cities experienced reductions in localized population density. The share of people living outside cities in the EBRD regions declined by 6 percentage points since 1990.

Economists think about the forces driving increasing or decreasing density in terms of agglomeration and dispersion effects, respectively. People gravitate toward larger cities in search of economic opportunities. Firms operating closely together in large markets benefit from easier sourcing of inputs, wider talent pools when hiring employees, and broader customer bases. In contrast, if density produces negative outcomes such as overcrowding, high levels of traffic congestion and pollution, then some individuals will likely forgo the higher wages and amenities available in cities, dispersing instead to areas with lower density.

Localized population density in the EBRD regions increased on average by about 1 per cent since 2000. However, the experience of individual communities varied greatly. Figure 57 shows the change in localized population density between 2000 and 2014 as a heat map. Dark blue areas, often representing capitals or provincial centres, show locations of high population gains. Brighter orange and red locations indicate more intense decreases.

Even between major cities, the change in density can vary. Consider the experience of Moscow and Warsaw. Moscow, shown in the upper-right window of Figure 57, exhibits greater population density growth at its core. Growth near the centre along roads, shown as black lines, was particularly fast. Meanwhile, some localities near roads at the periphery appear to have been drained. Moscow thus exhibits dominating agglomeration effects. In contrast, the centre of Warsaw lost density as the periphery gained, as shown in the upper-left window. Improvements in commuting options may have driven Warsaw's dominating dispersion effects.

Combining the localized population data constructed for cities with data on economic output shows that more densely populated markets also tend to be more productive. Research into "agglomeration economies" produce policy-relevant insights. Identifying places with accelerating densification and high productivity can help policy makers take steps early on to harness their potential, such as setting zoning policies promoting adequate housing and social integration. Areas losing population can bolster opportunities for education in those regions. Safety-net programs can ease the strain on households as local economies pursue new growth opportunities.

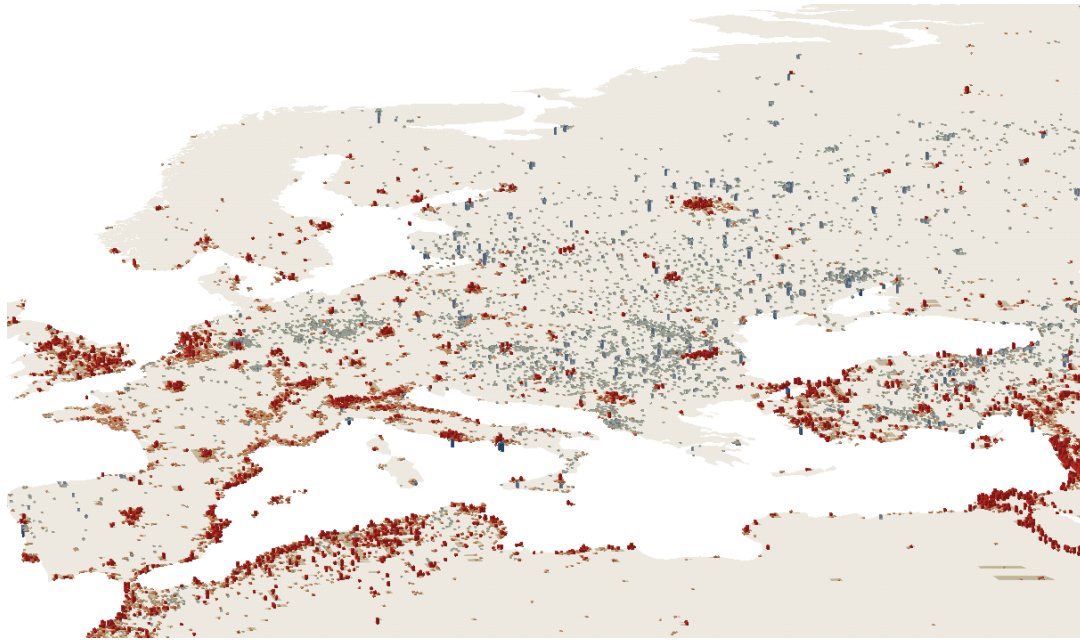


Figure 56 Population Growth by 100 km-square grid cells from 1990-2014. Positive changes in red and negative in blue.

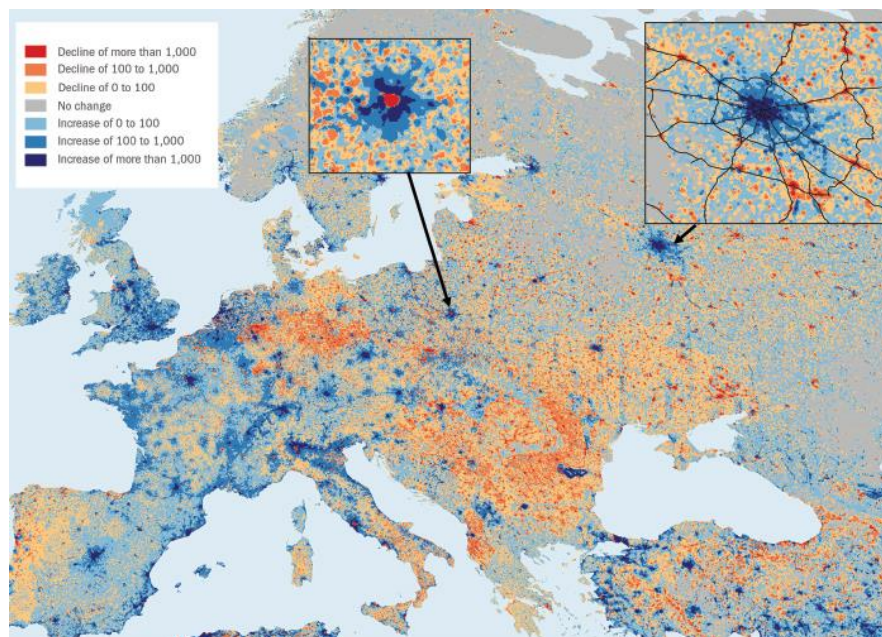


Figure 57: Changes in localized population density, 2000-2014. Notes: Localised population density is a measure of the number of people living within 5 km of a person, discounted by distance. The unit of change is the number of people in a 5 km radius.

References:

K. Desmet, D. K. Nagy, D. Nigmatulina and N. Young (2018), Chapter 4: Geographic Transition. Transition Report 2018-19. Work in Transition, EBRD London.

European Commission (Joint Research Centre) and Columbia University (Center for International Earth Science Information Network) (2015) GHSL population grid, derived from GPW4, multitemporal (1975, 1990, 2000, 2015).

J. De La Roca and D. Puga (2017) "Learning by working in big cities", The Review of Economic Studies, Vol. 84, pp. 106-142.

3.2.9 Analysing global megacities with GHSL data

Urban growth from 1975 to 2015

Rae A., Hoole C.

The problems posed by rapid and large-scale urbanisation are profound, and are recognised in the UN's New Urban Agenda; a declaration that aims to meet such challenges head-on, facilitated by the systematic tracking and analysis of global urban growth and change. In this context, the release in 2016 of the new Global Human Settlement Layer (GHSL) – a tool for exploring human presence on earth at the granular level – marks a watershed moment in our ability to understand, compare and contrast over time urban development across the world in a consistent and precise way. Our analysis of population growth in global megacities over time is therefore an attempt to show how advances in the availability of global data can help urban and regional authorities plan, predict and provide for growth at the local level.

The GHSL provides high resolution, small area global population data for 1975, 1990, 2000 and 2015. Using this rich new GHSL data set, our analysis (Hoole et al., 2019) provides a comparative analysis of global population growth and density change over four decades. The analysis was concentrated on a sample of 30 megacities that contained more than 558 million people and almost 8% of the world's population in 2015. We adopted a geospatial approach through the use of simple visualisation functions and zonal statistics that are readily achievable in proprietary and open-source GIS software.

Overall, this analysis highlighted the intense urbanisation processes seen across the globe in recent decades, particularly in the global South (see Figure 58), confirming what is already known about the scale difference of the population growth of megacities between the global North and South. While this is well known, however, it is much less well documented, analysed or visualised at a micro-scale across the entire globe in a systematic manner. By undertaking this analysis, we hope to demonstrate its utility for policymakers, by looking beyond traditional administrative boundaries that often 'underbound' metro areas, by highlighting the ways in which global cities can learn from the experience of others, and by demonstrating the value of standardised global data sources for local analysis.

The analysis offers a number of particularly striking findings. First, in 1975 the 30 megacities contained less than half their population total in 2015, at 261 million or 6.4 per cent of the global population at the time. Second, the level of growth in some of the urban agglomerations included in this study equates to entire megacities of 10 million people or more arriving in existing megacities, such as Jakarta in the past 15 years. This rate of urbanisation is often seen as neither sustainable nor desirable, yet it is the lived reality for residents and policy makers in many large cities across the global South. Third, from the analysis of individual densities, especially high maximum density figures of more than 100,000 people per square kilometre were found in Cairo, Kolkata, Guangzhou–Shenzhen, Manila, and Shanghai in 2015. Visual representations of these densities are shown for more focused areas in Figure 59, first for China and its neighbours and then for the eastern seaboard of the United States. A 100km grid is displayed on each map here, in order to aid comparison. While density in itself is not necessarily problematic – the affluent urban centres of Seoul, Hong Kong and Tokyo are good examples of successful high-density megacity living – this requires infrastructure, long-term planning and significant capital investment; none of which are available to the required level in cities such as Kolkata. Therefore, the question of what level of density is 'sustainable' will inevitably vary between urban and national contexts and needs to be carefully considered on a city-by-city basis. The new GHSL dataset provides an additional tool policymakers can use to achieve this.

The capability of urban and regional planners to respond to the social and environmental challenges of rapid urbanisation and the rising number of megacities on a global scale is dependent on the collation of evidence of urban change, especially in places where urban expansion has been unplanned and is difficult to track. This research shows the potential of the GHSL data set for generating creative visualisations and descriptive data to assist the development of progressive policy-oriented measurement frameworks and facilitate the closer monitoring and evaluation of urban growth in different regional contexts.

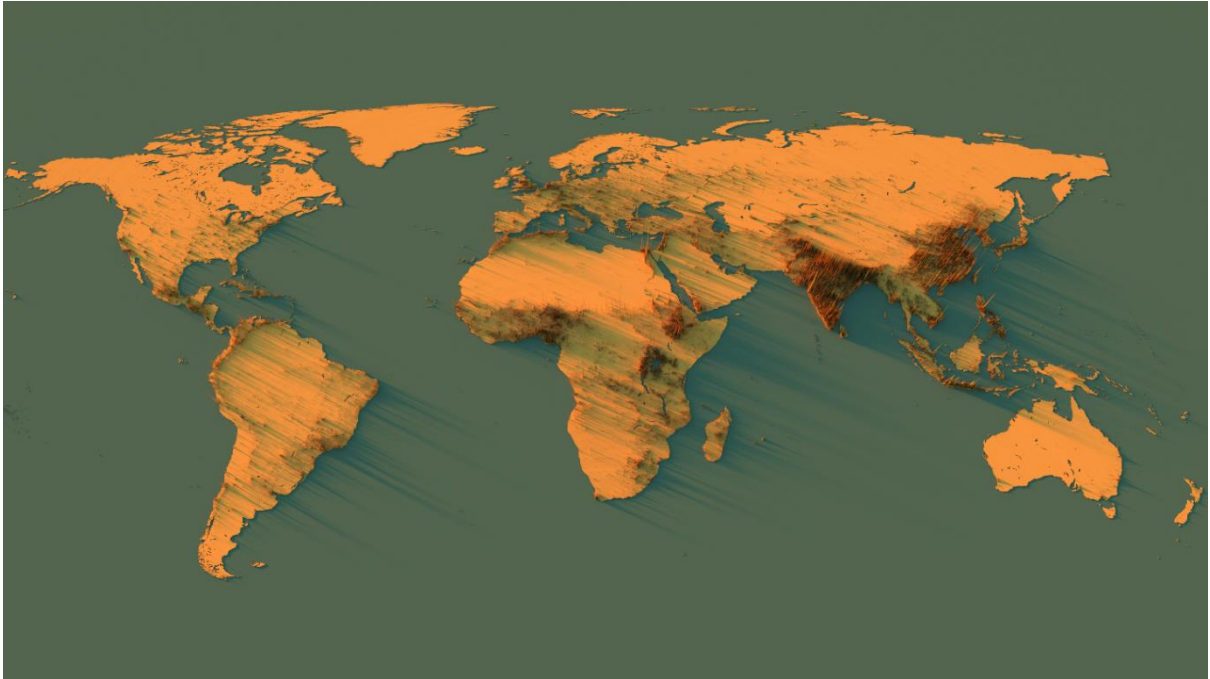


Figure 58 Global population density in 2015 (mapped using GHS_POP 2015 data)

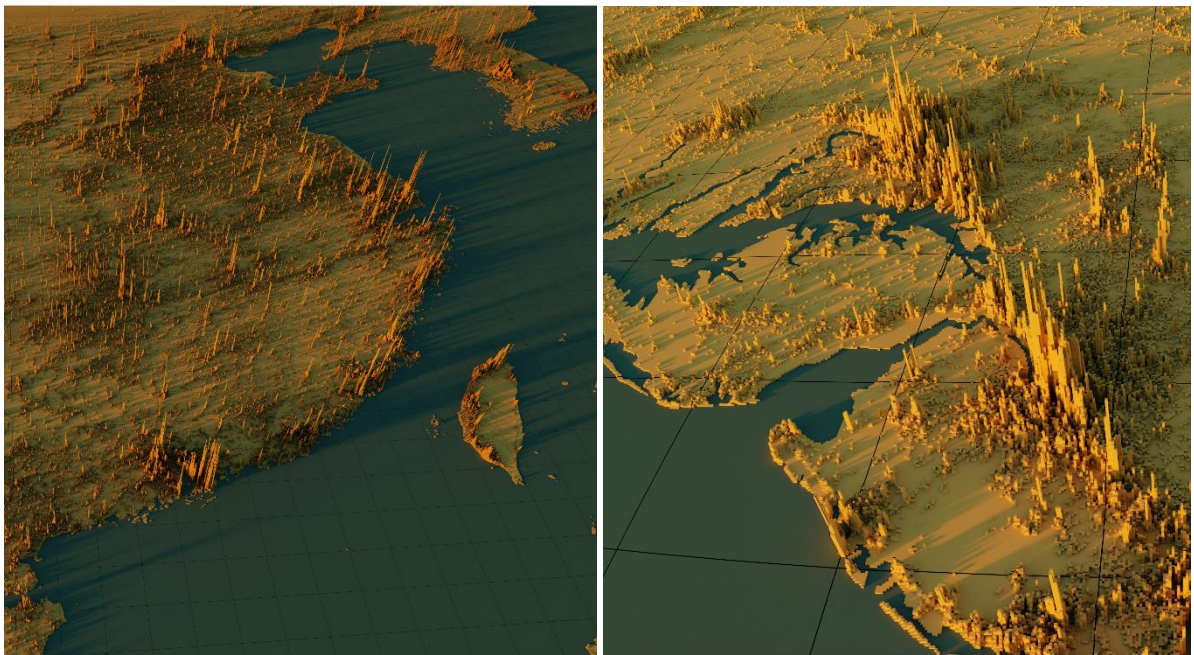


Figure 59 Global population density in China (left) and its neighbours, and the eastern United States (right)

References:

Hoole C, Hincks S & Rae A (2019). The contours of a new urban world? Megacity population growth and density since 1975. *Town Planning Review*, 90(6), 653-678.



3.3 Development

3.3 Development

Data and knowledge for development are a key priority for global organisations and donors. Knowing where people are, how they live and which place-based policies are most needed would help making the transition towards sustainable development more effective. The 2030 Agenda for Sustainable Development and its respective 17 Goals have put evidence-based policymaking, and implementation monitoring at the core of sustainable development strategies.

Showcases presented in this section address innovative ways to establish a solid knowledge base to inform policymaking by providing consistent, comparable, and spatially explicit data.

The showcase on the **Rural electrification planning tool for Burkina Faso** (3.3.1) demonstrates how important it is to produce data disaggregated at local level, to target specific needs especially in rural areas in developing countries. Countries in transition also experience a data gap arising from the time needed to conduct population and housing census, in such cases, place based modelling can help **Estimating Small-Area Population Density** (3.3.2): this is presented for the case of Sri Lanka, where surveys and geospatial data were combined to fill population data gaps.

Accessibility is also a key variable for development, and the showcase **Estimating travel time to urban areas of different population sizes** (3.3.3) explains the advantages of knowing how remote populations and places are from urban centres around the globe. The showcase on **LUISA4Africa** (3.3.4) presents a model to project into the future (to 2050) how human settlements in Africa will develop thus providing key resources for policy formulation. The showcase **Estimating climate change induced migration** presents the application of GHSL dataset to produce new data to quantify net migration and to study its nexus with climate change at global level (3.3.5).

Urban and rural areas do not just differ regarding development trajectories and policy demand, but also in terms of displacement trends. The showcase by IOM **Estimates of Rural and Urban Displacement Trends** (3.3.6) shows how to disaggregate IDP figures by settlement class and what salient information planners have at hand to better identify and address the varying needs and challenges faced by internally displaced populations from across urban, peri-urban and rural environments.

Another branch of applications focuses on monitoring, characterising and quantifying different aspects of development. The showcase **Detecting spatial patterns of inequality from Earth Observation** (3.3.7) looks at how human settlements across the globe differ in terms of combination of night-time light, population density and built-up areas to identify affluent sparsely populated settlements with extensive built-up areas and high light emission, versus very crowded and little lit-up settlements. The geographic locations of these different trends help identifying inequalities. The showcase on **Tracking Infrastructural Transitions** (3.3.8) also presents a method to combine multi-source Earth observation data to characterise human settlements linking urbanisation and development proposing different categories of human settlement morphology typical of population density, built-up area and night-time light combinations. Finally, the **SDG Voluntary Local Reviews** (3.3.9) proposes a review of methods and datasets that could assist local authorities in developing SDG monitoring at sub-national level.

3.3.1 Rural electrification planning tool for Burkina Faso

Outil de Planification de l'Électrification Rurale -Burkina Faso (OPER-BU): a web hosted GIS analytical tool
Moner-Girona M., Luisa Barbosa A., Arevalo J., Martino M., Valdes A.M., Leone A., Sawadogo N.

Rural electrification is a major concern for the development of energy access in West Africa and in the Sahel region in general. Improving access to electricity will help eradicating poverty while energy decarbonisation is crucial in mitigating climate change and reaching the UN Sustainable Development Goals (SDG7). Access to sustainable and affordable energy services in sub-Saharan Africa is limited and remains a critical challenge for the economic growth and industrialisation of the continent. Burkina Faso in particular suffers from a very low level of access to modern energies, especially in rural areas where only 21 % of rural population has access to electricity. The current electricity mix is based on electricity imports, fossil fuel generation, hydropower and solar energy. Burkina Faso heavily depends on imports. Due to the cost, grid extension is developing at a much slower pace than planned.

The rural electrification strategy for Burkina Faso is scattered within two different institutions the Rural Electrification Agency (ABER) and the Burkina Faso Electricity Transmission Company (SONABEL): there is a need of defining a coordinated action plan. Planning and coordination between grid extension and off-grid electrification programmes is essential to reach a long-term sustainable energy model and to avoid high unnecessary infrastructure investments. For several decades, the energy sector in Burkina Faso has been characterised by a dominance of the traditional use of biomass, by a primarily thermal productivity of electricity at national level (based on imported fossil fuels) and, below the demand from a population that is constantly growing, by one of the highest costs of electricity in the region. In order to facilitate the investments of private capital into the energy sector and to promote the development of cost-effective renewable energy projects, the government launched in 2017 a new law regulating the energy sector.

Following a request of the EU Delegation in Ouagadougou, experts of the EU Technical Assistance Facility (TAF) developed in collaboration with the JRC an analytical spatial tool to support the stakeholders involved in rural electrification planning in Burkina Faso (Figure 61 and Figure 62). Based on the current energy status and local resources, the tool so-called “Outil de Planification de l'Électrification Rurale -Burkina Faso” (OPER-BU), aims to support the Rural Electrification Agency, national government and development partners in evaluating off grid rural electrification options. The OPER-BU tool can indirectly support the private sector in identifying the most suitable areas for investment depending on their priorities.

The least-cost technology, at the basis of OPER-BU model, is based on population distribution, local electricity demands (including social infrastructure and productive uses), rate of electrification, distance to the existing grid, local prices of diesel, and the prices of the components of renewable energy systems. The innovative feature of the new methodology is the disaggregation of the population from data point (based on official data provided by Burkina Faso authorities) to a more accurate distribution of the population represented by polygons using GHS-BUILT as ancillary data source.

The results of our analysis suggest that an electrification plan mainly based on further grid extension is not always the best option in terms of efficiency and unsustainability in order to reach the national energy access targets. The calculated cumulative investment for Burkina Faso to reach universal access to electricity by 2030 is about EUR 1.7 billion, including electricity provision to the population of settlements already connected, but without access to electricity. Our results also suggest that Burkina Faso's rural electrification strategy should be driven by distributed minigrids powered by local renewable resources. We find that this approach would connect more people to power more quickly, and would reduce imported fossil fuel dependence/consumption that would otherwise be necessary for grid extension options. Smaller local electrification projects based on indigenous resources are in the long term expected to be more feasible than centralised ones based on fuel oil thermal plants or large scale solar plants. Our results suggest that up to 65 % of the non-electrified settlements are to be served by decentralised technologies. Findings shall support the Burkina Faso government and development partners to define the least-cost rural electrification options within the framework of the national action plans of the Sustainable Energy for All (SE4ALL).

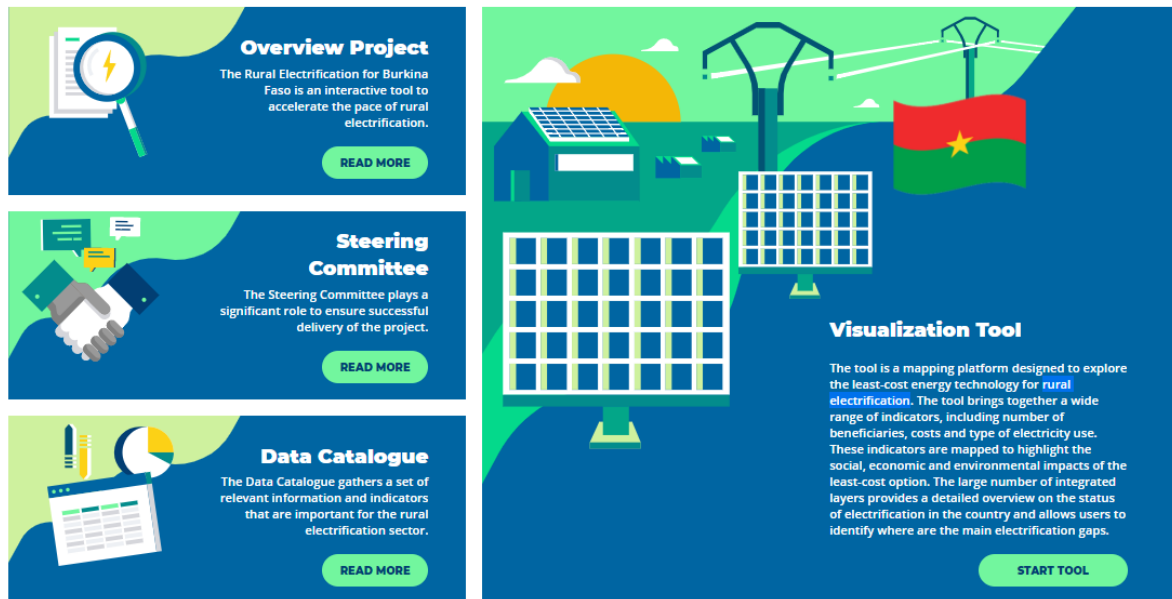


Figure 61 Landing page: OPER-BU web-hosted analytical tool

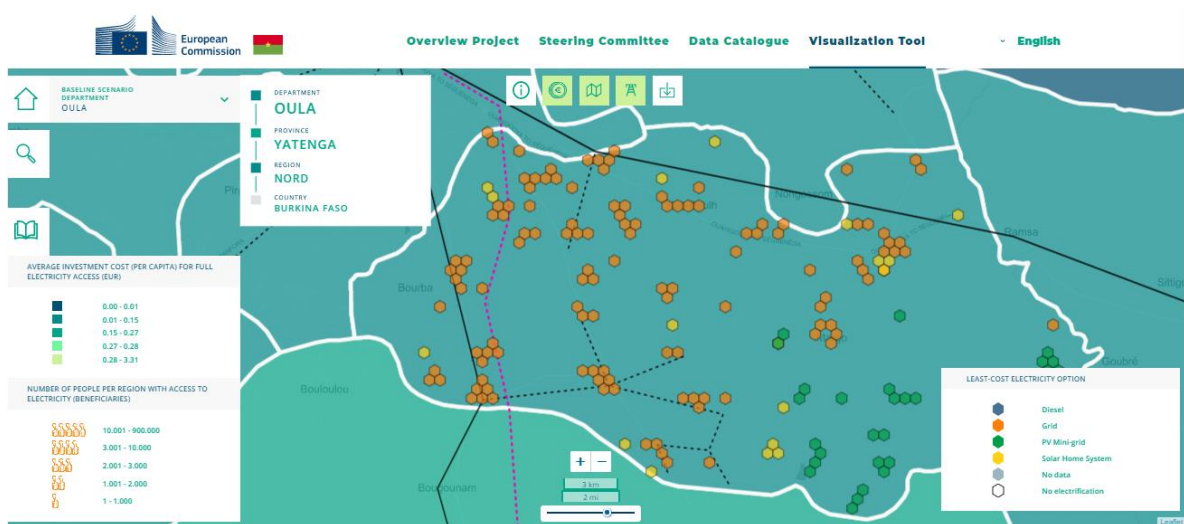


Figure 62. OPER-BU least-cost option per settlement (grid extension, diesel generator, PV mini-grid or PV stand-alone system)

Datasets:

Built-up area density BUILT_LDS2014_GLOBE_R2018A_54009_250_V_1_0

3.3.2 Estimating Small-Area Population Density in Sri Lanka using Surveys and Geospatial Data

Bottom Up Population Estimates in Sri Lanka
Engstrom R., Newhouse D., Soundararajan V.

Population changes are rapid due to conflicts, migration, urbanization, and natural disasters. As a result, decennial census data are unreliable to track population changes, especially in small areas, such as, villages and towns. While surveys can be frequently conducted, their coverage is not universal, and they are not representative at small administrative levels. Obtaining high frequency local population density estimates can assist in policy making and policy delivery, by, for example, facilitating efficient delivery of public goods/services, tracking migration, and understanding the impact of place-based infrastructure and economic policies.

In this work in Sri Lanka, we demonstrate a method of obtaining local population density estimates using a combination of survey data at the village level and geospatial data. The method estimates a statistical relationship between population density derived from a 2012/13 Household Income and Expenditure Survey (HIES) and a suite of satellite imagery derived geospatial indicators. Using this relationship, we model population density predictions in the non-survey villages for all of Sri Lanka using a Poisson regression model. Since we have a large number of geospatial, imagery-based layers, using too many variables can overfit the Poisson model and lead to less accurate predictions. Therefore, we select the best predictor variables of population density using the Least Absolute Shrinkage and Selection Operator (LASSO) method, and only the selected variables/indicators were used in the final model.

Overall, we find that our model estimates approximate the 2012 census density accurately in non-survey villages and are more precise than other studies that apply similar methods using geo-spatial data (Figure 63). We categorized satellite imagery-based indicators as (1) open-source (low to high resolution), and (2) commercially available (very high resolution). We tested the accuracy of each imagery type in predicting village level population density. Overall, open source indicators predict about 75% of the out-of-sample variation in the village population density (panel A, Figure 64); adding commercial indicators to the model does not improve the accuracy significantly beyond this (panel B in Figure 64). Among the open source indicators, the Global Human Settlement Layer (GHSL)'s built-up area measure was highly significant as it alone explains 69% of the out-of-sample variation in the village level population density (panel C in Figure 64).

The method used is called a "bottom-up" method because it uses local-level survey data to scale up and make predictions. This differs from a "top-down" method, which works by redistributing population, for large aggregated areas from a census and redistributes it to lower (local) geographic levels using geospatial and other contemporaneous data. Most open-source population products use the top-down method. While these top-down methods can be easier to execute, the estimates become less accurate as the census itself ages. Bottom-up methods circumvent the problem of aging census data by relying instead on more up-to-date household surveys and frequently updated, satellite data based indicators.

While our population density estimates can never substitute for a full census, we believe they can serve as the next best option in between-census years and in areas with little to no available census data. While this model was created for Sri Lanka, this methodology can be run in any geographic area, if nationally representative household surveys with local administrative region identifiers, local administrative shape files, and satellite imagery-based data are available.

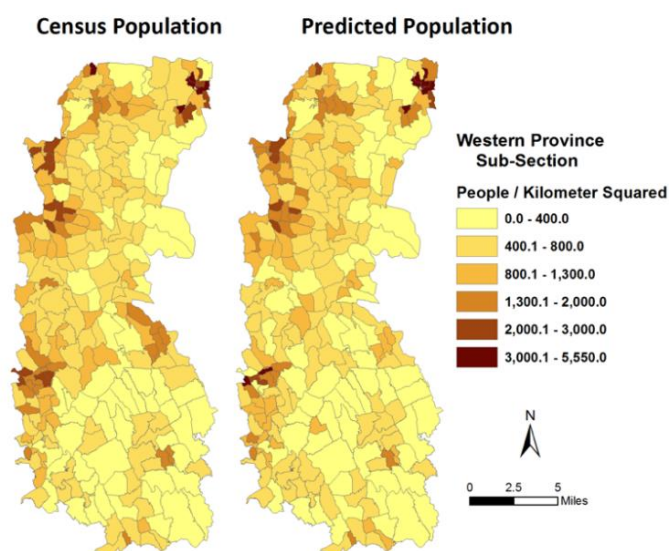


Figure 63 Census and our in-sample, model predicted population density for the Western Province Sub-section of Sri Lanka.

	Population Density			Mean RE	Median RE
	R ²	SRC	Mean AE		
A. Open source imagery					
HIES-based	0.75	0.92	663	34%	28%
Census-based	0.76	0.91	750	58%	36%
B. Commercially procured & open-source imagery					
HIES-based	0.79	0.91	664	37%	28%
Census-based	0.81	0.91	679	50%	28%
C. GHSL					
HIES-based	0.69	0.84	824	72%	37%
Census-based	0.68	0.84	887	107%	44%

Figure 64. Accuracy of predicted population density based on the model with all imagery, only open-source imagery, and only with GHSL. All models include district fixed effects, urban-area dummy, and log village area. HIES=the Household Income and Expenditure Survey. The accuracy measures for the predictions such as R², SRC (Spearman Rank Correlation), AE (Absolute error), RE (Relative Error), are calculated with respect to actual density from the census data. Higher values of the first two measures, and lower values of the latter two measures indicate better prediction accuracies. For reference, we report the prediction accuracies of the same model, but that uses census-density as the dependent variable.

Datasets:

- 1) Census of Sri Lanka
- 2) 2012/13 Household Income and Expenditure Survey of Sri Lanka
- 3) Open source satellite imagery-based indicators such as VIIRS, Global Forest Change, ASTER, Global Urban Footprint, Global Human Settlement Layer, Facebook's High Resolution Settlement Layer (HRSL)
- 4) Commercially procured satellite imagery-based indicators from Maxar (formerly DigitalGlobe)

3.3.3 Estimating travel time to urban areas of different population sizes*

New indicators of access to the resources and opportunities in urban areas

Nelson A., Weiss D. J., van Etten J., Cattaneo A., McMenomy T. S., Koo J.

Access to the resources, services and opportunities that are concentrated in urban areas is an important indicator for development. Urban areas and the transport networks that connect them together and to their surrounding rural areas are essential infrastructure. This infrastructure provides the means for people and products to travel from A to B. It enables social and economic interactions and the delivery of basic services such as education and healthcare. People with good access generally have greater opportunity for social and economic development, reduced costs and greater levels of interaction, whereas those with poor access generally face higher costs, fewer opportunities and poorer health and education outcomes.

The degree to which people have physical access to these resources – represented here as the time required to travel to the nearest city – has been previously mapped globally for 2000^[1] and 2015^[2] for all urban areas of 50,000 or more people. However, it is important to make a more nuanced assessment to account for population size since the nearest urban area could be a megacity with ten million or more people or a small regional city of 50,000 people and anything in between. There are enormous differences in the availability of resources, services, and opportunities within this spectrum of city sizes. To address this we developed, validated and published a set of global, high resolution maps for the year 2015 that estimate the travel time from any land-based pixel to the nearest urban settlement in a given size category. We made a nine-level stratification of human settlement sizes from 5,000 to more than 5 million inhabitants based on the 2016 version of the Joint Research Centre's Global Human Settlement Layer (GHSL) datasets. Urban areas were represented by GHS-SMOD and population per urban area came from GHS-POP. We generated nine, one-kilometre resolution, global travel time maps, using the same method as [2] (Figure 65 shows the map for one of the nine levels). Travel time estimates were validated against journey times reported by Google Maps (using the Google Maps Platform Distance Matrix API). We compared the travel times between the two for over 47,000 journeys distributed around the world. We observed a very good agreement, with a median difference of only –13.7 minutes. Our travel estimates were frequently shorter than Google's (Figure 66) but were representative of actual travel times. The travel time maps, the underlying friction surface, and the code to make the and validate the global maps are all Open Access resources^[3] and have been published as a Data Descriptor^[4].

The accessibility layers are relative measures of the ease of access from a given location to the nearest target in each urban area size category. They can function as part of a toolbox to improve economic planning in countries by allowing policymakers to focus on the linkages between urban centres and their surrounding rural areas. Inequalities in access can lead to greater social and economic divides. Poorly planned expansions of transport networks can also degrade the natural environment, leading to deforestation and the over exploitation of easily accessed natural resources. On the other hand, well planned improvements in access can lead to better outcomes in rural health, wealth and economic livelihoods whilst limiting environmental impacts. The variation in the provision of resources, services and opportunities across settlements of different size implies that our nuanced assessment of access across settlements of different sizes will be of interest for regional planners and service providers when considering the impact of investments and policies that affect the level of access to education and health services, markets and job opportunities, amongst others.

Access to the resources, services and opportunities that are concentrated in urban areas is underpins the 'leave no one behind' agenda of the United Nations Sustainable Development Goals (SDGs). Because of this, accessibility is directly or indirectly relevant for several targets and indicators within SDGs 1, 2, 3, 4, 5, 6, 7, 9, 10, 11 and 12, such as: indicator 1.4.1 "Proportion of population living in households with access to basic services"; target 2.1 "By 2030, end hunger and ensure access by all people, in particular the poor and people in vulnerable situations, including infants, to safe, nutritious and sufficient food all year round"; and target 3.8 "Achieve universal health coverage, including financial risk protection, access to quality essential health-care services and access to safe, effective, quality and affordable essential medicines and vaccines for all". This globally consistent representation of travel time has led to its inclusion in the GHSL in two different layers. Firstly, the Urban Centre Database (GHS-UCDB) includes an attribute of travel time to the capital city for all urban centres of 10,000 or more people. And secondly the Functional Urban Areas (GHS-FUA) layer, where the FUA are defined based on travel time to urban centres amongst other characteristics.

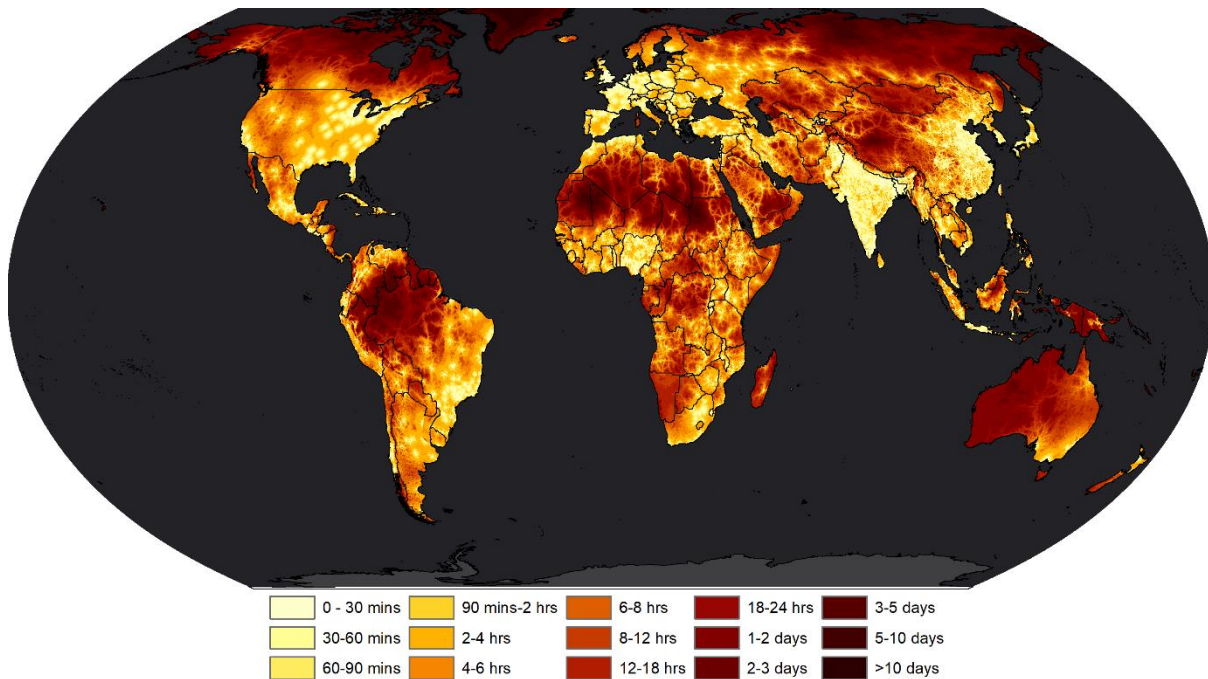


Figure 65. Travel time to the nearest human settlement in the year 2015 for GHSL settlements with $\geq 100,000$ and $< 200,000$ people. Country boundaries from GADM v3.6

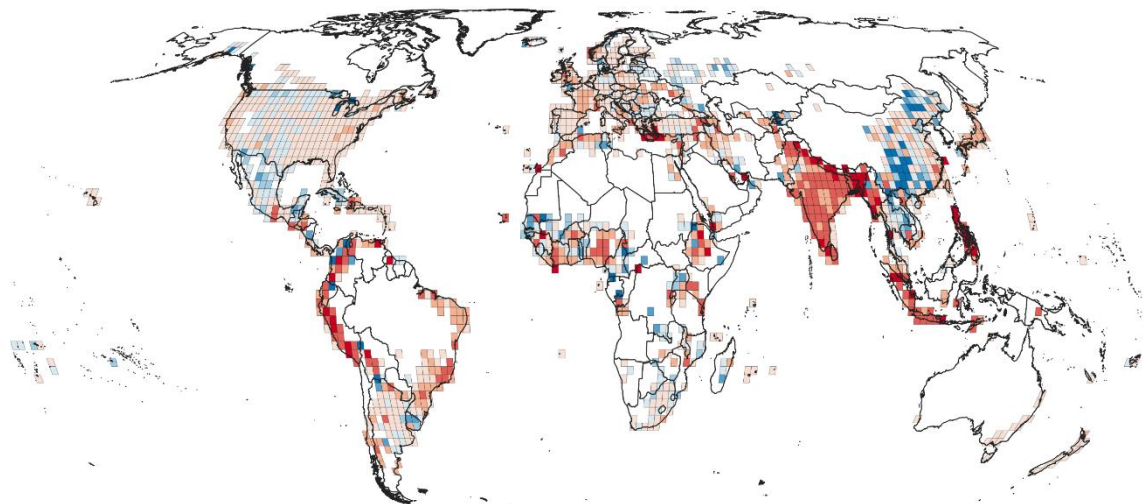


Figure 66. Difference in travel time estimates in minutes and hours (our estimated travel time minus Google journey time) based on journeys between locations within each of the $2^\circ \times 2^\circ$ tiles shown in the map. Country boundaries from GADM v3.6.

Datasets:

- 1) Nelson, A. Travel time to major cities: a global map of accessibility. Global Environment Monitoring Unit, Joint Research Centre of the European Commission, <http://forobs.jrc.ec.europa.eu/products/gam> (2008).
- 2) Weiss, D. J. et al. A global map of travel time to cities to assess inequalities in accessibility in 2015. *Nature* 553, 333–336 (2018)
- 3) Nelson, A. Travel time to cities and ports in the year 2015. figshare, <https://doi.org/10.6084/m9.figshare.7638134.v3> (2019)
- 4) Nelson, A. D., Weiss, D., van Etten, J., Cattaneo, A., McMenomy, T., & Koo, J. A suite of global accessibility indicators. *Scientific Data*, 6, 1-9. (2019) <https://doi.org/10.1038/s41597-019-0265-5>

* This text is based on Nelson, A. D., Weiss, D., van Etten, J., Cattaneo, A., McMenomy, T., & Koo, J. A suite of global accessibility indicators. *Scientific Data*, 6, 1-9. (2019) <https://doi.org/10.1038/s41597-019-0265-5>

3.3.4 GHSL: A crucial input for LUISA4Africa

Maistrali A., Baranzelli C., Jacobs-Crisioni C., Perpiña Castillo C., Lavalle C.

Africa is experiencing rapid urbanisation, continuous socio-economic changes and population growth. As urbanisation continues in cities of Africa, it is crucial to understand its patterns and their potential impacts. Since 2018, the Joint Research Centre's LUISA team (JRC.B.3) is developing the LUISA4Africa land-use model as an extension of the European LUISA territorial modelling platform. The Global Human Settlement Layer (GHSL) data on the presence of built-up land (GHS-BUILT) and population (GHS-POP) have been used as a key input for the projections that are computed by the LUISA4Africa model. LUISA4Africa is a fine resolution (at a square lattice of 1 km grids) model that can simulate the consequences of policies and expected demographic, economic or climate changes on local activity distributions. The results are captured in population distribution, land-use patterns and accessibility indicators.

LUISA4Africa consists of a population model integrated in a doubly constrained land-use optimisation model, as described in Jacobs-Crisioni et al (2017). Thus, population changes depend on concurrent land-use patterns and a function that describes attractiveness for settlement. Within specified constraints, land uses are redistributed by maximising locational advantages. These advantages are specified through dynamic maps that describe locational attractiveness. In the development of this model, GHSL data have been used as reference population maps; to refine reference land-use maps; as dependent variables in regressions that were setup to calibrate models of local attractiveness for population and land-use patterns; and as an input to calibrate models of national changes in urban density. The role of GHSL data in the model calibration exercise will be further detailed in the next sections.

To specify how attractive a place is for built-up land and population settlements, we created functions to describe historical changes of built-up land and population based on a range of variables. The resulting attractiveness maps are used to model likely locations for urban expansion and population growth, under the assumption that historical location preferences remain valid in the foreseen future. To quantify the effect that the included variables must have had to result in the observed changes, regression analyses were performed using GHSL 1 km population and built-up land grids as dependent variables. With regard to national population density functions, those drive space requirement expectations as a consequence of projected population size and economic output. The effects of the variables in those functions (per capita economic output, population increase and prior densities) were again estimated by regression analyses describing changes in built-up density according to GHSL data.

A selection of modelling results that can be obtained, owing to the GHSL datasets, are shown in the remainder of this paper. All the reported results are computed according to the Shared Socio-Economic Pathway 3 (SSP3). According to the SSP3 global narrative, economic development is slow, consumption is material-intensive, and inequalities persist or worsen over time; population growth is low in industrialized and high in developing countries; and a low international priority for addressing environmental concerns leads to strong environmental degradation in some regions. (O'Neill et al., 2017; Riahi et al., 2017).

To the best of our knowledge, GHSL built-up and population grids are the only available data-source in which the recorded values are measured with a consistent method for multiple years. They thus provide a unique vantage point for modelling calibration, as observed changes cannot be attributed to differences in the measuring method. GHSL inputs have been instrumental in the scenarios to obtain general trends in urban density and degree of urban expansion, and inform the shape of the projected local urban patterns. Figure 67 shows simulated urban growth in the cities of Johannesburg and Tshwane (Pretoria) from 2015 to 2050, according to the modelled SSP3 scenario. At national level, both urban areas and population are increasing. Figure 68 captures the share between urban and rural population in South Africa over the same simulation period (2015-2050). In 2050, urban population is expected to cover 75,8% of the total population of the country. Lastly, Figure 69 presents the associated significant decline of both urban expansion rate that will go from 10,9% down to 3,4%, along with the urban population growth rate that will go from 13,9% down to 5%, in South Africa over time.

Output and indicators for African cities are made available in the Urban Data Platform Plus (<https://urban.jrc.ec.europa.eu>).

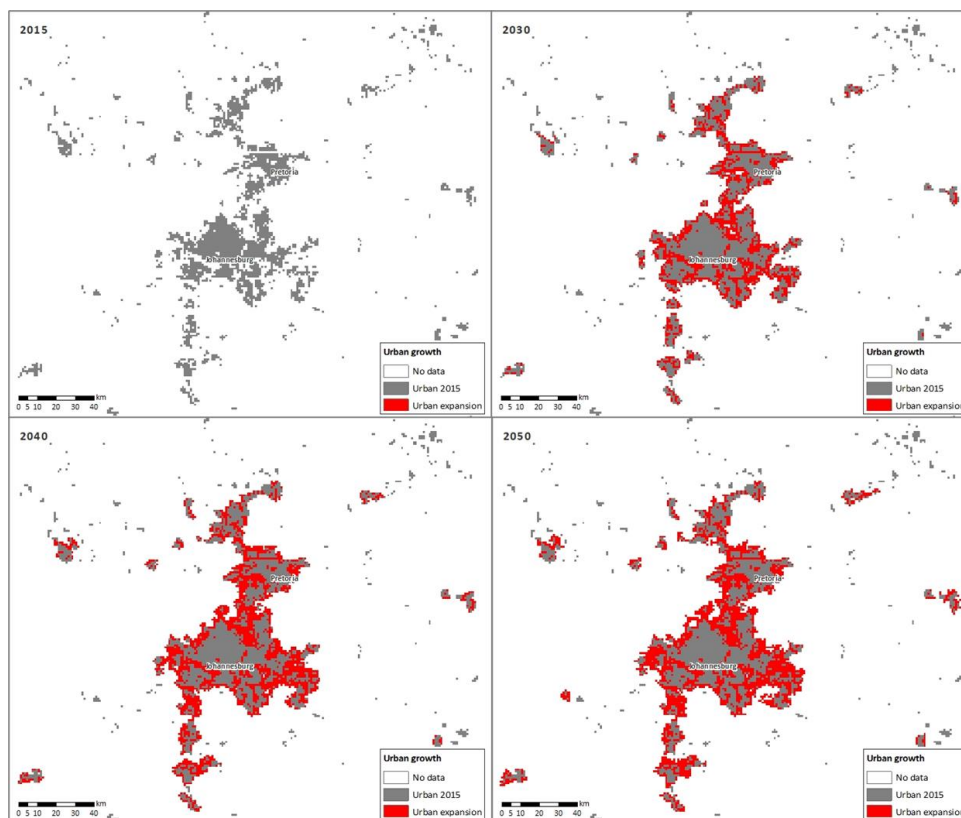


Figure 67. Urban growth of City of Johannesburg and City of Tshwane (Pretoria), for 2015-2050, according to modelled SSP3 scenario.

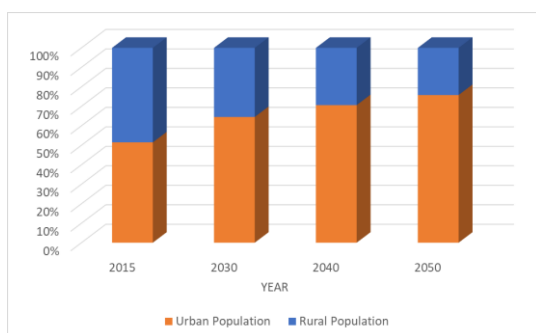


Figure 68. Urban and Rural population share in South Africa (2015-2050) according to modelled SSP3 scenario.

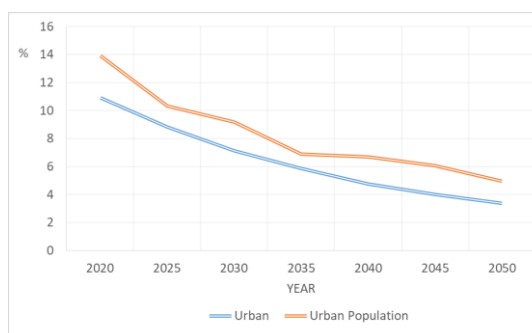


Figure 69. Urban growth rate and urban-population growth rate in South Africa (2015-2050), according to modelled SSP3 scenario. Urban growth rate refers to pixels containing a substantial share of built-up land, while urban population growth rate refers to the population living in there, both computed every 5 years.

References and Datasets:

Global Human Settlement Layer (GHSL), GHS Built-Up Grid, GHS_BUILT_LDSMT_GLOBE_R2015B
 Chris Jacobs-Crisioni, Vasco Diogo, Carolina Perpiña Castillo, Claudia Baranzelli, Filipe Batista e Silva, Konstantin Rosina, Boyan Kavalov, Carlo Lavalle. 2017. *The LUISA Territorial Reference Scenario 2017: A technical description*. JRC Working Papers JRC108163, Joint Research Centre
 O'Neill, B.C., Kriegler, E., Kristie L.E., Kemp-Benedict, E., Riahi, K., Rothman, D.S., van Ruijven, B.J., van Vuuren, D.P., Birkmann, J., Kok, K., Levy, M., Solecki, W. 2017. *The Roads Ahead: Narratives for Shared Socioeconomic Pathways Describing World Futures in the 21st century*. Global Environmental Change 42: 169-180
 Riahi, K., van Vuuren, D.P., Kriegler, E., Edmonds, J., O'Neill, B.C., Fujimori, S., Bauer, N., Calvin, K., Dellink, R., Fricko, O., et al. 2017. *The Shared Socioeconomic Pathways and Their Energy, Land Use, and Greenhouse Gas Emissions Implications: An Overview*. Global Environmental Change 42: 153-168

3.3.5 Estimating climate change induced migration

A focus on Africa

Migali S., Natale F., Alessandrini A., Ghio D., Petroliaqkis, T.

The European Commission's Knowledge Centre on Migration and Demography (KCMD) employs GHSL data to develop new estimates of net migration at high spatial detail. These estimates will serve to generate new evidence on the climate change-migration nexus, in the context of the KCMD Climate Change Induced Migration (CLICIM) project. Collections of in- and out-migration data at high geographical resolution are rare and their development at international level is at earliest stage. The most recent database of net migration data at high spatial resolution and global coverage is developed by the Centre for International Earth Science Information Network (CIESIN) for the period 1970-2010 (de Sherbinin, 2015). By following a similar approach to CIESIN, KCMD produces new net migration estimates, provided as a spatial raster dataset, (Alessandrini et al., 2020) on the basis of GHSL data. Indeed, GHSL provide not only highly spatially disaggregated data, but also the most recent population estimates up to 2015. Most importantly, GHSL data implement an internationally harmonized definition of cities, urban and rural areas. This allows not only to distinguish net migration in urban and rural areas, but also to compare them across countries and over time.

Net migration is the difference between the number of immigrants and the number of emigrants. When these numbers are not directly available, net migration can be obtained through an indirect estimation method. The change of population over two periods derives from the difference between births and deaths (natural increase) during the observed interval and the difference between in-migration and out-migration (net migration) during the same interval. It follows that net migration can be derived indirectly as the difference between population change and its natural increase. In this framework, KCMD uses GHSL data to compute population change every 5-years over the period 1975 - 2015, and UN DESA estimates of births and deaths to estimate the natural increase of population at high geographical detail. Figure 70 provides an example of the new estimates at resolution of 25km x 25km for the period 2010-2015. Orange cells represent areas with negative net migration, while blue cells show positive net migration. The former experience population losses since in-migration is lower than out-migration, while the latter population gains since in-migration exceeds out-migration. Dashboards with the full set of estimates are included in the [KCMD Dynamic Data Hub](#).

The new net migration data are used in the context of CLICIM project. The ultimate objective of CLICIM is the estimation of the relation between climate change and migration, particularly in Africa, the continent most affected by environmental and demographic factors.

As an illustrative example, Figure 71 shows the correlation between temperatures and net migration over the period 1975-2015 for the region of Kayes, Mali. The region – characterized mainly by rural areas – has been affected by extreme climatic events, such as droughts in the 70s and 80s, and increasing temperatures. The region is also a well known historical example of climate related migration. Figure 71 confirms an inverse relation between climate and migration also for most recent periods. Indeed, those territories in Kayes with higher temperatures tend to have lower net migration. This means that higher temperatures correlate with less attractive areas in terms of migration. CLICIM starts from these figures to model the climate-migration nexus for broader areas in Africa and disentangle climate change from the multiple drivers of migration, such as urbanisation, social and economic development.

The knowledge stemming from the CLICIM project will feed into the final step of formulating scenarios on how many people will be exposed and eventually move due to climate change. This would give insights to the policy debate on where the combined effects of local demographic patterns and contextual climatic factors would increase populations' vulnerability, thus requiring the definition of tailored policy interventions. The project is expected to contribute to development and climate adaptation policies by providing a mapping of populations exposed to slow onset climate events and their mobility patterns. This mapping exercise will help to target policy interventions towards areas which are already suffering the impacts of climate change both in terms of displacements and trapped populations. From the development perspective, the CLICIM project will also take into account how population response, in terms of mobility, to climate change varies with socio-economic development, poverty, and agricultural conditions in the affected areas.

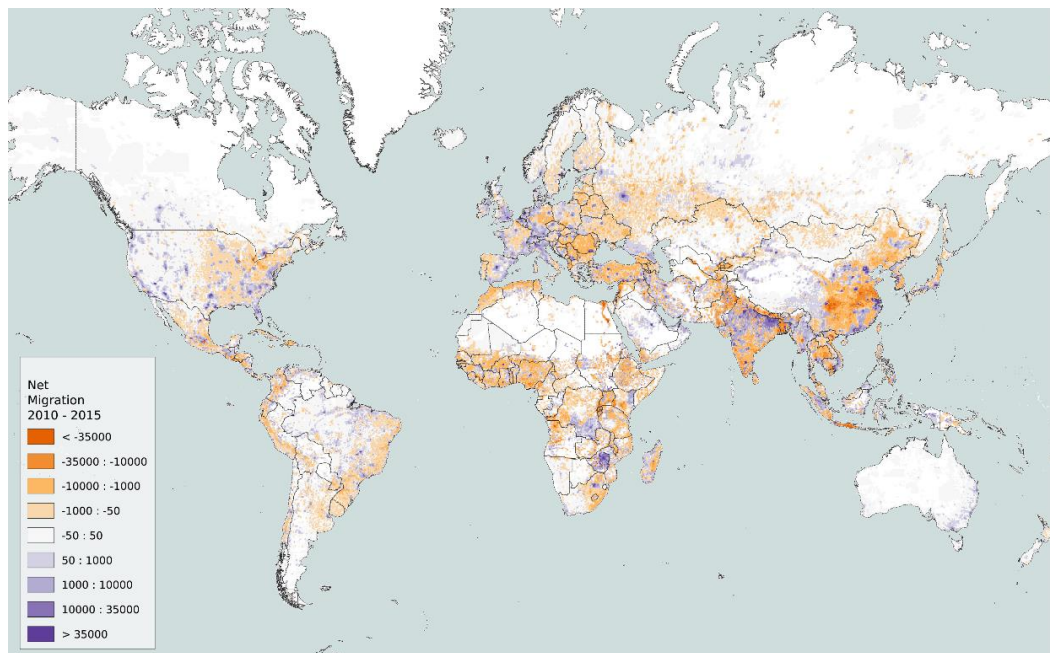


Figure 70 Net migration estimates (0.25 x 0.25 degree), 2010-2015

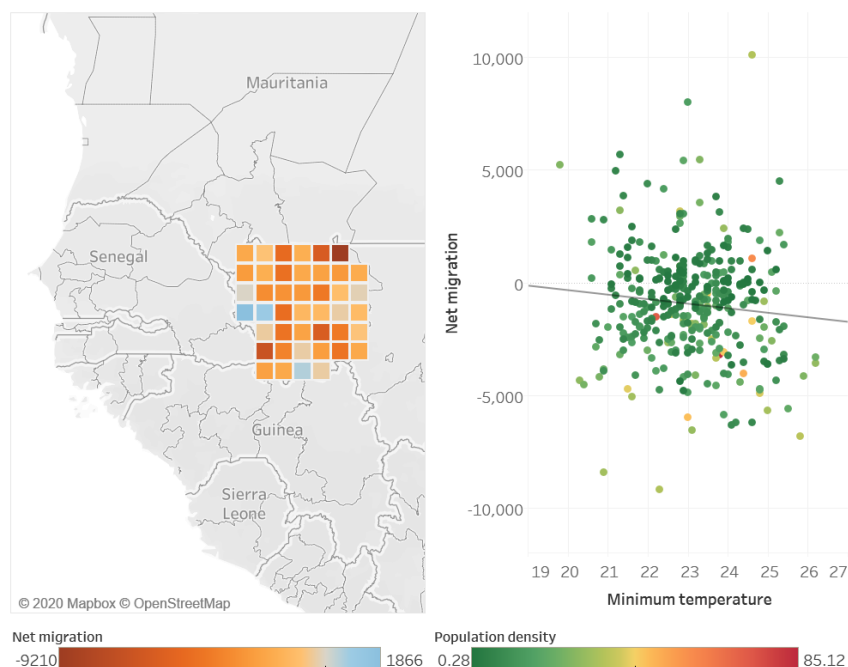


Figure 71 Net migration in Kayes region (Mali, 0.5 x 0.5 degree), 2010-2015 (left panel). Correlation between temperatures and net migration in Kayes region, by population density. 1970 – 2015 (right panel).

References

- Alessandrini, D. Ghio, S. Migali, Estimating net migration at high spatial resolution, EUR 30261 EN, European Union, Luxembourg, 2020, ISBN 978-92-76-19669-3, doi:10.2760/383386, JRC121003
- Alessandrini, D. Ghio, S. Migali, Population and climate dynamics in Western Africa: the case of Sahel regions (JRC technical report, forthcoming)
- De Sherbinin, A. (2015). Global Estimated Net Migration Grids By Decade: 1970-2000[Data set]. Palisades, NY: NASA Socioeconomic Data and Applications Center (SEDAC). <https://doi.org/10.7927/H43195VC>.
- Schiavina, M., Freire, S., MacManus, K. (2019). GHS population grid multitemporal (1975, 1990, 2000, 2015) R2019A. European Commission, Joint Research Centre (JRC) DOI: [10.2905/42E8BE89-54FF-464E-BE7B-BF9E64DA5218](https://doi.org/10.2905/42E8BE89-54FF-464E-BE7B-BF9E64DA5218) PID: <http://data.europa.eu/89h/0c6b9751-a71f-4062-830b-43c9f432370f>.

3.3.6 Estimates of Rural and Urban Displacement Trends

A Disaggregation of Internal Displacement by Level of Urbanization
Bueermann G., Klatt J., Sullivan D., Zambrano E.

As the number of people internally displaced due to conflicts and disasters around the world continually rises, humanitarian actors - including the International Organization for Migration (IOM) - strive to better understand the displacement dynamics, which provide them with the information they need to develop improved responses and policies for those forced to flee.

One underexplored aspect in this sector is the geographical distribution of internally displaced persons (IDPs) across urban, peri-urban, and rural areas. Recent research by the International Organization for Migration's (IOM) Displacement Tracking Matrix (DTM), conducted in collaboration with The World Bank and the European Commission Joint Research Centre (JRC) sheds light on this by proposing a data-driven approach to quantifying shares of urban/rural displacement.

IOM's Displacement Tracking Matrix (DTM) is an information system and set of tools developed to gather and analyse data to disseminate critical multi layered information on the mobility, vulnerabilities, and needs of displaced and mobile populations. The tool enables decision makers and responders to provide these populations with better context specific assistance.

This study utilizes GHSL data to obtain more nuanced understanding of the disaggregation level of urbanisation in internal displacement. GHSL provided a comprehensive labelling of geographic areas across 28 countries, within a square kilometre of resolution of urban centres, urban clusters, and rural areas. Ultimately, the GHS-SMOD provided a granular level of global spatial information about the human presence on the planet over time, which was essential to the investigation and classification of internal displacement.

This work shows how to disaggregate IDP figures by settlement class. Figure 72 shows the sketch of the method. It constitutes the first step to its operational usage. This study, bolstered by continually improving displacement data and consistently granular GHSL data, has abundant scope to further this methodological approach and subsequently improve the policy implications the team explored. Developing methods to better understand the disaggregation of displaced populations by level of urbanisation is essential to understanding how the evolution of needs and conditions relates to physical geographic location. A more nuanced and granular understanding of these breakdowns and trends will ultimately lead to more informed policies and program implementations.

The population data provides the foundation for a comparative analysis between IDPs and non-IDPs in rural and urban areas. For example, the analysis found that almost half of Nigerian population (48.5%) lives in peri-urban and urban areas. By contrast, over 63% of IDPs are concentrated in urban and peri-urban settlements. This allowed for a detailed investigation into related issues, such as economic mobility and access to services. The results of this analysis highlight that support for essential services is needed more in the case of rural IDPs in Nigeria. At the same time, they suggest re-evaluating the assumption that access to income and economic opportunities are far higher in urban centres.

Our findings can support planners and policy makers understanding to better identify and address the varying needs and challenges faced by internally displaced populations from across urban, peri-urban and rural environments within a country to better anticipate and inform context specific assistance in all phases of response. Additionally, DTM data can help to identify not only whether access to services is addressed but why it is or is not accessed. This can help to pinpoint practices that support both immediate and longer-term needs, particularly as displacement is increasingly becoming protracted, with the average length of displacement ranging from 17 years 25 to 23 years.

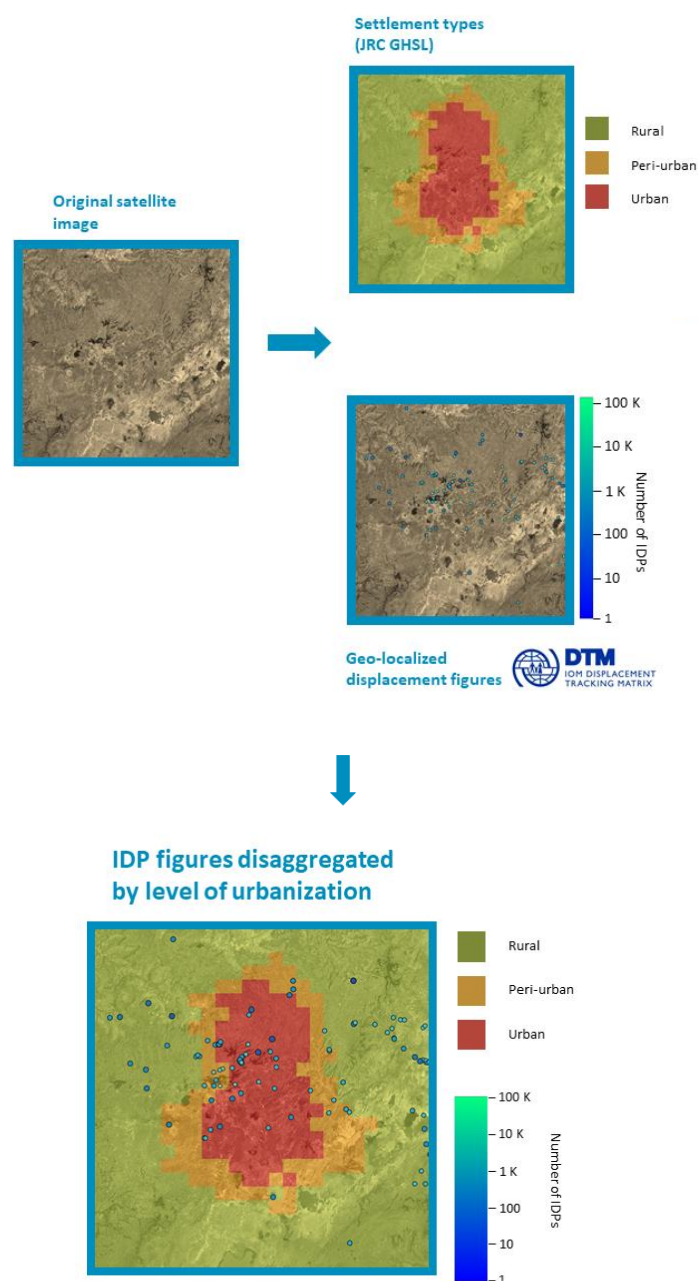


Figure 72 Algorithm for Urban Disaggregation of IDPs from area-based assessments. The procedure comprises a matching between the Global Human Settlement Layer and geo-localised displacement figures.

Datasets:

DTM Baseline and Location Assessments (displacement.iom.int), GHS population grid multitemporal (1975-1990- 2000-2015),

3.3.7 Detecting spatial patterns of inequality from Earth Observation

Towards mapping deprived communities

Ehrlich D., Schiavina M, Pesaresi M Kemper T,

Spatial inequalities in income, health and education, challenge the social and economic progress and sustainable development of many developing countries. This spatial inequality of economic and social indicators of wellbeing across geographical units is particularly important when spatial and regional divisions align with political and ethnic tensions to undermine social and political stability. Mapping inequalities is a challenge and there is little systematic evidence on the extent of spatial inequality within countries of the globe or across countries. This study case provides a global overview of inequality based on three global variables: built-up, population and night-lights (Ehrlich, Schiavina, et al. 2018). It is a preliminary global qualitative comparison, intended to provide complementary information to more traditional methods for inequality mapping.

Figure 73 shows socio-economic patterns across the globe. It is produced by combining nightlights (Elvidge et al., 2017); population density (Freire et al. 2016), and built-up area (Pesaresi, Ehrlich, et al. 2016) in 2015, respectively colour coded with red, green and blue. The regions where the blue dominates indicates high energy use and include the Gulf energy producing countries as well as the high income country in Europe, Australia, East Asia and Southern Africa. The red pattern shows the low lit and high population human settlement patterns that are typically of low income countries and clearly visible in East Africa. The green patterns show high built-up and population and no lights are typical of High-income countries. The lack of lights is visible also in rural and central China. Middle-income and emerging economies display intermediate night lit patterns.

Many human settlement spatial patterns of inequality seem to be associated with countries income. Typically, high-income countries are very well lit at night, low income countries are poorly lit at night. The most striking example is visible between South Korea that is very well night lit and North Korea that is very poorly night-lit (Figure 74 left). All larger cities of the world are night lit, those in low-income countries are often less well lit than cities in high-income countries. In addition, the peripheries of many large cities in low-income countries are very poorly lit. Figure 2 shows that settlement patterns are related also to internal strife or conflict. Figure 74 (right) shows part of Syria centred on Damascus in 2015. Damascus is represented by two distinct patterns with the western part of the city that is well lit and the eastern part that appears as not lit. In 2015 the government-controlled area west of the city has continuous electricity supply that was not available in the rebel-held area.

The demand for providing up-to-date global scale information on societal activity in settlements have prompted researchers and scientists to combine socio-economic data from field surveys and population census with EO data or satellite derived products. Most importantly, that demand originates from policy makers addressing humanitarian and development aid. In fact, data on poverty and inequality are needed to monitor the post-2015 framework agreements. This work contributes to the discussion on the development of all SDG indicators and in particular for SDG 1 (end poverty in all its forms everywhere”) and SDG 7 (ensure access to affordable, reliable, sustainable and modern energy for all”).

The demand is also generated by the scientific community striving to understand the human impact on the planet and the impact of hazardous events on human society. The unique characteristics of the input data – that of nightlight, of built-up and residential population – may be used to developing applications requiring frequent updates, for nowcasting or projection of deprivation, poverty, and the resilience of human communities. There might as well be potential to measure the impact of major crises and disasters at a local level.

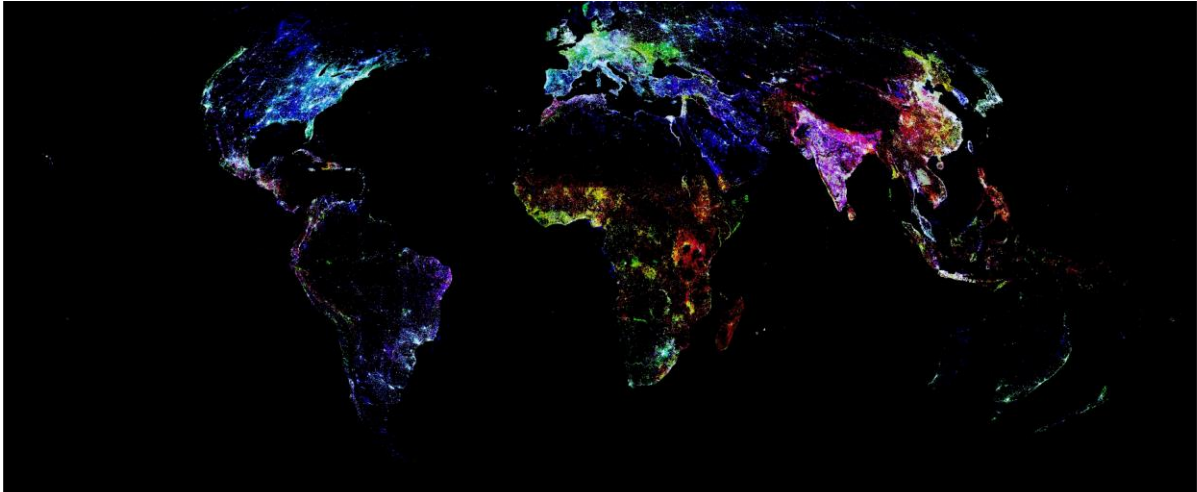


Figure 73 Global patterns of inequality detected by combining global population density, built-up density and night light emission for 2015

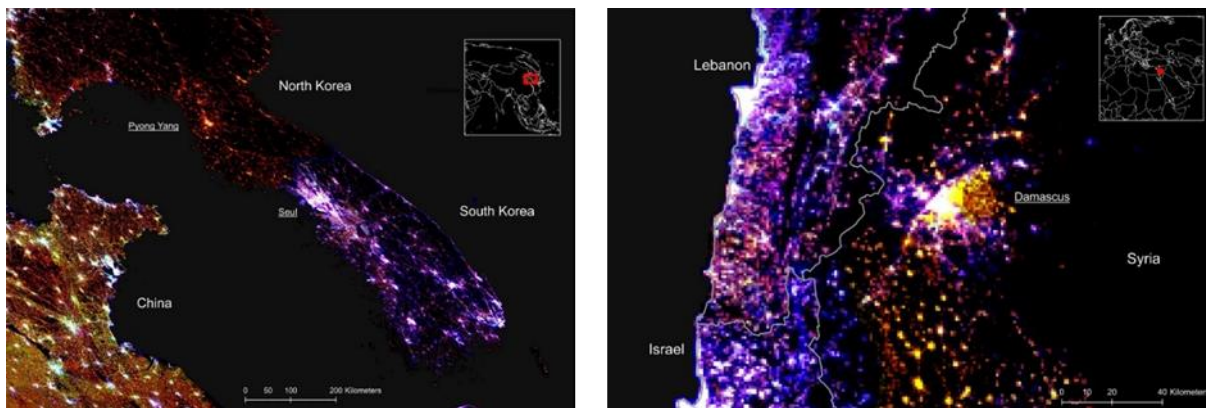


Figure 74 Inequality creating sharp contrast between neighbouring countries, examples of the Korea peninsula (left) and Middle East (right).

Datasets:

Ehrlich, D., Schiavina, M., Pesaresi, M., Kemper, T., 2018. Detecting spatial patterns of inequality from remote sensing (EUR - Scientific and Technical Research Reports No. 29465). Luxembourg: Publications Office of the European Union.

Elvidge, C.D., Baugh, K., Zhizhin, M., Hsu, F.C., Ghosh, T., 2017. VIIRS night-time lights. *International Journal of Remote Sensing* 38, 5860–5879. <https://doi.org/10.1080/01431161.2017.1342050>

Freire, S., MacManus, K., Pesaresi, M., Doxsey-Whitfield, E., Mills, J., 2016. Development of new open and free multi-temporal global population grids at 250 m resolution, in: *Proceedings of AGILE 2016*. Presented at the AGILE 2016, Helsinki, Finland.

Pesaresi, M., Ehrlich, D., Ferri, S., Florczyk, A.J., Freire, S., Halkia, M., Julea, A., Kemper, T., Soille, P., Syrris, V., 2016. Operating procedures for the production of the Global Human Settlement Layer from Landsat data of the epochs 1975, 1990, 2000, and 2014. Joint Research Centre, Luxembourg: Publications Office of the European Union.

3.3.8 Tracking Infrastructural Transitions using Multi-Temporal GHSL, Black Marble, and GPW Population Data

Stokes E. C., Seto K. C.

Though urbanization is often linked to economic development, in some regions, cities have grown in population and land area while remaining bereft of basic services like reliable electricity. Satellite data has been used to track urban growth for decades, but there have been few studies that have monitored whether infrastructure investment—which is directly linked to quality of life and economic prosperity—is keeping pace with demographic and land transitions. This research explores how using multi-temporal population, land, and nighttime lights data in tandem can add to our understanding of two infrastructure focused SDGs—Goal 7.1 (ensure universal access to affordable, reliable and modern energy services) and Goal 11.1 (ensure access for all to adequate, safe and affordable housing and basic services and upgrade slums).

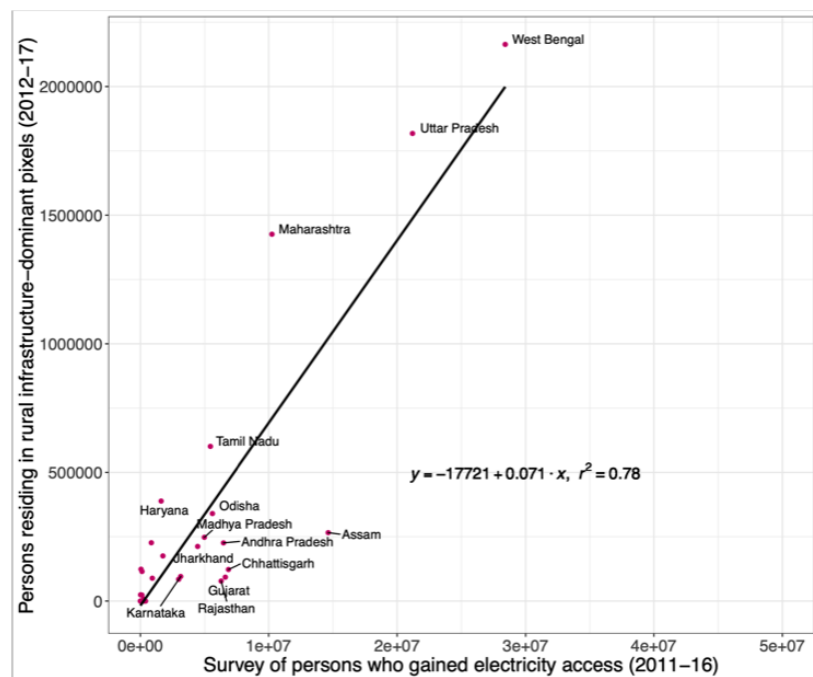
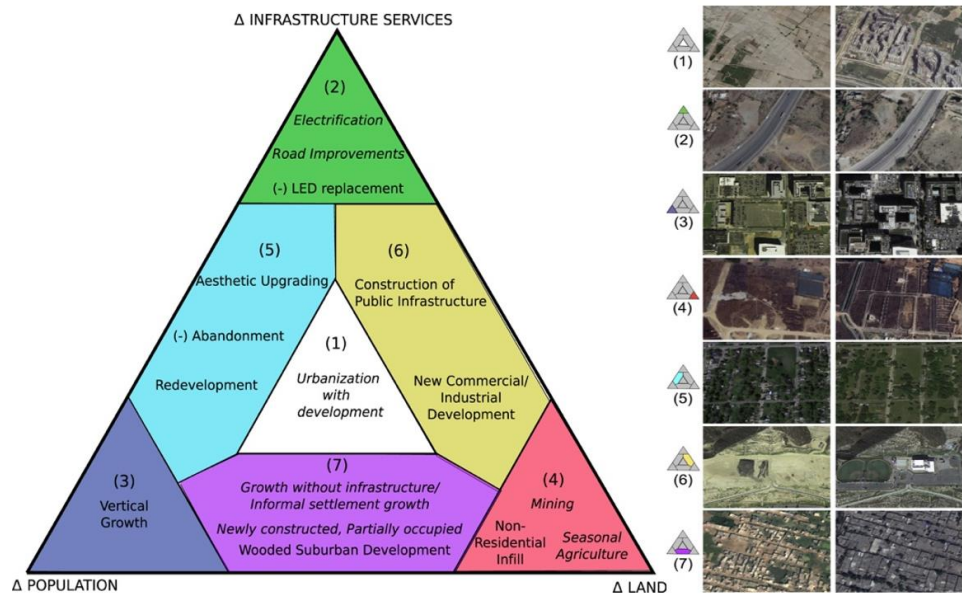
Key inputs to completing this study are independent, multi-temporal datasets on population change (from GPW 4.10 (CIESIN, 2018)), urban land change (from GHS-BUILT layer (GHSL) (Corbane et. al, 2018)), and electric infrastructure change (from satellite-derived nightlights). For nightlights, we use a new product, called NASA's Black Marble Product Suite (Roman et. al, 2018), created from data acquired by the Visible Infrared Imaging Radiometer Suite (VIIRS) day-night band. Radiance measurements from the day-night band are corrected to omit light from the moon and straylight, and to reduce effects from snow, vegetation, and the atmosphere. We use daily Black Marble data from 2012 to 2017 to regress a trendline describing change in nightlights at a 1 km² spatial resolution.

Because these three datasets measure intrinsically different urban transitions (population, land, and infrastructure changes), their fusion allows for the identification of places that may be urbanizing without increased electricity access (informal settlements), or areas benefiting from electrification. An unsupervised classification based on slopes from the three time-series yields seven urbanization classes in India and the US, two of which are especially relevant to the SDGs; *dark growth* (class 7 in Figure 75) and *electrification* (class 2 in Figure 75). Dark growth corresponded to growing informal settlements within major Indian cities, like Kolkata and Mumbai. Electrification was observed in small villages in the north of India — e.g. Jharkhand, Uttar Pradesh, Bihar, Madhya Pradesh, and Haryana — and along newly developed primary and secondary transportation corridors. The classification shows the *electrification* class tracks district level statistics on electricity access expansion reported from India's national surveys (Figure 76).

The classification results also show that Indian urbanization is dominated by two main classes: concurrent change and dark growth. Concurrent change, which corresponded to the construction of large-scale new developments on previously agricultural or wild land, is well-represented when using population datasets, NTL radiances, or built-up land area as parallel proxies. In contrast, dark growth areas, highlighting lags in public infrastructure development, are only identified when the datasets are not used as proxies of one another, but as independent descriptors of different urbanization processes.

In addition, uni-dimensional proxies of urban change do a particularly poor job of capturing urbanization occurring in developed countries. Whereas concurrent change accounted for 83% of the high change land area in India, it only comprised 41% of high change areas in the US, which were dominated by population growth or decline unaccompanied by land change. In the US, more than half of the “urbanization” signal could be overlooked by tracking urbanization as any singular variable of change.

The classes resulting from this study are interesting for urban policy and development researchers and practitioners alike, showing variations in how urban areas are changing in form, use, and quality. They also advance understanding of how urbanization impacts sustainability, and particularly human well-being. The methodology developed can help researchers and practitioners monitor the success of electrification initiatives, track whether slums are expanding and target infrastructure development resources to the areas that need them most. The ability to differentiate between different archetypes of urbanization also facilitates the study of urbanization's linkages to other global change and sustainability issues of importance (e.g. emissions or light pollution from new electricity infrastructure vs. biodiversity or agricultural loss from land changes).



Datasets:

GHS built-up grid, Joint Research Centre (JRC), Gridded Population of the World (SEDAC), Black Marble product suite (NASA).

Stokes, Eleanor C., and Karen C. Seto. "Characterizing urban infrastructural transitions for the Sustainable Development Goals using multi-temporal land, population, and nighttime light data." *Remote Sensing of Environment* 234 (2019): 111430.

3.3.9 SDG Voluntary Local Reviews: using GHSL layers to measure SDGs in European cities

Informing local authorities monitoring of the 2030 Agenda
Siragusa A.

The scope of the project URBAN2030, developed by the JRC with the support of DG REGIO, was to provide EU local authorities with a guide to set up local monitoring systems for the Sustainable Development Goals (SDGs), which serve both for monitoring of the achievements of the local administrations, but also as tools to foster the cooperation among city departments. The SDG local monitoring system would enable cities to prepare Local Voluntary Reviews (VLRs) to assess their achievement of the SDGs and to quantify their contribution towards the Agenda 2030. In 2018 a number of cities started to produce VLRs, but in absence of a common framework and guidelines, every city used different local indicators. Indeed, the indicators used for the global monitoring of the SDGs, defined by the Inter-agency and Expert Group on SDG Indicators (IAEG-SDGs), are designed at country level and can hardly be applied to the local scale. As a result, the first generation of VLRs (2018-2020) does not allow to compare the obtained results among cities (Pipa & Bouchet, 2020, p. 23).

The assessment of the SDGs should be evidence-based and tailored to the local situation, but also based and measured using comparable and sound indicators. It should include considerations on the local context and actions. Moreover, there was a gap in the identification of a set of local indicators that consider the European context. Sound methodologies and examples for the SDGs monitoring in cities were necessary to support cities in overcoming challenges related to capacity, data availability and relevance, sectorial silos.

The Joint Research Centre (JRC) elaborated the first European Handbook for SDG Voluntary Local Review (Siragusa et al., 2020), launched in February 2020 at the World Urban Forum 10. The Handbook has been downloaded more than 9,000 times since then and it has been acknowledged as a relevant reference for several studies published by international organizations (OECD, 2020; UCGL and UN-Habitat, 2020; Sarah Bentz, 2020). The Handbook includes 71 indicators, both official and experimental, harmonised and not harmonised (Figure 77). The indicators have been selected considering two main characteristics: meaningfulness for cities and comparability over space and time (Figure 78). The indicators included in the first Handbook are based on different sources including European Commission's services (JRC, DG REGIO, EUROSTAT), the European Environmental Agency, the Organization for Economic Co-operation and Development, etc.

The GHSL layers have been used as reference for the calculation of the "Built-Up Area Per Capita", suggested for Goal 11. In the Handbook, the "Built-Up Area Per Capita" has been preferred to the Land Use Efficiency indicator, usually calculated as the ratio between the land consumption rate and the population growth rate. The "Built-Up Area Per Capita" expresses a concept that the authors considered easier to communicate to citizens and more relatable (area occupied by each person) (Siragusa et al. 2020, pp. 146–147).

The GHSL has been also indicated as reference for the calculation of the "Urban Greenness" indicator, suggested for Goal 15. This specific indicator is included in the Level 3 classification of the European Settlement Map 2019 release and it gives the total amount of green area in square meters in the area of interest (Siragusa et al. 2020, pp. 188–189).

Among the characteristics that SDG local indicators should have, some are clearly stated in the *Handbook*: relevance at local scale; being of competence of local governments; geographical coverage and availability in different countries; timeliness, time coverage and comparability over time; affordability of data collection and production over time.

In consideration of those characteristics, the use of indicators computed using the GHSL for the SDG monitoring comes with advantages related to: (i) comparability among cities because of data at grid level; (ii) timeliness, thanks to the scheduled release plan of the products; (iii) affordability, since every user can get the data for free online; (iv) and accuracy of the GHSL layers compared to similar products. The use of official and experimental indicators as the ones calculated with the GHSL, that are available and ready-to-use to cities, are extremely relevant to enable local authorities with limited resources and capacity to set up SDG monitoring system and Voluntary Local Reviews tailored to their local needs and priorities, while preserving at the same time the possibility to benchmark with peers around the world.

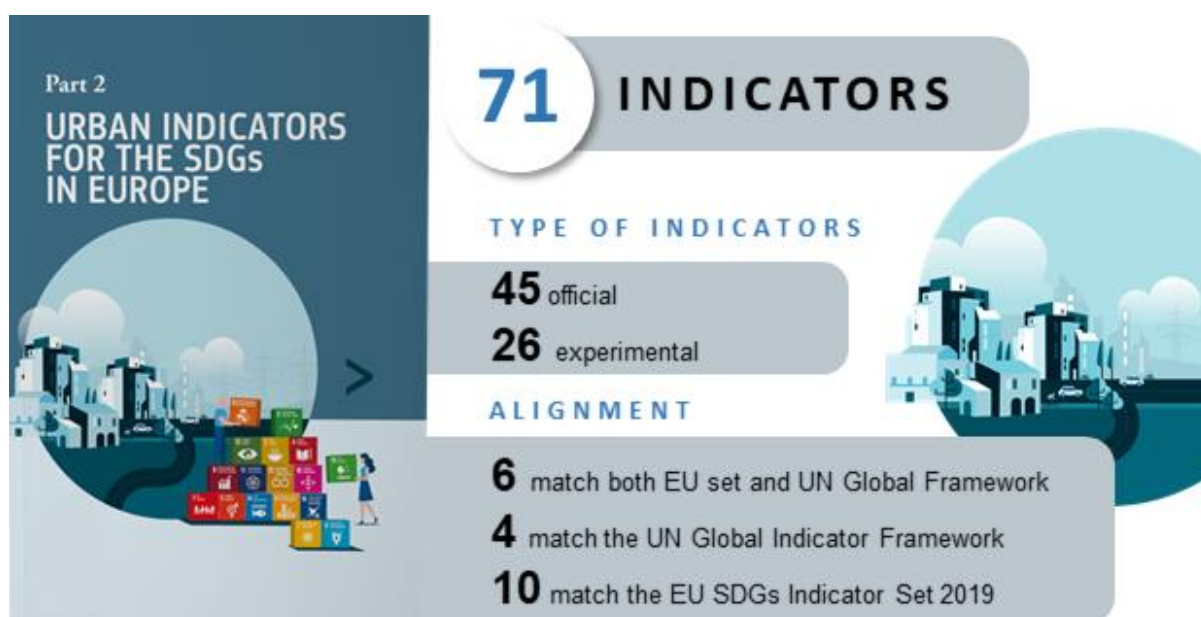


Figure 77 Types and alignment of the urban indicators proposed in the European Handbook for SDG Voluntary Local Review

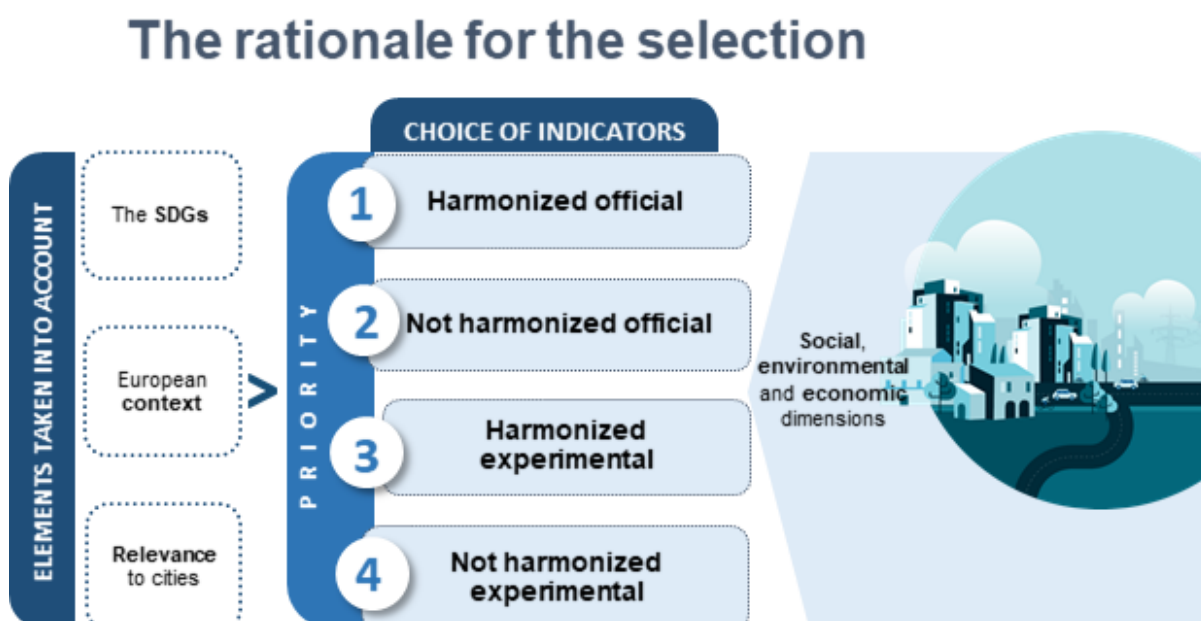


Figure 78 Rationale for the selection of the indicators proposed in the European Handbook for SDG Voluntary Local Review

Datasets:

Florczyk, A. J., Melchiorri, M., Corbane, C., Schiavina, M., Maffenini, M., Pesaresi, M., & Kemper, T. (2019). Description of the GHS Urban Centre Database 2015. Joint Research Centre, for the methodology see (Florczyk et al. 2019). Joint Research Centre. Joint Research Centre. European Settlement Map 2019 release. <https://ec.europa.eu/jrc/en/publication/european-settlement-map-2019-release>

OECD. (2020). A Territorial Approach to the Sustainable Development Goals: Synthesis report. <https://www.oecd.org/cfe/a-territorial-approach-to-the-sustainable-development-goals-e86fa715-en.htm>

Pipa, T., & Bouchet, M. (2020). Next generation urban planning level through voluntary local reviews (VLRs). February.

Sarah Bentz, N. N.-M. (2020). How local & regional government associations bring the SDGs to life. PLATFORMA and the Council of European Municipalities and Regions (CEMR). https://www.ccre.org/img/uploads/piecesjointe/filename/CEMR_PLATFORMA_study_SDGs_2019_EN.pdf

Siragusa, A., Vizcaino, P., Proietti, P., & Lavalle, C. (2020). European Handbook for SDG Voluntary Local Reviews. Publications Office of the European Union. <https://doi.org/10.2760/670387>

UCGL and UN-Habitat. (2020). Guidelines for Voluntary Local Reviews (VLRs) - Volume I. <https://unhabitat.org/guidance-for-voluntary-local-reviews-vol1-a-comparative-analysis-of-existing-vlrs>

3.4

Supporting the European Green Deal



3.4 Supporting the European Green Deal with new knowledge

Climate change and environmental degradation are an existential threat to Europe and the world. To overcome these challenges, the European Commission proposes a new growth strategy with the aim to transform the Union into a modern, resource-efficient and competitive economy, where there are no net emissions of greenhouse gases by 2050. In the strategy, the economic growth is decoupled from resource use and no person and no place is left behind. The European Green Deal is a central initiative of the European Commission and extends to many different sectors, including biodiversity, energy, transport, construction and food.

This section presents examples of how spatially detailed information on the presence of population and settlements in combination with other data sources can inform the decision making process for achieving the goals of the European Green Deal. The first reason for concern, used by the IPCC to illustrate the implications of global warming for people, economies and ecosystems, are the “unique and threatened systems: ecological and human systems that have restricted geographic ranges constrained by climate-related conditions and have high endemism or other distinctive properties. Examples include coral reefs, the Arctic and its indigenous people, mountain glaciers and biodiversity hotspots.”²¹ This Atlas includes two showcases that analyse specifically the population changes in two of these habitats: the **Arctic** (3.4.1) and **mountainous areas** (3.4.2).

In the context of global warming, man-made emissions of air pollutants play a central role. The Emissions Database for Global Atmospheric Research (EDGAR) provides consistent greenhouse gas and air pollutant emissions at the global scale from 1970 until today. In order to improve the **spatial distribution of emissions** in EDGAR (3.4.3), new population-based proxies have been developed using the six settlement types delineated in the GHS-SMOD settlement classification grid.

A central point in the European Green Deal is the change of the energy system of Europe. This requires a decarbonisation of the energy system to reach the climate objectives in 2050. The production and use of energy across economic sectors account for more than 75% of the EU's greenhouse gas emissions. Therefore, the new energy system must be developed based largely on renewable sources. A showcase analyses the potential **energy autarky in Europe** (3.4.4) and another one provides an assessment of the **photovoltaic potential** (3.4.5) of buildings using the high-resolution data of the European Settlement Map.

More than 34% of the European population live in cities and 56% including also the commuting zone. Cities are continuing to grow reducing the green areas in an around the cities. The EO data of GHSL and the ESM allow a detailed analysis of the **green spaces in cities** (3.4.6) and the fragmentation of **natural areas in the functional urban areas** (3.4.7) that include the commuting zones.

²¹ International Panel on Climate Change Special Report 1.5: <https://www.ipcc.ch/sr15/chapter/spm/b/spm2/>

3.4.1 Monitoring Arctic populations dynamics and urbanisation

Potential of the GHSL in remote regions

Koffi B., Wilson J., Ehrlich D., Dubois G., Mandrici A., Vernaccini L., Delli G.

The Arctic region covers territories from 8 countries (USA, Canada, Iceland, Norway, Finland, Sweden, Denmark and Russian Federation) and is home to about 4 million inhabitants. It is one of the “*Unique and threatened systems*” defined by the Intergovernmental Panel on Climate Change as having a high level of risk of adverse consequences from global warming. In addition to the direct impacts of climate change, which is particularly significant in the region, resource extraction, tourism and shifting political relationships are also contributing to changes, which include ice melting, sea levels rising, erosion of coastal areas, permafrost thawing, shifts in the areas where people, plants and animals live, human culture, self-government and livelihood. In 2016, the JRC began working on an Arctic research project to support the integrated EU Arctic policy. One specific work-package of the project is dealing with international collaboration for the Arctic, including a JRC contribution to the international Arctic Resilience Action Framework, which aims *inter-alia* to provide the Arctic Council, states, and peoples with a set of guiding principles and priorities for actions to build resilience in the region.

Arctic populations are expected to be significantly affected in the future by both demographic and migratory changes, as a result of the ever-accelerating climate and socio-economic changes in the region. Long-term monitoring based on an integrated approach and including explorations of the linkages between demographic, social, economic, and natural influences can help understand these changes. We will use 40-year records of built-up, population and settlements data in the Arctic that are available from the GHS data package (Florczyk et al., 2019) as the base from which we can quantify human and environmental exposure to various human pressures and natural hazards. To assess human population pressures in the region, we used the harmonised datasets themselves to generate multi-scale integrated population and urbanisation trends.

The GHS-POP 1 km x 1 km spatial grid was first used to analyse Arctic population dynamics and settlement size to compare with national estimates. We then used GHS-SMOD 1km x 1km spatial grid to quantify urbanisation patterns and trends for the circumpolar region, and national, regional and local scales. Between 1990 and 2015 Arctic national populations increased by 17% overall. National trends vary, ranging from a slight decrease (-3%) for the Russian Federation to high increase (+31%) for Iceland. A slight decrease (-3%) in population is observed in the Arctic sparsely populated regions, resulting from both positive (USA, Canada, Iceland, Kingdom of Denmark, Kingdom of Norway) and negative (Finland, Russian Federation and Sweden) population trends. The mapping of the changes (Figure 80) shows the diversity in population trends across the region, with some areas experiencing high positive (Yukon; Svalbard and Jan Mayen) and negative (Russian Krasnoyarsk region) changes.

Urbanization trends in the Arctic regions of North America, “Europe” (Iceland, Greenland and Norwegian, Finnish and Swedish Arctic territories) and Russian Federation show quite different regional patterns and trends as a result of demography and migration. North America shows a clear urbanisation trend with a corresponding decline in rural populated areas due to the movement of the rural population to larger settlements since 1990. Arctic-Europe and Russia show respectively a small increase and a decrease in urban population (Figure 81). Further analyses, including a comparison between national, regional and municipal population data clearly show the value of GHSL open free products in providing a spatially detailed and harmonised cross-scale documentation of Arctic population dynamics and settlements.

In a further step, GHSL datasets will be used together with other data layers to monitor both environmental and human threats in selected natural, managed and human systems of interest in the Arctic, such as cities, low-lying coastal and river basin areas, and vulnerable land ecosystems. The goal is to define a set of indicators that can be used to identify and monitor major risks, exposure and resilience of the Arctic on regions and scales of interest, using a socio-ecological-based approach where possible. The overall aim is to identify both policy needs at the local and regional scale that reinforce resilience and in the longer term to evaluate the effectiveness of policy interventions for maintaining or increasing socio-ecological resilience in the Arctic.

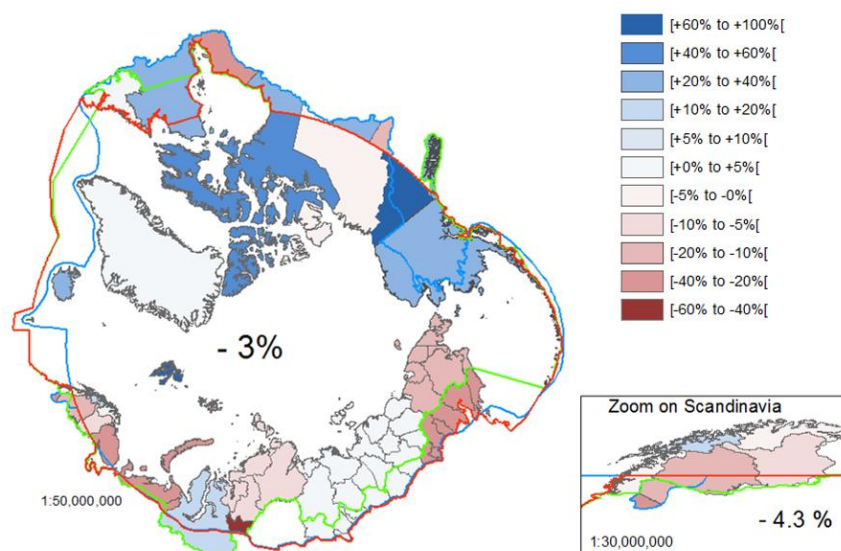


Figure 80 Map of 1990-2015 population change (%) in the Arctic study domain



Figure 81 Low Density grid Cells (LDC; left), Moderate Density Clusters (MDC, right) and High Density Clusters (HDC, right) cells in the Arctic regions of North America (NA; including Alaska and Canadian regions), "Europe" (EUR; including Iceland, Greenland and Norwegian, Finnish and Swedish Arctic territories) and Russian Federation (RUS). The origin is set above 0 in LDC plots to better highlight the temporal trend

Datasets:

Florczyk A.J., Corbane C., Ehrlich D., Freire S., Kemper T., Maffneni L., Melchiorri M., Pesaresi M., Politis P., Schiavina M., Sabo F., Zanchetta L., GHSL Data Package 2019, EUR 29788 EN, Publications Office of the European Union, Luxembourg, 2019, ISBN 978-92-76-13186-1, doi:10.2760/290498, JRC 117104.

3.4.2 Population changes and urbanisation in mountain ranges of the world

Insights from the GHSL

Ehrlich D., Melchiorri M.

Decision makers and donors have at disposal few global datasets that can help in prioritizing needs for development aid and identify path to sustainability in mountain regions of the world. Global mountain issues are addressed mostly in descriptive terms and few datasets are available to quantify societal developments, the deprivation of some of its inhabitants, the impact of natural hazards, and that of a changing climate. Questions including - Where in the world are mountainous environments most affected by human presence? How to improve the sustainability of mountain communities while preserving biodiversity and ecosystem functions? - are difficult to address also for the lack of suitable datasets, indicators or models that provide population and settlement data with global coverage for multiple points in time.

This work delivers statistics on mountain population change between 1975 and 2015 and urbanization on a global scale. The work uses the World Conservation Monitoring Centre (WCMC) global definition of mountains (Kapos 2000) and over 1048 mountain ranges outlines made available through the Global Mountain Biodiversity Assessment (GMBA) initiative (Körner et al. 2017). The data are intersected with the population grids of GHSL (Freire et al., 2016) and Urbanization statistics based on the *Degree of Urbanisation*.

The analysis shows that in 2015, mountain areas host 14% of total world population and that it has increased from 550 million in 1975 to 1050 million in 2015. The comparison of mountain ranges by population density, population increments and urbanization identifies significant differences. The most populated ranges are large in size, but many large ranges host very small populations (Figure 82). The share of urban population in mountain areas is half of that of lowlands that is estimated to be about 75% based on the Degree of Urbanisation applied to GHSL data.

The most populated mountain ranges are at low latitudes (Figure 82). The 30 most populated ranges, those with more than 5 million people (class 1 in Figure 82) account for nearly 40% of total mountain population, while occupying only 10% of total surface of mountain areas. The 180 GMBA ranges with more than 500K people (class 1 and 2) account for 60% of total mountain population, while occupying only 18% of total mountain area.

The most populated ranges include the Ethiopian Highlands, the Himalayas, Yunnan Guizhou Highlands (China), and Eje Volcanico Transveral (Mexico) that accounted for more than 20 million people each in 2015 (Figure 83). In Europe, mountain population is stable or declining, with the European Alps and the Carpathian being the most populated ranges. Highest increment occurs in Africa's mountain ranges with the exceptions of the Nuba Mountains, the only range that decreases in population. Asia hosts the largest mountain population that is more than that of all other continents combined except Africa, and that grows significantly (with the exception of mountain ranges in China and Russia). Latin America is known for its high degree of urbanization and a growing population, while North America for its very low population except for Sierra Nevada and Appalachian. Oceania hosts a negligible mountain population.

Understanding population sizes and growth as well as urbanization patterns is a preliminary step towards understanding sustainability trajectories in mountains. This work may be used to quantifying additional population characteristics including livelihoods, exposure and vulnerability to natural hazards, and underlying risk factors that are specific to mountains. Thanks to GHSL it was possible to analyse over time settlements and populations dynamics for otherwise marginalised area in order not to *leave* mountain people *behind* the sustainable development process.

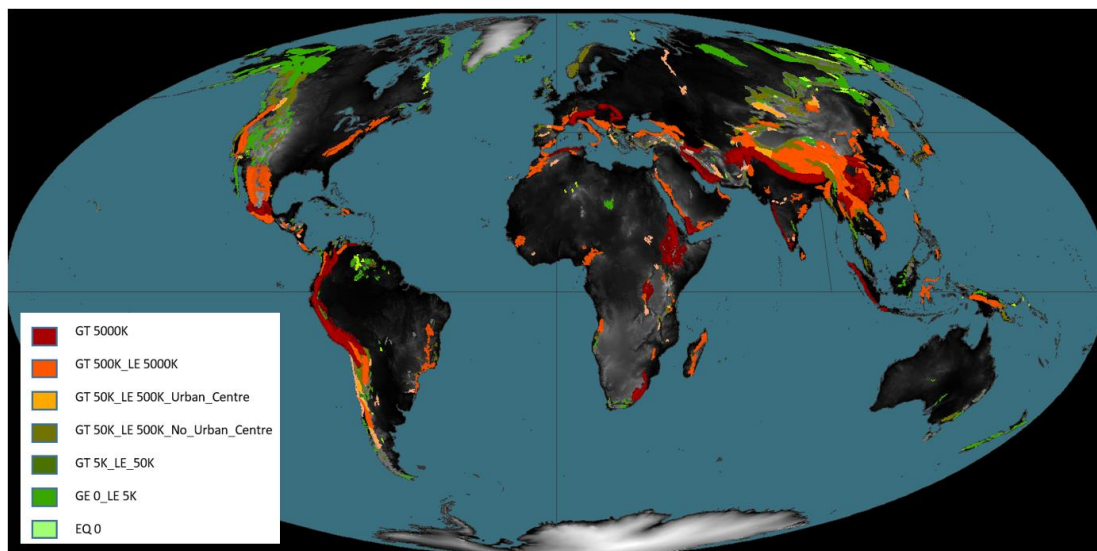


Figure 82 Map of the GMBA mountain ranges coloured in classes of population size. The most populated mountain ranges are located in low latitudes

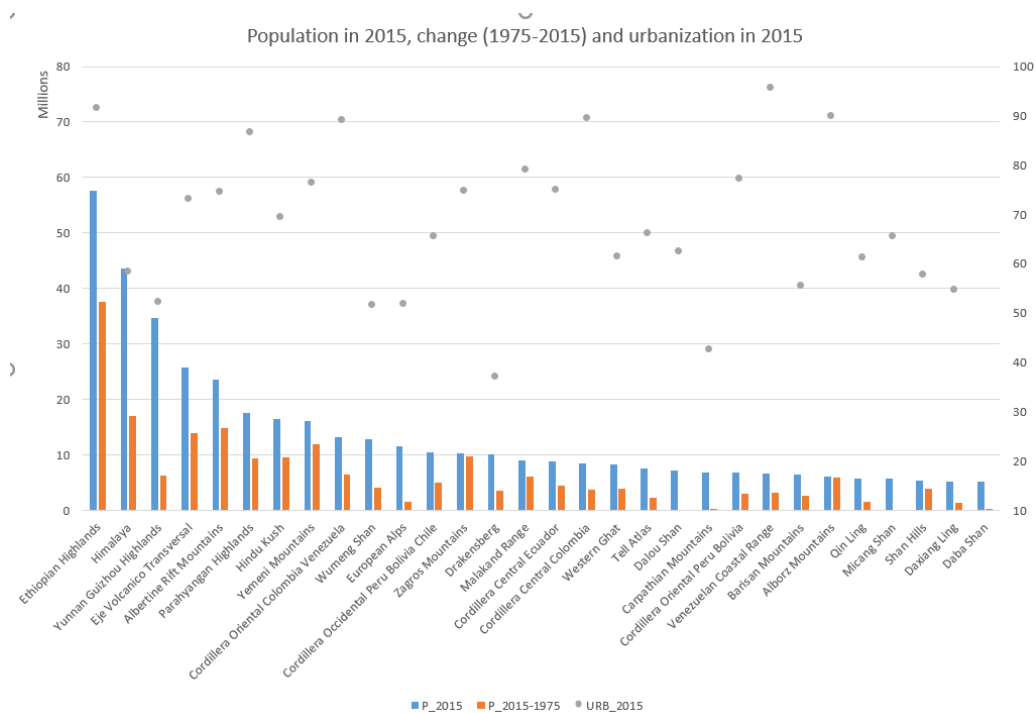


Figure 83 Population change and share of urban population in mountain ranges

Datasets:

Schiavina, Marcello; Freire, Sergio; MacManus, Kytt (2019): GHS population grid multitemporal (1975, 1990, 2000, 2015) R2019A. European Commission, Joint Research Centre (JRC)

Freire, S., MacManus, K., Pesaresi, M., Doxsey-Whitfield, E., Mills, J., 2016. Development of new open and free multi-temporal global population grids at 250 m resolution, in: Proceedings of AGILE 2016. Presented at the AGILE 2016, Helsinki, Finland.

Kapos, V., 2000. Mountains and Mountain Forests. Mountain Research and Development 20, 378–378. Körner, C., Jetz, W., Paulsen, J., Payne, D., Rudmann-Maurer, K., M. Spehn, E., 2017. A global inventory of mountains for bio-geographical applications. Alpine Botany 127, 1–15. <https://doi.org/10.1007/s00035-016-0182-6>

3.4.3 Global air pollutant emissions in urban centres

Forty-five years of emission evolution across world regions, settlements type and sectors
Crippa M., Guizzardi D.

The Emissions Database for Global Atmospheric Research (EDGAR) provides consistent greenhouse gas and air pollutant emissions at the global scale from 1970 until nowadays. EDGAR spatially distributes anthropogenic emissions over global gridmaps at 0.1°0.1 degree resolution (approx. 11 km at the equator), allowing the investigation of where emissions happen and supporting the development of mitigation measures. In order to improve the spatial distribution of the emissions in EDGAR, new population-based proxies have been developed using the six settlement types delineated in the GHS-SMOD settlement classification grid at Level 2 (Florczyk et al., 2019a). The novelty of this approach relies on the possibility to accurately quantify emissions from urban centres compared to rural areas at the global level and to look at their evolution over the past 4.5 decades. Using more accurate gridded population maps increases the quality of the emissions distribution in EDGAR, which are largely used in atmospheric modelling and policymaking. Results from this analysis can help the identification of most polluting areas all over the world and the definition of adequate mitigation measures to improve local, regional and global air quality.

Globally, anthropogenic emissions remained rather stable or increased up to 1.3 times from 1970 to 2015 depending on the pollutant, in particular due to the fastest increase in the emissions of developing countries. For example, in developing regions, NO_x and CO₂ emissions increased more than 4 times in the past 4.5 decades (e.g. SO₂ by 3.1 times, PM₁₀ by 1.4 times, CO by 1.5 times and NH₃ by 1.8 times), partly associated with the fast population growth and economic development. On the contrary, emissions in industrialised regions were stable or decreased mainly due to the implementation of air quality policies and the policy-industry interplay leading to technological advancements that helped in reducing the emissions (e.g. NO_x decreased by 18%, PM₁₀ by 37%, CO by 50% and SO₂ by 66%).

Urban areas are of a growing importance because nowadays almost half of global population lives in urban centres and urban population tripled compared to 1970, while rural population increased only by 45%. In 2015, around a third of global anthropogenic emissions is emitted in urban centres (Figure 84), which represent only a minor fraction of the global area. The share of emissions from urban centres are 35% for CO₂, 29% for NO_x, 27% for PM₁₀, 26% for CO, 37% for SO₂; however, these fractions vary for industrialised and developing regions. Emissions varied across settlement types over the years, for example, CO₂, NO_x and PM₁₀ emissions showed the fastest growth in urban centres compared to the other settlement classes from 1970 to 2015 both for developing and industrialised countries, reflecting the enhancement of anthropogenic activities related with combustion processes. On the contrary, over the same time period CO emissions showed reductions in urban centres due to more efficient combustion in particular in industries and their delocalisation outside urban centres, while they increased in villages/towns and rural areas in particular in developing countries. A different pattern is found for NH₃ with the fastest growth happening in urban centres in industrialised countries (in particular in North America and to a lesser extent in the EU) due to the deployment of selective catalytic reduction systems to abate NO_x while producing NH₃. Finally, SO₂ emissions decreased over the past decades mainly in urban centres thanks to the implementation of fuel quality directives and international treaties which lead to the desulphurisation of the fuel used in vehicles, power plants and industries, while they increased in the other settlement classes in developing regions.

Emissions of air pollutants and GHGs in urban centres are mostly associated with combustion activities related with the production of energy, industrial processes, residential and transport (Figure 85). For example, NO_x is mostly emitted by the energy-industry (69%) and transport sectors (24%), with a higher share from transport in industrialised countries (29% on average, and higher shares for countries mostly using gasoline vehicles). CO emissions come mainly from the transport sector, with a global share of 36% which increases up to 47% in industrialised regions where emissions of CO, SO₂ and PM₁₀ decreased from 1970 to 2015 thanks to the higher energy efficiency and implementation of new technologies and abatement measures despite the increase in fuel consumption. Differently, NH₃ is mostly emitted in rural areas, villages and towns, although 9% of NH₃ emissions still happens in urban centres. In industrialised countries NH₃ is emitted not only from agriculture, but also from transport and waste and NH₃ emissions are increasing in particular in urban centres, while NO_x emissions are rather stable. In developing regions contributions come also from the power-industry sector and residential.

This study highlights the need of defining targeted measures also on urban centres to abate almost a third of global air pollutant emissions. When considering not only urban centres but also their suburbs, roughly 50% of global emissions is produced (over a total emitting area less than 1%). The analysis of sector specific emissions

can also help in identifying the most effective measures to tackle air quality and climate change issues at the global scale.

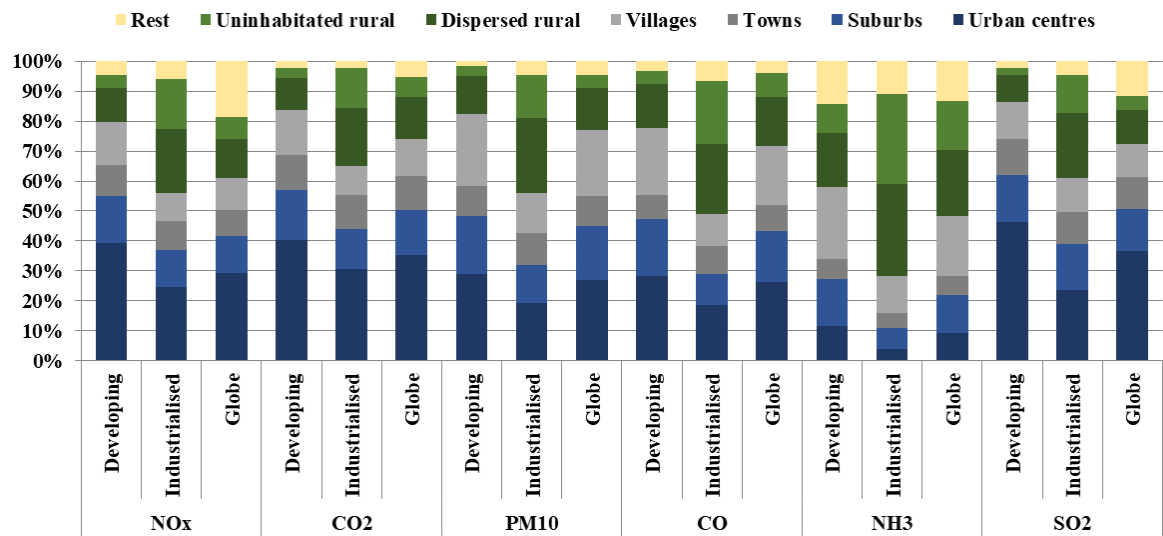


Figure 84 Air pollutant and CO2 emissions in different settlement areas in 2015

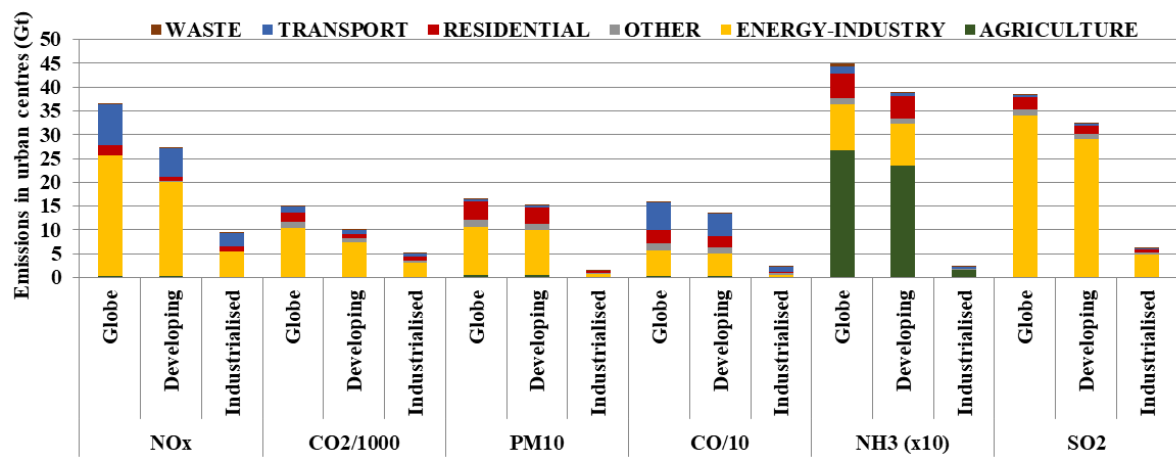


Figure 85 Air pollutant and CO2 emissions by sector in urban centres in 2015

Datasets:

https://edgar.jrc.ec.europa.eu/overview.php?v=50_GHG

https://edgar.jrc.ec.europa.eu/overview.php?v=50_AP

3.4.4 The possibility for renewable electricity autarky in Europe

European countries, regions, and municipalities powered by sun and wind only

Tröndle T., Pfenninger S., Lilliestam J.

A rapid decarbonisation of the European electricity sector is necessary to fulfil commitments under the Paris climate agreement. Renewable electricity is a promising option for a full decarbonisation but, compared to current options for electricity supply, it has a lower power density and therefore requires larger amounts of land. For this and other reasons, there is an ongoing political and societal debate on where to generate electricity. One solution is to generate electricity locally, close to where it is consumed. Proponents of this solution point to local economic benefits and to the independence which this autarkic structure offers in their eyes.

However, it is not known whether such renewable electricity autarky would actually be possible in Europe. A necessary condition for renewable electricity autarky is that the generation potential exceeds local electricity demand. While previous studies indicate that the potential is large enough for Europe as a whole, the generation potentials of all countries, and in particular of all subnational regions and municipalities in Europe are not known. The Europe-wide consistency and high resolution of data from the Global Human Settlement Layer allow us to assess the possibility for renewable electricity autarky on all levels in this study – from the continental down to the municipal level. We use the data in two ways: First, we combine the spatial distribution of built-up areas provided within the European Settlement Map with other data to estimate generation potentials of solar and wind power with high spatial resolution. Second, we combine the spatial distribution of population provided within GHS-POP with further data to estimate the distribution of electricity demand. Whenever the potential exceeds demand, we deem renewable electricity autarky possible for the whole continent, individual countries, regions, or municipalities.

We find that the potential of renewable electricity in Europe is large enough to cover current electricity demand, even if, next to technical restrictions, we consider environmental protection, land use conflicts with agriculture, and allow to use only 10% of the remaining surfaces. We also find sufficient potentials for all countries in Europe, although some countries, like Belgium, Luxembourg, and Germany, have to employ larger amounts of their available land to be able to fulfil demand domestically because land is scarce and electricity demand is high in these countries.

On the regional and municipal levels, however, we find many regions and especially municipalities whose potentials of renewable electricity are too low to satisfy local demand, see red areas in Figure 86. These are usually places with high population density and limited land availability. If all municipalities in Europe were to strive for electricity autarky, one in four Europeans would suffer from insufficient renewable electricity supply. In addition, enforcing renewable electricity generation to be close to demand centres means high pressure on the little non-built-up land that remains in densely populated areas. By accepting higher densities of generation infrastructure, more regions and municipalities could become autarkic, see light green and light red regions in Figure 87.

The data from the Global Human Settlement Layer allows us to show that renewable electricity autarky is possible for Europe as a whole, for all countries, and for most regions and municipalities in Europe. While electricity autarky even at local level is an option in most places, we also show the trade-off that comes with local-level autarky: pressure on non-built-up land close to the homes of Europe's population rises. In regions and municipalities where full autarky is not possible, electricity must be imported to support the insufficient local generation potential. With imports, all regions and municipalities in Europe can be supplied with fully renewable electricity that is generated either locally or in neighbouring regions.

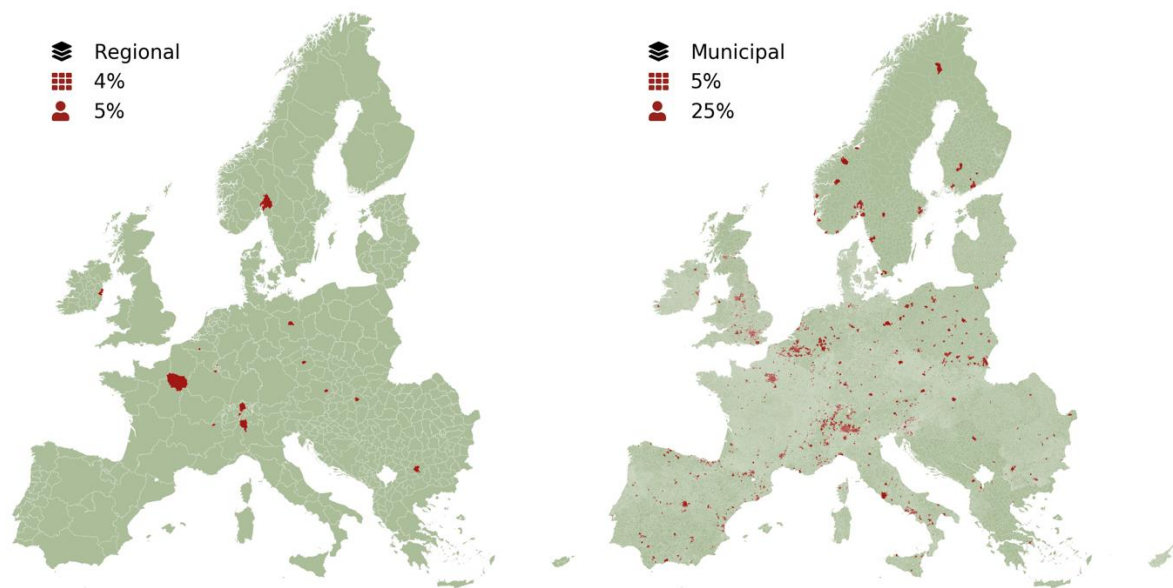


Figure 86 Areas where the generation potential exceeds electricity demand (light/green) and where it does not (dark/red), for all subnational regions and municipalities in Europe. For both levels the text box furthermore shows from top to bottom: the name of the level, the fraction of undersupplied administrative units, and the fraction of the European population living in undersupplied administrative units. Source: Tröndle et al (2019), Energy Strategy Reviews

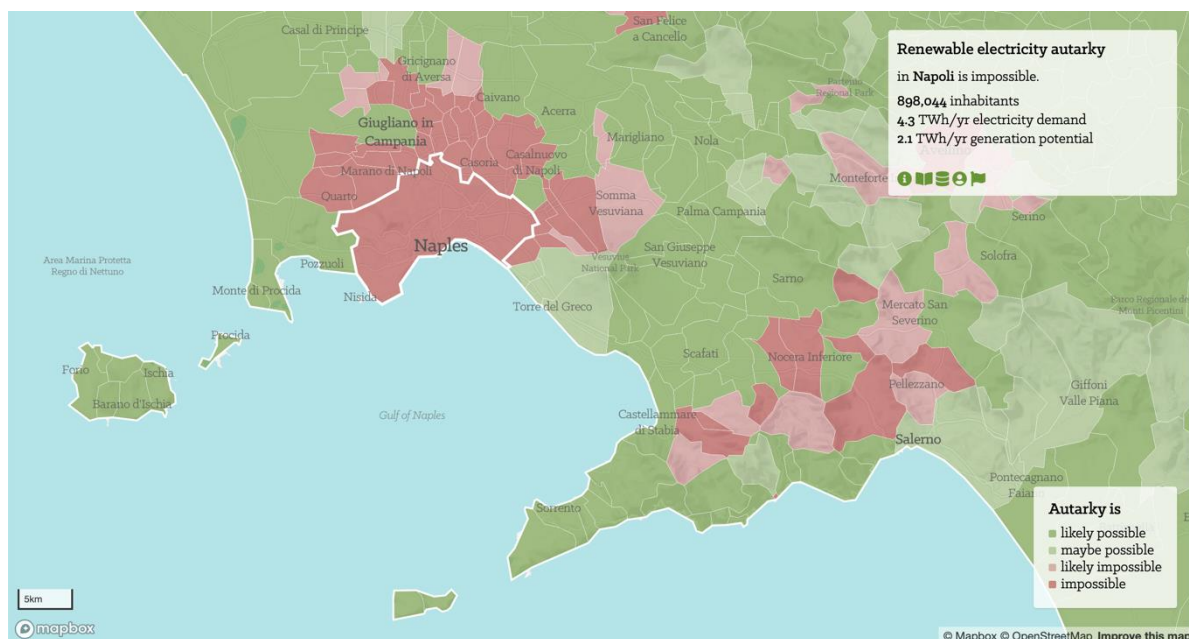


Figure 87 Screenshot of the interactive map visualising the main results of our study. The map visualises the potentials for each of the 34 countries, 502 regions, and 122,635 municipalities. Municipalities coloured light green and light red may be able to achieve renewable electricity autarky by allowing for higher local densities of electricity infrastructure. Available at: <https://timtroendle.github.io/possibility-for-electricity-autarky-map/>

Datasets:

Tröndle, T., Pfenninger, S., & Lilliestam, J. (2019). Result data related to "Tröndle et al (2019) — Home-made or imported: on the possibility for renewable electricity autarky on all scales in Europe" [Data set]. Zenodo. <https://doi.org/10.5281/zenodo.3244985>

3.4.5 Using the European Settlement Map to assess the rooftop solar photovoltaic potential in the European Union

Kougias i., Szabó S., Jäger-Waldau A., Taylor N., Kakoulaki G., Bódis K.

Solar photovoltaic (PV) systems play an important role in the transition towards low-carbon energy systems and European Union's (EU) climate targets. Rooftop systems in homes and commercial/industrial buildings currently represent 60% of the total installed solar power in Europe. The implementation of the new European Green Deal with updated 2030 EU climate targets to reduce greenhouse gas emissions by 55% will require an increase of the installed capacity from 133 GW (end of 2019) to 455-605 GW, depending on the scenario [1]. Energy efficient and near-zero energy buildings have a big role to play in this. Accordingly, there is a strong possibility that installation rates of rooftop PV systems in the EU will increase at high rates in the following years.

The design of effective policy measures that enable such deployment rates require reliable estimations of the available solar potential of EU roofs. Nevertheless, roof area data is not available at EU level and except from fragmented and not harmonized pieces of information. This limitation is not expected to be solved in the near future and requires alternative approaches. An effective option is the consideration of satellite earth observation data, specifically the European Settlement Map (ESM) that is based on satellite imagery and developed in the Global Human Settlement Layer (GHSL) framework. Satellite imagery can provide an overview of the EU building stock at continental-scale and in a harmonised manner. Due to scale and the specifications of input satellite imagery, the present ESM cannot provide refined representation of individual structures to allow an accurate quantification of EU rooftop areas. This limitation is shown in Figure 88, where certain areas evident in the aerial photo in Figure 88A (e.g. stadium, open space) are misinterpreted as building areas in the ESM image in Figure 88B. A sample comparison of ESM satellite imagery with reference cadastre data confirmed an overestimation of rooftop area (Figure 88C). To overcome this limitation, we developed a scaling factor methodology by comparing the ESM layer with accurate high-resolution cadastre information for selected regions, where such data is available. In this way, the model was trained in a machine learning process and the obtained scaling factors could be applied to the ESM layer in any location (Figure 88D shows the result for the sample area).

Coefficients were calculated for discrete building density classes. The analysis followed the definition of urban and rural areas by Copernicus, the EU's Earth Observation Programme. Accordingly, for urban areas the analysis harmonized with the definition of European Urban Atlas, while on rural areas with the corresponding Corine Land Cover classes. The application of the calculated scaling factors on the ESM layer allows a reliable estimation of building density at EU level. Figure 89 presents a sample of the obtained building density raster for the region of Lombardy, in Italy. The resulted building density raster was then combined with spatial information of solar irradiance. After applying the PVGIS energy yield model for photovoltaics [4], the final result was a unique high-resolution assessment of EU's rooftop solar PV technical potential. Overall, the existing EU building stock could generate up to 680 TWh of electricity, annually, covering up to 1/4 of EU's total electricity consumption.

This data was further processed to determine economic potential, by calculating a levelised cost of electricity (LCOE) for each rooftop over EU. Findings show that, for the majority of EU buildings, generation costs are lower than current retail electricity tariffs. The competitive part of the available resource –known as economic potential– is estimated at 468 TWh and represents nearly 70% of the available technical potential.

The policy relevance of applying ESM to assess solar PV options was shown in an analysis covering the EU Coal Regions in Transition (CRiT) [3]. The spatial analysis revealed a technical solar PV potential of 88 GW in CRiT rooftops, a power capacity that could yield nearly 100 TWh, annually. Further development of the approach will aim to support regional studies that build on additional high-resolution reference data. Analyses at neighborhood- and building-level would enable the design of net zero energy buildings. Such integrated implementation of energy and building asset policies could connect with the renovation wave and support a recovery programme in line with the "Build Back Better" paradigm.



Figure 88 (A) Aerial photo (B) Overlay of ESM (grey patches) and cadaster data (red polygons). (C) Observed overshoot in the ESM (red patches) to be filtered out. (D) Calculated scaling factors per land cover class. Source: [2]

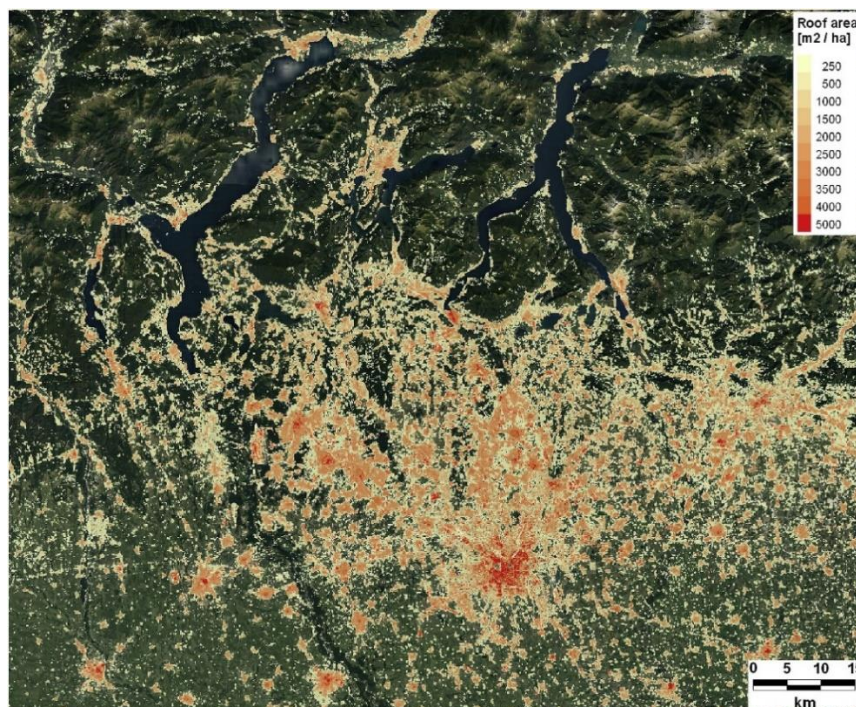


Figure 89 Example of obtained building density raster for the Lombardy region in northern Italy. Source: [2]

References:

- 1) Jäger-Waldau, A., Kougias, I., Taylor, N. and Thiel, C., 2020. How photovoltaics can contribute to GHG emission reductions of 55% in the EU by 2030. *Renewable and Sustainable Energy Reviews*, 126, p.109836.
- 2) Bódis, K., Kougias, I., Jäger-Waldau, A., Taylor, N. and Szabó, S., 2019. A high-resolution geospatial assessment of the rooftop solar photovoltaic potential in the European Union. *Renewable and Sustainable Energy Reviews*, 114, p.109309.
- 3) Bódis, K., Kougias, I., Taylor, N. and Jäger-Waldau, A., 2019. Solar photovoltaic electricity generation: a lifeline for the European coal regions in transition. *Sustainability*, 11(13), p.3703.
- 4) European Commission, Joint Research Centre. Photovoltaic Geographical Information System (PVGIS). 2020. Available online: <https://ec.europa.eu/jrc/en/pvgis> (accessed on 26 May 2020).

3.4.6 The European Settlement Map (ESM 2015) green component

Assessment of Access to Green Open Spaces

Corbane C., Sabo F.

Green open spaces are an essential infrastructure that contributes to the physical and mental health of urban area residents. In fact, the provision of accessible green open spaces is part of the whole urban planning process and integrated with other sector policies (such as housing, transport, health, sustainability, biodiversity) (WHO Europe Urban Green Space expert panel and Hunter 2017).

Measuring proximity to green open spaces within European cities enhances our information on the presence and availability of green urban areas in their functions for urban population. The European Settlement Map (ESM 2015) produced in the framework of the GHSL initiative enables such an assessment thanks to availability of a scientific product characterizing the urban areas in terms of access/distance to green open spaces (Corbane, Sabo, et al. 2019). ESM is a spatial raster dataset that uses Copernicus Very High Resolution optical coverage to map human settlements in Europe (VHR_IMAGE_2015). The ESM 2015 includes two publically available products describing built-up areas and building typologies at spatial resolutions of 2 and 10 meter respectively. It also includes a third scientific product available upon request estimating the distance to green open spaces. The production of this dataset with a spatial resolution of 10 m builds on the combination of: 1) the urban/rural settlement model (GHS-SMOD) for delineating the urban centres, 2) the built-up areas derived from the ESM 2015, 3) the open spaces derived from the Urban Atlas (2012). The integration of these layers allows deriving meaningful indicators (people weighted access to open spaces, average distance to open spaces, km² of open spaces per inhabitant) describing the European cities in a consistent way.

Accessibility to open spaces is typically measured using rules for spatial proximity between objects, such as the distance between peoples permanent place of residence and open spaces. The methodology developed in the ESM 2015, consists in calculating the distance from built-up areas, with resident population, to any open space (without discriminating between classes of open spaces). For that purpose a distance function based on the geodesic time algorithm has been applied (F. Sabo, Corbane, and Kemper 2019). The integration of the obtained accessibility maps with gridded population data for Europe (GHS_POP_EUROSTAT_EUROPE_R2016A) allows deriving meaningful metrics for assessing the amount of people living in proximity to open spaces for several classes of distances. The results of this analysis are summarized in the charts of Figure 90. They illustrate the type of metrics that can be derived from the analysis of access to open spaces in combination with fine scale population data Figure 90 chart shows the percentage of people living within predefined distances classes in the 12 biggest urban centres in Europe (area > 400 km²). It reveals that Milano, Naples and Rotterdam have the highest shares of their population living in distances greater than 1 km from any open space while Katowice in Poland has 40% of its population living very close to green open spaces within a distance of 100 meters. The chart in Figure 91 ranks the 12 largest urban centres in Europe by the percentage of open spaces compared to the size of the urban centre. With more or less similar sizes of the urban centre, Katowice has a much bigger share of open spaces than Berlin.

The computed indicators are expected to be particularly relevant when discussing urban quality of life issues. In addition, they are closely linked to one of the targets of United Nations Sustainable Development Goal 11: "By 2030, provide universal access to safe, inclusive and accessible, green and public spaces, in particular for women and children, older persons and persons with disabilities". Another application of this work is the analysis of public open spaces in European cities to inform the SDG indicator 11.7.1 which looks at green and non-green open spaces (e.g. public squares and pedestrian streets). The current work is being updated for reference year 2018 hence opening the way to multi-temporal analysis for monitoring of access to open spaces.

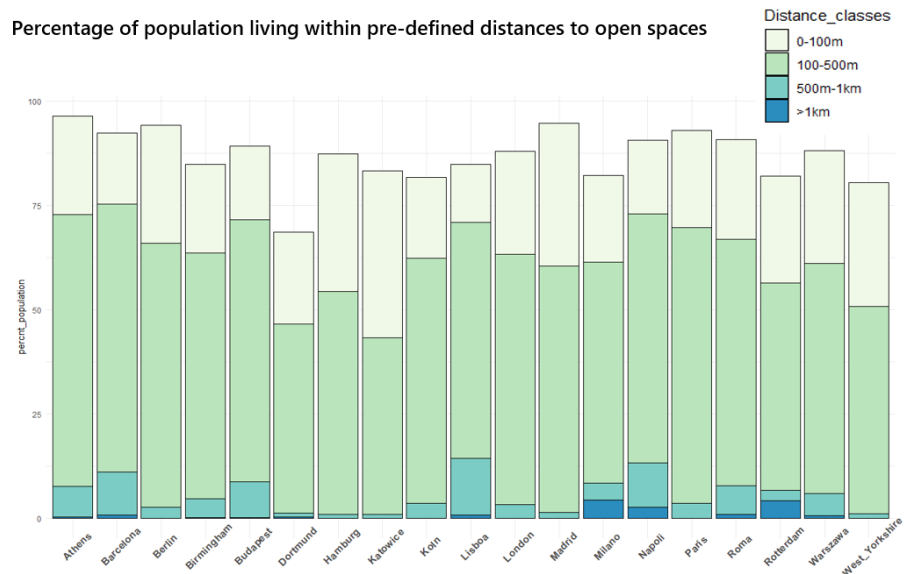


Figure 90 Percentage of people living within pre-defined distances to open spaces for the 12 biggest urban centres as defined by GHS settlement model (GHS-SMOD)

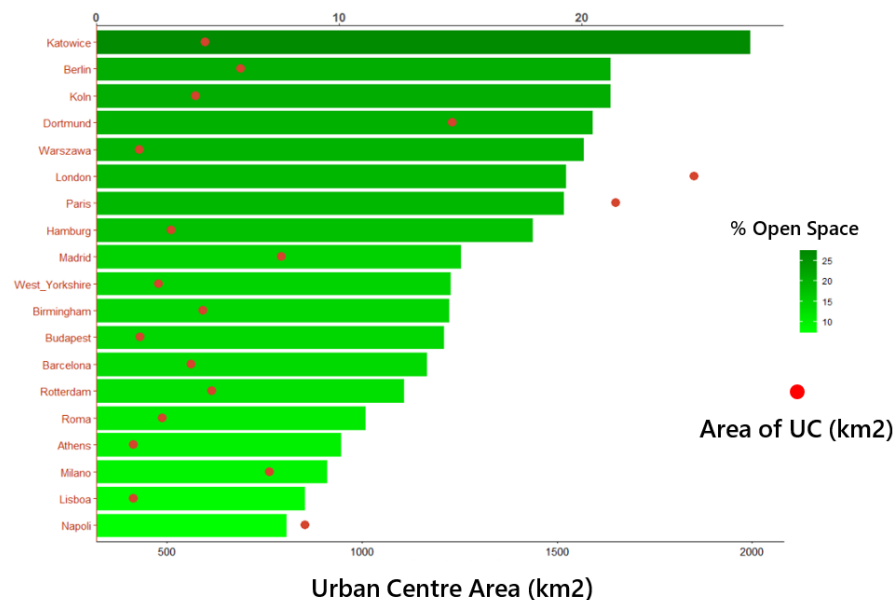


Figure 91 The top 12 biggest cities in EU ranked by the percentage of open spaces compared to the size of the urban centre as defined by GHS-SMOD)

Datasets:

ESM 2015 - Corbane, Christina; Sabo, Filip (2019): ESM R2019 - European Settlement Map from Copernicus Very High Resolution data for reference year 2015. European Commission, Joint Research Centre (JRC)

GHS_POP_EUROSTAT_EUROPE_R2016A- Freire, S.; Halkia, M.; Pesaresi, M. (2016): GHS population grid, derived from EUROSTAT census data (2011) and ESM R2016. European Commission, Joint Research Centre (JRC)

References:

- 1) WHO Europe Urban Green Space expert panel and R. Hunter, Urban green spaces: a brief for action. 2017.
- 2) C. Corbane et al., "Application of the Symbolic Machine Learning to Copernicus VHR Imagery: The European Settlement Map," IEEE Geosci. Remote Sens. Lett., pp. 1–5, 2019.
- 3) F. Sabo, C. Corbane, and T. Kemper, "The European Settlement Map 2019 release," Luxembourg: Publications Office of the European Union, EUR 29886, 2019.

3.4.7 The structure of urban green in European functional urban areas

Zulian G., Maes J. Marando F.

Spatial integrity is an important property of Urban Green Infrastructure (UGI). It describes two important attributes: the size and the structural connectivity of green patches that have a key role for the provision of ecosystem services, such as microclimate regulation, pollination or flood regulation.

Through the European Settlements Map (ESM) (Ferri et al. 2016), a high-resolution data set available at European scale, complemented by Urban Atlas (UA)²², we analysed urban green in 700 European cities (Maes et al. 2019).

Spatial integrity of green areas was calculated using the Fragmentation analysis at a fixed Observation Scale (FOS) module from the Guidos toolbox²³ (Vogt and Riitters 2017). The model reclassifies the share of green patches, in a surrounding fixed-area zone, in 6 degrees of spatial integrity going from rare to intact. In this application, we used a fixed-area zone of 12.25 ha and we included all natural and semi-natural areas in core cities and their surroundings, including very small patches of green areas.

Figure 92 shows an example of spatially explicit results for Austrian Functional Urban Areas (FUAs) and relative core cities. In Innsbruck and Klagenfurt, more than 50% of the urban green is classified as “Intact” (patches > 12.2 ha), whereas “Rare” patches (< than 1.1 ha) are practically absent in all cities. Figure 93 shows the Share of Dominant-Interior-Intact green areas in European core cities. In 26.7% of European core cities, less than 40% of the UGI is represented by patches bigger than 7 ha. In 36.6% of cities, a fraction between 40 and 65% of the UGI is represented by patches bigger than 7 ha. In the remnant 36 % of the cities, more than 65% of the UGI is characterised by dominant and intact green spaces.

The current analysis was implemented in the project EnRoute, which stands for “Enhancing Resilience Of Urban Ecosystems through Green Infrastructure”. The project, managed by the European Commission and funded by the European Parliament, aimed to promote the deployment of UGI at a local level and delivered guidance on the management and governance of UGI (<https://oppla.eu/groups/enroute>).

In EnRoute, the MAES²⁴ framework for the assessment of urban ecosystems condition was tested for the first time on 700 European functional urban areas. The project informed the New Biodiversity Strategy 2030²⁵: “...a comprehensive, ambitious, long-term plan for protecting nature and reversing the degradation of ecosystems”, which, for the first time, considers urban ecosystems (Section 2.2.8 “Greening urban and peri-urban areas”).

²² <https://land.copernicus.eu/local/urban-atlas/urban-atlas-2012>

²³ <https://forest.jrc.ec.europa.eu/en/activities/lpa/gtb/>

²⁴ https://ec.europa.eu/environment/nature/knowledge/ecosystem_assessment/pdf/5th%20MAES%20report.pdf

²⁵ https://ec.europa.eu/environment/nature/biodiversity/strategy/index_en.htm

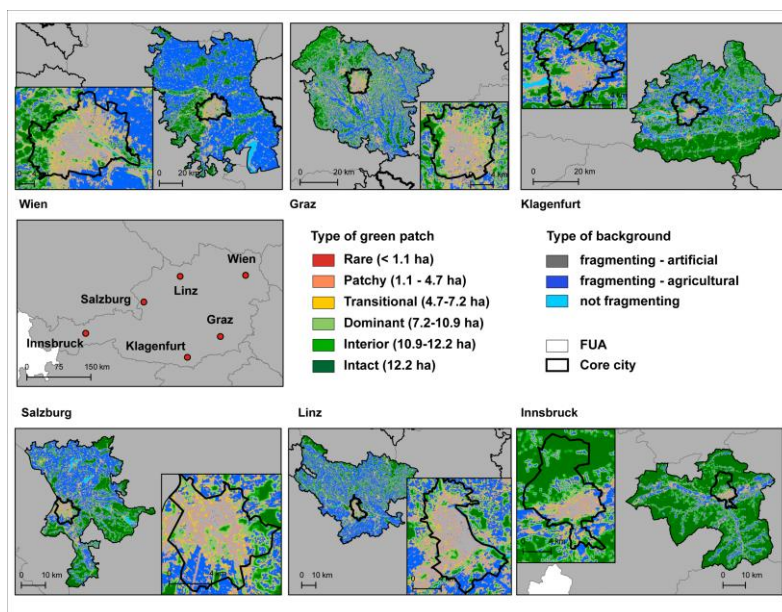


Figure 92 Spatial configuration of urban green areas, example in Austrian cities

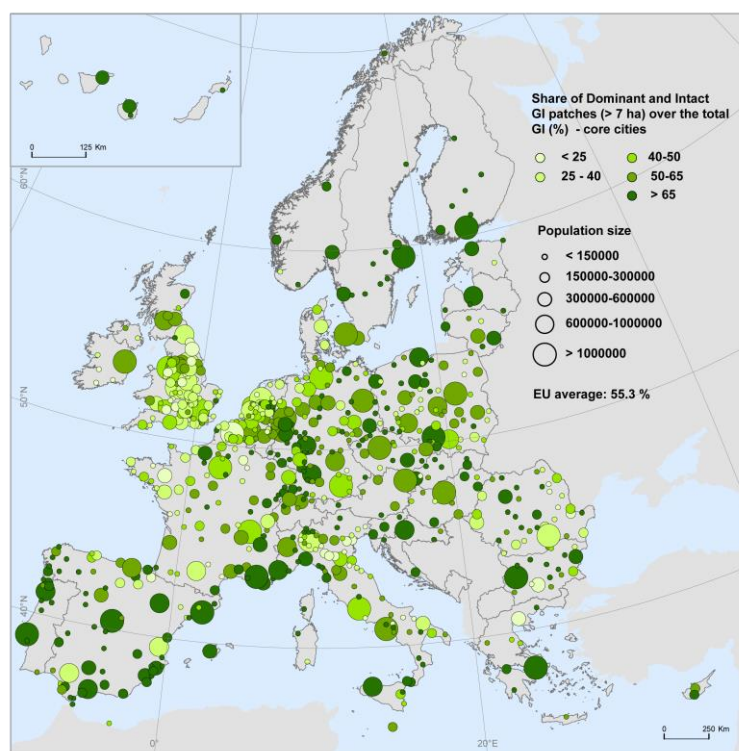



Figure 93 Spatial configuration of urban green areas in European core cities. Share of Dominant – Interior – Intact green areas (% on the total GI)

Datasets:

Vogt, P., Riitters, K., GuidosToolbox: universal digital image object analysis. Eur J Remote Sens 50(1): 352–361, 2017. doi: 10.1080/22797254.2017.1330650.

Stefano FERRI, Alice SIRAGUSA, Matina HALKIA; The ESM green components. A dedicated focus on the production of the green in the European Settlement Map's workflow; 2016, EUR 28024 EN; doi:10.2788/022426

Maes J, Zulian G, Günther S, Thijssen M, Raynal J, Enhancing Resilience Of Urban Ecosystems through Green Infrastructure. Final Report, EUR 29630 EN, Publications Office of the European Union, Luxembourg, 2019, ISBN 978-92-79-98984-1, doi:10.2760/602928, JRC115375.



4.0

4 Challenges and trends in human settlements research

The multidisciplinary case studies of this Atlas 2020 show the usefulness of open geospatial information and Earth Observation (EO) for understanding human settlements, the societal processes within, and their complex relationships with natural environment. Today, Earth observation technology generates large volumes of data referred as “Big Earth Data (BED)” used to understand natural and human phenomena on planet Earth (Goodchild et al. 2012). The analysis of remote sensing data with ancillary data sets combined with advanced analytics and widespread availability of high performance computing platforms are used to generate scientific knowledge for an urbanizing planet. In the context of increasing urbanisation, rising vulnerabilities to climate change impacts, timely open and global information about human settlements and urban areas are required for informed decisions.

We identify eight research areas that can advance our understanding of urbanization and generate knowledge for policy decisions. This includes improvements in the analysis of EO data (a-f), the modelling of the population distribution (g) and the need for capacity building (h):

- (a) fine-scale mapping of built-up areas at global scale and across the urban-rural gradient;
- (b) continuous spatial and temporal monitoring of human settlements growth, sprawl and change by integrating data from different sensors;
- (c) quantifying intra-urban variations and the different settlement types;
- (d) understanding of urban morphology, in particular the vertical structure of urban areas which reflects several biophysical and socioeconomic processes of the urban environments;
- (e) mitigating the sensor-dependency estimates of urban measures derived from remote sensor data by introduction of robust sub-pixel continuous modelling estimates;
- (f) improve causal modelling combining remote sensing data with socio-economic data to better understand the drivers of urban development and establish scenarios for spatially explicit projections of built-up land patterns and the associated future population growth;
- (g) spatio-temporal mapping of population, especially useful for Disaster Risk Management.
- (h) capacity building to facilitate information sharing and production as well as collective knowledge building

In order to make sure that the community of practice and decision-makers benefits from these developments, we need to raise awareness of the potential of big earth data and geospatial information for public purposes. These research activities require investments, institutional capacity building as well as data-driven regulation and policymaking.

The Global Human Settlement project together with the GEO Human Planet initiative are collaborating with the scientific community, different stakeholders and practitioners to help addressing those challenges. This chapter discusses some of the challenges related to our knowledge of human settlements and advocates a new research agenda adequately directed to real-problem applications and aimed at closing the gaps between technology, science and policy.



Figure 95 © Adobe Stock

4.1 Fine scale global mapping of human settlements

Recent years have seen a proliferation of global maps describing human settlements. The most recent datasets include the Global Urban Footprint (GUF) with its 12 m cell or pixel size product derived from TerraSAR-X imagery acquired in 2011–2013 (Esch et al. 2017); the World Settlement Footprint (WSF) with the 10 m resolution datasets based on Landsat-8 and Sentinel-1 sensors for reference year 2015 (Marconcini et al. 2019) and the FROM-GLC10 landcover map which includes a dedicated class for artificial surfaces derived from Sentinel-2 data acquired in 2017 (Gong et al. 2019). Unlike the GUF, which was generated from commercial imagery, all the other products were derived from free and open-access satellite image datasets, primarily from Landsat and the European Copernicus Sentinel missions. These products are freely available (absence of restrictions on their use for multiple types of applications) and can be updated at relatively low cost. Although these datasets have been widely used in different application areas, they present a certain number of limitations. These limitations are mostly related to accuracy, sensor-scale dependency, quantitative surface measurements in the extrema of the settlement density range, and the continuous monitoring of urban land cover changes. Compelling challenges and opportunities still lie ahead in high-resolution mapping and accurate classification of built-up areas over large areas. Several initiatives are targeting the fine scale delineation of human settlements from commercial, very high resolution satellite data. As an example, Facebook has recently made available for public use high resolution settlement grids (aggregated at a spatial resolution of 30 meters) in the frame of “Data for Good” Facebook program that supports international humanitarian efforts (‘Facebook’s Data for Good Program’ 2020). While the delineation of sparse settlements in particular in rural Africa was remarkably accurate, the mapping of large urban areas shows systematic omission errors.

Within the GHSL project, considerable effort has been invested in the development of a deep-learning based framework (GHS-S2Net) for large-scale mapping of human settlements from Sentinel-2 Copernicus data. The deployment of the model on the global Sentinel-2 image composite provided the most detailed and complete map reporting about built-up areas for reference year 2018 (Figure 96). The results are validated with an independent reference dataset of building footprints covering 277 sites across the world. The most noticeable achievement of the GHSL approach is the capacity of the model to classify built-up areas in remote areas (e.g. in Africa and in Asia), reported in none of the global products (i.e. GUF, WSF, FROM GLC10). The resulting dataset will be used as a baseline for the production of the GHSL 2020 data package (see Box 1 p. 118). This work contributes to cutting-edge research in the field of automated built-up areas mapping from remote sensing data and establishes a new reference layer²⁶ for the analysis of the spatial distribution of human settlements across the rural-urban continuum (Corbane, Syrris, et al. 2020).

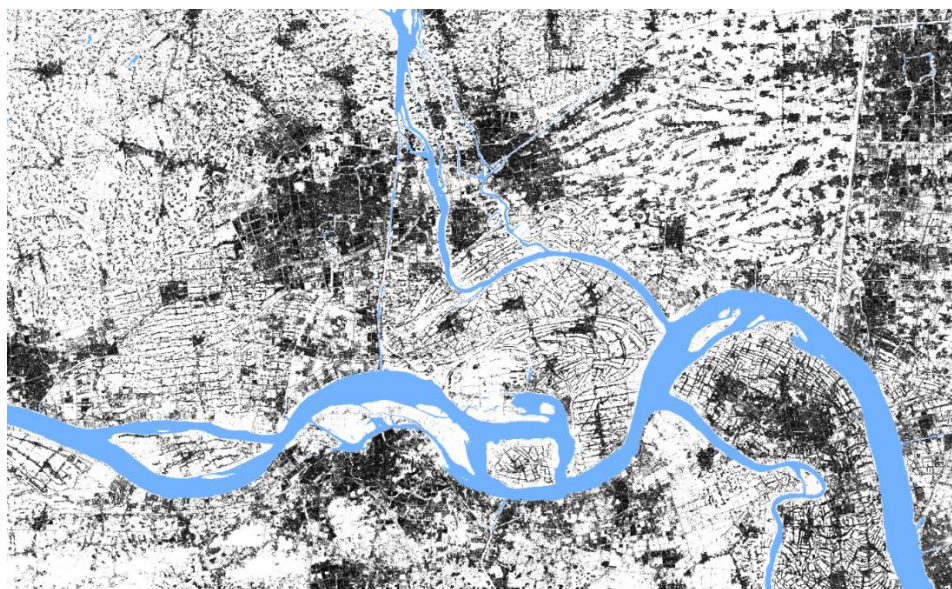


Figure 96. The most detailed and up-to-date map of built-up areas derived from Sentinel-2 Copernicus data in the framework of GHSL. The example here is taken from China.

²⁶ Corbane, Christina; Sabo, Filip; Politis, Panagiotis; Syrris Vasileios (2020): GHS-BUILT-S2 R2020A – built-up grid derived from Sentinel-2 global image composite for reference year 2018 using Convolutional Neural Networks (GHS-S2Net). European Commission, Joint Research Centre (JRC) PID: <http://data.europa.eu/89h/016d1a34-b184-42dc-b586-e10b915dd863>, doi:10.2905/016D1A34-B184-42DC-B586-E10B915DD863

4.2 Multi-sensor monitoring of human settlements

Considering the complexity of human settlements, it is of great importance to characterize the long-term spatio-temporal dynamics of built-up areas and link them with socio-economic data to better understand the urbanization process, develop urban growth models, and investigate environmental impacts of human settlements encroachment on natural and agricultural landscapes (X. Li et al. 2018). Although built-up areas are considered relatively stable in comparison to daily or seasonally changing land covers (e.g. Forest, agricultural areas), they are highly dynamic both horizontally and vertically at yearly or multi-annual temporal frequency observation that is consistent with the sustainable development policy frameworks. Information on built-up areas dynamics has been widely addressed with remote sensed observation with relatively coarse temporal resolution (e.g. five-year or decade (Corbane, Pesaresi, et al. 2019)). In rapidly developing regions such as China and India, information on built-up areas dynamics derived from coarse temporal resolution observations, can hardly capture the subtle changes in the urban environments such as urban disturbances and accelerated growth.

At a global scale, annual global products had coarse spatial resolutions in the order of hundreds of meters or kilometres. At a spatial resolution of 30 meters became available only recently from the processing of Landsat data collections available in cloud computing platforms such as Google Earth Engine (Liu et al. 2020; Gong et al. 2020). The multi-temporal built-up layer produced in the framework of GHSL from Landsat data collections (Corbane, Pesaresi, et al. 2019) was the first global dataset to map the dynamics of human settlements between 1975 and 2014 at a spatial resolution of 30 meters. The advent of Sentinel-2 satellite, proved to bring the mapping of built-up areas to the next level thanks the increased spatial resolution (10 m in comparison to Landsat 30 m) and revisit time (5 days for the combined constellation Sentinel-2A and Sentinel-2B). Studies have suggested that Sentinel-2 adds value to the mapping of built-up areas, over predecessor Landsat-based products (Pesaresi, Corbane, et al. 2016; Corbane, Syrris, et al. 2020).

The advances brought by this new open and free satellite datasets stimulate a variety of new urban remote sensing algorithms and applications. It is very likely that next generation global built-up grids will rely on the combination of Sentinel-1 and Sentinel-2 data. However, the challenge will be to combine Sentinel-1 and Sentinel-2 observations or derived built-up maps with Landsat historical data to contribute to long-term time series data collections. Some initiatives are currently investigating the potential to harmonize data coming from Landsat-8 and Sentinel-2 satellites programs to ease their combined use (e.g. the Harmonized Landsat 8 OLI and Sentinel-2 MSI (HLS) project (Claverie et al. 2018)). With the increasing number of Earth observation satellites, observations from multiple observatories can be merged to provide improved temporal coverage (J. Li and Roy 2017) hence creating a so-called “Virtual Constellation”.



Figure 97 © Adobe Stock

4.3 Human settlements spatial patterns and typologies

The GHSL approach uses remotely sensed data to generate built-up surfaces or urban areas following the INSPIRE definition of buildings (INSPIRE Thematic Working Group 2013). That built-up detection is complicated by the fact that almost any material can be used as building roof, producing high spectral confusion between built-up and not-built-up areas as observed from remote sensors. The GHSL approach also infers *use type* of the building – this is the next challenge – based on physical characteristics including roof material, shape, size, and context).

Information on intra-urban variations and the different settlement types is a key input for capturing spatial and temporal patterns of energy consumption, for analysing urban socioeconomic features dominated by human activities and for more accurate population modelling. Several studies have identified persistent overestimation of population density in rural areas or areas where buildings are largely non-residential (e.g. industrial sites) and underestimation of population density in high-density urban settings, particularly where multistorey buildings are common. This suggests that contextual information, such as residential vs. non-residential buildings may improve the accuracy of population disaggregation models (Wardrop et al. 2018). In (X. Huang et al. 2020), Open Street Map (OSM) land use data including was used to eliminate non-residential buildings for disaggregating the American Community Survey into a 100 m population grid product. The results confirmed that the OSM trimming process removes non-residential buildings and thus provides a better representation of population distribution within complicated urban fabrics.

Mapping building typologies is a challenging task. For instance, there are limitations to identify detailed building types using remote sensing data, while there are challenges to map building types over large areas using social sensing data such as OSM. Texture, context, and proportional land cover data have been used in conjunction with spectral data to characterize the built-up environment and derive information on the usage of buildings (Gong and Howarth 1990). Most of the remote sensing based studies for mapping building typologies have exploited LIDAR data or very high resolution multispectral imagery through a combined use of spatial and landscape attributes (Z. Lu et al. 2014). These approaches may be successful over specific types of landscapes and for limited areas but are hardly applicable over large scales and certainly not at global scale.

Within the GHSL initiative, advanced machine learning methods are being developed for large scale characterization of human settlements type from remote sensing data. The European settlement Map produced in 2015 by the GHSL team is the first Pan-European datasets that includes a classification of residential versus non-residential buildings at high spatial resolution (Corbane, Sabo, et al. 2020) (Figure 98).

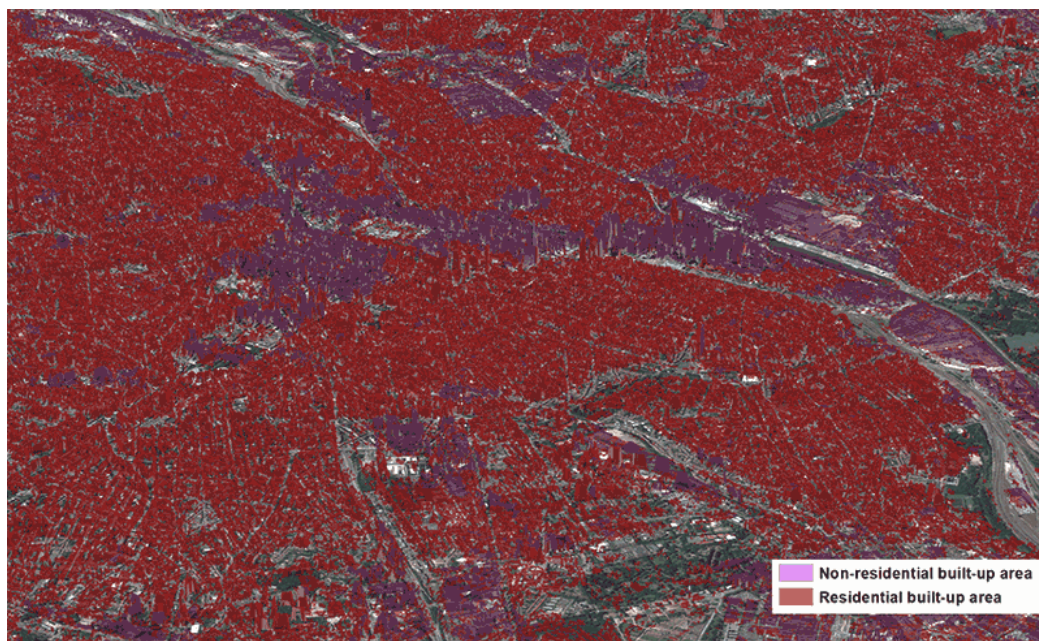


Figure 98. European Settlement Map from Copernicus Very High Resolution data for reference year 2015, Public Release 2019. European Commission, Joint Research Centre (JRC) doi: 10.2905/8BD2B792-CC33-4C11-AFD1-B8DD60B44F3B
PID: <http://data.europa.eu/89h/8bd2b792->

4.4 Describing the vertical component of built-up areas over large scales

In response to the increasing urban population and higher demand for land and infrastructure, cities adopt different urban growth expansion strategies. Usually combining horizontal growth, the addition of new settlements; and vertical growth promoting concentration of population and economic activity in central locations (Zambon, Colantoni, and Salvati 2019). Information about the vertical component of the built-up areas are important in urban analysis, urban planning, and required in many studies in the built environment. Knowledge of the vertical dimension (i.e. building heights and volume) is necessary for a comprehensive characterization of urban morphology, especially for projecting future carbon emissions under scenarios of continuous urbanization and climate change (Salat, Labbé, and Nowacki 2011) (Zhu et al. 2019). For example, the vertical dimension of urban areas is closely linked to the distribution of population densities (Steinnocher et al. 2019) and may support urban climatology studies and related adaptation and mitigation actions (Bechtel et al. 2018) (Y. Xu et al. 2017). Besides, the vertical dimension of built-up areas plays a major role in urban heat islands by affecting the urban energy balance (H. Huang et al. 2017), and is key in Earth System Modelling (Balsamo et al. 2018).

Compared to the horizontal information, the vertical component reflects urban compactness and can be extracted through optical stereo photogrammetry, airborne light detection and ranging and analysis of Synthetic Aperture Radar (SAR). Methods fusing data from airborne and spaceborne sensors, operating at the metric scale, target small clusters of buildings, and both direct and indirect methods have been developed for extracting three-dimensional information. Direct approaches consist in assessing building heights from LiDAR data (Z. Lu, Im, and Quackenbush 2011), stereoscopic satellite data (Shaker et al. 2011) or aerial imagery, or through a fusion of LiDAR and optical or radar imagery (Y. Huang et al. 2017; Sportouche, Tupin, and Denise 2009). Indirect approaches use proxy variables to determine the volume of buildings such as building shadows (Comber et al. 2012) (Kadhim and Mourshed 2017) or image derivatives and filtering of Digital Surface Models (DSM). Most of these datasets are scarce and typically costly. Consequently, they are rarely available in low-income countries and they are hard to use for globally exhaustive comparative studies. In order to support the monitoring of the sustainable development frameworks, there is an urgent need of addressing these information requirements by global remote sensing data available in the public open and free use domain.

Considering the challenges in data availability at global scale and the heterogeneities in the built-up environments, The GHSL project has investigated the potential of global open DSMs for indirect mapping of building heights and volumes under different terrain and urban density conditions (Pesaresi et al. in press). The Generalized Vertical Components (GVC) of built-up areas are used to summarize relevant geometric characteristics of the three-dimensional built-up environment. They statistically describe the height of the built-up surfaces assessed at a fine scale to a given, broader generalization scale of 250 meters (Figure 99 and Figure 100).

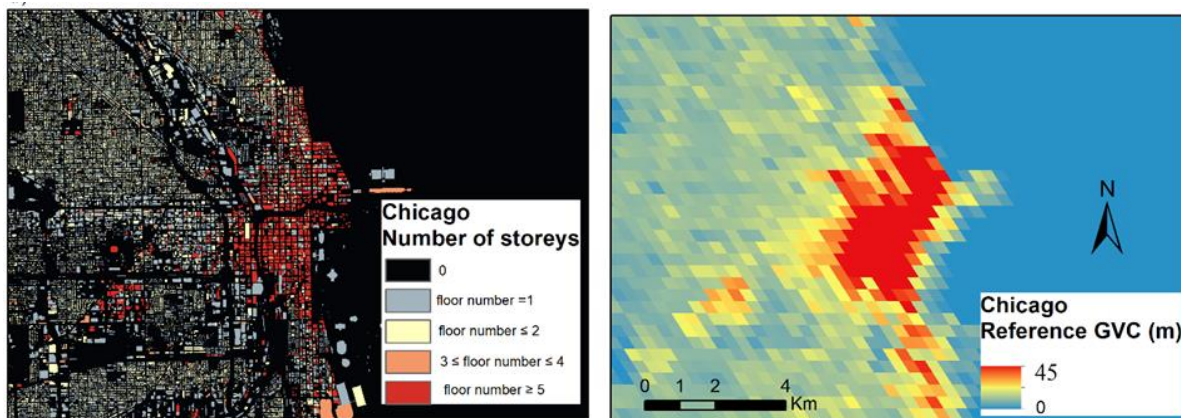


Figure 99 Reference data on number of floors per building for the city of Chicago –left), and estimated Gross Vertical Component derived from open and global Digital Surface Models –right.

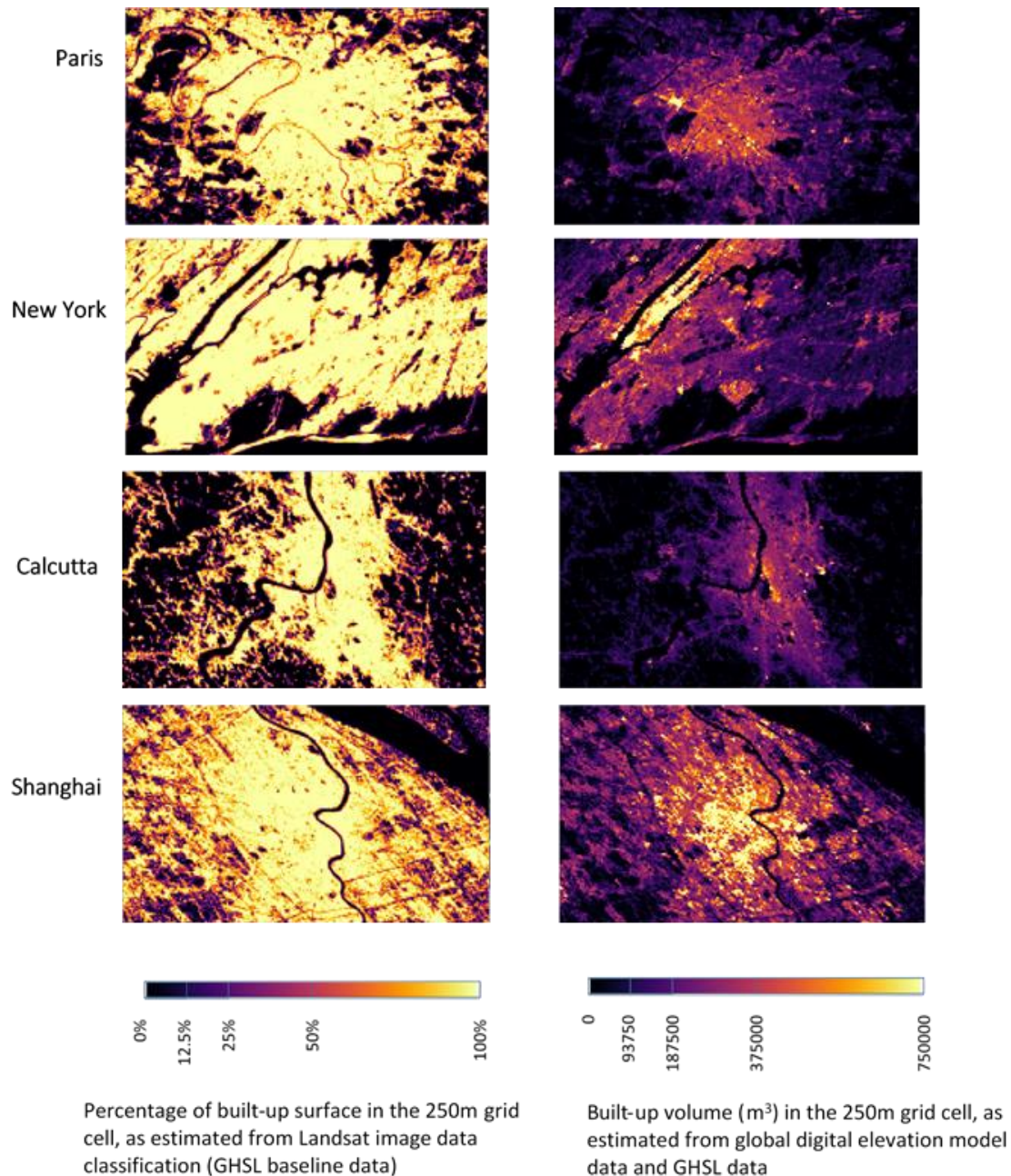


Figure 100 Built-up surface and estimated building volume in the 250m grid cell for selected cities

4.5 Mitigating sensor-dependent built-up area estimation

Nowadays, with the routine collection of Earth Observation data from a variety of satellites, there is increasing number of datasets describing built-up areas at regional, continental and global scales. When considering solely the maps of built-up areas produced in the framework of the GHSL we can notice the diversity of products derived from different sensors: at global scale, the main input sensors are Landsat, Sentinel-1 and Sentinel-2, while at the European scale there is a combination of very high resolution satellite data (e.g. SPOT5-6, Pléiades, Worldview-2). Although estimates of maps of built-up vary significantly in part due to differences in the spatial resolution, the methods for information extraction and the varying accuracies across the globe (Klotz et al. 2016), these datasets in addition to the plethora of other European and global products have been instrumental in developing our knowledge about human settlements and their imprint on Earth. Users of these different products should get minimum guidance on which dataset to use and for what purpose. Besides, to fully exploit the synergies between the different sensors and possibly integrate those products in the future, it is essential to understand the potential and limitations of each of them and identify complementarities (Filip Sabo et al. 2018).

As built-up areas exhibit complex forms and uneven distributions over space, their precise detection is required to accurately convey the human settlements dynamics through derived products. The spatial resolution of input satellite images is crucial for determining the amount of information that can be extracted. The advantage of high-resolution satellite images (5 m) in capturing complex landscape patterns over medium (80–15 m) and low (100 m) datasets have been highlighted in published literature (Kawakubo et al. 2019).

Closely linked to the issue of spatial resolution and its influence on the capacity to detection built-up areas, is the problem of pixel-mixing effects, which is amplified by the characteristics of urban areas connoted by the presence of heterogeneous material surfaces with high spatial frequency variation (Small 2003). “The spectral-mixing effect occurs when a given pixel registers the energy signal coming from two or more targets or materials on the surface. Therefore, the intensity of the mixing effect basically depends on the spatial configuration of the land use (extrinsic factor) and the spatial resolution of the image (intrinsic factor)” (Kawakubo et al. 2019). Such a mixture becomes especially prevalent in urban areas where buildings with different roof material surfaces, trees, lawns, concrete, and asphalt roads and parking lots occur within a pixel. Mixed pixels have been recognized as a problem affecting the effective use of remotely sensed data in quantitative analysis and change detection (D. Lu and Weng 2004).

The preponderance of mixed pixels registered in Landsat imagery (30 m) occurs due to the decorrelation of urban reflectance observed at 10–20 m. Even in higher spatial-resolution imagery, such as the Sentinel-2 multispectral images (10 m), the proportion of mixed pixels found in the image is quite significant (R. Xu, Liu, and Xu 2018).

In order to support robust multi-sensor quantitative modelling of the built environment, it is necessary to improve the capacity to describe sub-pixel surface fractions from remotely sensed data.

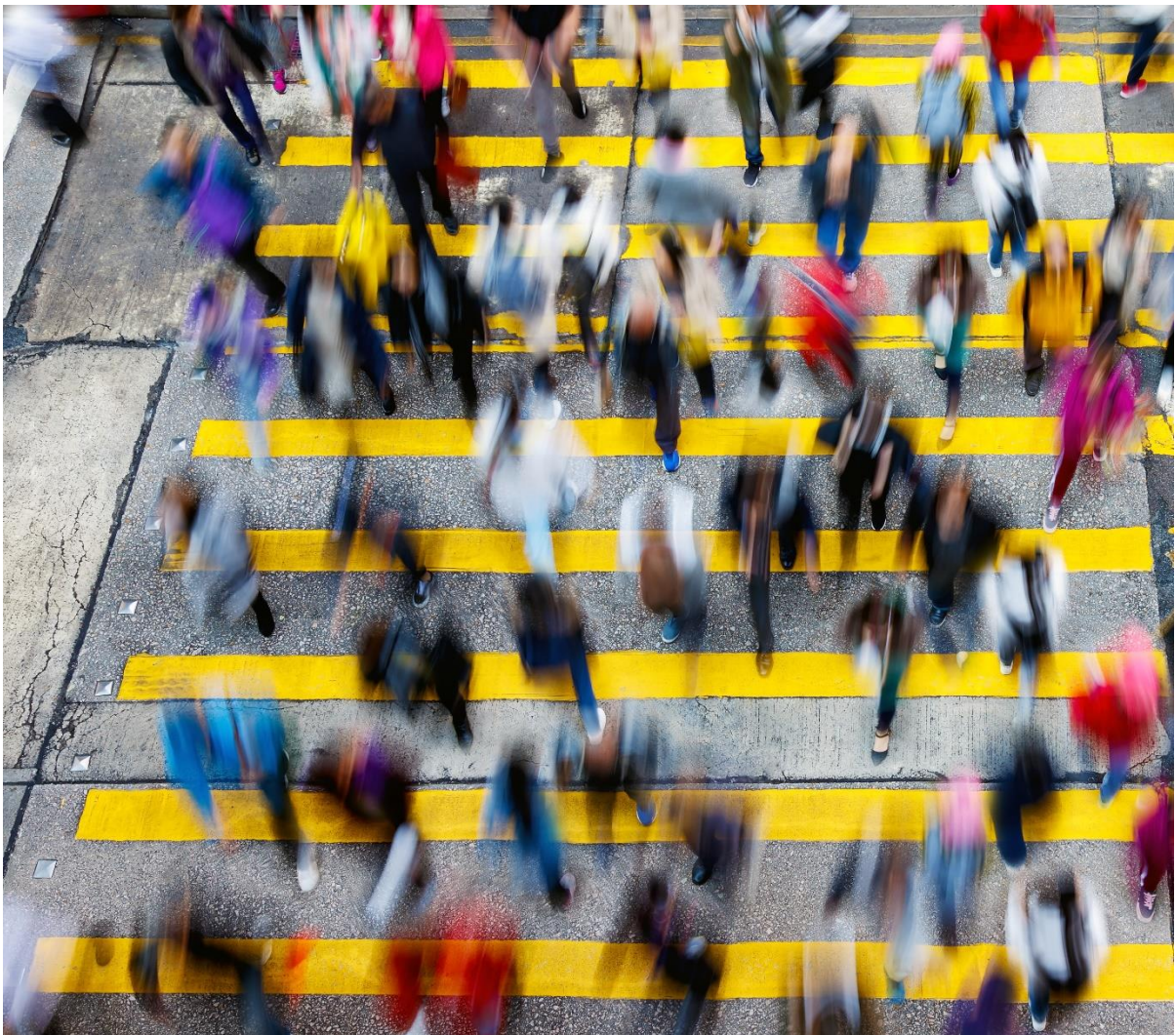


Figure 101 © Adobe Stock

4.6 Improving the mapping of global population distribution

Despite all the recent progress and initiatives in mapping global population distribution, several challenges remain. These include **increasing the availability of updated and reliable population statistics**.

The quality, detail, and age of available census data varies significantly by country and despite mitigation and harmonisation procedures implemented to derive global time series, some limitations propagate to derived population grids and their applications. ‘Total population’, despite being the most simple, basic, and neutral demographic variable is still affected by significant uncertainties. Therefore, it is likely these are even greater for more complex and sensitive variables (e.g. sex, age, ethnicity).

Addressing the UN ‘leaving no one behind’ imperative of the 2030 Agenda for Sustainable Development requires that all people are counted and accounted for, namely where they live. While the targets and monitoring needs (i.e. indicators) of these development agreements (e.g. SDGs) place great demands and responsibility on geospatial population data, they also present an opportunity for improving related statistics and enhancing their supporting infrastructures. The combination of new methods (e.g. machine learning) with the synoptic capacities of satellite imagery can contribute to fill information gaps and supplement existing statistics by mitigating some major shortcomings in population data. This is especially true in poor, remote, unsafe, disputed, very large, and/or highly dynamic areas of the globe where conventional data gathering and updating is challenging. Remote sensing imagery and methods have been evolving towards constituting a more detailed, objective and independent data source on human presence on the Earth surface (Figure 102).

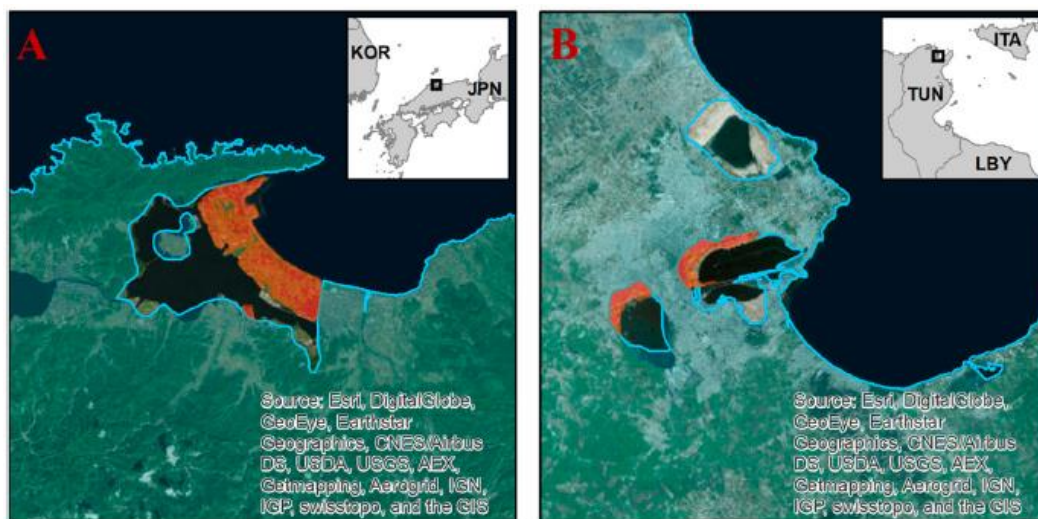


Figure 102 Examples of discrepancies (patches larger than 1 km²) between census geometries (blue line) and detected built-up areas in GHS-BUILT 2014 (orange) along the coasts of (A) Japan (JPN) and (B) Tunisia (TUN) (from Freire et al. 2020).

For instance, improved mapping of built-up presence and changes captured by satellite imagery can enable more accurate and frequent update of population distribution maps. However, efforts to improve modelling of population distribution should go in parallel with (and contribute to) strengthening national institutional capacities to produce better data and making it freely available to all stakeholders. GRID3²⁷ (Geo-Referenced Infrastructure and Demographic Data for Development) is one such project working with countries to generate, validate, and use geospatial data on population, settlements, infrastructure, and boundaries.

Non-withstanding the importance of ‘total population’ in analyses and as denominator of many indicators in post-2015 development agendas, additional demographic variables (e.g. sex, age) are also relevant for many issues and there is increasing demand for their spatially-explicit mapping. This calls for improved modelling of the distribution of these attributes, which are likely to benefit from enhanced source data and modelling of total population.

4.6.1 Mapping and assessing present population and their dynamics

Accurate maps showing where people live (i.e. resident population) are essential as baseline information for planning and policy design, but knowing where people actually are can be invaluable for decision-making.

²⁷ GRID3 Project: <https://grid3.org/>

Accounting for population spatiotemporal dynamics is essential for a range of applications, from disaster risk assessment to transportation planning. For instance, when disasters strike, information on the actual population present in the affected area is invaluable for tailoring the emergency response. Mapping present population in a region also requires considering presence of migrants and refugees, which often are not accounted as resident population.

The recent explosion in the port of Beirut, Lebanon (04/08/2020) underlined the importance and difficulties of providing a detailed, accurate, and updated population distribution grid in a country without a detailed recent census and with significant presence of refugees. Improving the mapping of present population would benefit from combining data on displaced populations such as that compiled and provided by IOM-DTM²⁸, a task which is not without challenges due to need to reconcile complex displacement dynamics with baseline census data to control the population budget.



Figure 103 © Adobe Stock

Challenges for population mapping also include increasing temporal resolution and providing more temporal segmentations (i.e., day- vs night-time distributions). At global scale, major advancements are expected from improvements in classifying building functions and estimating their height (in urban areas), and from better detection and mapping of dispersed settlement patterns (in rural areas). However, the actual contribution of these additional descriptors of built-up areas and their cost-benefit needs investigation: data on building height is likely more relevant in urban contexts where census data is coarse and building height displays high intra-unit variation. Improvements in remote sensing data (e.g. Copernicus Sentinel) and information extraction methods (e.g. machine learning) are showing promise for supplying some of these data, in open and free framework (e.g. Corbane and Sabo 2019) and should be further pursued. Promising research paths involve combinations of conventional with unconventional data sources, including big data (from VGI, social media, mobile phones) (Aubrecht et al. 2017; 2018) but their use is not without problems (e.g. completeness, sustainability of approaches, data access and ownership, privacy and anonymity, representation bias) that deserve attention. The project ENACT²⁹ (ENhancing ACTivity and population mapping) was successful at producing consistent, seamless, multi-temporal, high-resolution and validated population density grids for Europe (EU-28) taking into account major daily (commuting to work or education) and monthly (tourism) variations. By combining official population statistical at regional level with geospatial data from conventional and non-conventional data sources, for the first time it was possible to produce spatially-explicit day- and night-time population grids per month of the year for a large-multinational region.

4.6.2 Spatially-explicit, high resolution population projections

For a variety of planning and policy issues it is also crucial to understand how the spatial distribution of human population may evolve over time into the next decades. Although population projections exist for countries and major cities, there is room for improvements of these statistical models as well as a demand for mapping these projections as spatially-explicit grids. Higher resolution grids showing potential future population distribution

²⁸ Displacement Tracking Matrix: <https://dtm.iom.int/>

²⁹ ENACT Project: <https://ghsl.jrc.ec.europa.eu/enact.php>

and urban extent are important for development and testing of models of related anthropogenic phenomena, and exploring scenarios and their policy implications. These projections can be mostly informed by past and present trends of population and built-up distribution and expansion, or more compliant with existing scenarios such as Shared Socioeconomic Pathways (SPPs). Such efforts are under way, enabled by improvements in remotely sensed spatial data products.

4.7 Capacity building

Although geospatial technologies, datasets and remote sensing imagery are getting more accessible, lack of skilled human resources and institutional capacities are major hurdles in their effective applications within the policy domain. There is a strong demand for ready-to-use tools that i) facilitate the use of available geospatial products describing human settlements, ii) facilitate the production of ad-hoc geospatial information describing settlement from analysis of open satellite data and iii) assist in the application of standardized geospatial statistical classification such as the “degree of urbanization” classification methodology to national data. In particular the last point is important, if we want to assure ownership by national institutions and therefore continued use of geospatial information in the decision making process. The GHSL has developed a suite of tools enabling the extraction of information from big earth data, modelling of population distribution and the classification of human settlements (see section 2.1.6). To ensure conscious implementation of the methods and facilitate uptake of the technology by different stakeholders, the GHSL has designed a training package and contributed to the manual that EUROSTAT and other Organisations are preparing in compliance to the mandate given by the 51st Session of the United Nations Statistical Commission. In addition GHSL has organised several training sessions and workshops around the world, in particular to support the development of the harmonised global definition of cities and settlements. The workshops are helping to strengthen national and local capacities to use urban definitions building on earth observation data, to evaluate and formulate policies and actions based on empirical evidence. Seven regional workshops were co-organized between 2018 and 2019 with UN-HABITAT and involved 86 members states. They aimed at:

- Strengthening technical and institutional capacity of national and local institutions competent to adopt a national monitoring framework based on scientifically proven methods that produce reliable, timely and disaggregated;
- Strengthening the capacity of countries to monitor and review of SDGs and through voluntary national reports using the harmonized definition of cities and rural areas.
- Strengthening the capacity of countries to translate evidence into policy and action generated transformation for the achievement of sustainable urban development.

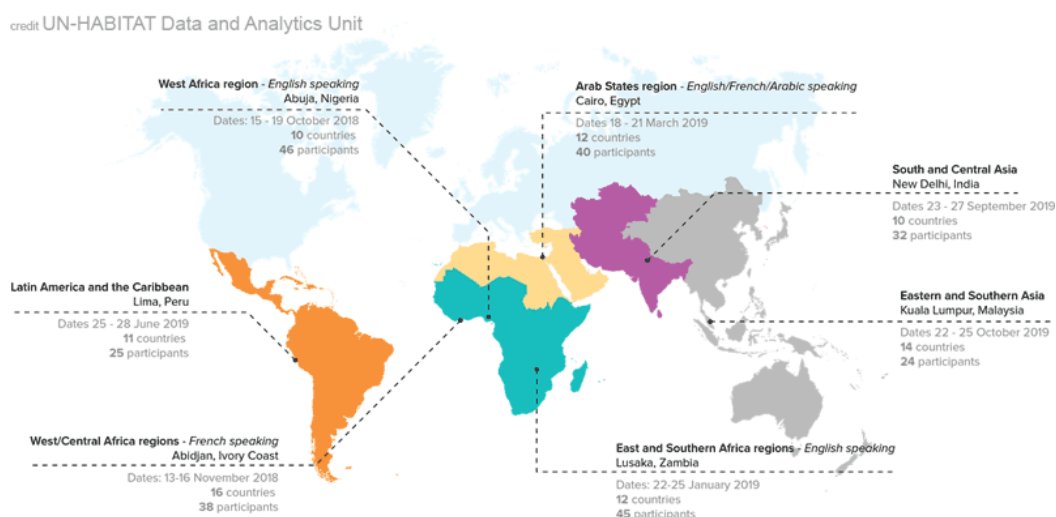
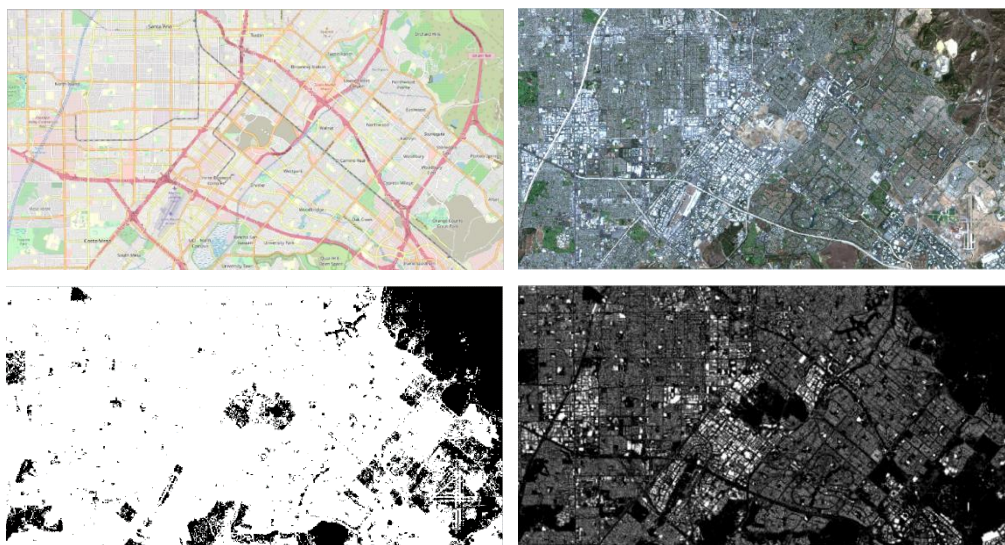


Figure 104. Regional workshops co-organized by the European Commission (DG REGIO and JRC) and UN-Habitat

As follow up to the workshops the JRC conducted dedicated training in the United Arab Emirates at the request of the Federal Competitiveness and Statistical Authority, and at the UN-Habitat Headquarter in Kenya for UN-Habitat staff. Indeed, GHSL implements a complete cycle from data to information to indicators to policy frameworks that finally feed into the co-design process. This established procedure is a model that can be replicated for any science-policy interface such as international, European and national policies by lifting the barriers from data to knowledge to address the sustainability challenges.

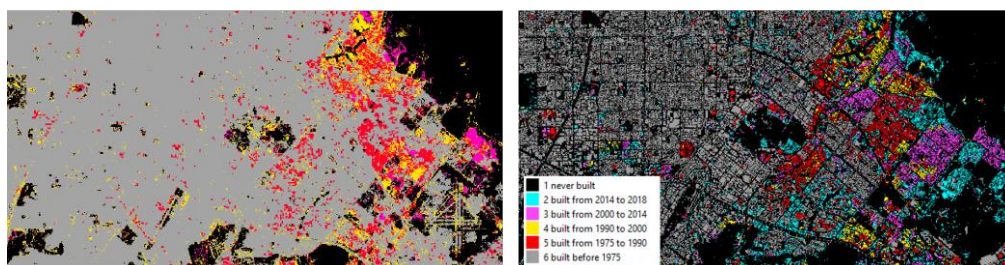
GHSL data release

The currently available GHSL data package stops at the epoch 2015. This was the year of adoption of the three international frameworks Sendai, SDG and Paris Agreement. It is obvious that the GHSL data need to be updated, if they want to support the monitoring of the frameworks. The next major release of the GHSL data is planned for the coming year 2021. The GHSL release will, for the first time, integrate Copernicus Sentinel-2 data for the reference year 2018 (Corbane et al., 2020)³⁰. This will increase the spatial resolution of the baseline built-up area data to 10 m (instead of 30m). This leads to a better thematic accuracy with significant improvements in detecting rural settlements as well as the more detailed delineation of open (non built-up spaces) in cities. The next release will move away from the binary built-up/non built-up dichotomy and provide built-up fractions instead. The built-up fraction model facilitates a multi-sensor monitoring of human settlements.



Example of built-up area map at 10 m extracted from Sentinel 2 (bottom right), compared to GHS-BUILT multi-temporal Landsat (bottom left), and to input imagery from Sentinel 2 (top right) and to OpenStreet Map layer (top left)

A strength of the GHSL data set is the multi-temporal aspect. The new release will combine the four Landsat epochs (1975, 1990, 2000, 2015) with the Sentinel-2 epoch (2018) passing the high-spatial resolution also to the earlier epochs. For many applications the full resolution of the Sentinel – and even Landsat data – are too detailed and the data volume is difficult to handle. Therefore, the GHSL build-up data are provided in an aggregated resolution. However, improvements also on the side of the population modelling allow increasing the detail from 250 to 100 (or even 50 m, still under discussion) for all five epochs (1975, 1990, 2000, 2015, 2018). At the highest aggregation level of 1 km, it is possible to model the dynamics of built-up and population change. The new data release will include annuals layers of built-up area and population for the timespan 1975–2020.



Examples of built-up area map temporal characterisation at 10 m in the period 1975–2018 processed from Sentinel 2

Box 1

³⁰ Corbane, C., Syrris, V., Sabo, F. et al. Convolutional neural networks for global human settlements mapping from Sentinel-2 satellite imagery. *Neural Comput & Applic* (2020). <https://doi.org/10.1007/s00521-020-05449-7>

4.8 Way Forward

This Atlas of the Human Planet 2020 is a turning point in the GHSL science for policy support. Since its first release in 2016, all atlases were based on GHSL data derived mainly from Landsat imagery, which were progressively integrated with EO data coming from Copernicus satellites along the GHSL evolution. The next data release in 2021 will start the new era based on Copernicus Sentinel data. However, since the applications also in this atlas have demonstrated the importance of time series, the consistency between the two sensors will be maintained.

The various applications presented in this Atlas and the integration of the GHSL data in a number of operational products of the Copernicus Emergency Mapping Service demonstrate the need for a sustainable production for future updates. Therefore, the European Commission is currently preparing the ground for the integration of the GHSL data production into the Copernicus Emergency Mapping Service portfolio.

It is expected that with the improvement of the spatial resolution of the built-up area product from 30 m to 10 m, we will see two effects. On the one hand, we will see a better detection of smaller rural settlements and hamlets. On the other hand, open spaces in cities will be delineated better leading to less dense built-up areas. This will have an impact on the population distribution, especially for countries with very large census units. In some countries, we could see a shift of population from urban to rural areas. Consequently, all the GHSL downstream products will be updated starting from the settlement model (GHS-SMOD) that will be delivered together with the built-up area and population data sets, the urban centre database (GHS-UCDB) and the functional urban areas (GHS-FUA) will follow.

The breadth of applications presented in this Atlas is demonstrating the impact of free and open data. It is expected that this is only a promising beginning, whereas an increasing amount of studies use GHSL data published in the scientific literature and in institutional reports. The GEO Human Planet Initiative should build on these developments and shift from the current focus on data production and improvement to the integration of Human Planet data with other data sets to create new knowledge. This knowledge can inform the SDG monitoring, but it should already look beyond the 2030 horizon, with an outlook on 2050 when Europe pledged to become the first carbon-neutral continent. There is a role for GEO to support this generational endeavour providing innovative data and knowledge for transformative policies.



5.0

5 Conclusions

This edition of the Atlas took stock of the long-term public availability of the GHSL 2019 data release and of a wide and engaged multidisciplinary community of GHSL data users including policy makers, researchers and practitioners.

The Atlas 2020, the fifth in the series of the Atlas of the Human Planet, represents an important landmark in the uptake of the GHSL framework. On the one hand, the report explained the GHSL evolution, both in terms of progressive technological and methodological improvements in the GHSL data production, and in terms of development of tools and systems for capacity development. On the other hand, this year's Atlas collects more than 30 concrete, action oriented and transformative applications of GHSL data across four thematic areas, which are at the core of international development strategies: disaster risk management and its reference global agenda – the Sendai Framework; urbanisation framed in SDG 11 and in the New Urban Agenda, the thematic section on development, capturing the Sustainable Development Goals at large; and the thematic section on environment and sustainability framed in the European Green Deal and in the UNFCCC Paris Agreement.

Each of the topical sections has revealed the importance of the key principles, unique features and products of the GHSL framework for specific applications.

In the field of disaster risk management, GHSL was integrated – among many other applications – in information systems to improve decision makers awareness, to save time during crises, and to identify how exposure to epidemics may vary with settlement typologies. These applications are of direct relevance in response to the four priorities of the Sendai Framework focussing on understanding disaster risk, strengthening its governance, investing in resilience and enhancing preparedness.

In the broad field of urbanisation and urban studies several applications benefitted from the long time series made available by GHSL data to understand changes in settlement structure and the distribution of populations, and several others relied on the global coverage to develop new methods to study human settlements. These applications indicate the many aspects of urbanisation and sustainable urban development that can be monitored and how this knowledge base can better inform policymaking.

In the key field of development, GHSL data were used in particular to fill data gaps or to source local data, where such information was not easily available. Several examples across the showcases are of direct relevance to a wide array of Sustainable Development Goals, including Goal 1 on poverty eradication, Goal 7 on clean and affordable energy, and more comprehensively on the elaboration of data collection methods to make sustainable development progress monitoring possible.

The thematic section on environment and sustainability is closely tied to the European Green Deal, but as the showcase on global emission shows, the challenge for a sustainable environment is a global one, clearly requiring global data. In that respect, GHSL showed its potential to supply data for areas for which data may not be systematically collected. These specific regions of the world like the Arctic or mountain ranges are fundamental ecological systems that should continue to sustain human life also in the future.

This year's Atlas also highlighted current research frontlines regarding geospatial information on human settlements. These include improved mapping capabilities made possible by innovative methods applied to the Copernicus satellite data, as well as new capacity to differentiate human settlement patterns and typologies, and to estimate the height of buildings over large areas. Additional challenges derive from the demographic component of human settlements, and include increasing the availability of updated and reliable population statistics (which currently vary significantly across countries and regions), the need to map and assess the actual present population in a region and their dynamics (including day vs. nighttime variations), and the modelling of future population distribution and densities.

As the GHSL evolves and adoption of the Degree of Urbanisation becomes more widespread, tools and capacity enhancement become increasingly important to allow stakeholders to produce data independently by ensuring global comparability of outputs, methods compliance and ease of implementation.

The upcoming release of a new GHSL data suite with considerable advances calls for a pause in the yearly issue of the Atlas of the Human Planet, whose next publication is scheduled for 2022.

References

- Aubrecht, Christoph, Dilek Özceylan Aubrecht, Joachim Ungar, Sérgio Freire, and Klaus Steinnocher. 2017. 'VGDI – Advancing the Concept: Volunteered Geo-Dynamic Information and Its Benefits for Population Dynamics Modeling'. *Transactions in GIS* 21 (2): 253–76. <https://doi.org/10.1111/tgis.12203>.
- Aubrecht, Christoph, Joachim Ungar, Dilek Ozceylan Aubrecht, Sérgio Freire, and Klaus Steinnocher. 2018. 'Mapping Land Use Dynamics Using the Collective Power of the Crowd'. In *Earth Observation Open Science and Innovation*, edited by Pierre-Philippe Mathieu and Christoph Aubrecht, 247–53. Cham: Springer International Publishing. https://doi.org/10.1007/978-3-319-65633-5_10.
- Balsamo, Gianpaolo, Anna Agusti-Panareda, Clement Albergel, Gabriele Arduini, Anton Beljaars, Jean Bidlot, Nicolas Bousserez, et al. 2018. 'Satellite and in Situ Observations for Advancing Global Earth Surface Modelling: A Review'. *Remote Sensing* 10 (12): 2038.
- Bechtel, Benjamin, Martino Pesaresi, Aneta J Florczyk, and Gerald Mills. 2018. 'Beyond Built-up: The Internal Makeup of Urban Areas'. *Urban Remote Sensing*.
- Claverie, Martin, Junchang Ju, Jeffrey G. Masek, Jennifer L. Dungan, Eric F. Vermote, Jean-Claude Roger, Sergii V. Skakun, and Christopher Justice. 2018. 'The Harmonized Landsat and Sentinel-2 Surface Reflectance Data Set'. *Remote Sensing of Environment* 219 (December): 145–61. <https://doi.org/10.1016/j.rse.2018.09.002>.
- Comber, Alexis, Masahiro Umezaki, Rena Zhou, Yongming Ding, Yang Li, Hua Fu, Hongwei Jiang, and Andrew Tewkesbury. 2012. 'Using Shadows in High-Resolution Imagery to Determine Building Height'. *Remote Sensing Letters* 3 (7): 551–56. <https://doi.org/10.1080/01431161.2011.635161>.
- Corbane, C., M. Pesaresi, T. Kemper, P. Politis, Aneta J. Florczyk, V. Syrris, M. Melchiorri, F. Sabo, and P. Soille. 2019. 'Automated Global Delineation of Human Settlements from 40 Years of Landsat Satellite Data Archives'. *Big Earth Data* 3 (2): 140–69. <https://doi.org/10.1080/20964471.2019.1625528>.
- Corbane, C., M. Pesaresi, P. Politis, V. Syrris, A.J. Florczyk, P. Soille, L. Maffenini, et al. 2017. 'Mass Processing of Sentinel-1 and Landsat Data for Mapping Human Settlements at Global Level'. In *Proc. of the BiDS'17*, 52–55. <https://doi.org/10.2760/383579>.
- Corbane, C., F. Sabo, V. Syrris, T. Kemper, P. Politis, M. Pesaresi, P. Soille, and K. Osé. 2019. 'Application of the Symbolic Machine Learning to Copernicus VHR Imagery: The European Settlement Map'. *IEEE Geoscience and Remote Sensing Letters*, 1–5.
- Corbane, C., F. Sabo, V. Syrris, T. Kemper, P. Politis, M. Pesaresi, P. Soille, and K. Ose. 2020. 'Application of the Symbolic Machine Learning to Copernicus VHR Imagery: The European Settlement Map'. *IEEE Geoscience and Remote Sensing Letters* 17 (7): 1153–57. <https://doi.org/10.1109/LGRS.2019.2942131>.
- Corbane, C., V. Syrris, F. Sabo, P. Politis, Michele Melchiorri, M. Pesaresi, P. Soille, and T. Kemper. 2020. 'Convolutional Neural Networks for Global Human Settlements Mapping from Sentinel-2 Satellite Imagery'. *ArXiv Preprint ArXiv:2006.03267*.
- Craglia, M, A Annoni, P Benczur, P Bertoldi, P Delipetrev, G De Prato, C Feijoo, et al. 2018. 'Artificial Intelligence–a European Perspective, EUR 29425 EN, Publications Office, Luxembourg'. *Doi* 10: 11251.
- Ehrlich, Daniele, Martino Pesaresi, Thomas Kemper, and Christina Corbane. 2018. 'Built-up and Population Densities: Two Essential Societal Variables to Address Climate Hazard Impact'. *Environmental Science & Policy*.
- Ehrlich, Daniele, Marcello Schiavina, Martino Pesaresi, and Thomas Kemper. 2018. 'Detecting Spatial Patterns of Inequality from Remote Sensing'. EUR - Scientific and Technical Research Reports 29465. Luxembourg: Publications Office of the European Union.
- Elvidge, Christopher D, Kimberly Baugh, Mikhail Zhizhin, Feng Chi Hsu, and Tilottama Ghosh. 2017. 'VIIRS Night-Time Lights'. *International Journal of Remote Sensing* 38 (21): 5860–79. <https://doi.org/10.1080/01431161.2017.1342050>.
- Esch, Thomas, Wieke Heldens, Andreas Hirner, Manfred Keil, Mattia Marconcini, Achim Roth, Julian Zeidler, Stefan Dech, and Emanuele Strano. 2017. 'Breaking New Ground in Mapping Human Settlements from Space

- The Global Urban Footprint'. *ISPRS Journal of Photogrammetry and Remote Sensing* 134: 30–42. <https://doi.org/10.1016/j.isprsjprs.2017.10.012>.
- European Commission , Joint Research Centre. 2018. *Atlas of the Human Planet 2018, a World of Cities*. Publications Office of the European Union. 10.2760/124503.
- . 2019. *Atlas of the Human Planet 2019: A Compendium of Urbanisation Dynamics in 239 Countries*. Publications Office of the European Union. 10.2760/445233.
- 'Facebook's Data for Good Program'. 2020. *Facebook's Data for Good Program* (blog). 2020. <https://data.humdata.org/organization/facebook>.
- Freire, Sergio, Kytt MacManus, Martino Pesaresi, Erin Doxsey-Whitfield, and Jon Mills. 2016. 'Development of New Open and Free Multi-Temporal Global Population Grids at 250 m Resolution'. In *Proceedings of AGILE 2016*. Helsinki, Finland.
- Gong, Peng, and Philip J. Howarth. 1990. 'The Use of Structural Information for Improving Land-Cover Classification Accuracies at the Rural-Urban Fringe.' In .
- Gong, Peng, Xuecao Li, Jie Wang, Yuqi Bai, Bin Chen, Tengyun Hu, Xiaoping Liu, et al. 2020. 'Annual Maps of Global Artificial Impervious Area (GAIA) between 1985 and 2018'. *Remote Sensing of Environment* 236 (January): 111510. <https://doi.org/10.1016/j.rse.2019.111510>.
- Gong, Peng, Han Liu, Meinan Zhang, Congcong Li, Jie Wang, Huabing Huang, Nicholas Clinton, et al. 2019. 'Stable Classification with Limited Sample: Transferring a 30-m Resolution Sample Set Collected in 2015 to Mapping 10-m Resolution Global Land Cover in 2017'. *Science Bulletin* 64 (6): 370–373.
- Goodchild, M. F., H. Guo, A. Annoni, Bian L, K. De Bie, F. Campbell, M. Craglia, et al. 2012. 'Next-Generation Digital Earth'. *Proceedings of the National Academy of Sciences of the United States of America* 109: 11088–94.
- Guo, Huadong. 2017. 'Big Earth Data: A New Frontier in Earth and Information Sciences'. *Big Earth Data* 1 (1–2): 4–20. <https://doi.org/10.1080/20964471.2017.1403062>.
- Huang, Huanchun, Yingxia Yun, Jiangang Xu, Rong Huang, Jing Fu, and Kaidi Huang. 2017. 'Scale Response of Summer Urban Heat Island to Building Plot Ratio and Its Warning Parameter'. *Tehnički Vjesnik* 24 (3): 877–886.
- Huang, Xiao, Cuizhen Wang, Zhenlong Li, and Huan Ning. 2020. 'A 100 m Population Grid in the CONUS by Disaggregating Census Data with Open-Source Microsoft Building Footprints'. *Big Earth Data*, July, 1–22. <https://doi.org/10.1080/20964471.2020.1776200>.
- Huang, Yuhua, Li Zhuo, Haiyan Tao, Qingli Shi, and Kai Liu. 2017. 'A Novel Building Type Classification Scheme Based on Integrated LiDAR and High-Resolution Images'. *Remote Sensing* 9 (7): 679. <https://doi.org/10.3390/rs9070679>.
- INSPIRE Thematic Working Group. 2013. 'D2.8.I.2 INSPIRE Data Specification on Buildings – Technical Guidelines" Version 3.0'. European Commission Joint Research Centre. <https://inspire.ec.europa.eu/id/document/tg/bu>.
- Kadhim, Nada, and Monjur Mourshed. 2017. 'A Shadow-Overlapping Algorithm for Estimating Building Heights from VHR Satellite Images'. *IEEE Geoscience and Remote Sensing Letters* 15 (1): 8–12.
- Kapos, Valerie. 2000. 'UNEP-WCMC Web Site: Mountains and Mountain Forests'. *Mountain Research and Development* 20 (4): 378–378. [https://doi.org/10.1659/0276-4741\(2000\)020\[0378:UWWSMA\]2.0.CO;2](https://doi.org/10.1659/0276-4741(2000)020[0378:UWWSMA]2.0.CO;2).
- Kawakubo, Fernando, Rúbia Morato, Marcos Martins, Guilherme Mataveli, Pablo Nepomuceno, and Marcos Martines. 2019. 'Quantification and Analysis of Impervious Surface Area in the Metropolitan Region of São Paulo, Brazil'. *Remote Sensing* 11 (8): 944. <https://doi.org/10.3390/rs11080944>.
- Klotz, M., T. Kemper, C. Geiß, T. Esch, and H. Taubenböck. 2016. 'How Good Is the Map? A Multi-Scale Cross-Comparison Framework for Global Settlement Layers: Evidence from Central Europe'. *Remote Sensing of Environment* 178 (June): 191–212. <https://doi.org/10.1016/j.rse.2016.03.001>.
- Körner, Christian, Walter Jetz, Jens Paulsen, Davnah Payne, Katrin Rudmann-Maurer, and Eva M. Spehn. 2017. 'A Global Inventory of Mountains for Bio-Geographical Applications'. *Alpine Botany* 127 (1): 1–15. <https://doi.org/10.1007/s00035-016-0182-6>.

- Lewis Dijkstra, and Hugo Poelman. 2014. 'A Harmonised Definition of Cities and Rural Areas: The New Degree of Urbanisation'. Regional Working Paper 2014 WP 01/2014. Bruxelles: European Commission, Regional and Urban Policy.
- Li, Jian, and David P. Roy. 2017. 'A Global Analysis of Sentinel-2A, Sentinel-2B and Landsat-8 Data Revisit Intervals and Implications for Terrestrial Monitoring'. *Remote Sensing* 9 (9). <https://doi.org/10.3390/rs9090902>.
- Li, Xuecao, Yuyu Zhou, Zhengyuan Zhu, Lu Liang, Bailang Yu, and Wenting Cao. 2018. 'Mapping Annual Urban Dynamics (1985–2015) Using Time Series of Landsat Data'. *Remote Sensing of Environment* 216 (October): 674–83. <https://doi.org/10.1016/j.rse.2018.07.030>.
- Liu, Xiaoping, Yinghuai Huang, Xiaocong Xu, Xuecao Li, Xia Li, Philippe Ciais, Peirong Lin, et al. 2020. 'High-Spatiotemporal-Resolution Mapping of Global Urban Change from 1985 to 2015'. *Nature Sustainability* 3 (7): 564–70. <https://doi.org/10.1038/s41893-020-0521-x>.
- Lu, D., and Q. Weng. 2004. 'Spectral Mixture Analysis of the Urban Landscape in Indianapolis with Landsat ETM+ Imagery'. *Photogrammetric Engineering and Remote Sensing* 70: 1053–62.
- Lu, Zhenyu, Jungho Im, and Lindi Quackenbush. 2011. 'A Volumetric Approach to Population Estimation Using Lidar Remote Sensing'. *Photogrammetric Engineering & Remote Sensing* 77 (11): 1145–56. <https://doi.org/10.14358/PERS.77.11.1145>.
- Lu, Zhenyu, Jungho Im, Jinyoung Rhee, and Michael Hodgson. 2014. 'Building Type Classification Using Spatial and Landscape Attributes Derived from LiDAR Remote Sensing Data'. *Landscape and Urban Planning* 130 (October): 134–48. <https://doi.org/10.1016/j.landurbplan.2014.07.005>.
- Maffenini, L., M. Schiavina, S. Freire, M. Melchiorri, M. Pesaresi, and T. Kemper. 2020. *GHS-POP2G User Guide*. Luxembourg: Publications Office of the European Union. <https://doi.org/10.2760/500887>.
- Maffenini, L., M. Schiavina, M. Melchiorri, M. Pesaresi, and T. Kemper. 2020a. *GHS-DUG User Guide*. Luxembourg: Publications Office of the European Union. <https://doi.org/10.2760/916217>.
- . 2020b. *GHS-DU-TUC User Guide*. Luxembourg: Publications Office of the European Union. <https://data.europa.eu/doi/10.2760/633624>.
- Marconcini, Mattia, Annekatrin Metz-Marconcini, Soner Üreyen, Daniela Palacios-Lopez, Wiebke Hanke, Felix Bachofer, Julian Zeidler, et al. 2019. *Outlining Where Humans Live – The World Settlement Footprint 2015*.
- Melchiorri, Michele, Martino Pesaresi, Aneta J. Florczyk, Christina Corbane, and Thomas Kemper. 2019. 'Principles and Applications of the Global Human Settlement Layer as Baseline for the Land Use Efficiency Indicator—SDG 11.3.1'. *ISPRS International Journal of Geo-Information* 8 (2): 96. <https://doi.org/10.3390/ijgi8020096>.
- Pesaresi, M. 2018. 'Principles and Applications of the Global Human Settlement Layer'. In *IGARSS 2018 - 2018 IEEE International Geoscience and Remote Sensing Symposium*, 2047–50. Valencia: IEEE. <https://doi.org/10.1109/IGARSS.2018.8519155>.
- Pesaresi, M., C. Corbane, A. Julea, A. Florczyk, V. Syrris, and P. Soille. 2016. 'Assessment of the Added-Value of Sentinel-2 for Detecting Built-up Areas'. *Remote Sensing* 8 (4): 299. <https://doi.org/10.3390/rs8040299>.
- Pesaresi, M., D. Ehrlich, T. Kemper, A. Siragusa, Aneta J. Florczyk, S. Freire, and C. Corbane. 2017. 'Atlas of the Human Planet 2017: Global Exposure to Natural Hazards'. EUR 28556 EN. European Commission, Joint Research Centre, Institute for the Protection and Security of the Citizen. <https://ec.europa.eu/jrc/en/publication/eur-scientific-and-technical-research-reports/atlas-human-planet-2017-global-exposure-natural-hazards>.
- Pesaresi, M., Daniele Ehrlich, Stefano Ferri, Aneta J. Florczyk, Sergio Freire, Matina Halkia, Andreea Julea, Thomas Kemper, Pierre Soille, and Vasileios Syrris. 2016. 'Operating Procedures for the Production of the Global Human Settlement Layer from Landsat Data of the Epochs 1975, 1990, 2000, and 2014'. Luxembourg: Publications Office of the European Union: Joint Research Centre.
- Pesaresi, M., M. Melchiorri, A. Siragusa, and T. Kemper. 2016. 'Atlas of the Human Planet - Mapping Human Presence on Earth with the Global Human Settlement Layer'. JRC103150. Publications Office of the European Union. Luxembourg (Luxembourg): European Commission, DG JRC.

- Sabo, F., C. Corbane, and T. Kemper. 2019. 'The European Settlement Map 2019 Release'. EUR 29886. Luxembourg: Publications Office of the European Union.
- Sabo, Filip, Christina Corbane, Aneta J. Florkczyk, Stefano Ferri, Martino Pesaresi, and Thomas Kemper. 2018. 'Comparison of Built-up Area Maps Produced within the Global Human Settlement Framework'. *Transactions in GIS*, November. <https://doi.org/10.1111/tgis.12480>.
- Salat, Serge, Françoise Labbé, and Caroline Nowacki. 2011. *Cities and Forms: On Sustainable Urbanism*. CSTB Urban Morphology Laboratory.
- Shaker, Ibrahim F., Amr Abd-Elrahman, Ahmed K. Abdel-Gawad, and Mohamed A. Sherief. 2011. 'Building Extraction from High Resolution Space Images in High Density Residential Areas in the Great Cairo Region'. *Remote Sensing* 3 (4): 781–91. <https://doi.org/10.3390/rs3040781>.
- Small, Christopher. 2003. 'High Spatial Resolution Spectral Mixture Analysis of Urban Reflectance'. *Remote Sensing of Environment* 88 (1–2): 170–86. <https://doi.org/10.1016/j.rse.2003.04.008>.
- Sportouche, Helene, Florence Tupin, and Leonard Denise. 2009. 'Building Extraction and 3D Reconstruction in Urban Areas from High-Resolution Optical and SAR Imagery'. In *2009 Joint Urban Remote Sensing Event*, 1–11. Shanghai, China: IEEE. <https://doi.org/10.1109/URS.2009.5137746>.
- Steinnocher, K., A. De Bono, B. Chatenoux, D. Tiede, and L. Wendt. 2019. 'Estimating Urban Population Patterns from Stereo-Satellite Imagery'. *European Journal of Remote Sensing* 52 (sup2): 12–25. <https://doi.org/10.1080/22797254.2019.1604081>.
- Wardrop, N. A., W. C. Jochem, T. J. Bird, H. R. Chamberlain, D. Clarke, D. Kerr, L. Bengtsson, S. Juran, V. Seaman, and A. J. Tatem. 2018. 'Spatially Disaggregated Population Estimates in the Absence of National Population and Housing Census Data'. *Proceedings of the National Academy of Sciences* 115 (14): 3529–37. <https://doi.org/10.1073/pnas.1715305115>.
- WHO Europe Urban Green Space expert panel, and Ruth Hunter. 2017. *Urban Green Spaces: A Brief for Action*.
- Xu, Rudong, Jin Liu, and Jianhui Xu. 2018. 'Extraction of High-Precision Urban Impervious Surfaces from Sentinel-2 Multispectral Imagery via Modified Linear Spectral Mixture Analysis'. *Sensors* 18 (9): 2873. <https://doi.org/10.3390/s18092873>.
- Xu, Yong, Chao Ren, Peifeng Ma, Justin Ho, Weiwen Wang, Kevin Ka-Lun Lau, Hui Lin, and Edward Ng. 2017. 'Urban Morphology Detection and Computation for Urban Climate Research'. *Landscape and Urban Planning* 167: 212–224.
- Zambon, Ilaria, Andrea Colantoni, and Luca Salvati. 2019. 'Horizontal vs Vertical Growth: Understanding Latent Patterns of Urban Expansion in Large Metropolitan Regions'. *Science of The Total Environment* 654 (March): 778–85. <https://doi.org/10.1016/j.scitotenv.2018.11.182>.
- Zhu, Zhe, Yuyu Zhou, Karen C. Seto, Eleanor C. Stokes, Chengbin Deng, Steward T.A. Pickett, and Hannes Taubenböck. 2019. 'Understanding an Urbanizing Planet: Strategic Directions for Remote Sensing'. *Remote Sensing of Environment* 228 (July): 164–82. <https://doi.org/10.1016/j.rse.2019.04.020>.

List of Figures

Figure 1	7
Figure 2. The evolutionary concept of GHSL EO data segment	10
Figure 3 © Adobe Stock	11
Figure 4	12
Figure 5 Schema of dependencies between input data and GHS products	13
Figure 6 Transition from Landsat imagery to built-up areas extraction (GHS-BUILT), population modelling (GHS-POP), and settlements classification (GHS-SMOD), examples in the area of Bangkok (Thailand) information layers of the epoch 2015.	14
Figure 7 Information extraction process from the satellite images of the earth surface (bottom) to the built-up area extraction (middle) to the aggregated built-up area density (top).	15
Figure 8 Combination of GHS-BUILT with the census data to produce a regular fine scale grid of population density.	16
Figure 9 Synthetic explanation of GHS-SMOD logics and definitions. An example from the area of Trapani (Italy)	17
Figure 10 Combination of GHS-SMOD urban centres and other variables to obtain the GHS-UCDB with geospatial data integration processing	18
Figure 11 Delineation of GHS-FUA as commuting area for all urban centres on the planet for the epoch 2015	19
Figure 12 Applying the Degree of Urbanisation process with GHSL Tools	20
Figure 13 GHSL process from imagery to settlement map in the area of Madrid (geospatial layers of the epoch 2015)	22
Figure 14	23
Figure 15 (c) Adobe Stock.....	23
Figure 16 Showcases by thematic area and main policy linkage	24
Figure 17	25
Figure 18 Population exposure analysis considering the degree of urbanisation, GHS-SMOD layer	28
Figure 19 Across-scale population exposure analysis using GHSL layers for A. River flood, B. Coastal Flood, C. Earthquake, hosted on the Risk Data Hub.	28
Figure 20 Global exposure to epidemics (INFORM Risk Index 2020)	30
Figure 21 Population exposed in Nigeria to selected epidemics by Degree of Urbanization grid settlement class at Level 1	30
Figure 22 SEDAC Global COVID-19 Viewer showing a population-weighted 7-day moving average of cases in Europe as of 1 December 2020 and an age pyramid for the combined populations of the UK, Spain, and Portugal.....	32
Figure 23 SEDAC Global COVID-19 Viewer showing charts of daily and 7-day moving average of COVID cases, and degree of urbanization population and land area estimates for India	32
Figure 24 Estimated difference in daytime (red) vs nighttime (blue) population in Milan, Italy, in 2011. Height of the bars is directly proportional to its population density.	34
Figure 25 Variation of potential population exposure to seismic hazard per month in 2011, for (A) Spain; (B) Greece, for Modified Mercalli Intensity (MMI) levels > VI (Strong). Blue bars represent nighttime exposure; orange bars represent daytime exposure.	34
Figure 26 Global drought hazard, exposure (including GHS-POP layer), and vulnerability as well as the risk resulting from the combination of all factors. Adapted from Vogt et al., 2018	36

Figure 27 Drought risk assessment in the UNCCD Drought toolbox. Source: https://maps.unccd.int/drought/ ..	36
Figure 28 Potential Burnable Area Proportion (0-100 %)	38
Figure 29 WUI in Europe, 2012: percentage of WUI land area (left), and population living in the interface (right). Population data from 2015, WCRP EUR-11 grid cell size: approximately 12.5 km (see footnote). From Costa et al., 2020.	38
Figure 30 View of the Rapid Risk Assessment available on the GloFAS website The Global administration regions are shaded according to an impact matrix (shown below) which combines the total population exposure to the flood hazard with the lead time of the flood event. Categories along the top of the matrix refer to the total number of people who live within the flood inundation footprint.	40
Figure 31 Application of the GloFAS RRA for the case study in Mozambique. The map shows overlay of the population density (in red) with the areas predicted to be flooded (in blue).	40
Figure 32 Population in low elevation coastal zones in Vietnam analysed using GHS-POP and settlements classification	42
Figure 33 (upper) infrastructures extracted from free open data for Sao Paulo (Brazil) Urban Area overlayed with the corresponding GHSL layer; (lower) map of infrastructures that are used as gazetteers to place tweets in a GHSL cell on the map	44
Figure 34 Aggregation of classified tweets according to different classes of impact	44
Figure 35 Earthquake in Turkey 24 January 2020: comparison of Aols generated by GDACS and the areas which were analysed under CEMS-Rapid Mapping for actual impact using satellite images. The satellite-based impact assessment confirmed damages in the GDACS Aols of the highest intensity class.	46
Figure 36 Typhoon Kammuri December 2019: comparison of Aols generated by GDACS (wind impact), actual storm track and the footprint of pro-actively tasked satellite images.	46
Figure 37 Example of one of the output formats of CEMS-Rapid Mapping products - a ready to print map - which provides a visual of the consequences table displaying among others the estimated population in the area of interest (Copernicus EMS © 2020, [EMSR436: Fire in Podlaskie Voivodeship, Poland: Delineation product, Monitoring 01])	48
Figure 38 Area of interest of the Risk & Recovery Mapping activation (EMSN054) extending over the transnational Drin River Basin. The European Settlement Layer and GHS population grid were used to facilitate the downscaling of economic information from the Global Assessment Report.	48
Figure 39 Spatial distribution of IDPs and Returnees with the vulnerable condition across entire Iraq	50
Figure 40 Snapshot of Mosul, Iraq, by combining the GHS-SMOD layer and DTM data.....	50
Figure 41	51
Figure 42 World population shares by degree of urbanisation, 1975-2050. In Cities of the World (OECD and EC, 2020) p. 17	54
Figure 43 Life satisfaction by degree of urbanisation, income group and gender. Based on Gallup World Poll, 2016-17, https://www.gallup.com/analytics/232838/world-poll.aspx ; elaborated by EC and OECD, 2019. In Cities of the World (OECD and EC, 2020) p. 41	54
Figure 44 Figure 1. Population Growth in urban centres 1990-2015, from the Urban Centres Database, as published in the Future of Cities Report. Web visualisation of the GHSL urban centre database in the Urban Data Platform Plus	56
Figure 45 Infographic showing one of the main key messages on demographics in European cities taken from the Future of Cities Report	56
Figure 46 Population growth in large cities in Africa 1975 - 2015	58
Figure 47 Map of annual density change for metropolises between 2000 and 2015 and average density in 2015.....	58
Figure 48 Degree of Urbanisation at level 1 in the area of Durban displayed at grid level GHS-SMOD on the left, and applied to local units on the right	60

Figure 49 Country deviation from global average built-up area per capita 2015	60
Figure 50 (left) The metropolitan area of Medellin, Colombia. (right) Development level and importance of commuting zones	62
Figure 51 A web-tool to explore Functional Urban Areas across the world. Source: www.worldcitiestool.org ..	62
Figure 52 General schema of the disaggregation/aggregation method. (source: ESPON FUORE)	64
Figure 53 High education attainment levels evolution in border areas (2000-2005-2010-2015), estimated by means of the FUORE methodology using ESM and GHSM as ancillary dataset. Source: Screenshot from the FUORE Analytical Tool	64
Figure 54 settlement patterns in Padova (Italy) in 1975 – 1990 -2000 - 2014. (Maes et al., 2020)	66
Figure 55 settlement pattern in European functional urban areas, short and long-term trends. (Maes et al., 2020).	66
Figure 56 Population Growth by 100 km-square grid cells from 1990-2014. Positive changes in red and negative in blue.	68
Figure 57: Changes in localized population density, 2000-2014. Notes: Localised population density is a measure of the number of people living within 5 km of a person, discounted by distance. The unit of change is the number of people in a 5 km radius.	68
Figure 58 Global population density in 2015 (mapped using GHS_POP 2015 data)	70
Figure 59 Global population density in China (left) and its neighbours, and the eastern United States (right) ..	70
Figure 60	71
Figure 61 Landing page: OPER-BU web-hosted analytical tool	74
Figure 62. OPER-BU least-cost option per settlement (grid extension, diesel generator, PV mini-grid or PV stand-alone system)	74
Figure 63 Census and our in-sample, model predicted population density for the Western Province Sub-section of Sri Lanka.....	76
Figure 64. Accuracy of predicted population density based on the model with all imagery, only open-source imagery, and only with GHSL. All models include district fixed effects, urban-area dummy, and log village area. HIES=the Household Income and Expenditure Survey. The accuracy measures for the predictions such as R2, SRC (Spearman Rank Correlation), AE (Absolute error), RE (Relative Error), are calculated with respect to actual density from the census data. Higher values of the first two measures, and lower values of the latter two measures indicate better prediction accuracies. For reference, we report the prediction accuracies of the same model, but that uses census-density as the dependent variable.....	76
Figure 65. Travel time to the nearest human settlement in the year 2015 for GHSL settlements with >=100,000 and <200,000 people. Country boundaries from GADM v3.6	78
Figure 66. Difference in travel time estimates in minutes and hours (our estimated travel time minus Google journey time) based on journeys between locations within each of the 2° × 2° tiles shown in the map. Country boundaries from GADM v3.6.	78
Figure 67. Urban growth of City of Johannesburg and City of Tshwane (Pretoria), for 2015-2050, according to modelled SSP3 scenario.	80
Figure 68. Urban and Rural population share in South Africa (2015-2050) according to modelled SSP3 scenario.....	80
Figure 69. Urban growth rate and urban-population growth rate in South Africa (2015-2050), according to modelled SSP3 scenario. Urban growth rate refers to pixels containing a substantial share of built-up land, while urban population growth rate refers to the population living in there, both computed every 5 years....	80
Figure 70 Net migration estimates (0.25 x 0.25 degree), 2010-2015	82
Figure 71 Net migration in Kayes region (Mali, 0.5 x 0.5 degree), 2010-2015 (left panel). Correlation between temperatures and net migration in Kayes region, by population density. 1970 – 2015 (right panel).	82

Figure 72 Algorithm for Urban Disaggregation of IDPs from area-based assessments. The procedure comprises a matching between the Global Human Settlement Layer and geo-localised displacement figures.	84
Figure 73 Global patterns of inequality detected by combining global population density, built-up density and night light emission for 2015.....	86
Figure 74 Inequality creating sharp contrast between neighbouring countries, examples of the Korea peninsula (left) and Middle East (right).	86
Figure 75 (left) New classes of urban change developed by comparing infrastructure, land, and population change. (based on GHS BUILT layer, GPW population density, Black Marble nighttime lights; (right) satellite images showing examples of each change class	88
Figure 76 Regression showing estimates of rural population gaining access to electricity between 2011 and 2017, based on the census and class-based estimates.....	88
Figure 77 Types and alignment of the urban indicators proposed in the European Handbook for SDG Voluntary Local Review	90
Figure 78 Rationale for the selection of the indicators proposed in the European Handbook for SDG Voluntary Local Review	90
Figure 79	91
Figure 80 Map of 1990-2015 population change (%) in the Arctic study domain	94
Figure 81 Low Density grid Cells (LDC; left), Moderate Density Clusters (MDC, right) and High Density Clusters (HDC, right) cells in the Arctic regions of North America (NA; including Alaska and Canadian regions), “Europe” (EUR; including Iceland, Greenland and Norwegian, Finnish and Swedish Arctic territories) and Russian Federation (RUS). The origin is set above 0 in LDC plots to better highlight the temporal trend	94
Figure 82 Map of the GMBA mountain ranges coloured in classes of population size. The most populated mountain ranges are located in low latitudes	96
Figure 83 Population change and share of urban population in mountain ranges	96
Figure 84 Air pollutant and CO2 emissions in different settlement areas in 2015	98
Figure 85 Air pollutant and CO2 emissions by sector in urban centres in 2015.....	98
Figure 86 Areas where the generation potential exceeds electricity demand (light/green) and where it does not (dark/red), for all subnational regions and municipalities in Europe. For both levels the text box furthermore shows from top to bottom: the name of the level, the fraction of undersupplied administrative units, and the fraction of the European population living in undersupplied administrative units. Source: Tröndle et al (2019), Energy Strategy Reviews.....	100
Figure 87 Screenshot of the interactive map visualising the main results of our study. The map visualises the potentials for each of the 34 countries, 502 regions, and 122,635 municipalities. Municipalities coloured light green and light red may be able to achieve renewable electricity autarky by allowing for higher local densities of electricity infrastructure. Available at: https://timtroendle.github.io/possibility-for-electricity-autarky-map/	100
Figure 88 (A) Aerial photo (B) Overlay of ESM (grey patches) and cadaster data (red polygons). (C) Observed overshoot in the ESM (red patches) to be filtered out. (D) Calculated scaling factors per land cover class. Source: [2]	102
Figure 89 Example of obtained building density raster for the Lombardy region in northern Italy. Source: [2]	102
Figure 90 Percentage of people living within pre-defined distances to open spaces for the 12 biggest urban centres as defined by GHSL settlement model (GHS-SMOD)	104
Figure 91 The top 12 biggest cities in EU ranked by the percentage of open spaces compared to the size of the urban centre as defined by GHS-SMOD)	104
Figure 92 Spatial configuration of urban green areas, example in Austrian cities	106

Figure 93 Spatial configuration of urban green areas in European core cities. Share of Dominant – Interior – Intact green areas (% on the total GI)	106
Figure 94	107
Figure 95 © Adobe Stock	108
Figure 96. The most detailed and up-to-date map of built-up areas derived from Sentinel-2 Copernicus data in the framework of GHSL. The example here is taken from China.	109
Figure 97 © Adobe Stock	110
Figure 98. European Settlement Map from Copernicus Very High Resolution data for reference year 2015, Public Release 2019. European Commission, Joint Research Centre (JRC) doi: 10.2905/8BD2B792-CC33-4C11-AFD1-B8DD60B44F3B PID: http://data.europa.eu/89h/8bd2b792-	111
Figure 99 Reference data on number of floors per building for the city of Chicago –left), and estimated Gross Vertical Component derived from open and global Digital Surface Models –right.....	112
Figure 100 Built-up surface and estimated building volume in the 250m grid cell for selected cities	113
Figure 101 © Adobe Stock.....	114
Figure 102 Examples of discrepancies (patches larger than 1 km ²) between census geometries (blue line) and detected built-up areas in GHS-BUILT 2014 (orange) along the coasts of (A) Japan (JPN) and (B) Tunisia (TUN) (from Freire et al. 2020).....	115
Figure 103 © Adobe Stock.....	116
Figure 104. Regional workshops co-organized by the European Commission (DG REGIO and JRC) and UN-Habitat.....	117
Figure 105	120

List of Boxes

Box 1	118
-------------	-----

GETTING IN TOUCH WITH THE EU

In person

All over the European Union there are hundreds of Europe Direct information centres. You can find the address of the centre nearest you at: https://europa.eu/european-union/contact_en

On the phone or by email

Europe Direct is a service that answers your questions about the European Union. You can contact this service:

- by freephone: 00 800 6 7 8 9 10 11 (certain operators may charge for these calls),
- at the following standard number: +32 22999696, or
- by electronic mail via: https://europa.eu/european-union/contact_en

FINDING INFORMATION ABOUT THE EU

Online

Information about the European Union in all the official languages of the EU is available on the Europa website at: https://europa.eu/european-union/index_en

EU publications

You can download or order free and priced EU publications from EU Bookshop at: <https://publications.europa.eu/en/publications>. Multiple copies of free publications may be obtained by contacting Europe Direct or your local information centre (see https://europa.eu/european-union/contact_en).

The European Commission's science and knowledge service

Joint Research Centre

JRC Mission

As the science and knowledge service of the European Commission, the Joint Research Centre's mission is to support EU policies with independent evidence throughout the whole policy cycle.



EU Science Hub
ec.europa.eu/jrc



@EU_ScienceHub



EU Science Hub - Joint Research Centre



EU Science, Research and Innovation



EU Science Hub



Publications Office
of the European Union

doi:10.2760/16432

ISBN 978-92-76-27388-2